

Holocene paleoenvironmental change, climate and human impact in Sierra Nevada, southern Iberian Peninsula



UNIVERSIDAD
DE GRANADA

María Josefa Ramos Román
PhD Thesis

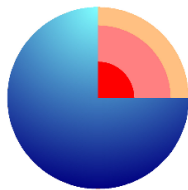


**UNIVERSIDAD
DE GRANADA**

Holocene paleoenvironmental change, climate and human impact in Sierra Nevada, southern Iberian Peninsula

María Josefa Ramos Román

**PhD Thesis
Department of Stratigraphy and Paleontology
University of Granada**



**Programa Doctorado
Ciencias de la Tierra**



**UNIVERSIDAD
DE GRANADA**

Holocene paleoenvironmental change, climate and human impact in Sierra Nevada, southern Iberian Peninsula

María Josefa Ramos Román

PhD Thesis

Directors:

Gonzalo Jiménez Moreno

R. Scott Anderson



**Programa Doctorado
Ciencias de la Tierra**

Editor: Universidad de Granada. Tesis Doctorales
Autora: María Josefa Ramos Román
ISBN: 978-84-9163-787-5
URI: <http://hdl.handle.net/10481/49719>

The doctoral candidate **María Josefa Ramos Román**
and the thesis supervisors **Dr. Gonzalo Jiménez Moreno** and **Prof. R. Scott
Anderson**

Guarantee, by signing this doctoral thesis, that the work has been done by the doctoral candidate under the direction of the thesis supervisor and, as far as our knowledge reaches, in the performance of the work, the rights of other authors to be cited (when their results or publications have been used) have been respected.

Granada, December 2017

Thesis supervisors:

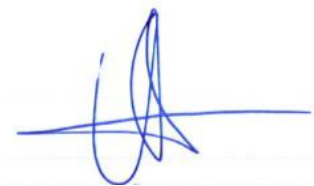


Gonzalo Jiménez Moreno



R. Scott Anderson

Doctoral candidate:



María Josefa Ramos Román

Agradecimientos

Durante estos años han sido muchas las personas e instituciones que han formado parte directa o indirectamente del desarrollo de esta tesis y a quienes quiero manifestar mi más sincera gratitud por todo el apoyo prestado y la confianza depositada en mí. La experiencia vivida en estos años me llena de entusiasmo para seguir fuera del mismo.

En primer lugar quiero agradecer a las instituciones que mediante su financiación han hecho posible el desarrollo de la presente tesis doctoral, a la Junta de Andalucía, por la financiación para el contrato de "Personal investigador en formación asignado a los programas Excelencia de la convocatoria 2011", al proyecto "Cambio climático en el sur de la Península Ibérica: Reconstrucción basada en sedimentos lacustres del Parque Nacional Sierra Nevada (P11-RNM-7332) " y al grupo de investigación RNM0190. Se brindó apoyo financiero adicional por el proyecto "Cambio ambiental y climático en el sur de Europa: el registro paleoecológico de El Padul, Sierra Nevada (MINECO: CGL2013-47038-R). A la Universidad de Granada y CEI BioTic por su financiación con una beca para una estancia breve dentro del programa de movilidad internacional.

Seguidamente quiero agradecer a mi director de tesis el Dr. Gonzalo Jiménez Moreno, por su meritoria dirección, con su dedicación, paciencia, criterio y guía sin los que el desarrollo de esta tesis no hubiera sido posible. Gracias por el conocimiento aportado, por estar pendiente de mí en cada situación y tener la palabra de aliento adecuada en el momento preciso.

También quiero agradecer a el Dr. R. Scott Anderson, mi codirector, por acogerme durante mi estancia en la Northern Arizona University, y por compartir conmigo sus amplios conocimientos.

Mi agradecimiento a demás miembros del grupo de trabajo involucrado en este proyecto, por sus colaboraciones al Dr. Francisco Jiménez-Espejo, Dra. Jaime L. Toney, Dr. José S. Carrión, y en especial a el Dr. Antonio García-Alix por su importante participación y ayuda en el progreso de esta tesis. También me gustaría

agradecer a mi compañero Jon Camuera, estudiante de doctorado, con el que he tenido la oportunidad de trabajar cómodamente, recibir su apoyo y compartir nuestros conocimientos desinteresadamente.

Gracias a Dirk Sachse por acogerme en su laboratorio en el German Research center of Geosciences (GFZ, Helmholtz Centre Potsdam), y a todo su equipo de trabajo por el apoyo prestado durante mi estancia allí.

Gracias a todo el departamento de Estratigrafía y Paleontología por estos casi cuatro años allí, en los que me he sentido como en casa desde el primer día. Agradecer profundamente a todos mis compañeros de despacho, Paola, Elena, Jon, Vedrana, Anja, Bob, Samuel, Weronika y Paula con los que he compartido momentos muy especiales e indeterminadas horas de trabajo.

Doy las gracias por tener tan buena experiencia dentro de la universidad, quien me ha permitido convertirme en la profesional que tanto me apasiona, gracias a cada compañero y tutor que ha formado parte de este proceso de formación, que hoy nos trae como recuerdo esta tesis.

A todos aquellos con los que he tenido la oportunidad de cruzarme durante mis estancias en el extranjero y que me hicieron sentir como en casa con su apoyo y cariño, Vera Markgraf, Pamela Anderson, Andrea Knappe, Alina, Hoda y Pauline: gracias.

A mis compañeras de piso, Mercedes y Cor, a las que considero mi familia en Granada, por estar en los buenos y malos momentos.

A mis padres: gracias por darme la libertad de elegir mi futuro y brindarme con las manos abiertas apoyo y confianza en mi preparación y mi profesión. No puedo olvidar al resto de mi familia, como mis hermanos, gracias por vuestro amparo, paciencia y ánimo durante todo este camino.

Y a mis amigas del pueblo, dónde me refugiaba para tener mis ratitos de desconexión: gracias por los buenos momentos que me hacéis pasar. Gracias por el apoyo y la amistad que siempre me demostráis.

Quiero agradecer a Juanma, mi compañero de vida, todo su apoyo incondicional y comprensión, su amor, sus consejos y el sacrificio de la distancia, porque gracias a él he cumplido una de mis mayores metas. Gracias por entender mis ausencias estando separados a miles de kilómetros durante largas temporadas y por tus visitas al otro lado del mundo. Por esto y por mucho más GRACIAS: sin ti, sin tu soporte ilimitado la finalización de esta tesis no hubiera sido posible.

Finalmente agradezco a quien dedica un espacio de su tiempo a leer este apartado y mi tesis, resultado de mis experiencias, investigaciones y conocimiento.

No existen palabras en el mundo que se acerquen a lo agradecida que estoy.
Y como dijo, Lao Tse, *La gratitud es la memoria del corazón*

Thesis outline

This PhD thesis is structured in seven chapters:

Chapter 1 is the introduction, starting with the background information about orbital and suborbital forcings driving climate change in the western Mediterranean and in the Iberian Peninsula during the Pleistocene and Holocene. Subsequently, background information about human impact in southern Iberia and the use of multi-proxy analysis in lakes and bog/wetlands areas as tools for the reconstruction of past climate change and human influence in these environments. In this chapter is described the hypothesis and objectives of the present PhD thesis. Finally, the regional settings of the studied sites are shown.

The following chapters, 2, 3, 4 and 5, are a compilation of the results of the currently PhD thesis in form of published or future publications in international scientific reviews in which the PhD student has been the main author or has made an important collaboration.

Chapters 6 and 7 correspond to the conclusions and future perspectives.

Table of Contents

Extended Abstract	1
Resumen extendido	5
Chapter 1: Introduction	13
1. Background	13
2. Hypothesis and objectives	32
3. Regional settings	35
Chapter 2: Millennial-scale cyclical environment and climate variability during the Holocene in the western Mediterranean region deduced from a new multi-proxy analysis from the Padul record (Sierra Nevada, Spain)	45
1. Introduction	47
2. Methodology	53
3. Results and proxy interpretation	59
4. Discussion	75
5. Conclusions	87
Chapter 3: Holocene climate aridification trend and human impact interrupted by millennial- and centennial-scale climate fluctuations from a new sedimentary record from Padul (Sierra Nevada, southern Iberian Peninsula)	97
1. Introduction	100
2. Regional setting: Padul, climate and vegetation	102
3. Material and methods	105
4. Results	109
5. Discussion	117
6. Conclusions	134
Chapter 4: Centennial-scale vegetation and North Atlantic Oscillation changes during the Late Holocene in the southern Iberia	143
1. Introduction	145
2. Methods	150
3. Results	154
4. Discussion	160
5. Conclusions	172
Chapter 5: Alpine bogs of southern Spain show human-induced environmental change superimposed on long-term natural variations	177
1. Introduction	179
2. Results	182
3. Discussion	187
4. Conclusions	196
5. Methods	197
Chapter 6: Concluding Remarks. Climate evolution and human impact in Sierra Nevada based on vegetation reconstruction dynamics	219

1. Long-term Holocene vegetation dynamics, environmental variability and climate change during in Sierra Nevada	219
2. Millennial-scale paleoenvironmental and climate variability during the Holocene in Sierra Nevada	224
3. Human Impact	228
Chapter 7: Conclusions and future perspectives	233

Extended Abstract

Sierra Nevada, located in southern Iberian Peninsula, is an interesting area to study past climate changes due to its situation between subtropical and temperate latitudes in the western Mediterranean region, being a sensitive area to climate fluctuations. Currently, one of the main atmospheric mechanisms directing climate in this area is the North Atlantic Oscillation (NAO) and many recent studies put a significant effort in trying to relate local and regional environmental variability with global atmospheric-oceanic dynamics. The Sierra Nevada ecosystems are specially protected (National Park since 1999) and have been declared an area of interest to study vegetation variability since its important situation between humid and arid climates, its location proximal to the last-glacial coastal shelves and its altitudinal gradient and biodiversity.

The Holocene (i.e., the last 11700 years BP) is an interesting period to study past climate change in the Mediterranean region, with the main objective of analyzing climate patterns, estimating future climate scenarios and to constrain future climate models. Understanding climate change related with orbital variability (i.e., changes in insolation) and suborbital processes and their links with solar activity and atmospheric-oceanic circulation and how these different scale climate changes affected the environments have been the main subject of scientific studies in the western Mediterranean region during the last decades. However, despite of the importance to understand climate variability and its environmental effects in this very sensitive area, a lack of high-resolution multi-proxy analysis exist. In addition, the study of Late Holocene continental records subjected to important anthropogenic impact is the key to disentangling natural versus anthropic impact and what is the main forcing directing the environmental change in the last millennia.

In this framework, multi-proxy analyses at high-resolution (from millennial to multi-decadal-scale) are necessary in sedimentary sequences of southern Iberia. In this sense, the present PhD thesis focusses in the study of vegetation, paleoenvironmental and climate change during the Holocene in the Sierra Nevada

ecosystems at orbital and suborbital-scale. In order to accomplish this, high-resolution multi-proxy analyses (lithological and sedimentological and physical properties, radiocarbon dating, pollen, charcoal, organic and inorganic geochemistry) were done on two sedimentary sequences from different altitudes and different environmental settings in Sierra Nevada: Borreguil de la Caldera (BdlC; ~2992 m), at higher elevation in the crioromediterranean vegetation belt, and Padul (~725 m), at lower elevation in the mesomediterranean vegetation belt.

The multi-proxy analysis carried out by pollen, non-pollen palynomorphs (NPPs), lithological, sedimentological, inorganic and organic geochemistry from the new Padul wetland sedimentary record (Padul-15-05) is based on seventeen accelerator mass spectrometry (AMS) radiocarbon dates used to build a robust age-model for the last approximately 11.6 cal ka BP. This study provided a reconstruction of vegetation, environmental and climate evolution, and human impact in the area during the Holocene. Results from the analyses show that the Holocene period could be divided in three different phases following a long-term trend related with orbital-scale climate variability. (1) The expansion of Mediterranean forest in the region, maximum regional humidity and a peatland environment in Padul characterized the record between ~11.6 and 7.6 cal ka BP, and was mostly controlled by a higher seasonality and greater summer insolation, locally producing higher evaporation rates and lower water levels. Within this period the maximum in humidity, represented by maxima in mesic species, was recorded between ~9.5 and 7.6 cal ka BP. (2) A transitional period, between 7.6 and 4.7 cal ka BP, was characterized by a slight decrease in deciduous taxa. The local environment during this period was featured by a higher water level variability related with the decrease in seasonality and millennial-scale climatic oscillations. (3) An abrupt regional change occurred at around ~4.7 cal ka BP, featured by a strong decrease in Mediterranean forest, pointing to regional aridification, and locally by the establishment of a shallow water lake and lacustrine sedimentation. This natural decrease in forest and the increase in water level could be explained by the decrease in summer insolation, providing lower winter rainfall and more aridity, but also lower evaporation rates in summer, triggering an increase in

the lake level. During the last 1.5 cal ka BP the shallow lake turned into an ephemeral lake environment and emerged in the last four centuries. This can be related to a combination of factors, including aridification, increase in soil erosion and draining of the basin by humans, this later factor supported by higher evidence of human activities in the area in the last 1.5 cal ka BP.

Rapid climatic events are also detected in this record during the entire Holocene at around 9.6, 8.5, 7.5, 6.5, 5.4, 4.7-4.2, 2.7 and 1.3 cal ka BP, coinciding with North Atlantic decreases in temperature and linked to variations in solar irradiance. These events are characterized in the Padul-15-05 record by decreases in Mediterranean forest, the increase in erosion and run-off and the increase in lake level and hygrophytes but decrease in algal productivity in the local environment. Time series analysis carried out in the regional signal (Mediterranean forest taxa) suggest two different climatic periodicities, a cyclicity of ~2100 and ~1100 yr period dominating regional climate between 11.6 and 4.7 cal ka BP and a periodicity of around ~1400 yr since 4.7 cal ka BP to Present. This change in cyclicity could be due to the establishment of the actual climate dynamic mainly controlled by the NAO. Our results thus agree with other time series analysis in the northern hemisphere, suggesting links between atmospheric-oceanic and solar dynamics at hemispheric scales.

The multi-proxy analysis from BdlC, is based on a chronological age-model build by five AMS radiocarbon dates recording the last ~4.5 cal ka BP. The multi-proxy analysis based on pollen, charcoal, magnetic susceptibility, inorganic and organic geochemistry provide a reconstruction of vegetation, fire, atmospheric dynamics, climate and human impact at higher elevation than Padul in the Sierra Nevada. An aridification process during the Late Holocene is also recorded in this record characterized here by the decrease in arboreal pollen, the expansion of xeric component and the increase in African dust input. The long-term aridification trend is also interrupted in the BdlC record by millennial and centennial-scale climatic variability linked with atmospheric dynamics mainly controlled by the NAO. With respect to this climatic variability, are detected periods such as the wetter Iberian-

Roman Humid Period (IRHP) depicted in this record by the increase in *Pinus* forest in the area, arid events occurred during the Dark Ages (DA) and Medieval Climate Anomaly (MCA), which were featured by increases in *Artemisia* and the Little Ice Age (LIA) showed higher variability, alternating between arid and humid pulses, related with NAO atmospheric dynamics and solar activity. Despite this regional aridification trend, the local environmental response in this record show an increase in the aquatic component during the Late Holocene in the BdIC, which could be explained by the geomorphological conditions of the basin and/or the decrease in summer insolation. During the last centuries higher anthropogenic impact was recorded, characterized by direct activities in the alpine ecosystem not affecting the natural vegetation changes. After the Industrial Revolution (IR), indirect anthropic effects are registered while the last glacier in Sierra Nevada disappeared.

Resumen extendido

Sierra Nevada está situada en el Sur de la Península Ibérica y es un área interesante para el estudio de cambios climáticos en el pasado debido a su localización entre una latitud subtropical y templada en la zona oeste del Mediterráneo, siendo un área muy sensible a las variaciones climáticas. Actualmente, uno de los principales mecanismos que controla el clima en esta zona es la Oscilación del Atlántico Norte (NAO, por sus siglas en inglés) y el objetivo principal de un gran número de estudios actuales es intentar relacionar variaciones medioambientales locales y regionales con dinámicas atmosféricas-oceánicas globales. Los ecosistemas de Sierra Nevada, de especial protección (es Parque Nacional desde 1999), han sido declarados áreas de interés para el estudio de la variabilidad en la vegetación debido a su importante situación entre un clima húmedo y árido, su gran diversidad vegetal, la localización cercana a las zonas costeras durante el último periodo glacial y a su gradiente altitudinal.

El Holoceno (es decir, los últimos 11700 años BP) es un periodo muy interesante para el estudio del cambio climático en el pasado en la región Mediterránea, con el objetivo principal de estimar escenarios y modelos climáticos futuros. El intento de entender la evolución del clima y su impacto en el medioambiente relacionado con cambios orbitales (i.e. insolación) y suborbitales y las relaciones con la actividad solar y la circulación atmosférica-oceánica ha sido una de las líneas de trabajo principales en los estudios de registros sedimentarios de la región oeste del Mediterráneo durante las últimas décadas. A pesar de la importancia de este tipo de estudios en esta área tan sensible al cambio climático, hay una carencia de análisis multi-proxy a alta resolución. En este sentido, el estudio a alta resolución de registros continentales depositados durante el Holoceno Tardío podría ser la clave para separar la señal del impacto natural del antrópico e identificar cuál fue el principal factor que controló el cambio ambiental durante los últimos milenios.

Los análisis multi-proxy a alta resolución (de escala milenaria a escala de multidécadas) en las secuencias sedimentarias del sur de la Península Ibérica son

necesarios para poder llevar a cabo estos objetivos. En este sentido, la presente tesis doctoral se centra en el estudio de la vegetación, el cambio paleoambiental y climático a escala orbital y suborbital durante el Holoceno en los ecosistemas de Sierra Nevada. Para ello, hemos realizado análisis multi-proxy de alta resolución (polen, carbonos, geoquímica orgánica e inorgánica, litología, sedimentología y propiedades físicas) basados en modelos cronológicos robustos, a través de dos secuencias sedimentarias a diferente altitud in Sierra Nevada. Uno de ellos a mayor altitud, Borreguil de la Cadera (~2992 m) en el piso de vegetación Crioromediterráneo y el otro, Padul (~725 m) a menor altitud, en el cinturón de vegetación Mesomediterráneo.

El análisis multi-proxy realizado mediante polen, palinomorfos no-polinicos (NPPs), litología, sedimentología, geoquímica inorgánica y orgánica del registro del humedal de Padul se basa en diecisiete fechas de radiocarbono por espectrometría acelerada de masas (AMS, en inglés) utilizadas para construir un modelo de edad robusto para los últimos 11.6 cal ka BP. Este análisis nos proporciona una reconstrucción de detalle de la vegetación, evolución ambiental, clima e impacto humano durante el Holoceno. Los resultados de dicho análisis muestran que el período Holoceno se puede dividir en tres fases climáticamente diferentes, siguiendo una tendencia a largo plazo que está relacionada con la variabilidad climática a escala orbital: (1) desde aproximadamente ~11.6 a 7.6 cal ka BP, caracterizada por la expansión del bosque Mediterráneo y de especies caducas, indicando máxima humedad (óptimo de humedad entre ~9.5 a 7.6 cal ka BP), y localmente por un ambiente de turbera, debido a una mayor estacionalidad e insolación de verano que produciría mayores tasas de evaporación y niveles de agua más bajos. (2) Una época de transición, entre ~7.6 y 4.7 cal ka BP, caracterizada por una pequeña disminución en el bosque mediterráneo, que queda formado principalmente por *Quercus* perenne. El ambiente local durante este período se caracterizó por una mayor variación del nivel de agua relacionado con la disminución de la estacionalidad. (3) Un cambio brusco alrededor de ~4.7 cal ka BP mostrado por la acusada disminución del bosque mediterráneo y el establecimiento de un lago somero. Esta disminución natural en el bosque y el aumento en el nivel del agua podría explicarse debido a la disminución

en la insolación de verano, proporcionando menor precipitación en invierno en la región y más aridez, pero también menores tasas de evaporación en verano y, por tanto, subidas en nivel del lago. Durante los últimos 1.5 cal ka BP, el lago pasa a ser un ambiente efímero, incluso llega a emerger en los últimos cuatro siglos. Esto estaría relacionado con una mayor aridez, que produciría un aumento en la escorrentía y erosión del suelo y también estaría conectado con la mayor evidencia de actividades humanas en la zona desde este periodo hasta la actualidad, incluyendo la desecación artificial del humedal.

En este registro también se detectan eventos climáticos rápidos a lo largo de todo el Holoceno, con eventos especialmente áridos alrededor de 9.6, 8.5, 7.5, 6.5, 5.4, 4.2, 2.7 y 1.3 cal ka BP, que coinciden con caídas en la temperatura del Atlántico Norte y vinculados con disminuciones en la actividad solar. Estos eventos vienen representados en el nuevo registro Padul-15-05 por la disminución del bosque mediterráneo, el aumento de la escorrentía superficial y el aumento de las condiciones de humedad en el medioambiente local. Además, el análisis espectral de la serie temporal del bosque mediterráneo, que indica medioambiente y clima regional, sugiere un cambio significativo en la periodicidad de los ciclos climáticos, detectando una periodicidad de alrededor de ~2100 y ~1100 años entre ~11.6 y 4.7 cal ka BP y una periodicidad de alrededor de ~1400 años desde ~4.7 cal ka BP hasta el presente. Este cambio se pudo deber al establecimiento de la dinámica climática actual principalmente controlado por la NAO. Nuestros resultados están de acuerdo con otros análisis de series temporales del Holoceno en el hemisferio norte, sugiriendo una fuerte vinculación entre los sistemas atmosféricos-oceánicos con la dinámica solar a escala hemisférica.

El análisis multi-proxy de los sedimentos del BdIC se basa en un modelo de edad construido por cinco fechas de radiocarbono por AMS que muestra un registro continuo de los últimos ~4.5 cal ka BP. El análisis multi-proxy basado en polen, carbón, susceptibilidad magnética, geoquímica inorgánica y orgánica proporciona una reconstrucción de la vegetación, incendios, dinámica atmosférica, clima e impacto humano en la zona durante el Holoceno tardío. Este estudio registra también

el proceso de aridificación que tuvo lugar durante los últimos milenios, caracterizado en el BdIC por la disminución del polen arbóreo, la expansión de hierbas xerofíticas y el incremento de la entrada de polvo africano. Esta tendencia a la aridez se encuentra, al igual que en Padul, intercalado por variabilidad climática a escala de milenios y centurias que se relaciona principalmente con la dinámica atmosférica mayoritariamente controlada por variaciones solares que afectaron a la NAO. Dentro de esta variabilidad climática, se detectan periodos más húmedos como el período húmedo Ibero-Romano (IRHP, en inglés) caracterizado por el aumento de *Pinus*, y áridos como la Edad Oscura (Dark Ages: DA, en inglés) y la Anomalía Climática Medieval (MCA, en inglés) caracterizadas por el aumento en *Artemisia* y la Pequeña Edad de Hielo (LIA, en inglés), que se manifiesta por una mayor variabilidad alternando entre pulsos áridos y húmedos. A pesar de esta tendencia a la aridificación, la respuesta del medioambiente local en este registro muestra un aumento en el componente acuático, que podría explicarse por las condiciones geomorfológicas de la cuenca y/o el descenso en la insolación de verano. Durante los últimos siglos se registra un mayor impacto humano en la zona, sobretudo por actividades directas en el ecosistema alpino local no aparentemente afectando a cambios en la vegetación. Después de la Revolución Industrial (IR, en inglés), se registran efectos antrópicos indirectos mientras desaparece el último glaciar in Sierra Nevad

CHAPTER 1

Chapter 1: Introduction

1. Background

In the last few decades the Earth has been affected by rapid global climate change with the increase in temperature mostly related with increasing greenhouse gases (e.g. CO₂, CH₄). Climate predictions estimate that southern Europe will be subjected to the increase in temperature, droughts and fires, affecting the landscapes and the productivity of the cultivated areas and thus societies (IPCC, 2013). Global warming is affecting the environments dramatically, in particular in fragile environments such as mountain and alpine wetlands.

Instrumental climate records show significant climate warming in the northern Hemisphere (Hurrell, 1995) together with an average decreasing trend in precipitation in southern Europe since 1950 (Haylock et al., 2008). This last three decades' decrease in precipitation in the Mediterranean area could be explained due to predominantly positive North Atlantic Oscillation (NAO) modes, being the longest trend during the last century (Bojariu and Gimeno, 2003). Climate models for Europe show that future heat waves will be more intense for this area and intensified by ongoing increase in greenhouse gases (Meehl and Tebaldi, 2004). In addition, projections of future climate change estimated the decrease in precipitation for the Mediterranean region suggesting that this area may be a special vulnerable area to global and climate change “hot-spots” (Giorgi, 2006; Giorgi and Lionello, 2008).

An essential question to answer is how will be the response of vulnerable ecosystems to future climate change. The absence of long-term monitoring data series make necessary the study of paleoclimate records for a better understanding of patterns and future climate response of these ecosystems (Douglas et al., 1994). In addition, a good understanding of large-scales past climate change help us disentangling natural vs. human induced changes on the environment during the rapid climate change events such as the one occurring at Present.

1.1. Quaternary orbital and suborbital-scale climate variability

The attempt to understand climatic evolution during the Quaternary has been the focus of a multitude of paleoclimatic studies in the last decades. Insolation is one of the principal factor affecting long-term cyclic climate change. Its changes are associated to the variations in geometry of the Earth's orbit around the sun (Berger, 1980, 1988). This was first discovered by Milutin Milankovitch, which linked changes in insolation with glacial-interglacial oscillations in the Northern Hemisphere, describing three principal elements of the computation of insolation (Fig. 1): a) eccentricity related with the earth orbit around the sun with a periodicity of approximately 100000 yr, b) obliquity related with the rotation of the earth axis (tilt between 21.5° to 24.5°; seasonality) with a periodicity of around 41000 yr and c) precession of the equinox according to the earth axis of rotation (wobbling motion; seasonality magnitude) with a periodicity of around 22000 yr (Milankovitch, 1941; Berger, 1980; Laskar et al., 2004).

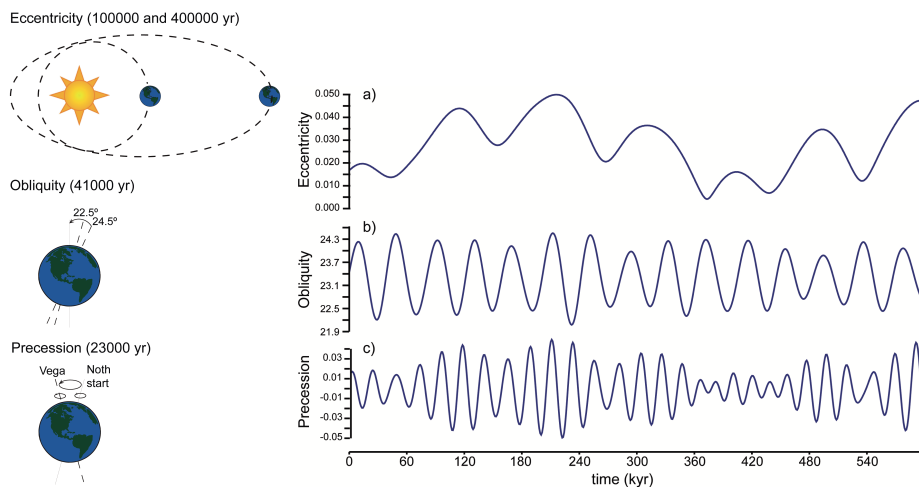


Figure 1. (Left) Scheme of the different parameters postulated by Milankovitch (modified from; <http://www.detectingdesign.com/milankovitch.html>). (Right) Periodicity of the insolation quantified for the Earth during the last 600 kyr: a) Eccentricity, around 100000 yr periodicity, b) Obliquity, around 41000 yr periodicity, c) Precession, around 23000 yr periodicity. The periodicity was calculated based in the (Laskar et al., 2004) method using the Analyseries 2.0 softward (Paillard et al., 1996).

More recently, the high-resolution analysis of ice and marine records have been excellent for the study of climate change during the Quaternary. Variations in the oxygen isotopic composition ($\delta^{18}\text{O}$) and other proxies of ice cores from Greenland drilled in the nineties have played an important role in the study of past climate change during the last four glacial-interglacial cycles (Johnsen et al., 1992; Dansgaard et al., 1993). Subsequently, the analysis of $\delta^{18}\text{O}$ in the calcite shells of benthic foraminifera from marine sediment cores was very useful providing information about ice volume and global temperatures at the time of shell formation. This analysis increased our knowledge about expansions and reductions of the ice sheets and sea level fluctuations in different marine sites in the last million years (Lisiecki and Raymo, 2005) and particularly well-resolved since the last four glacial cycles (Shackleton, 2000; Waelbroeck et al., 2002; Fig. 2).

The Northern hemisphere was also affected by suborbital climate variability at millennial-scales, especially studied during the last glacial period (Dansgaard, 1987; Dansgaard et al., 1993; Cacho et al., 1999; Sánchez Goñi et al., 2002). Although, the cause of these millennial-scale changes are not really well known, they have been noticed through the detailed study of ice core records and marine sediment cores and were named as Dansgaard/Oeschger- (D/O) and Heinrich-like (H) variability (Broecker, 1992; Bond et al., 1993; Grootes et al., 1993; Alley et al., 2000). These events have also been described worldwide implying strong connections between Northern and Southern Hemisphere climates (Ahn and Brook, 2008; Fig.3).

The Mediterranean area have also been shown to be a very sensitive region recording millennial-scale climate variability during the last glacial cycle (D/O and H events), and paleoclimatic records show a strong correlations between vegetation changes, sea surface temperatures and ice sheet fluctuations from Greenland ice cores (Cacho et al., 1999; Sánchez Goñi et al., 2002; Fletcher and Sánchez-Goñi, 2008). This is deduced by the comparison of pollen analysis from marine sediments and SSTs from the western Mediterranean area with terrestrial vegetation records (Padul; southern Iberian Peninsula) and marine isotope stages, demonstrating a strong connection between vegetation and millennial-scale climate variability (Fletcher and Sánchez-Goñi et al., 2008; Fig. 4).

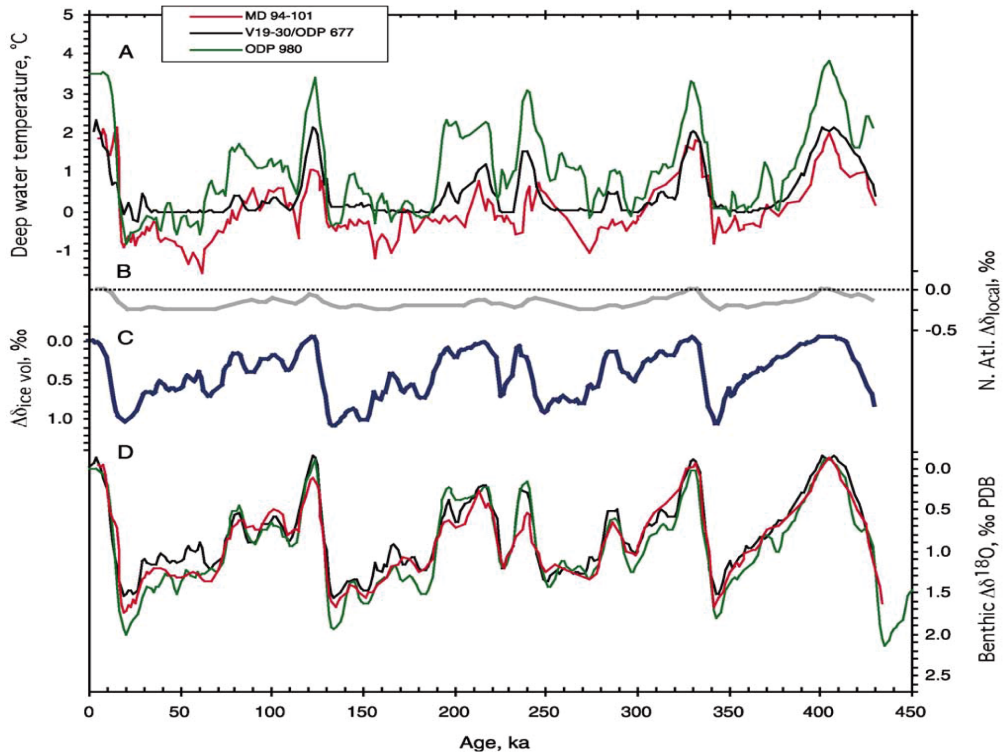


Figure 2. A) Computed deep water temperatures from North Atlantic, S. Indian and Pacific Ocean sites, B) Model variation from N. Atlantic bottom water with respect to present N. Atlantic local bottom water, C) Reconstructed ice volume changes, D) Smoothed $\delta^{18}O$ benthic ratios with respect to Present (same legends than in A). From *Waelbroeck et al., 2002*.

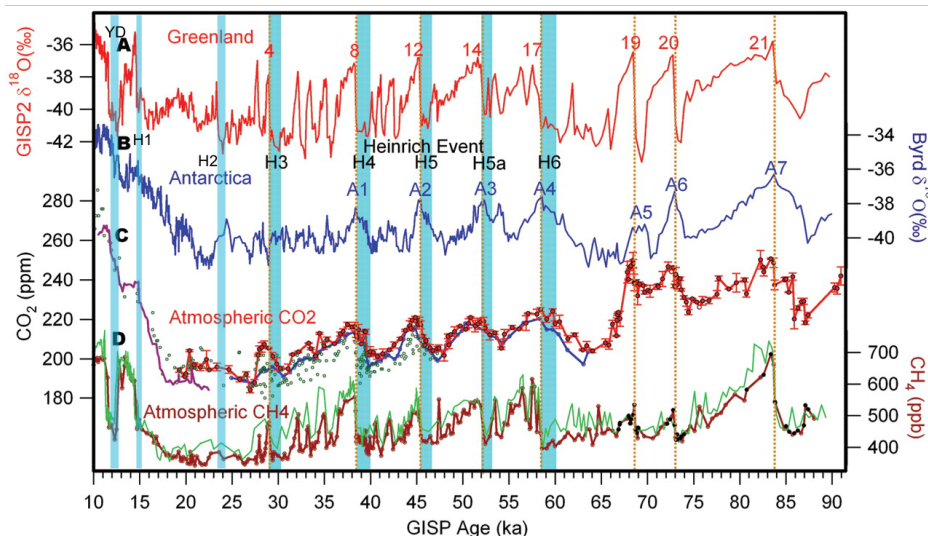


Figure 3. Atmospheric CO₂ composition and climate during the last glacial period. Comparison between: (A) Greenland temperature. Red numbers denote D/O events, (B) Antarctic temperature, (C) Atmospheric CO₂ from an Antarctic record and (D) CH₄ from Greenland (green line) and Antarctic records (brown line). YD = Younger Dryas, H = Heinrich events. Slightly modified From *Ahn and Brook. (2008)*.

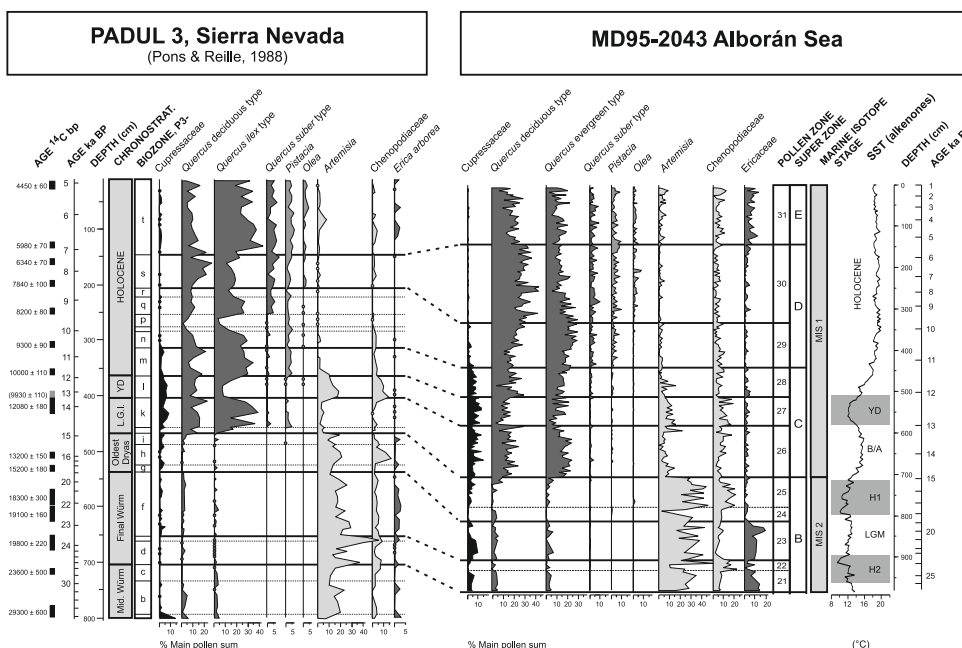


Figure 4 Comparison of pollen record from Padul 3 (Sierra Nevada), and MD95-2043 Alborán Sea. Alkenone SST from Cacho et al. (1999). From *Fletcher and Sánchez-Goñi (2008)*.

1.2. Holocene climate change in the western Mediterranean

Climate has gone through different phases since the last glacial period. This is deduced by many Holocene paleoclimate studies in the northern hemisphere and the western Mediterranean suggesting that climate changed mostly controlled by orbital-scale variability (i.e., precession/insolation mechanism). Studies focusing in the analysis of global climate models shown that the Early Holocene was characterized by wetter conditions around the Mediterranean (Meijer and Tuenter, 2007). Jalut et al. (2009), in a circum-Mediterranean synthesis study, show three different climatic phases through the Holocene, describing an Early humid Holocene (from 11.5 to 7 cal ka BP), a transition phase (from 7 to 5.5 cal ka BP) and a Late Holocene characterized by an aridification process (from 5.5 to Present). Recent data support this hypothesis, showing a Middle Holocene climate transition around 6 ka BP in the western Mediterranean (Carrión et al., 2010a; Anderson et al., 2011; Roberts et al., 2011; Fletcher et al., 2013). Identifying and constraining the timing of the Holocene humidity optimum and the Middle Holocene climate transition have been the focus of recent studies, however, no consensus has been reached regarding this matter and different ages are given for these climatic transitions in the Mediterranean. For example, Magny et al. (2011) show contrasting patterns between paleohydrological records from north-south and east-western Mediterranean. Roberts et al., (2011) also observed that precipitation in the eastern Mediterranean started to decline previously than in the western Mediterranean. Other studies focusing in this latitudinal and longitudinal climatic differences suggested that contrasting seasonal patterns of precipitations may be explained by differences between paleoclimatic records depending on the proxy used to reconstruct climate variabilities (Magny et al., 2012). A higher consensus exists about the Late Holocene aridification process and the shift in oceanic and atmospheric dynamics in the western Mediterranean (Fletcher and Sánchez-Goñi, 2008; Combourieu-Nebout et al., 2009; Carrión et al., 2010a; Anderson et al., 2011; Jiménez-Moreno and Anderson, 2012; Pérez-Sanz et al., 2013; Aranbarri et al., 2014; Jiménez-Espejo et al., 2014; Jiménez-Moreno et al., 2015). However, the aridification process in the Mediterranean region occurred together

with the expansion of human activities in this area (Jalut et al., 2000; Roberts et al., 2011) and separating the main forcing directing environmental change within the Late Holocene period is still unclear. Some authors suggest that carrying out multi-proxy analysis in these records, comparing primary climate sources (e.g. lake and cave isotopes) with pollen or microcharcoal particles, which could be better indicating the environmental response to human impact, could be a good tool in order to clarify this matter (Roberts et al., 2011).

Millennial-scale climatic variability are also observed in paleoclimatic records through shifts between warm-cold and humid-dry periods during the Holocene, modulating the previously mentioned long-term trends (e.g. Combourieu-Nebout et al., 2009; Fletcher et al., 2010). These studies show that this short-scale variability is thus not unique of the last glacial period and also occurred during the currently interglacial epoch (deMenocal et al., 2000; Bond et al., 2001; Mayewski et al., 2004). According to (Bond et al., 1997), Holocene millennial-scale climate shifts (with a cyclicity of $\sim 1470 \pm 500$ yr) observed in the North Atlantic records, would be caused by the same forcing that produced the abrupt shifts (i.e., D-O variability) detected during the last glaciation in the ice core records. Posteriorly, other study suggested that solar forcing (solar irradiance), with a cyclicity of around ~ 1500 yr period, controls these fluctuations in climate, at least during the Holocene (Bond et al., 2001). Other studies related this periodicities with oceanic oscillations (Schulz et al., 2007; Denton and Broecker, 2008). Mayewski et al. (2004) also related these millennial-scale climatic changes with solar activity (Stuiver et al., 1998). Furthermore, Fletcher and Zielhofer (2013) associated some of these millennial-scale climatic oscillations with solar irradiance, reconstruction based on ice core ^{10}Be (Steinilber et al., 2009). In the last few years, a study of non-stationary times series detected a shift in the periodicity of these cyclical climatic changes around the Middle Holocene, with a predominant ~ 1000 yr cycle for the Early Holocene (and ~ 2500 yr for the entire Holocene), and a ~ 1500 yr periodicity for the second part of the Holocene, showing also a change from mostly insolation (external) forcing to oceanic (internal) forcing (Debret et al., 2007, 2009). Fletcher et al. (2013) studied a marine record from the Alboran sea and also detected this climatic shift, with a change in the periodicity

around the Middle Holocene transition at ~6 cal ka BP, suggesting the establishment of the actual climate system (mainly controlled by the NAO) since this time. A more recent paleoclimatic study in the western Mediterranean show that decreases in rainfall are associated with cool episodes during the Early Holocene, while during the end of the African Humid Period (~5 ka) and the establishment of the NAO present-day system, a change in climatic forcing occurred, relating coolings with winter rain maxima associated with solar minima. This study also show millennial- to centennial-scale decrease in western Mediterranean winter rain (Zielhofer et al., 2017). Jalut et al. (2000) also described millneial-scale aridification phases for the western Mediterranean region ralted with North Atlantic records. Some arid events around ~9.6-9.5, 8.4-8 and 6-5.5, have also been identified as arid and cool events in a study from the eastern and western Mediterranean region (Dormoy et al., 2009). These studies show specially arid events co-occurring in different sites in the Mediterranean associated with North Atlantic cooling events, which point to a reginal climate variability response to global-scale climate variability.

Currently, climate in the North Atlantic and in the western Mediterranean region is strongly influenced by the NAO, which is mostly managed by the difference of pressures between the Azores (high) and Icelandic (low) controlling the latitudinal situation of the winter storm track (Visbeck et al., 2001). The NAO is considered as one of the mechanism that modulate the climate at interannual and decadal-scale and during positive NAO phases, higher differences in pressures are predominant between the Azores and Icelandic producing drier and colder conditions over the Mediterranean region while wetter and warmer conditions occur over northern Europe (Visbeck et al., 2001), and inversely during negative NAO conditions (Fig. 5). In the last years an effort has been made to reconstruct long sequences of past NAO conditions (Trouet et al., 2009; Olsen et al., 2012; Baker et al., 2015) and past NAO variations seem to have a very strong influence on climate in the northern hemisphere, affecting the oceanic overturning circulation and Artic sea-ice distribution (Seierstad and Bader, 2009; Strong et al., 2009). In this respect, evidences of moisture cycles in southern Iberian Peninsula, such as during the Iberian-Roman Humid Period (IRHP), have been associated with persistent negative NAO conditions

(Martín-Puertas et al., 2009). Trouet et al. (2009) carried out a multi-decadal NAO reconstruction for the last ~940 yr, finding centennial-scale climatic variability, such as a persistent positive NAO phase during the Medieval Climate Anomaly (MCA) with a change to negative NAO conditions into the Little Ice Age (LIA). This shift could be associated with a global climate transition probably related with intensified Atlantic meridional overturning circulation (AMOC) during the MCA. Subsequently, a longer NAO reconstruction of the last 5200 yr, showed a shift from persistent positive NAO to intermittent conditions around 4500 and 650 yr ago (Olsen et al., 2012).

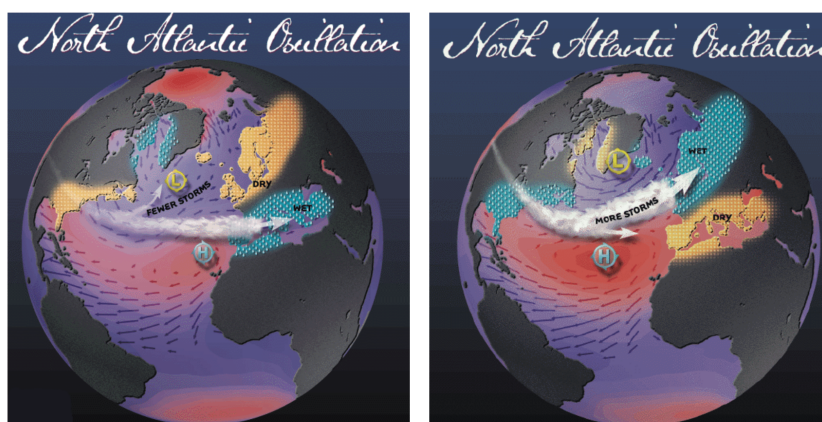


Figure 5. Scheme of the North Atlantic Oscillation (NAO) variability and its influence in the northern Hemisphere climate. To the left negative NAO conditions. To the right positive NAO conditions. From: <http://www.ldeo.columbia.edu/NAO> by *Martin Visbeck*.

1.3. Climate change in the Iberian Peninsula during the Holocene

The Iberian Peninsula constitute an interesting area for the study of paleoenvironmental, paleoclimatic and human impact due to the complexity in geological, geographical and historical cultures (Carrión et al., 2010b). A multitude of Holocene paleoclimate records have been carried out in northern and central Iberia at millennial and centennial-scale resolution (González-Sampériz et al., 2006; Lebreiro et al., 2006; Gil García et al., 2007; Moreno et al., 2008, 2012, Morellón et al., 2009, 2011; Corella et al., 2013; Pérez-Sanz et al., 2013; Aranbarri et al., 2014).

Sediment cores from numerous lakes and bog environments from southern Iberian Peninsula and adjacent areas, such as marine sites from the Alboran Sea and continental records from North Africa have been studied with the objective of characterizing climate variability during the Holocene, showing most of them long-term trends and millennial-scale climate variability (Florschütz et al., 1971; Pons and Reille, 1988; Lamb and van der Kaars, 1995; Reed et al., 2001; Carrión, 2002; Carrión et al., 2001a, 2010a, 2003, 2007; Ortiz et al., 2004; Martín-Puertas et al., 2008, 2011; Gil-Romera et al., 2010; Anderson et al., 2011; Jiménez-Moreno and Anderson, 2012; García-Alix et al., 2012a, 2013; Fletcher et al., 2013; Fletcher and Zielhofer, 2013; Aranbarri et al., 2014; Jiménez-Espejo et al., 2014; Jiménez-Moreno et al., 2015; Zielhofer et al., 2017). However, a multidisciplinary and multi-proxy analysis at centennial-scale resolution for the Holocene of southern Iberia including a time series analysis has never been performed.

The earliest Holocene in southern Europe and the Mediterranean is described as a warming period characterized by an open woodland (Fig. 6). However, paleoenvironmental reconstructions show different patterns along the Iberian Peninsula. In the northeastern part of the Iberian Peninsula, in inner continental regions, cool and arid conditions occurred, marked by a higher representation of steppe (Sánchez-Goñi and Hannon, 1999; Aranbarri et al., 2014) and conifer forest (e.g. Pérez-Sanz et al., 2013; Aranbarri et al., 2014), as well as, lower lake levels that can be attributed to the increase in summer temperatures and higher evaporation rates (Morellón et al., 2011; Aranbarri et al., 2014). In the southeastern part of Iberia in inner continental areas, the earliest Holocene is also described as a relatively dry period characterized by the occurrence of conifer forests (Carrión and Van Geel, 1999; Carrión et al., 2001a; Carrión, 2002). In the southernmost Iberian Peninsula, an alpine lake record from Sierra Nevada also show xeric conditions and *Pinus* forests occurrence (Anderson et al., 2011).

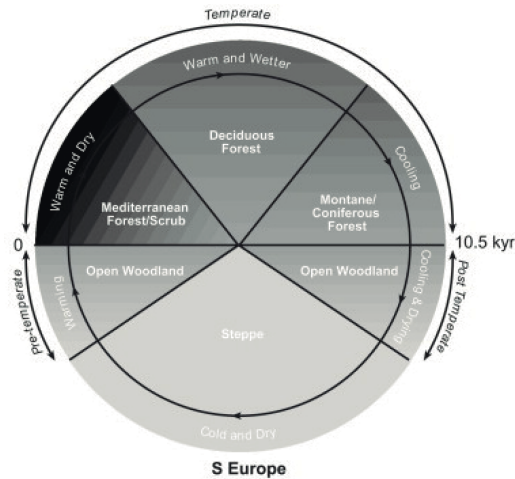


Figure 6. Idealized vegetation phases in southern European sites with sufficient moisture availability. From (Tzedakis, 2007).

Around the second half of the Early Holocene warmer and more humid conditions and the related mesic forest occurred in the eastern and southern part of the Iberian Peninsula although conifer forests still prevailed. In the northeast and mountain areas of the south high values of *Pinus* are recorded (Carrión et al., 2001a; Carrión, 2002; Morellón et al., 2009; Pérez-Sanz et al., 2013; Aranbarri et al., 2014), and higher water levels are depicted in the northeastern region (Morellón et al., 2009; Aranbarri et al., 2014). In the southernmost areas of Iberia, and the nearly Alboran sea and northern Africa, higher values of Mediterranean forest occurred mainly dominated by evergreen *Quercus* (Pons and Reille, 1988; Lamb and van der Kaars, 1995; Fletcher and Sánchez-Goñi, 2008) and increasing deciduous forest (Pons and Reille, 1988; Fletcher and Sánchez-Goñi, 2008). Lake levels in southern Iberia around this period seem to be greater at high altitude (Anderson et al., 2011) and lower at low altitude (Reed et al., 2001). According to Anderson et al. (2011), during the Early Holocene larger difference in seasonality and insolation could be reflect in higher snowpack during winter and snowmelt during summer providing water availability and high lake levels in alpine environments but not necessarily at lower altitudes where higher evaporation rates due to insolation maxima occurred. In the Middle Atlas, (Zielhofer et al., 2017) also indicated higher lake levels at higher altitude during this time.

The Middle Holocene, has been generally described as a period of transition from the humid optimum towards more aridity (Jalut et al., 2009), showing in some areas of the Iberian Peninsula higher moisture than during the Early Holocene (Sánchez-Goñi and Hannon, 1999; Carrión, 2002; González-Sampériz et al., 2006; Pérez-Sanz et al., 2013; Aranbarri et al., 2014). Lake level maximum is also recorded in some sites (Reed et al., 2001; Carrión, 2002; Morellón et al., 2009; Aranbarri et al., 2014), probably due to local lake responses to decreasing summer insolation and decrease in seasonality, favoring the increase in effective moisture (Lamb and van der Kaars, 1995). Carrión et al. (2010a) in a study from southeastern Iberia, described the Middle Holocene as a period of mesic maximum and xeric minimum. In the Sierra Nevada record and the Alboran Sea, the mesic maximum was recorded during the first half of the Middle Holocene and a decrease in mesic arboreal component occurred around ~7 cal ka BP (Pons and Reille, 1988; Combourieu-Nebout et al., 2009; Anderson et al., 2011; Jiménez-Moreno and Anderson, 2012) and alpine lake levels decreased since this time (Anderson et al., 2011; García-Alix et al., 2012a; Jiménez-Moreno and Anderson, 2012). According to Zielhofer et al. (2017), the hydro-climatic conditions differed with the altitude between different vegetation belts in the western Mediterranean. Carrión et al. (2010a), described the vegetation transition process since the Middle Holocene in southern Iberian Peninsula, taking into account the different altitudinal gradient, fire occurrence and human influence (Fig. 7).

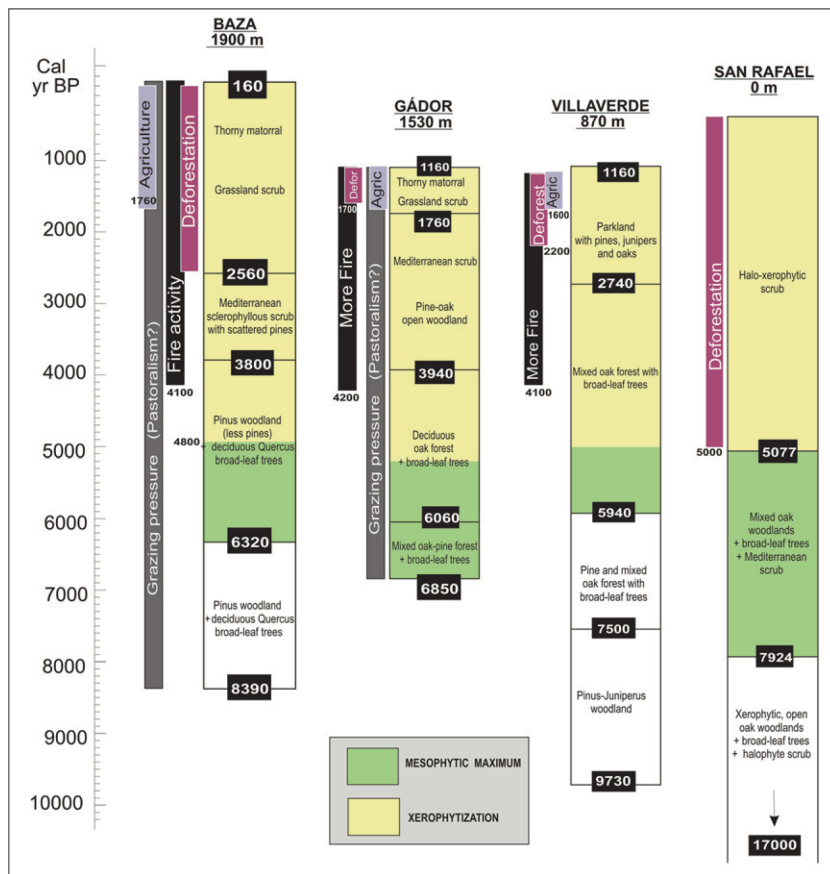


Figure 7. Comparison of Holocene vegetation patterns from four important pollen sequences from southeastern Spain from high to littoral elevation. Showing the xerophytization process, modulated by fire occurrence and suggesting human influence. From (Carrión et al., 2010a).

The aridification process recorded in the western Mediterranean between the Middle Holocene transition and the Late Holocene has been identified at different times depending on latitude, altitudinal gradient, as well as, the masking effect of human impact, which increased considerably in the last millennia (Jalut et al., 2000; Carrión et al., 2007, 2010a; Roberts et al., 2011; Sadori et al., 2011). The Late Holocene period has been described in southern Europe as characterized by a progressive cooling after the warm and humid previous phase of the Early and Middle Holocene (Fig. 6). In inner continental areas of northeastern Iberia it was associated with regression of mesic component and the increase in *Pinus* and lower lake levels (Pérez-Sanz et al., 2013; Aranbarri et al., 2014). On the contrary, expansion of scrubs and

xeric components occurred in the lowlands and littoral areas in southern Iberia. For instance, an increase in herbs during the last ~5.5 cal ka BP is described in southern lowland areas, at the same time that a gradual sediment infilling of the lake (Reed et al., 2001). Jiménez-Moreno et al. (2015) also described this aridification process with the expansion of semi-desert vegetation during the Late Holocene, in a study from the Doñana National Park in southern Spain. A decrease in lake levels, an increase in xeric vegetation and an increase in Saharan dust is also observed during the Late Holocene in the alpine areas of Sierra Nevada (Anderson et al., 2011; Jiménez-Moreno and Anderson, 2012; Jiménez-Moreno et al., 2013a). In the Middle Atlas region, the Late Holocene was characterized by the replacement of *Quercus* forest by *Cedrus atlantica*, being this interpreted as due to the decrease in summer insolation and increasing effective moisture during summer. This is supported in the area by recorded higher lake (Lamb and van der Kaars, 1995). Some authors suggest, that the link between forest decline and the expansion of scrubs and xeric vegetation in southern Iberia and the nearly Alboran Sea have been associated with the natural orbital process of decrease in summer insolation (Jiménez-Moreno and Anderson, 2012; Fletcher et al., 2013; Jiménez-Moreno et al., 2015; Fig. 8), agreeing with the assumption of climate as the main forcing directing this aridification process in the western Mediterranean (Magny et al., 2002, 2012).

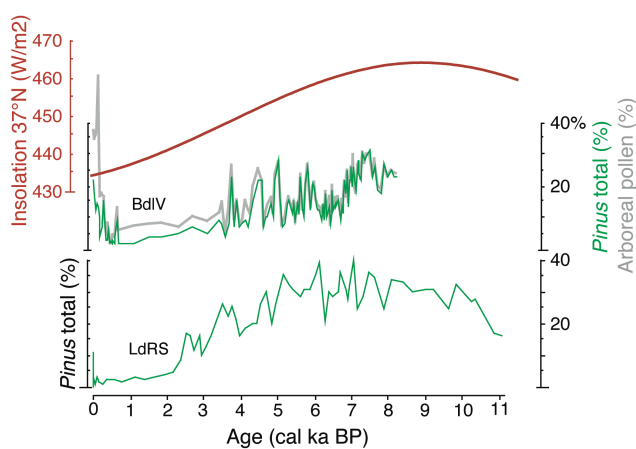


Figure 8. Comparison of *Pinus* and Arboreal pollen percentage from Sierra Nevada records [Laguna de Rio Seco (LdRS) and Borreguil de la Virgen (BdlV)] and summer insolation at 37° N. Modified from Jiménez-Moreno and Anderson (2012).

1.4. Human impact in the southern Iberian Peninsula and Sierra Nevada

The Mediterranean area has had a long history of civilization settlements and land uses during the Holocene being the different civilizations also very dependant of climatic changes (Mercuri et al., 2011). In southern Iberia and the western Mediterranean, abrupt climate changes have been identified in continental and marine paleoclimatic records and have been associated with atmospheric, oceanic and solar dynamics (see above). It is well-known that these abrupt fluctuations have been the detonating of the collapse and proliferation of societies in areas sensitives to climatic change such as arid and semi-arid regions (Carrión et al., 2007; González-Sampériz et al., 2009). Jalut et al. (2009) suggested, societies had to adapt to natural environment variations, being the climatic change determinant in the semiarid Mediterranean biome.

Human occupation in the Iberian Peninsula has been relevant since prehistorical times and the study of societies and anthropogenic impact has been the focus of a multitude of analyses during the last decade (e.g. Jiménez-Espejo et al., 2007; Carrión et al., 2007, 2010a; González-Sampériz et al., 2009; Cortés Sánchez et al., 2012; García-Alix et al., 2013; López-Sáez et al., 2014; Lillios et al., 2016). Most of these studies in southern Iberia have focused in the exploration of climatic periods related with societies since the Middle Holocene, the moment in which is appreciated a higher evidence of human settlements in the western Mediterranean (Roberts et al., 2011). According to Carrión et al. (2010a), humans have been shaping the environment in southern Iberia since the Middle Holocene, with grazing, agricultural activities, mining, coppicing, slash and burn, concluding that is difficult to unravel how much humans contributes to this modification in the landscape. A record from southern Iberia suggests a decrease in arboreal and the infilling of the lake related with anthropogenic impact since the last ~3.4 cal ka BP (Reed et al., 2001). Anthropogenic impact related with lead pollution has been described in southern Spain and the Alboran Sea, finding Pb anomalies since the end of the Bronze Age (Martín-Puertas et al., 2010). García-Alix et al. (2013) also detected lead pollution in alpine lake sediments from Sierra Nevada since ~3.9 cal ka BP, probably caused by

metallurgical activities at lower elevations, being lead pollution especially important during the Late Bronze Age (from ~3.5 to 2.8 cal ka BP; Fig. 9). Increase in charcoal since ~4 cal ka BP has also been recorded in southern Spain from Sierra de Baza and Sierra Nevada archives, related with increase in aridity but could be also due to human induced burning as the evidences of pasturing or agricultural activities seem to start to be recorded also during this period (Carrión et al., 2007; Anderson et al., 2011; Fig. 9). Jiménez-Moreno et al. (2013a), concluded that in the southeastern Iberian Peninsula the increase in fire frequency in the Late Holocene could be due to both factors climate and human influence.

Nevertheless, human presence only became more evident in the Sierra Nevada alpine ecosystems during the last millennia. This is probably due to the remote location of this area (Anderson et al., 2011; Jiménez-Moreno and Anderson, 2012; Fig. 10). Other important human-related feature of the Sierra Nevada paleoenvironmental studies is the record of *Olea* cultivation, which seems to start several hundred years earlier (since ~2.7 cal ka BP) than the Roman occupation of the Iberian Peninsula. However, the strongest increase in this taxon began in the last centuries, coinciding with the increase in oil production in southern Spain. In addition, an increase in *Pinus* is also recorded during the last century, which is most likely due to reforestation in the last decades to combat erosion (Anderson et al., 2011).

Finally, it is of important interest to remark that some proxies used to disentangle natural versus anthropic effects such as the fire frequency, need to be taken carefully as fires have been recognized as a natural disturbance phenomenon in Mediterranean ecosystems (Gil-Romera et al., 2010). According to Riera et al. (2004), differentiating human and natural impact in the environment could be only unraveled by multi-proxy analysis.

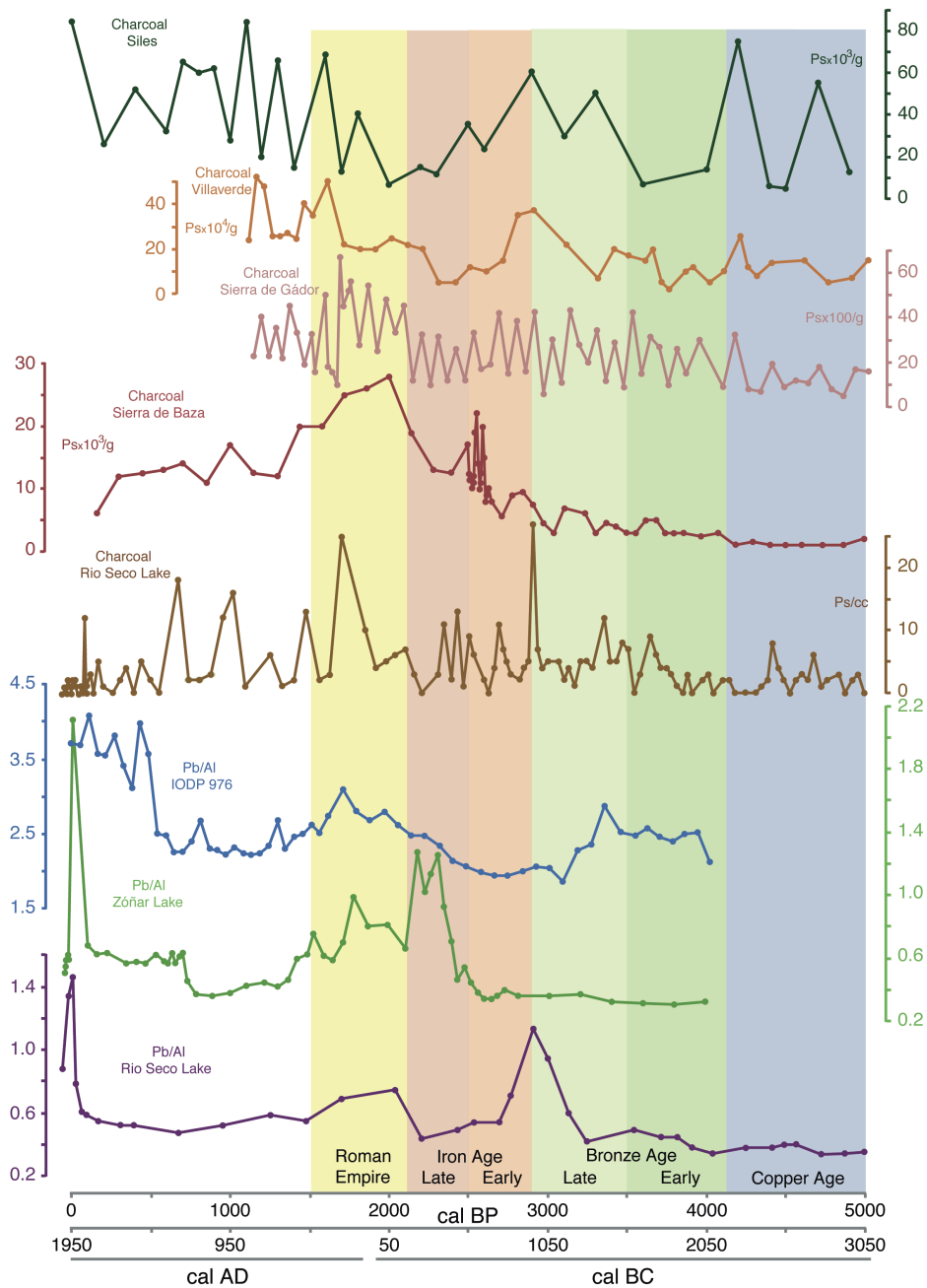


Figure 9. Pb/Al rate comparison from Riso Seco (Sierra Nevada), Zóñar Lake and Alboran Sea and charcoal comparison between Sierra Nevada, Sierra de Baza, Sierra de Gádor, Villaverde and Siles. From *García-Alix et al., 2013*.

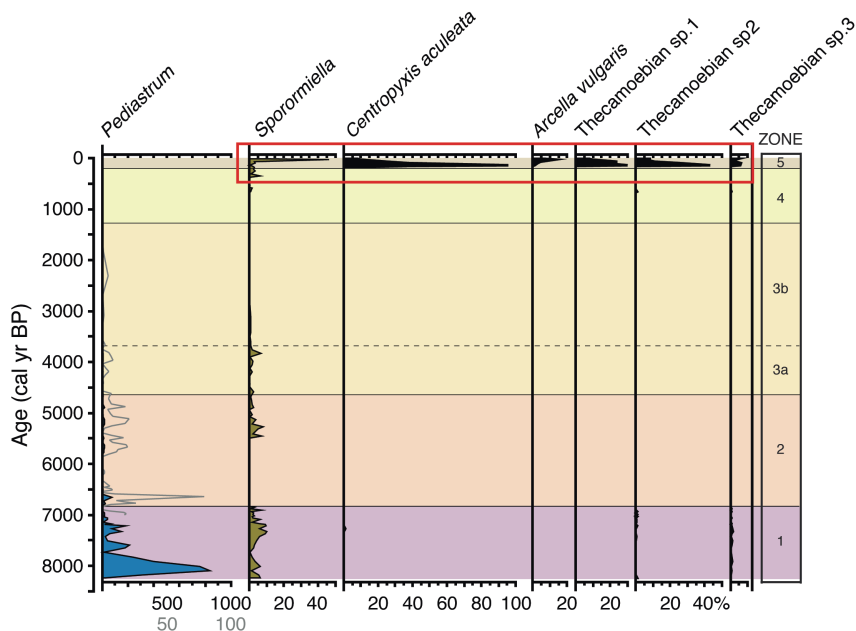


Figure 10. Algae, spores and thecamoebians from the Borreguil de la Virgen record (Sierra Nevada) showing the increase in proxies probably related with the introduction of livestock in this alpine area in the last centuries. Slightly modified from *Jiménez-Moreno and Anderson (2012)*.

1.5. The importance of multi-proxy analysis in lakes, peat bogs/wetlands for the reconstruction of past climate change and human impact

The study of past climate change using paleoclimate archives such as lake sediments is necessary in the absence of long term climatic and environmental monitoring data (e.g. Smol et al., 2005). Dating techniques of the sediment strata and the study of multi-proxy analyses (e.g. pollen, charcoal, geochemistry organic and inorganic, physical properties, macroscopic biological remains) allow the paleoenvironmental and climate reconstruction of these systems during the Quaternary (e.g., Wick et al., 2003). In these studies, pollen, non-pollen palynomorphs (NPP) and charcoal grains can provide with information about the evolution of the nearby vegetation of lake and wetlands ecosystems and human impact since thousands of years (Anderson, 1990; Whitlock and Anderson, 2003). Sedimentary changes through physical and geochemical signals could indicate hydrological variability in the lake system (e.g. precipitation or evaporation,

elemental geochemical composition, organic composition of the sediments) helping with the reconstruction of the lake level variability and/or changes in the sedimentary input (Magny et al., 2003, 2007; Morellón et al., 2011). Another important issue of many paleolimnological and peat deposit reconstructions is identifying the source of the organic matter from the catchment area of the study site (Meyers, 1994; Ficken et al., 2000; Meyers, 2003). All these paleoenvironmental variabilities could be affected by anthropogenic impact during the last several millennia. Recent studies in the Mediterranean, an area intensively occupied since historical times, demonstrated that the use of multi-proxy analysis is necessary in order to distinguish between climate and humans affecting the environments in the past (Roberts et al., 2011).

2. Hypothesis and objectives

2.1. Hypothesis

Future climate projections for the for southern Iberian Peninsula forecast an increase in temperature and a decrease in precipitation (specially during the warm season) (Giorgi and Lionello, 2008). This climatic change will have profound consequences in the environment (i.e., biodiversity losses) as well as in the economy (i.e., bad harvest, soil degradation) and society (very dependent on water supply) in this arid area (Sardans and Peñuelas, 2004). It is then extremely important to study past environmental responses to climate change in times when climate was warmer and drier than at present in order to predict the response of the environments to these changes.

Sierra Nevada (southern Iberia Peninsula) is a very sensitive area with respect to climate change, as it is located near the boundary between temperate (humid) and subtropical (arid) climates in the Mediterranean region (Alpert et al., 2006). It is also one of the tallest (highest peaks in the Iberian Peninsula) and longest mountain range in the Iberian Peninsula and the southernmost areas to be glaciated during the Late Pleistocene in Europe. Therefore, its present-day landscape was intensely influenced by glacial erosion during the coldest phases of the Pleistocene (Schulte, 2002). In addition, Sierra Nevada contains one of the highest plant diversity in the western Mediterranean region (Blanca, 2001). These features make Sierra Nevada very vulnerable to future climate change and thus very interesting from a paleoenvironmental point of view. Several studies have previously been performed in the Sierra Nevada alpine lakes and bogs (Anderson et al., 2011; Jiménez-Moreno and Anderson, 2012; García-Alix et al., 2012a, 2013; Jiménez-Moreno et al., 2013a; Jiménez-Espejo et al., 2014), which aroused the interest for the study of longer records in which it would be possible to analyze past climatic changes during periods with similar climatic conditions or even warmer than at present. In this regard, the well-known Padul wetland site, located at the western foot of the Sierra Nevada, bears one of the longest continental records in southern Europe, with a sedimentary sequence of ca. 100 m thick that could represent the last 1 Ma. However, the Late

Holocene was never recorded and never studied in these previous analysis (Florschütz et al., 1971; Pons and Reille, 1988; Ortiz et al., 2004), being probably the part of the sequence most influenced by human activities and that could provide information about the main forcing driving environmental change in the Sierra Nevada ecosystems.

Despite being a very interesting study area, Sierra Nevada is one of the regions of southern Europe with fewer studies dealing with natural and anthropogenic climate change. Alpine ecosystems located above the treeline are very suitable areas for the study of global change because they are remote and not so altered by human influence (Battarbee et al., 2002), making the comparison with lower elevation montane ecosystem as Padul, possibly involved in a higher human influence since historical times, very interesting. The consequences of anthropic effects in the natural climate system are still unknown for this area, so, deeper studies are needed to attempt to quantify the human impact in the current climate development. It is of great interest to study past warmer and/or drier periods than present, when humans were not impacting the ecosystems, to compare with present-day patterns and separate the effect of the two (natural vs. human) signals on the environments. The comprehension of these past climate changes is the key to provide information, as far as possible, for future climate scenarios and climate models in order to analyze the effect of global change in the Sierra Nevada ecosystems and the western Mediterranean. Consequently, the study proposed in this PhD thesis, with the study of Holocene climate change and human influence in Sierra Nevada ecosystems at high and low elevations, will help increasing the information available so far about these matters.

2.2. Objectives

The main objective of the present thesis is to describe the Holocene environmental and vegetation history related with climate variability and human impact in the southern Iberian Peninsula throughout the study of the fossil record and physical-chemical properties recorded in the sediments of wetlands and lakes in Sierra Nevada.

Under this framework, the principal goals for the current PhD thesis were arranged as follows:

1. To determine the chronology and paleoenvironmental variabilities from two different altitude sedimentary records from Sierra Nevada during the Holocene, with the support of AMS radiocarbon dates and a multi-proxy analysis of pollen, charcoal, lithological, sedimentological, physical and geochemical properties.
2. To understand the mechanism of Mediterranean climate and vegetation development, with the objective of understanding how the Sierra Nevada ecosystems respond to climate change.
3. To compare the results obtained for the multi-proxy analysis at orbital and suborbital-scale from Sierra Nevada with other regional and global paleoclimate records, with the objective of understanding the links between atmospheric, oceanic and solar dynamics and their influence on the western Mediterranean ecosystems.
4. To disentangle the principal forcing (i.e. natural vs human) driving vegetation and environmental change during the Late Holocene in Sierra Nevada.
5. To determine human activities and the indirect/direct effects of human impact during the last centuries in the Sierra Nevada alpine ecosystems.

Learning and performing multidisciplinary laboratory techniques, carried out over a great number of samples, were also supplementary objectives for this PhD study. Drilling in the Padul wetland (43 m of sedimentary sequence), sampling for diverse proxies, lithological description, sample preparation for the measurement of the elemental analysis of carbon/nitrogen/hydrogen/sulfur (CNHS), palynological treatment and identification, were carried out at the University of Granada. X-ray fluorescence analysis were measured throughout a stay at the University of Barcelona. Charcoal treatment and identification were completed during a stay in the Northern Arizona University. Sample preparation and analysis of biomarker were realized while a stay in the German Research Center for Geoscience (GFZ).

3. Regional settings

Sierra Nevada is a W-E aligned mountain range situated in the internal zone of the Betic Range (southern Iberia; Fig. 11). Sierra Nevada has an elevation range between approximately ~900 to more than 3400 m, which includes the three highest peaks in the Iberian Peninsula, Mulhacen (3479 m asl), Veleta (3396 m asl) and Alcazaba (3366 m asl). Previous studies suggest that this was the southernmost European area to be glaciated during the last glacial period, however, the Early Holocene is not well dated and the exact chronology is unknown (Schulte, 2002). Within the Sierra Nevada mountain range, the Veleta cirque was the southernmost glaciated area during the LIA, making this area the most interesting place in southern Spain for the study of glacier shifts (Schulte, 2002). Melting during deglaciation generated glacier cirque basins that allowed the formation of small lakes and posteriorly bogs (“borreguiles”) during warmer periods like the Holocene (Castillo Martín, 2009).

The Sierra Nevada mountain range is formed by three main complexes characterized by different metamorphic facies: the Maláguide, the Alpujárride and the Nevado-Filábride. The area of study is located within the influence of the Alpujárride and the Nevado-Filábride complex. The Nevado-Filábride complex at higher elevations is characterized by Paleozoic siliceous metamorphic rocks (mostly mica-schists and quartzites) and the Alpujárride complex, situated at lower elevations, is mostly featured by Triassic dolomites and limestones (Sanz de Galdeano et al., 1998).

The regional climate in the Mediterranean region is principally affected by the NAO (Lionello and Sanna, 2005). Sierra Nevada is influenced by Mediterranean thermal effect (with cold and humid winters and hot and drier summers) because the nearby location to the Mediterranean Sea (Gómez-Ortiz et al., 2004). The annual mean precipitation at 2500 m of elevation is approximately 700 mm and the temperature ~4.5 °C (Oliva et al., 2009). At lower elevations in the adjacent Granada basin at ~700 m of elevation, mean annual precipitation and temperature are around 445 mm and 14.4 °C, respectively (www.aemet.es). According to elevation,

conditioning temperature and precipitation, Sierra Nevada is divided in different vegetation belts, which are strongly influenced by this large altitudinal gradient (Table 1).

Sierra Nevada is considered one of the most important biodiversity centers in the western Mediterranean region and is characterized by a higher number of endemism (Blanca, 1996). During the Quaternary glacial periods tundra and alpine species coming from central and northern Europe were refuged in Sierra Nevada, at the end of the last glacial period and the transition to the Holocene many of this species were “trapped” on the summits of Sierra Nevada (Hernández Bermejo and Shinz Ollero, 1984). Sierra Nevada also contain a considerable number of Tertiary relict species, which got protected in valleys subjected to thermal protection and/or constant water supply (Blanca, 1996). This highest elevation environments from Sierra Nevada were declared a part of the UNESCO Biosphere Reserve in 1986, Natural Park in 1989 and National Park in 1999 (Gómez-Ortiz et al., 2004).

Table 1. Modern vegetation in the different Sierra Nevada vegetation belts. From *Jiménez-Moreno et al. (2013a)*.

Vegetation belt	Elevation (m)	Most characteristic taxa
Crioromediterranean	>2800	<i>Festuca clementei</i> , <i>Hormatophylla purpurea</i> , <i>Erigeron frigidus</i> , <i>Saxifraga nevadensis</i> , <i>Viola crassiuscula</i> , and <i>Linaria glacialis</i>
Oromediterranean	1900 –2800	<i>Pinus sylvestris</i> , <i>P. nigra</i> , <i>Juniperus hemisphaerica</i> , <i>J. sabina</i> , <i>J. communis</i> subsp. <i>nana</i> , <i>Genista versicolor</i> , <i>Cytisus oromediterraneus</i> , <i>Hormatophylla spinosa</i> , <i>Prunus prostrata</i> , <i>Deschampsia iberica</i> and <i>Astragalus sempervirens</i> subsp. <i>nevadensis</i>
Supramediterranean	1400 –1900	<i>Quercus pyrenaica</i> , <i>Q. faginea</i> , <i>Q. rotundifolia</i> , <i>Acer opalus</i> subsp. <i>granatense</i> , <i>Fraxinus angustifolia</i> , <i>Sorbus torminalis</i> , <i>Adenocarpus decorticans</i> , <i>Helleborus foetidus</i> , <i>Daphne gnidium</i> , <i>Clematis flammula</i> , <i>Cistus laurifolius</i> , <i>Berberis hispanicus</i> , <i>Festuca scariosa</i> and <i>Artemisia glutinosa</i>
Mesomediterranean	600 –1400	<i>Quercus rotundifolia</i> , <i>Retama sphaerocarpa</i> , <i>Paeonia coriacea</i> , <i>Juniperus oxycedrus</i> , <i>Rubia peregrina</i> , <i>Asparagus acutifolius</i> , <i>D. gnidium</i> , <i>Ulex parvi florus</i> , <i>Genista umbellata</i> , <i>Cistus albidus</i> and <i>C. lauri flolius</i>

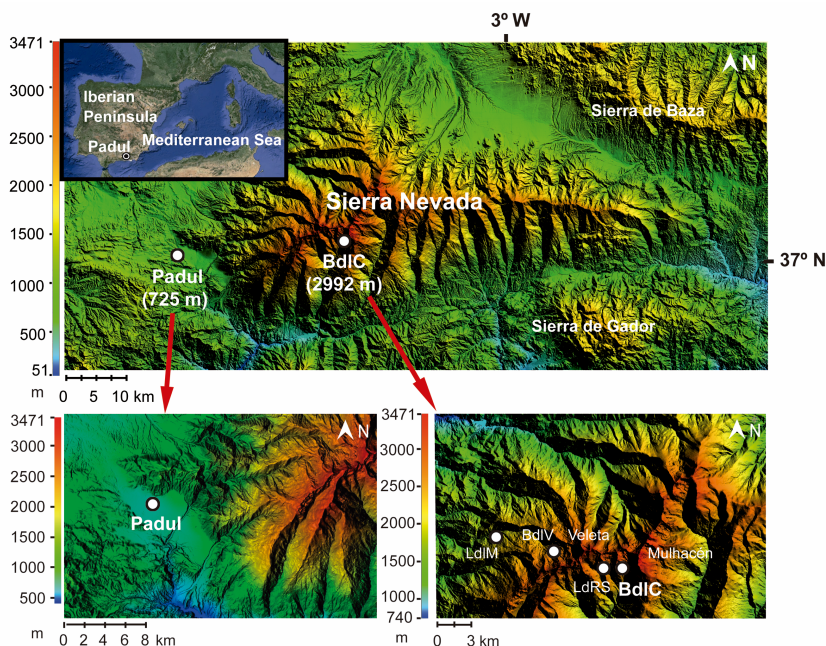


Figure 11. (Above) Location of Sierra Nevada (southern Iberia) in the western Mediterranean region. (Below to the left) Location of Padul wetland area in the mesomediterranean vegetation belt and Borreguil de la Caldera (BdlC) to the right Sierra Nevada alpine area. Sierra Nevada maps were performed using the GIS software Global Mapper and modified with Adobe Illustrator.

The sites studied during this PhD thesis are two sedimentary basins located at different altitudes in Sierra Nevada:

3.1. Borreguil de la Caldera

Borreguil de la Caldera (BdlC), is located in the Sierra Nevada range at ca. 2992 masl in the Nevado-Filabride complex (Fig. 11). This high-elevation peat bog has an area of around ~0.17 hectares and the catchment basin is around ~62 hectares, and is situated in the south facing glacially eroded Poqueira River Valley. This bog is located just below Laguna de la Caldera, a glacier cirque lake basin enclosed in the upper drainage part of the Mulhacén river. The studied bog is located within the crioromediterranean vegetation belt, which is mainly non-vegetated, being the vegetation limited to the water courses and peat bogs and characterized by tundra-like vegetation and mainly featured as the most representative species by grasses and

Cyperaceae (Fig. 12). Around this peat bog other plant species occur, such as *Armeria splendens*, *Agrostis nevadensis*, *Ranunculus acetosellifolius*, *Plantago nivalis* and *Lepidium stylatum* (Molero-Mesa et al., 1992). The altitudinal gradient, and the biogeographical location of Sierra Nevada between Europe and Africa make Sierra Nevada unique with respect to fauna and flora, with a considerable number of endemic plants (e.g. *Erigeron frigidus*, *Saxifraga nevadensis*, *Viola crassiuscula*, *Plantago nivalis*; *Artemisia granatensis*; Fig. 12). The plant and algae growth in these areas is limited to the snow-free season that occur normally between July and October.



Figure 12. (Above) Present-day vegetation (mainly Cyperaceae) covering the Borreguil de la Caldera (BdlC) bog. (Below) Secondary plant species represented in the BdlC and surroundings. On the left *Gentiana* sp. and on the right, *Erigeron frigidus* (endemic plant from Sierra Nevada).

3.2. *Padul*

The Padul wetland, located at ~725 m asl, is a basin area of around 45 km², at the foothill of the southwestern Sierra Nevada (Andalusia, Spain; Fig. 11). It is located in the northeastern area of the Lecrin Valley, around 20 km south of Granada city. Padul is a small extensional basin approximately 12 km long, which is bounded by the Padul normal fault, located in an endorheic and asymmetric basin surrounding by the Albuñuelas and Manar ranges (Ortiz et al., 2004). This is one of the most seismically active areas in southern Iberian Peninsula, with numerous faults in NW-SE direction, with the Padul fault being one of these active normal faults (Alfaro et al., 2001). The basin fill is asymmetric, with thicker sedimentary and peat infill to the northeast (~100 m thick; Florschütz et al., 1971; Domingo-García et al., 1983; Nestares and Torres, 1997) and progressively becoming thinner to the southwest (Alfaro et al., 2001). Depending on the distance from the fault, previous cores taken in the Padul peat bog showed different thickness and sedimentation ranges (Menéndez Amor and Florschütz, 1964; Florschütz et al., 1971; Pons and Reille, 1988; Ortiz et al., 2004). In this sense, the Padul contains one of the best Pleistocene continental sedimentary records found in southern Europe and we know from previous studies that it contains a record of the last ~1 Ma (Ortiz et al., 2004). The sedimentary in-filling of the basin consists of Neogene and Quaternary deposits; Upper Miocene conglomerates, calcarenites and marls, and Pliocene and Quaternary alluvial sediments, lacustrine and peat bog deposits (Domingo-García et al., 1983; Sanz de Galdeano et al., 1998; Delgado et al., 2002).

The Padul area is one of the most important wetlands in the southeast part of Iberia. This wetland is protected as a reserve area within the Sierra Nevada Natural Park, included in the Inventory of Natural Parks of Andalucía since 1989, in the wetland inventory since 2004 and considered in the Ramsar Convention since 2006. Its protection mostly comes from the fact that a number of birds live and reproduce in the area, being considered since 1979 as ‘Zona de Protección Especial para las aves’ (ZEPA). As well as, ‘lugar de importancia comunitaria’ (LIC) within Sierra Nevada according to the normative Hábitat 92/43/CEE.

It is well-known by historical sources that since the late XVIII century this depression was drained by a multitude of canals, called ‘madres’, with the main goal of using this area for agricultural purposes (Villegas Molina, 1967). The species cultivates might have changed in the past but there not historical records available for a deeper review. At present the areas surrounding the Padul lake are cultivated with cereals, such as *Triticum* spp., *Prunus dulcis* and *Olea europea*. Peat mining activities have been carried out in the area since 1943 (Carrasco Duarte, 1999).

Despite of the human impact on the environment since historical times, diversity of aquatic and wetland plants in the surroundings of the present-day Padul lake is high, being considered one of the most extensive reed areas of Andalucía (Fig. 13). The lake environment is dominated by aquatic and wetland communities (Pérez Raya and López Nieto, 1991). Some sparse riparian trees occur in the northern lake shore.

Besides the present-day natural value of this area, Padul is also significant from a paleontological and paleoclimatic point of view. This wetland yielded southernmost European remains of mammoths during the Pleistocene, dating around ~40-30 cal ka BP (within last glacial period), having important paleobiogeographical and paleoclimatic implications (García-Alix et al., 2012b).



Figure 13. (Above) Picture of Padul wetland, peat mine (dark area in the center-right) and cultivated crops in the Padul basin. Note the alluvial fans and Sierra Nevada mountains in the background. (Below) Picture of the present-day Padul lake, surrounded by wetland plants (mainly reeds; *Phragmites australis*).

CHAPTER 2

Chapter 2: Millennial-scale cyclical environment and climate variability during the Holocene in the western Mediterranean region deduced from a new multi-proxy analysis from the Padul record (Sierra Nevada, Spain)

María J. Ramos-Román¹, Gonzalo Jiménez-Moreno¹, Jon Camuera¹, Antonio García-Alix¹, R. Scott Anderson², Francisco J. Jiménez-Espejo³, Dirk Sachse⁴, Jaime L. Toney⁵, José S. Carrión⁶, Cole Webster²

¹ Departamento de Estratigrafía y Paleontología, Universidad de Granada, Spain

² School of Earth Sciences and Environmental Sustainability, Northern Arizona University, USA.

³ Department of Biogeochemistry, Japan Agency for Marine-Earth Science and Technology (JAMSTEC), Japan.

⁴ Helmholtz Centre Potsdam, German Research Centre for Geosciences GFZ, Section 5.1 Geomorphology, Organic Surface Geochemistry Lab., Germany

⁵ School of Geographical and Earth Sciences, University of Glasgow, UK

⁶ Departamento de Biología Vegetal, Facultad de Biología, Universidad de Murcia, Murcia, Spain

This chapter will be submitted to:

Quaternary Science Reviews

. Impact factor (JCR): 4.797 (2016)

. Rank: Q1

Abstract

A high-resolution pollen, geochemical and sedimentological analysis has been carried out on the Holocene part of the Padul sedimentary record in southern Iberian Peninsula reconstructing vegetation, environment and climate oscillations for the last ~11.6 cal ka BP in this part of the western Mediterranean area. The expansion and highest occurrence of deciduous forest in the Padul area from ~9.5 to 7.6 cal ka BP represents the Holocene humidity optimum probably due to enhanced winter precipitation during a phase of highest seasonal anomaly and maximum summer insolation. Locally, insolation maxima induced high evaporation, counterbalancing the effect of relatively high precipitation, and triggered very low water table in Padul and the deposition of peat sediments. A transitional environmental change towards more regional aridity occurred from ~7.6 to 4.7 cal ka BP and then aridification enhanced in the Late Holocene most likely related to decreasing summer insolation. This translated into higher water levels and a sedimentary change at ~4.7 cal ka BP in the Padul wetland, probably related to reduced evaporation during summer due to lower seasonality. Millennial-scale variability is superimposed on the Holocene long-term trends. The Mediterranean forest regional climate proxy shows significant cold-arid events around ~9.6, 8.5, 7.5, 6.5 and 5.4 cal ka BP with cyclical periodicities (~1100 and 2100 yr) during the Early and Middle Holocene. A change is observed in the periodicity of these cold-arid events towards ~1430 yr in the Late Holocene, with forest declines around ~4.7-4, 2.7 and 1.3 cal ka BP. The comparison between the Padul-15-05 data with North Atlantic and Mediterranean paleoclimate records suggests common triggers for the observed climate variability, being the Early and Middle Holocene forest declines mostly controlled by external forcing (i.e. solar activity) and the Late Holocene variability dominated by internal mechanisms (oceanic-atmospheric).

Keywords: Holocene, Padul, wetland, Sierra Nevada, western Mediterranean Sea, North Atlantic Oscillation, atmospheric-oceanic dynamics, wavelet analysis, arid events

1. Introduction

The western Mediterranean region, located between subtropical and tropical latitudes (Alpert et al., 2006), is a sensitive area to detect past climate variability and has been the focus of several previous Holocene studies. Present-day climate in this area is characterized by a strong seasonality, principally dominated by dry (hot) summers and wetter (mild) winters (Lionello et al., 2006) and one of the main mechanisms generating climate variations is the North Atlantic Oscillation (NAO) (Hurrell, 1995; Moreno et al., 2005).

During the Holocene orbital-scale (i.e. insolation) variations triggered climate changes that in turn produced significant environmental changes worldwide. Paleoclimate records show a Holocene climatic optimum between 9.5-7.5 ka BP (Dormoy et al., 2009), characterized in the western Mediterranean area by high temperatures and precipitation, which has been related with high summer insolation (Lamb and van der Kaars, 1995; Fletcher and Sánchez-Goñi, 2008; Anderson et al., 2011). Regional climate models described that the most important climatic transition towards cooler and drier conditions during the Holocene occurred around ~6 ka BP (Huntley and Prentice, 1988; Cheddadi et al., 1997). This shift is also described in the western Mediterranean, suggesting the establishment of the actual NAO-like system at ~ca. 6 cal ka BP (Fletcher et al., 2013). However, other studies differ in the timing of this climate shift indicating a transition phase between 7 and 5.5 cal ka BP (Jalut et al., 2009). These differences could be related with changes in altitudinal vegetation gradient, geomorphological changes in the study area and/or human perturbation of the landscape (Anderson et al., 2011). According to Roberts et al. (2011), combining different proxies indicative of vegetation and geomorphological changes could be a useful tool to discern the timing and the main forcing triggering this mid-Holocene environmental change.

During the last decades, a multitude of continental, marine and ice records worldwide have shown rapid climate variability at millennial-scales during the Holocene (Johnsen et al., 1992; Bar-Matthews et al., 2003; Mayewski et al., 2004). A considerable number of studies have detected this climate variability in the North

Atlantic area (i.e., Bond et al., 2001; Debret et al., 2007, 2009), with a prominent ~1500 yr cycle (Bond et al., 2001). However, others have demonstrated that Holocene climate variability was not stationary but that the Holocene exhibited variable periodicity (Debret et al., 2007, 2009). In this respect, high-resolution Mediterranean records have also shown rapid environmental variability related to millennial-scale climate change (Cacho et al., 2001; Fletcher and Sánchez-Goñi, 2008; Peyron et al., 2013). Previous palynological analyses from the western Mediterranean, showed vegetation responses at millennial-scales that seem to co-vary with climate variability from North Atlantic records, demonstrating hemispheric-scale teleconnections during the Holocene (Combourieu-Nebout et al., 2009; Fletcher et al., 2013). Other marine and terrestrial studies found centennial and millennial-scale Holocene frequency climatic patterns (Rodrigo-Gámiz et al., 2014a; Ramos-Román et al., 2016; García-Alix et al., 2017). However, there is a lack of non-stationary time-series analysis at millennial-scales from terrestrial records in the western Mediterranean area, which is necessary to understand terrestrial-ocean-atmospheric dynamics and the connections with high-latitude North Atlantic climate records. This is key for learning about past environmental change and climate variability in the western Mediterranean region and more robustly predict change under future climate scenarios.

Multi-proxy studies in continental records in southern Iberia and the western Mediterranean that could help understanding this environmental variability during the Holocene are rare. In order to improve our knowledge about this subject, we present a high-resolution multidisciplinary analysis recording sedimentation, geochemistry, vegetation, and climate variability during the Holocene (from ~11.6 cal ka BP to Present) from the Padul-15-05 record. Previous sedimentary records and paleoecological studies have been carried out on the Padul archive, detecting climate variability from the Pleistocene to the Middle Holocene (Florschütz et al., 1971; Ortiz et al., 2004; Pons and Reille, 1988). Nevertheless, a high resolution multi-proxy analysis on the same sediment samples has never been performed in this site for the entire Holocene. Recently, a multi-proxy analysis has been done focusing on the Late Holocene part of Padul-15-05 record (Ramos-Román et al., in press.) providing interesting results and renewing the interest to carry out a more complete study for

the entire Holocene. This time we used high-resolution radiocarbon dating, inorganic and organic geochemistry, pollen, lithology and macrofossil analysis to determine the Padul area paleoenvironmental evolution and millennial-scale vegetation and climate fluctuations in the western Mediterranean region during the Holocene. In this framework, two main goals direct this work: 1) understanding regional vegetation changes and local environmental evolution and making climate interpretations during the Early, Middle and Late Holocene, specifically focusing on the transitions, and 2) comparing millennial-scale vegetation and water-level oscillations (regional and local signal) with global climatic events.

1.1. Location and environmental setting

The Padul basin is an endorheic area at around 725 m of elevation at the foothill of the southwestern Sierra Nevada in Andalusia, southern Spain (Fig. 1). Today's climate in the region is characterized by a mean annual temperature of 14.4 °C and a mean annual precipitation of 445 mm (<http://www.aemet.es/>). The Sierra Nevada mountain range shows strong thermal and precipitation differences due to the altitudinal gradient (from ~700 to more than 3400 m), which control plant taxa distribution in different bioclimatic vegetation belts due to the variability in temperature and precipitation (Valle Tendero, 2004). According to this climatophilous series classification (Table 1), the Padul basin is situated in the Mesomediterranean vegetation belt (from ~ 600 to 1400 m of elevation), which is largely defined by the dominance of *Quercus rotundifolia* and, to a lesser extent, *Q. faginea*, which is normally accompanied by *Pistacia terebinthus*. *Q. coccifera* also occur in crests and very sunny rocky outcrops.

Sedimentation in the Padul basin is made up of (1) allochthonous detritic material coming for the surrounding mountains, principally from Sierra Nevada, which is characterized at higher elevations by Paleozoic siliceous metamorphic rocks (mostly mica-schists and quartzites) from the Nevado-Filabride complex and, at lower elevations and acting as bedrock, by Triassic dolomites, limestones and phyllites from the Alpujárride Complex (Sanz de Galdeano et al., 1998), (2) autochthonous organic material coming from plants growing in the wetland area of the basin itself and (3)

biogenic carbonates from charophytes, ostracods and gastropod shells, prominent organisms that lived in the lake. The water contribution to the Padul wetland comes from groundwater input and in less amounts by rainfall. Groundwater comes from different aquifers: the Triassic carbonate aquifers to the north and south edge of the basin, the out-flow of the Granada Basin to the west and the conglomerate aquifer to the east (Castillo Martín et al., 1984; Ortiz et al., 2004). The main water output is through evaporation and evapotranspiration and more recently also by water wells and by canals (locally called “madres”) (Castillo Martín et al., 1984). The canals were built around the end of the XVIII century with the goal of draining the basin water to the Dúrcal river to the southeast for cultivation purposes (Villegas Molina, 1967). In the early 2000’s the Padul wetland was placed under environmental protection and the peat mine stopped pumping water out of the basin and the Padul lake increased its size considerably.

The Padul-15-05 drilling site is located around 50 m south of the present-day Padul lake shore area. The edge of the lake area is at present principally dominated by the grass *Phragmites australis*. The lake environment is also characterized by emerged and submerged macrophytes communities dominated by *Chara vulgaris*, *Myriophyllum spicatum*, *Potamogeton pectinatus*, *Potamogetum coloratus*, *Typha dominguensis*, *Apium nodiflorum*, *Juncus subnodulosus*, *Carex hispida*, *Juncus bufonius* and *Ranunculus muricatus* among others (Pérez Raya and López Nieto, 1991). *Populus alba*, *Populus nigra*, *Ulmus minor* and several species of *Salix* and *Tamarix* grow on the northern lake shore.

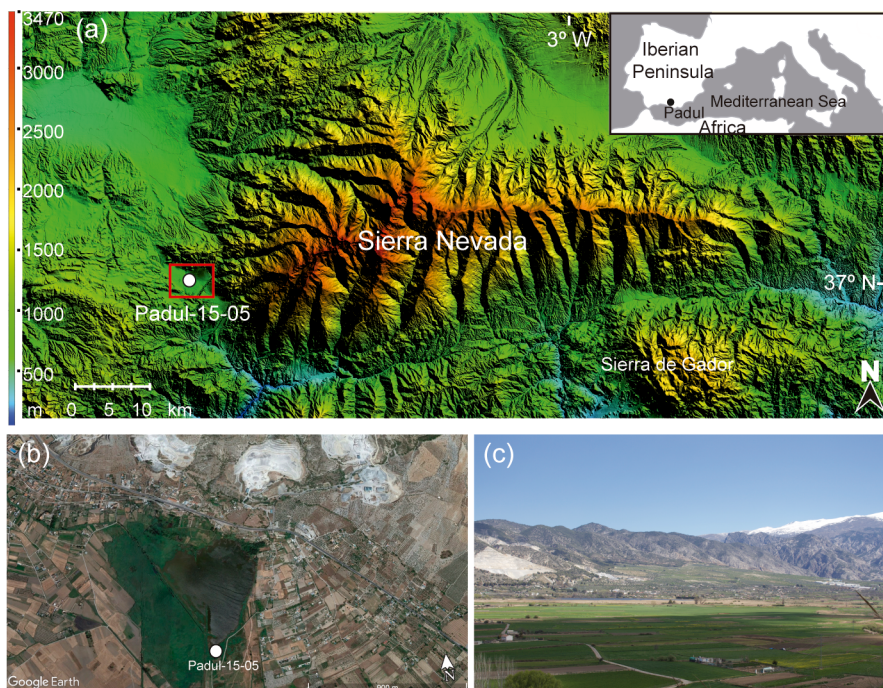


Figure 1. Location and pictures of Padul wetland. (a) Location of Padul wetland in Sierra Nevada, southern Iberian Peninsula, western Mediterranean region. (b) Padul basin area showing the coring location. (c) Picture of Padul wetland, peat bog and crops area in the Padul basin, and the alluvial fans and Sierra Nevada mountains in the background. Software use: Above, Sierra Nevada map was performed using the GIS software Global Mapper (<http://www.globalmapper.com>) and modified with Adobe Illustrator. The inset map (the western Mediterranean region) was created with Adobe Illustrator (<https://www.adobe.com/>). Below, to the left, is the Google Earth image (<http://www.google.com/earth/index.html>) of Padul basin showing the coring locations.

Table 1. Modern vegetation belts from Sierra Nevada (El Aallali et al., 1998; Valle, 2003).

Vegetation belt	Elevation (m)	Principally characteristic taxa
Crioromediterranean	> 2800	Tundra vegetation including members of Poaceae, Asteraceae, Brassicaceae, Gentianaceae, Scrophulariaceae and Plantaginaceae.
Oromediterranean	1900-2800	<i>Pinus sylvestris</i> , <i>P. nigra</i> and <i>Juniperus</i> spp. and other shrubs such as species of Fabaceae, Cistaceae and Brassicaceae.
Supramediterranean	1400-1900	<i>Quercus pyrenaica</i> , <i>Q. faginea</i> and <i>Q. rotundifolia</i> and <i>Acer opalus</i> ssp. <i>granatense</i> and other trees and shrubs, with some species of Fabaceae, Thymelaeaceae, Cistaceae and <i>Artemisia</i> sp.
Mesomediterranean	600-1400	<i>Quercus rotundifolia</i> , some shrubs, herbs and plants as <i>Juniperus</i> sp., and some species of Fabaceae, Cistaceae and Liliaceae

2. Methodology

2.1. Padul site core drilling

Two sediment cores Padul-13-01 (37°00'40''N; 3°36'13''W) and Padul-15-05 (37°00'39.77''N; 3°36'14.06''W) with a length of 58.7 cm and 42.64 m, respectively, were collected between 2013 and 2015 from the Padul lake shore (Fig. 1). The cores were taken with a Rolatec RL-48-L drilling machine equipped with a hydraulic piston corer from the Scientific Instrumentation Center of the University of Granada (CIC-UGR). The sediment cores were wrapped in film, put in core boxes, transported and stored in a dark cool room at +4 °C at the University of Granada. In this study, we focus on the uppermost ~3.67 m from the 42.6-m-long Padul-15-05 core.

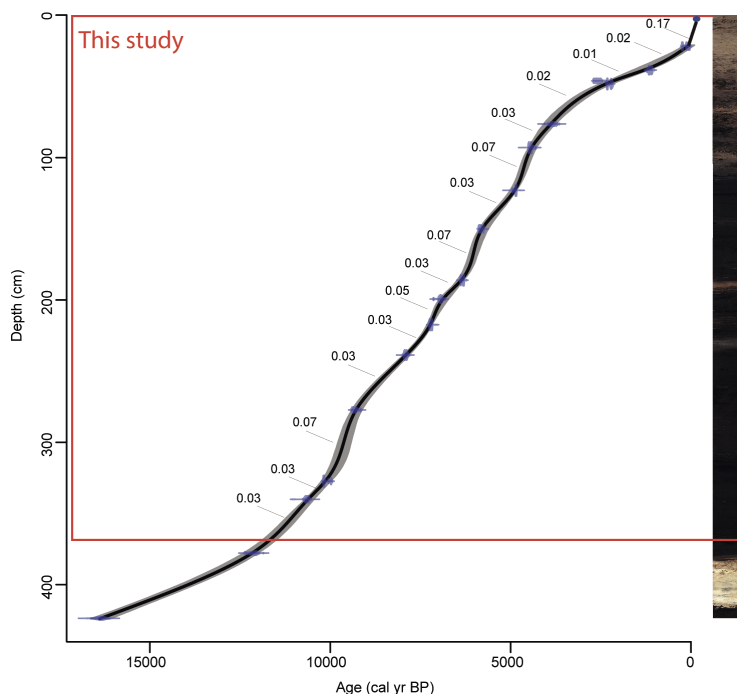


Figure 2. Picture of the Padul-15-05 sediment core with the age-depth model showing the part of the record that was studied here (red rectangle) corresponding with the last ~11.6 cal ka BP. The sediment accumulation rates (SAR) between radiocarbon dates are marked. See the body of the text for the explanation of the age reconstructions.

2.2. Chronology and sedimentation rates

The sedimentary record chronology was constrained using seventeen AMS radiocarbon dates from plant remains and organic bulk samples taken throughout the cores (Table 2). In addition, four samples were rejected, because one plant sample was too young and three gastropod shell samples provided old dates due to the reservoir effect. Sixteen of these samples came from Padul-15-05 and one from the nearby Padul-13-01 (Table 2). We were able to use the date from Padul-13-01 core because there is a very significant correlation between the upper part of Padul-15-05 and Padul-13-01 cores, shown by identical lithology and geochemistry changes (Ramos-Román et al., in press.). The age model for the upper ~4.24 m until 21 cm from the surface was built using the R-code package ‘Clam 2.2’ employing the calibration curve IntCal 13 (Reimer et al., 2013), a 95% confident range, a smooth spline (type 4) with a 0.20 smoothing value and 1000 iterations (Fig. 2). The chronology of the uppermost 21 cm of the record was built using a lineal interpolation between the last radiocarbon date and the top of the record, which was assigned the age when coring (2015 CE).

2.3. Lithology and magnetic susceptibility (MS)

The Padul-15-05 core was split longitudinally and was described in the laboratory with respect to lithology and color (Fig. 3). High-resolution continue scanning images were taken with an Avaatech core scanner at the University of Barcelona (UB). MS was measured with a Bartington MS3 operating with a MS2E sensor. MS measurements (in SI units) were obtained directly from the core surface every 0.5 cm (Fig. 3).

Table 2. Age data for Padul-15-05 record. All ages were calibrated using R-code package ‘clam 2.2’ employing the calibration curve IntelCal 13 (Reimer et al., 2013) at 95 % of confident range. * Rejected data. a Sample number assigned at radiocarbon laboratory.

Laboratory number ^a	Core	Material	Depth (cm)	Age (¹⁴ C yr BP ± 1σ)	Calibrated age (cal yr BP) 95% confidence interval	Median age (cal yr BP)
Reference ages			0	2015CE	-65	-65
D-AMS 008531	Padul-13-01	Plant remains	21.67	103 ± 24	23-264	127
Poz-77568	Padul-15-05	Org. bulk sed.	38.46	1205 ± 30	1014-1239	1130
BETA-437233	Padul-15-05	Plant remains	46.04	2480 ± 30	2385-2722	2577
Poz-77569	Padul-15-05	Org. bulk sed.	48.21	2255 ± 30	2158-2344	2251
BETA-415830	Padul-15-05	* Shell	71.36	3910 ± 30	4248-4421	4343
BETA- 437234	Padul-15-05	Plant remains	76.34	3550 ± 30	3722-3956	3838
BETA-415831	Padul-15-05	Org. bulk sed.	92.94	3960 ± 30	4297-4519	4431
Poz-74344	Padul-15-05	Plant remains	122.96	4295 ± 35	4827-4959	4871
BETA-415832	Padul-15-05	Plant remains	150.04	5050 ± 30	5728-5900	5814
Poz-77571	Padul-15-05	Plant remains	186.08	5530 ± 40	6281-6402	6341
Poz-74345	Padul-15-05	Plant remains	199.33	6080 ± 40	6797-7154	6935
BETA-415833	Padul-15-05	Org. bulk sed.	217.36	6270 ± 30	7162-7262	7212
Poz-77572	Padul-15-05	Org. bulk sed.	238.68	7080 ± 50	7797-7999	7910
Poz-74347	Padul-15-05	Plant remains	277.24	8290 ± 40	9138-9426	9293
BETA-415834	Padul-15-05	Plant remains	327.29	8960 ± 30	9932-10221	10107
Poz-77573	Padul-15-05	Plant remains	340.04	9420 ± 50	10514-10766	10640
Poz-74348	Padul-15-05	* Plant ramains	375.62	9120 ± 50	10199-10412	10305
Poz-79815	Padul-15-05	Org. Bulk sed.	377.83	10310 ± 50	11847-12388	12144
Poz-79817	Padul-15-05	* Shell	411.02	13910 ± 60	16588-17088	16838
Poz-79818	Padul-15-05	* Shell	414.89	14130 ± 50	17001-17419	17210
Poz-77574	Padul-15-05	Org. Bulk sed.	423.65	13580 ± 80	16113-16654	16384

2.4. Inorganic geochemistry

High-resolution X-Ray fluorescence (XRF) was applied continuously throughout the core surface, taking measurements of elemental geochemical composition. An Avaatech X-Ray fluorescence (XRF) core scanner® located at the UB was used. Chemical elements were measured in the XRF core scanner at 10 mm of spatial resolution, using 10 s count time, 10 kV X-ray voltage and an X-ray current of 650 μ A for lighter elements and 35 s count time, 30 kV X-ray voltage, X-ray current of 1700 μ A for heavier elements. Thirty-three chemical elements were measured but only the most representative with a significant number of counts were considered (Si, K, Ca, Ti, Fe, Zr, Br, S and Sr). Results for each element are expressed as intensities in counts per second (cps) and normalized for the total sum in cps in every measure (Fig. 4).

2.5. Organic geochemistry

Several organic geochemical proxies have been studied from bulk sediment samples throughout the record: total organic carbon (TOC), atomic Carbon-Nitrogen ratio (C/N) and atomic Hydrogen-Carbon ratio (H/C). In addition, several indices of leaf wax biomarkers (*n*-alkanes) were calculated: the average chain length (ACL), the carbon preference index (CPI) and the portion of aquatic (Paq). In addition, three new indices have been calculated based on the relative abundance of odd carbon number from *n*C₁₇ to *n*C₃₃ alkanes, except for *n*C₂₇ alkanes (See Section 3.2.2 for justification of new indices).

Samples for elemental analyses in bulk sediment were analyzed every 2 or 3 cm throughout the Padul-15-05 record, with a total of 206 samples analyzed. Samples were decalcified with 1:1 HCl to eliminate the carbonate fraction. Carbon, nitrogen and hydrogen content of the decalcified samples were measured in an Elemental Analyzer Thermo Scientific Flash 2000 model at the CIC-UGR. Percentage of TOC, total nitrogen (TN) and total hydrogen (TH) per gram of sediment was calculated from the percentage of organic carbon, nitrogen and hydrogen yielded by the elemental analyzer, and recalculated by the weight of the sample prior to

decalcification. The atomic C/N and H/C ratio was calculated from the carbon, nitrogen and hydrogen measurements (Fig. 4).

Biomarkers from the Padul-15-05 record were extracted every 5 cm from sedimentary record, with a total of 68 samples analyzed. Furthermore, thirty-one modern plant leaves/algae and bryophyte samples were taken from the surroundings of the Padul basin and analyzed for biomarkers. The total lipid extraction (TLE) from the freeze-dried samples was obtained using an accelerated solvent extractor (ASE) Thermo DIONEX 350, with a dichloromethane:methanol (9:1). Plant biomarkers were extracted manually using dichloromethane:methanol (9:1) by means of sonication and low temperature (38°C). The TLE from plants and sediments was separated into three different fractions using a silica gel column. Before the separation three internal standards were added to the TLE (5 α -androstane, 5 β -androstane-17-one and 5 α -androstane-3 β -ol) in order to assess the biomarker extraction as well as to quantify them. Compounds of the aliphatic fraction (*n*-alkanes) were recovered in the first fraction eluted with Hexane. The *n*-alkanes were identified and quantified using a Gas Chromatography flame detection and mass spectrometry (GC-FID and GC-MS) by means of an Agilent 5975C MSD by comparison to an external *n*-alkane standard mixture from *n*C₁₀ to *n*C₄₀.

2.6. Pollen

Samples for pollen analysis (1-3 cm³) were taken with a resolution between 1-5 cm throughout the core, with a total of 176 samples. Pollen extraction methods followed a modified Faegri and Iversen, (1989) methodology. Processing included the addition of *Lycopodium* spores for calculation of pollen concentration. Sediment was treated with NaOH, HCl, HF and the residue was sieved at 250 μ m before an acetolysis solution. Counting was performed using a transmitted light microscope at 400 magnifications to an average pollen count of around ~250 terrestrial pollen grains. Fossil pollen was identified using published keys (Beug, 2004) and modern reference collections at the UGR. Pollen counts were transformed to pollen percentages based on the terrestrial pollen sum, excluding aquatics. Non-pollen palynomorphs (NPP) include algal spores. The NPP percentages were also calculated

and represented with respect to the terrestrial pollen sum (Fig. 5). Several pollen and NPP taxa were grouped according to present-day ecological data in Mediterranean forest, xerophytes and algae (Fig. 6). The Mediterranean forest taxa include *Quercus* total, *Olea*, *Phillyrea* and *Pistacia*. The Xerophyte group includes *Artemisia*, *Ephedra*, and Amaranthaceae. The *Algae* group is composed of *Botryococcus*, *Zygnema* type, *Mougeotia* and *Pediastrum*.

2.7. Statistical analysis

Statistical treatment was performed using the Past software (http://palaeo-electronica.org/2001_1/past/issue1_01.htm). Principal component analysis (PCA) was conducted on different geochemical elements (XRF data) to clarify the lithological elemental composition of the core (Supplementary; Figure S1). Prior to the PCA analysis we pretreated the data normalizing the element counts by subtracting the mean and dividing by the standard deviation (Davis and Sampson, 1986). As data spacing was different in all the study proxies the data were also resampled to the average value of 80-yr (linear interpolation) to obtain equally spaced time series. Posteriorly, a Pearson correlation was made to different organic/inorganic geochemistry and pollen proxies to find affinities between the different proxies.

In this study spectral analysis was accomplished on the Mediterranean forest pollen taxa time series, to identify regional millennial-scale periodicities in the Padul-15-05 record (Supplementary Fig. S4). We used REDFIT software (Schulz and Mudelsee, 2002) on the unevenly spaced pollen time series in order to identify cyclical changes. In addition, we carried out a Wavelet transform analysis by the Past software (Torrence and Compo, 1998) with the goal of identifying non-stationary cyclical variability in the regional vegetation evolution, the pollen was previously detrended and resampled at 80-yr age increments. In this study, a Morlet wavelet was chosen, the significant level (plotted as contour) corresponded to a p-value = 0.05, and a white-noise model was used.

3. Results and proxy interpretation

3.1. Chronology and sedimentary rates

The age-model of the studied Padul-15-05 core (Fig. 2) is constrained by seventeen AMS ^{14}C radiocarbon dates from the top 4.24 m of the record (Table 2). In this work, we studied the uppermost ~3.67 m that continuously cover the last ~11.6 cal ka BP. This interval is chronologically constrained by sixteen AMS radiocarbon dates. Fifteen distinct sediment accumulation rates (SAR) intervals can be differentiated between 3.67 m and the top of the record between radiocarbon dates (Fig. 2). The highest SAR occurred above ~0.21 m with an average of 0.17 cm/yr. The average SAR below 0.21 m varied from around 0.01 to 0.07 cm/yr, showing the lowest values from 0.21 to 0.58 cm averaging values of approximately 0.01 cm/yr and showing an increase from 0.58 m to 3.67 m with average values of 0.05 cm/yr.

3.2. Lithology, inorganic and organic geochemistry

3.2.1. Lithology and inorganic geochemistry

Inorganic geochemistry informs us about variations in the lithology and the local depositional environment. Variations in these proxies could also be useful for estimating water level fluctuations in the wetland environment. Sediments bearing aquatic fossil remains (i.e. gastropods and charophytes) and then rich in carbonates have previously been related to shallow water lakes (Riera et al., 2004). Lower water levels, more subjected to be occupied by wetland vegetation, and ephemeral lakes are characterized by the increase in organics and clastic input and more influenced by terrestrial-fluvial deposition (Martín-Puertas et al., 2008). Magnetic susceptibility (MS) measure the propensity of the sediments to bring a magnetic charge (Snowball and Sandgren, 2001).

Framboidal pyrite (FeS_2) and barite (BaSO_4) with Sr have been found covering exceptionally preserved mammals remains from 40 to 30 ky at the Padul peat bog (García-Alix et al., 2012b) pointing towards a peat-bog environment with enhanced anoxic conditions. The presence of pyrite and organic-sulfur compounds is common

in peat bogs (Wieder and Lang, 1988; Feijtel et al., 1989; Chapman, 2001) and other organic rich sediments under anoxic conditions (López-Buendía et al., 2007). Increasing values of organic carbon, and bromine have been related with higher organic matter deposition generated in high productivity environments (Kalugin et al., 2007). In marine records Br XRF scanning counts can be used to estimates sedimentary total organic carbon (Ziegler et al., 2008).

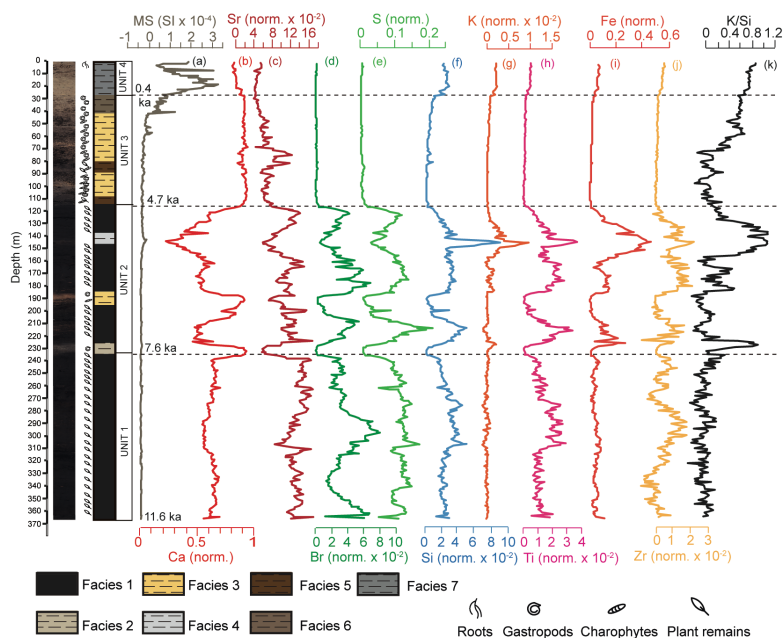


Figure 3. Inorganic geochemistry results for the ~3.67 m of the upperpart from Padul 15-05 record. Picture of the Padul-15-05 record, facies interpretations with paleontology, magnetic susceptibility (MS) and X-ray fluorescence (XRF). XRF elements (Ca, Sr, Br, S, Si, K, Ti, Fe, Zr) represents as counts per second normalized to the total counts (norm.). (a) MS in SI, (b) Ca normalized (norm.), (c) Sr normalized (norm.), (d) Br normalized (norm.), (e) S normalized (norm.), (f) Si normalized (norm.), (g) K normalized (norm.), (h) Ti normalized (norm.), (i) Fe normalized (norm.), (j) Zr normalized (norm.), (k) K/Si ratio.

A visual lithological inspection was made for the upper ~3.67 m of the Padul-15-05 sediment core and was compared with the elemental geochemical composition (XRF) and the MS data (Fig. 3). For the geochemical elements, we conducted a PCA analysis to summarize and better understand the correlation between the visual lithological features and the geochemical signal of the sediments (Supplementary Fig. S1 and Table S1). The PCA analysis in the study sedimentary sequence help us

identify three main groups of sediments consisting of clays with variable content in (1) carbonates of endogenic formation with high values of Ca, related with the occurrence of shells and charophyte remains, (2) siliciclastics (Si, K, Ti, Fe, Zr) and (3) vegetal organics probably associated with anoxic/reducing environment with high values of S, Sr and Br. To differentiate the clays input to the basin the K/Si ratio have been calculated. The use of K/Si ratio is based in the fact that clay fraction is enriched in filosilicates (illite, muscovite), compared with the coarser particles that are mainly quartz, dolomite and schists. This correlation between K and clay content has been observed in lacustrine systems (e.g. Lake Enol, Iberian Peninsula) and associate to an increase in detrital input (Moreno et al., 2011). We were able to identify four different lithological units: Units 1 and 2 are principally made up of peat sediments and Unit 3 and 4 by clays with variable carbonates (Fig. 3). Unit 1, from the bottom (3.67 m; ~11.6 cal ka BP) to around 2.31 m (~7.6 cal ka BP), is characterized by *facies* 1 - dark organic peat – high S, Sr and Br values. Unit 2, from 2.31 to 1.15 m (~7.6 to 4.7 cal ka BP), is also generally characterized by *facies* 1 but with the intercalation of three other different *facies*: *facies* 2 from 2.31 to 2.21 m (~7.6 to 7.3 cal ka BP) depicted by grey clays with gastropod remains (featured by the increase in Ca and the increase in K/Si ratio), *facies* 3 from 1.95 to 1.85 m (~6.6 to 6.4 cal ka BP) made up of brown clays with the occurrence of gastropods and charophytes (showing a decrease in S, Br and Sr and higher values of Ca) and *facies* 4 around 1.46 to 1.40 m (~5.7 to 5.4 cal ka BP) characterized by grey clays (related with the increase in siliciclastic material and clays input). Unit 3, from around 1.15 to 0.28 m (~4.7 to 0.40 cal ka BP), is mostly characterized by high Ca values and the trend to increase in K/Si ratio, and the decrease in S, Br and Sr. This unit is made up of three different *facies*: *facies* 5 between 1.15-1.10 m depth (~4.7 to 4.65 cal ka BP) and 0.89-0.80 m depth (~4.3 to 4 cal ka BP), are characterized by dark brown organic clays that bear charophyte and plant remains, *facies* 3 between 1.10-0.89 m (~4.65 to 4.3 cal ka BP) and 0.80-0.42 m depth (~4 to 1.6 cal ka BP), are made up of brown clays, with the occurrence of gastropods and charophytes and *facies* 6, between 0.42-0.28 m (~1.6 to 0.4 cal ka BP), which are characterized by grayish brown clays with

the occurrence of gastropods. Unit 4, between 0.28 and 0 m depth (~0.4 cal ka BP to Present), is composed of *facies* 7 and made up of light grayish brown clays depicted by a decreasing trend in Ca and an increase in K/Si ratio and MS.

3.2.2. Organic geochemistry

Variations in TOC, C/N and H/C ratios reflect changes in paleoenvironmental dynamics in bogs and lakes (García-Alix et al., 2017; Meyers and Lallier-vergés, 1999; Ortiz et al., 2010). TOC concentration is the principal indicator of organic matter content in sediments. Typical organic matter contains 50 % of carbon so the concentration of organic matter in sediments is twice the TOC (Meyers et al., 1999). C/N ratio helps us learn about the proportion of algal and terrestrial vascular plant organic matter in the sediments (Meyers, 1994). Fresh organic matter from algae has usually molar C/N values that are between 4 and 10, whereas cellulose-rich terrestrial plants are characterized by values of 20 and greater (Meyers et al., 1994). H/C values are a good proxy for the source of the organic matter in sediments, as algal/bacterial/amorphous remains are richer in hydrogen than herbaceous and woody plant material, with values over 1.7 indicative of algal/amorphous organisms. In addition, lower values of H/C (<0.8) could also be indicative of organic matter transport or diagenesis after deposition (Talbot, 1988; Talbot and Livingstone, 1989).

N-alkanes biomarkers abundance and distribution can provide information about different biological sources of organic matter accumulated in bog and lake sediments (Ficken et al., 2000; Meyers and Lallier-vergés, 1999; Sachse et al., 2006). Several of these sources are characterized by distinct predominant *n*-alkanes chain-lengths have been identified according to the biological sources to the sediments : (1) In general, *n*-alkanes with 17 or 19 carbon atoms (nC_{17} or nC_{19}) are found predominantly in algae (Cranwell, 1984; Gelpi et al., 1970) and with photosynthetic bacteria (Cranwell et al., 1987), (2) nC_{21} , nC_{23} or nC_{25} are associated with submerged and floating aquatic plants (Cranwell, 1984; Ficken et al., 2000), while (3) *n*-alkane distribution with predominant $> nC_{27}$, nC_{29} , nC_{31} represent higher terrestrial plant input (Cranwell et al., 1987) as well as emergent macrophytes (e.g. *Juncus* sp., *Typha* sp. or *Phragmites*

australis) (Cranwell, 1984; Ficken et al., 2000; Ogura et al., 1990). CPI (illustrating the relative abundance of odd vs. even carbon chain lengths) is a proxy for preservation of organic matter in the sediments, with values lower than 2 indicating diagenetic alteration or algal/bacterial influence and, higher than 2 (see Bush and McInerney, 2013 review) indicating terrestrial influence and thermal immaturity of the source rock. Ficken et al. (2000) formulated the Paq (proportion of aquatics) to discern the origin of the organic inputs in the sediments, giving average values for present-day plants of <0.1 for terrestrial plants, 0.1-0.4 for emerged aquatics and 0.4-1 for submerged/floating aquatic species. However, García-Alix et al., (2017), showed that the meaning of the different indices of the distribution of the *n*-alkane chain length cannot be generalized, being important to know the present *n*-alkane distribution of the vegetation in the study site.

To better constrain the origin of the organic input in the Padul-15-05 record, we analyzed *n*-alkanes from present day terrestrial and aquatic plants as well as algae/bryophyte in the Padul basin area (Supplementary information; Figs. S2 and S3). Our results show that the predominant *n*-alkanes in the samples are nC_{27} , nC_{29} and nC_{31} . There is also a strong odd over even carbon number predominance (CPI values higher than 2). This basin is currently dominated by wetland plants, such as *Phragmites australis* with predominant carbon chain between C_{27} and C_{29} *n*-alkane. The Paq for present-day plants average values of 0.16 ± 0.16 for terrestrial plants, 0.29 ± 0.34 for aquatic plants and 0.32 ± 0.21 for algae-bryophyte.

Table 3. Summary of the *n*-alkane indices from the studied plant, algae and moss samples from the surroundings of the present-day Padul peatland (For more information see in the Supplementary Figure S2 and S3).

Samples	n-alkane indices					
	Paq	ACL	CPI	Short-chain (%)	Mid-chain (%)	Long-chain (%)
Algae-Bryophyte	0.32 ± 0.21	27.97 ± 0.74	9.52 ± 7.69	13.02 ± 21.07	35.26 ± 19.82	51.71 ± 33.84
Aquatics plants	0.29 ± 0.34	28.78 ± 1.86	11.60 ± 7.35	1.33 ± 4.40	28.36 ± 32.44	70.31 ± 34.64
Terrestrial	0.16 ± 0.16	28.23 ± 0.74	20.64 ± 10.84	-	17.44 ± 19.34	82.56 ± 19.34

ACL average values were around 28.23 ± 0.74 for emerged-terrestrial plants, 28.78 ± 1.86 for aquatic plants and 27.97 ± 0.74 for algae-bryophyte (Table 3; Supplementary Fig. S3). These results led us to the need to create three new *n*-alkane indices with the goal of characterizing the source of organic matter in our sediment samples from the Padul-15-05 record, taking in consideration the relative abundances of the odd carbon chains except for *n*C₂₇ (due to higher values in all the plant/algae samples): (1) Short-chain (%), where higher values are typical from algae or bacterial, (2) Mid-chain (%), where higher values are typical of aquatic plants, and (3) Long-chain (%), where higher values are obtained when the source is vascular emerged aquatic or terrestrial plants (Table 3).

1. Short-chain:

$$[C_{17}-C_{19}] = [(C_{17}+C_{19})/(C_{17}+C_{19}+C_{21}+C_{23}+C_{25}+C_{29}+C_{31}+C_{33})] \times 100$$

2. Middle-chain:

$$[C_{21}-C_{23}-C_{25}] = [(C_{21}+C_{23}+C_{25})/(C_{17}+C_{19}+C_{21}+C_{23}+C_{25}+C_{29}+C_{31}+C_{33})] \times 100$$

3. Long-chain:

$$[C_{29}-C_{31}-C_{33}] = [(C_{29}+C_{31}+C_{33})/(C_{17}+C_{19}+C_{21}+C_{23}+C_{25}+C_{29}+C_{31}+C_{33})] \times 100$$

The results for the organic geochemistry (TOC, C/N ratio, H/C ratio and *n*-alkane indices) from the Padul-15-05 record are depicted in Figure 4, showing the following results:

TOC values range from 0.8 to 61%, with an average value of 27.5 %. Highest TOC values are registered during the deposition of sedimentary Unit 1 averaging values of 41 %, associated with the peatland environment related with anoxic/reducing conditions (showing higher correlation with S, Br; Table 4). Higher TOC variability occurred during Unit 2. The transition between Unit 1 and 2 is marked by a TOC decrease with values around 14 % at ~ 7.6 cal ka BP. Other decreases occurred between 2-1.89 m (~ 6.9 to 6.4 cal ka BP) and between 1.48-1.39 m (~ 5.7 to 5.4 cal ka BP), reaching values around 20 and 30 %, respectively. The transition between Unit 2 and 3 (~ 4.7 cal ka BP/ ~ 1.13 m) is marked by a significant decline to values

below 15 %. The lowest TOC values are recorded during Units 3 and 4 with average values around 4.6 %. Atomic C/N ratios were higher during the lithological Units 1 and 2 and ranged between 53 and 11, with an average value of 26. A decrease in C/N occurred during the transition from Units 2 to 3 down to average values of 17. The lowest values occurred during Unit 1, recording C/N values in a range between 14 and 10. Atomic H/C ratios ranged between 1.13 and 6.66 with an average value of 1.65. The lowest values were recorded between the bottom of the record and approximately 0.77 m (~3.9 cal ka BP) with ranging values between 1.13 and 2.26 with an average of 1.39. Highest values are depicted from 0.77 m to the top of the record averaging values of 2.62.

The *n*-alkane data obtained from the Padul-15-05 sediments show that shorter carbon chains were abundant during Unit 1. CPI values were higher than 2, averaging values of around 7 and representing an odd over even carbon chain and a good preservation of the organic matter in the sediments, the lowest values, with an average of 2.6, occurred during the Unit 1 around 3.07-2.31 m depth (~9.7 to 7.6 cal ka BP), and the highest values averaging 11.8 occurred around 2.31 to 2.15 m depth (from ca. 7.5 to 7.2 cal yr BP). Short-chain shows peaks of higher values at 3.10 m (~9.6 cal ka BP), 2.55 m (~8.5 cal ka BP), 2.30 m (~7.5 cal ka BP), 1.40 m (~5.4 cal ka BP), from 1.15 to 0.8 m (~4.7-4 cal ka BP), 0.52 m (~2.7 cal ka BP) and from 0.4-0.33 m (~1.3-0.8 cal ka BP). Mid-chain shows the highest values between the bottom and 2.26 m (between ~11.6 and 7.6 cal ka BP) with an average of around 24 %, depicting a maximum between 2.90 and 2.31 m (~9.5 to 7.6 cal ka BP) with average values of around 40 %. The lowest values are recorded during the last 1.15 m (~4.7 cal ka BP). Long-chain index shows high values averaging ~81 % between 2.26 and 1.40 m (~7.5 to 5.4 cal ka BP) and reached maximum values around 0.60 m (~3.2 cal ka BP) and between 0.45 m (~1.9 cal ka BP), and the last 0.22 cm (~0.1 cal ka BP).

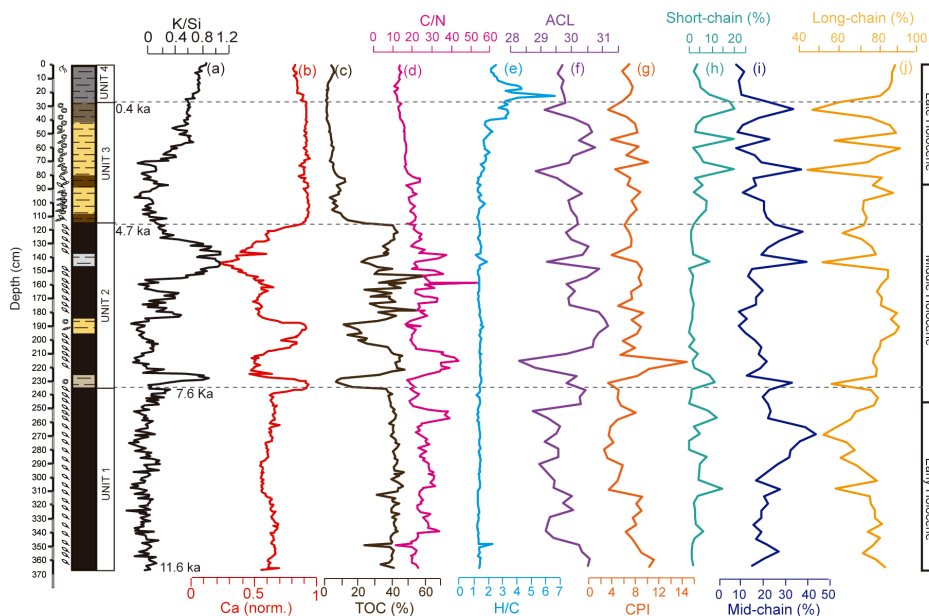


Figure 4. Organic geochemistry results for the ~3.67 m of the upperpart (Holocene part) from Padul-15-05 record and comparison with inorganic index calculated from the PCA analysis performed to XRF elements in the same record. (a) K/Si ratio, (b) Ca (norm.), (c) Total organic carbon percentage (TOC %), (d) Carbon-Nitrogen ratio (C/N), (e) Hydrogen-Carbon ratio (H/C), (f) Average chain length (ACL), (g) Carbon preference index (CPI), (h) Short-chain (%), (i) Mid-chain (%), (j) Long-chain (%).

3.3. Pollen and Spores

Pollen grains from terrestrial and aquatic species were identified and the most representative taxa are plotted in a summary pollen diagram (Fig. 5). In this study, we used the variations between Mediterranean forest taxa, xerophytes, hygrophytes and algae for paleoenvironmental and paleoclimatic variability in the study area. The fluctuations in arboreal pollen (AP, including Mediterranean tree species) have previously been used in other nearby Sierra Nevada records as a proxy for regional humidity changes (Jiménez-Moreno and Anderson, 2012; Ramos-Román et al., 2016). The abundance of the Mediterranean woods (i.e., evergreen and deciduous *Quercus*, *Olea*, *Pistacia*) has been used as a proxy for climate change in many other studies in the western Mediterranean region, with higher forest development generally meaning higher humidity (Fletcher and Sánchez-Goñi, 2008; Fletcher et al., 2013). On the other hand, increases in xerophyte pollen taxa (i.e., *Artemisia*, *Ephedra*,

Amaranthaceae), representative of steppe vegetation, have been used as an indication of aridity in this area (Anderson et al., 2011; Carrión et al., 2007). Variability in wetland angiosperms and algae could be indicative of local change in the surrounding vegetation and lake level fluctuations. Singh et al. (1990) suggested that Cyperaceae and *Typha* could be taken like swamp-indicative when occurring with freshwater algae (*Cosmarium*, Zygnemataceae). Currently, the dominant plant species in the Padul wetland is the common reed, *Phragmites australis*, in fact very common in semi-arid wetlands with shallow water levels (Moro et al., 2004). This species has thrives whenever a wetlands becomes drier (Hudon, 2004). Van Geel et al., (1983) described the occurrences of *Zygnema* and *Mougeotia* as characteristic of shallow lake water environments. The chlorophyceae *Botryococcus* is an indicator of freshwater environments in relatively productive fens, temporary pools, ponds or lakes (Guy-Ohlson, 1992). Clausen (1999) point out that *Botryococcus* abundance is higher in sediment of shallow water lakes and/or littoral environment in deeper lakes.

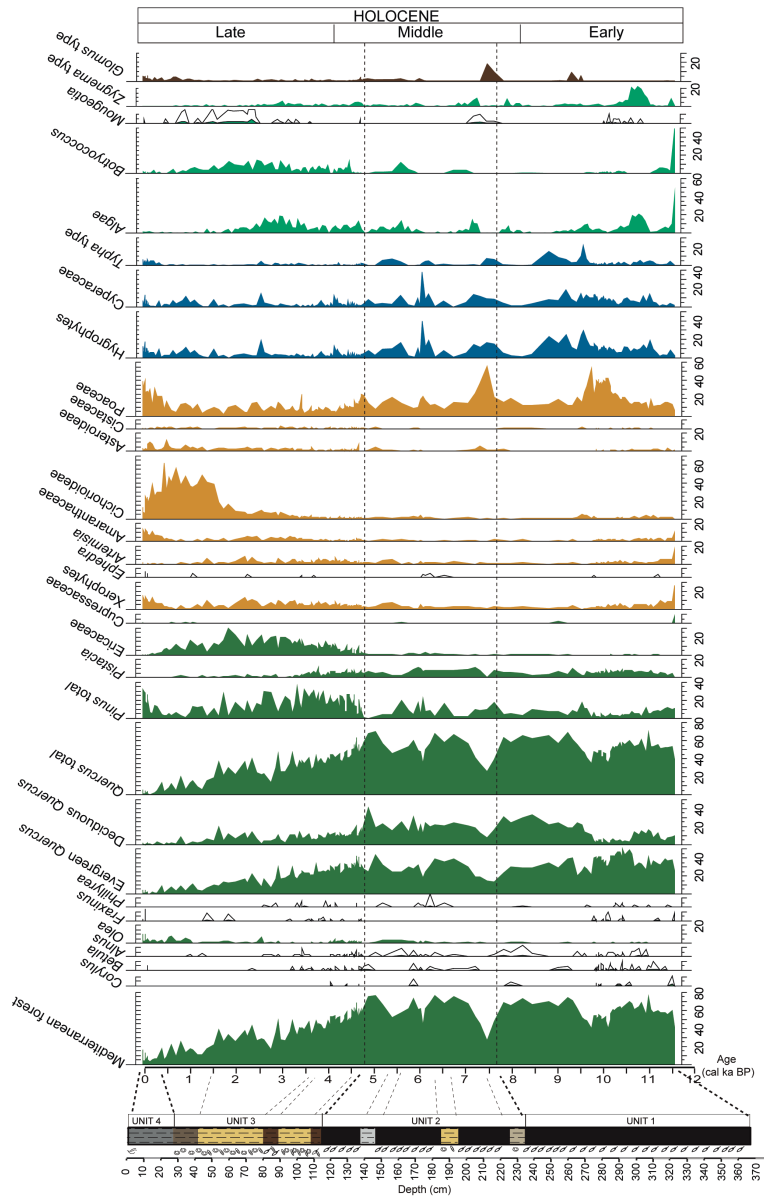


Figure 5. Percentages of selected pollen taxa and non-pollen palynomorphs (NPPs) from the Holocene part of Padul-15-05 record, represented with respect to terrestrial pollen sum. Silhouettes show 7-time exaggerations of pollen percentages. Tree and shrubs are showing in green, herbs and grasses in yellow, aquatics in dark blue, algae in blue and fungi in brown. The Mediterranean forest taxa is composed of *Quercus* total, *Olea*, *Phillyrea* and *Pistacia*. The xerophyte group includes *Artemisia*, *Ephedra*, and *Amaranthaceae*. Hygrophytes group is composed by *Cyperaceae* and *Typha* type. Algae group is formed by *Zygea* type, *Botryococcus*, *Mougeotia* and *Pediastrum*.

The pollen results are described thereafter, distinguishing three different phases during the Holocene:

3.3.1. From ~11.6 to 7.6 cal ka BP (from ~3.67 to 2.31 m)

The Early and early Middle Holocene, from ~11.6 to 7.6 cal ka BP, is characterized by high abundance of Mediterranean forest, averaging relative percentage values of approximately 58%. The most representative arboreal tree taxon between ~11.6 to 9.7 cal ka BP is evergreen *Quercus*, reaching maximum values of ca. 50%. A decrease in the Mediterranean forest and an increase in hygrophytes and Poaceae occurred between 10.1 and 9.6 cal ka BP (from 3.28 to 3.01 m). Deciduous *Quercus* show increasing trends between 9.5 and 7.6 cal ka BP (~2.91 to 2.31 m), recording average maxima with values of around 22% at that time. Hygrophytes reach maxima average values of approximately 17%, from ~9.8 to 8.8 cal ka BP (from 3.16 to 2.63 m). Algae display a decreasing trend from around 9% (from ~11.6 to 9.9 cal ka BP/3.67 to 3.20 m) to 2% (from ~9.9 to 7.6 cal ka BP/3.20 to 2.34 m). This algal decline between ~11.6 and 9.9 cal ka BP is due to the lowering of *Zygnema* spores. An increase in the soil mycorrhizal fungus *Glomus* type occurs from ~9.6 to 9.3 cal ka BP (from 3.01 to 2.80 m).

This transition between the Early and Middle Holocene is featured by a slight decrease in deciduous *Quercus* and in wetland plants such as Cyperaceae and *Typha* type.

3.3.2. From ~7.6 to 4.7 cal ka BP (from ~2.34 to 1.13 m)

The Middle Holocene from ~7.6 to 4.7 cal ka BP was still characterized by high values of Mediterranean forest (averaging values of ca. 58%) interrupted by several events of forest decrease. One of the most significant Mediterranean forest declines (up to 26%) parallel hygrophyte and Poaceae rise between ~7.5 and 7.3 cal ka BP (2.28 to 2.21 m). A slight increase in algae also occurred around ~7.6 to 7.1 cal ka BP (2.31 to 2.11 m). A second decrease in the Mediterranean forest occurred at ~6 cal ka BP (from around 1.65 m), also characterized by the increase in hygrophytes to

maximum values around 40 %, and the increase in *Pinus* of around 5 to 12 %. A third remarkable decrease in Mediterranean forest occurred between ~5.5 to 5.4 cal ka BP (around 1.43 to 1.39 m), also characterized by the increase of the aquatic component. These three previous events of decrease in forest decline are accompanied by slight *Glomus* type increases.

3.3.3. From ~4.7 to Present (from ~1.13 m to top)

The Middle to Late Holocene transition (from ~ 4.7 cal ka BP/~1.13 m) is characterized by the decrease in Mediterranean forest, in particular in the deciduous tree taxa, from average values around 58% during the Middle Holocene to about 25 %. Other significant changes are: the increase in shrubs such as Ericaceae from values around 1% to ~8% reaching maxima of ~30%, a strong increase of xerophytes and Asteraceae (mainly Cichorioideae), and a *Pinus* expansion from 8% to 17%. An increase in algae between ~4.7 to 1.5 cal ka BP (from ~1.13 to 0.28 m), reaching a peak at around 2.5 to 1.7 cal ka BP (from around 0.5 to 0.43 m), is also remarkable within this period.

Even though Mediterranean taxa show an overall decreasing trend during this phase, they increased relatively between ~ 2.6 and 1.6 cal ka BP to average values around 31%. This peak in Mediterranean forest was accompanied with an increase in algae, which as largely dominated by *Botryococcus*, to average values of 13 %.

The most important pollen changes during the last ~1.5 cal ka BP are the decline in arboreal pollen and algae and the increase of Cichorioideae, and during the last ~0.4 cal ka BP the significant increase in Poaceae.

3.4. Correlations for the environment reconstruction

A linear r (Pearson) correlation analysis was carried out between the obtained local proxy dataset (MS, Ca, S, Br, Sr, K/Si ratio, C/N ratio, H/C ratio, TOC, short-chain, mid-chain and long-chain abundances, Poaceae, Algae and Hygrophytes; Table 4]. This correlation analysis helped us associating all these proxies and understanding environmental change in the Padul area. This analysis assisted us differentiate proxies

characteristic of organic-rich sediments, primarily those peatland environment under very shallow lake conditions (higher TOC, C/N ratio, S, Br, Sr and mid-chain) to deeper shallow water environments characterized by the increase in endogenic carbonates and more influenced by terrestrial-clays input (higher Ca, K/Si, MS, Algae).

3.5. Spectral analysis

Spectral analysis was performed in order to find cyclical periodicities in the Mediterranean forest from the Padul-15-05 record using REDFIT analysis (Schulz and Mudelsee, 2002) detecting a periodicity of around ~2067, 1431 and 1095 yr. Wavelet transform analysis is a useful tool for detection of periodicities in time series with nonstationary cyclical patterns (Torrence and Compo, 1998). Wavelet analyses show significant cycles ($p = 0.05$) in the Mediterranean forest taxa time series with periodicities around ~2067 and 1095 yr during the Early and Middle Holocene period and ~1431 yr during the last ~4.7 cal ka BP.

Table 4. Linear r (Pearson) correlation between geochemical proxies and pollen data from the Padul-15-05 record. Statistical treatment was performed using the Past software (http://palaeo-electronica.org/2001_1/past/issue1_01.htm).

	C/N ratio	H/C ratio	TOC	MS	Poaceae	Algae	Hygrophyte	Short-chain	Mid-chain	Long-chain	S	Br	K/Si	Ca	Sr
C/N ratio		5.33E-16	6.30E-33	9.48E-13	9.41E-07	7.14E-02	2.11E-10	3.67E-05	0.0093249	9.69E-01	2.15E-30	1.24E-13	4.56E-08	1.05E-24	5.60E-20
H/C ratio	-0.60595		4.97E-16	1.25E-54	0.24997	0.83873	0.014101	1.36E-11	0.16571	0.040739	4.80E-11	3.45E-08	1.03E-10	9.55E-09	9.85E-17
TOC	0.79396	-0.60645		1.03E-12	8.08E-08	0.00097023	5.41E-10	1.26E-11	0.00011256	0.80183	2.41E-65	1.04E-36	1.02E-10	2.05E-39	6.36E-49
MS	-0.54666	0.90279	-0.54594		0.58699	0.64816	0.018814	2.33E-09	1.03E-01	0.12274	4.44E-09	2.02E-07	2.83E-11	1.60E-06	4.34E-15
Poaceae	0.39277	-0.095815	0.42633	-0.045323		0.00096771	5.25E-07	0.37586	5.61E-01	0.99854	8.46E-08	0.00018098	0.019496	6.83E-06	0.00031762
Algae	-0.14967	-0.016988	-0.27025	-0.038078	-0.27031		0.0028618	0.6669	9.08E-05	0.0073904	0.0043751	8.23E-05	0.00030366	0.13141	0.00039267
Hygrophyte	0.49514	-0.20278	0.4852	-0.19424	0.40108	-0.24514		0.29595	1.53E-08	0.00034311	1.54E-12	5.19E-10	0.016645	1.67E-10	1.44E-06
Short-chain	-0.33565	0.52387	-0.52465	0.4706	-0.074081	0.036044	-0.087385		0.0010611	5.42E-22	6.36E-08	1.93E-08	4.50E-05	8.70E-08	2.48E-11
Mid-chain	0.21524	-0.11572	0.31522	-0.13612	0.048675	-0.31926	0.44853	0.26917		1.93E-48	5.05E-05	3.19E-03	6.52E-02	0.00011163	3.23E-05
Long-chain	0.0032797	-0.17016	0.021023	-0.12875	-0.00015362	0.2216	-0.29331	-0.6921	-0.88146		0.66657	0.66508	5.68E-01	0.7461	0.99199
S	0.77416	-0.51013	0.93201	-0.46179	0.42573	-0.23457	0.54234	-0.43076	0.32998	-0.036081		9.63E-42	3.78E-12	4.77E-34	5.58E-40
Br	0.56396	-0.43716	0.81996	-0.41423	0.30507	-0.32002	0.48565	-0.44574	0.24327	0.036253	0.84907		2.40E-07	8.36E-27	7.26E-26
K/Si	-0.43366	0.50252	-0.50258	0.51532	-0.19316	0.29481	-0.1979	0.33204	-0.15353	-0.047753	-0.53426	-0.41189		0.22728	2.33E-21
Ca	-0.72099	0.45282	-0.83631	0.38503	-0.36269	0.12543	-0.49757	0.42671	-0.31537	0.027119	-0.80209	-0.74218	0.10054		5.65E-19
Sr	0.6649	-0.61781	0.88208	-0.59051	0.2939	-0.28956	0.38657	-0.51813	0.33788	0.00084107	0.83951	0.73296	-0.68263	-0.65119	

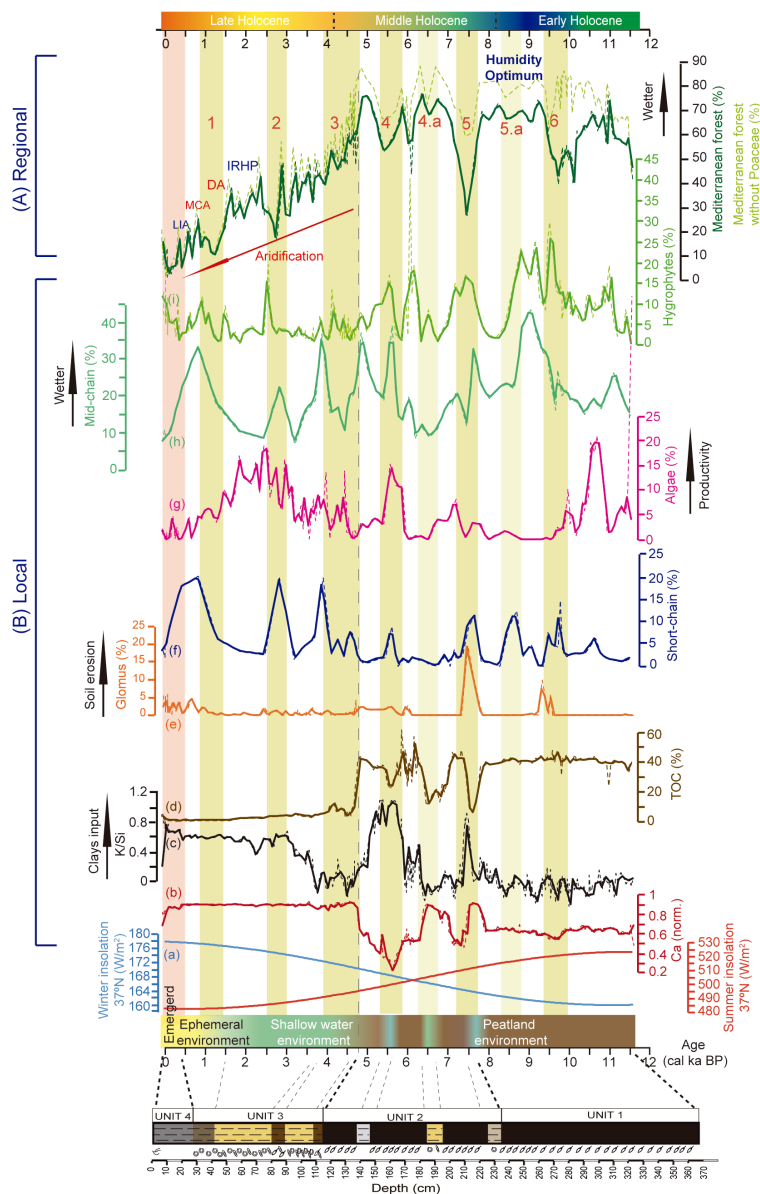


Figure 6. Padul-15-05 local environment development during the Holocene deduced for a comparison between different pollen, organic and inorganic geochemistry proxies from the Holocene part of the Padul-15-05 record and summer and winter insolation for the Sierra Nevada latitude. A) Regional response determined by Mediterranean forest taxa (%). B) Local response: (a) Summer and winter insolation calculated for 37°N (Laskar et al., 2004), (b) Ca (norm.) (c) K/Si ratio (clays input), (d) Total organic carbon percentage (TOC %), (e) *Glomus* type (%) (f), Short-chain (%), (g) Algae percentage from the pollen analysis (h) Mid-chain (%), (i) Hygrophytes percentage. Beige shadings are showing arid and cold event during the Early and Middle Holocene determined by the decline in Mediterranean forest component and

showing the response in the local environment. Proxies were resampled at 80 yr (in bold) by lineal interpolation using Past software (http://palaeo-electronica.org/2001_1/past/issue1_01.htm).

4. Discussion

4.1. Holocene climate change in Padul and the western Mediterranean region

4.1.1. The earliest Holocene

During the earliest Holocene (~11 to 10 cal ka BP) a transition period from glacial to interglacial conditions occurred in the Padul area and the pollen assemblages were dominated by evergreen *Quercus* and to a lesser extent, mesic forest species such as deciduous *Quercus*. Local environment proxies show a development of a peatland environments in the Padul basin (organic facies featured by higher values of TOC and C/N and lower values of mid-chain, short-chain and S; Fig. 6), which indicate low water levels at that time. The increase in Mediterranean forest taxa may be interpreted as a regional vegetation response to a climate change to warmer and more humid conditions than earlier on during the cold and dry Younger Dryas, agreeing with the increasing trend in SSTs reconstructions from the Alboran Sea (Cacho et al., 1999; Rodrigo-Gámiz et al., 2014b; Fig. 7). The observed peak of evergreen *Quercus* is consistent with previously described glacial-interglacial vegetation transition from Southern Europe indicating that a cold-dry steppe was followed by pre-temperate open woodland [including *Juniperus*, *Pinus*, *Betula*, *Quercus*; Van der Hammen et al. (1971)]. These results agree with the previous pollen records from Padul, which also show a widespread evergreen *Quercus* forest after the postglacial epoch (Pons and Reille, 1988) and other high-resolution pollen study in the western Mediterranean region that show a similar forest change with high abundance of Mediterranean taxa (Fletcher and Sanchez-Goñi et al., 2008; Fig. 7). These results are also consistent with vegetation variability in the Middle Atlas Mountains of Morocco depicting high values of evergreen *Quercus rotundifolia* (Lamb and van der Kaars, 1995). A forest expansion is also observed in the nearby, but higher elevation site, Laguna de Rio Seco in Sierra Nevada, but in this case it is mostly due to *Pinus* expansion after a pollen assemblage dominated by steppe vegetation (Anderson et al., 2011; Fig. 7).

This dissimilarity is probably explained by the altitudinal difference between the two sites (Padul=750 vs. Laguna de Rio Seco=3000 m), being influenced by different vegetation belts (mesomediterranean vs. oromediterranean belt; see Table 1). The continental pollen record of the cave site Carihuela, inland Granada at the supramediterranean, also shows a clear oak dominance during this period (Carrión et al., 1999; Fernández et al., 2007).

A punctual increase in algae (principally dominated by *Zygnema* type) also occurred within this peat-dominated and shallow water period at around ~10.5 cal ka BP. We suggest that this increase in algae could probably be linked with an increase in productivity in the wetland due to increased temperatures during a warm pulse recorded in the North Atlantic ice record (Bond et al., 2001; Fig. 9).

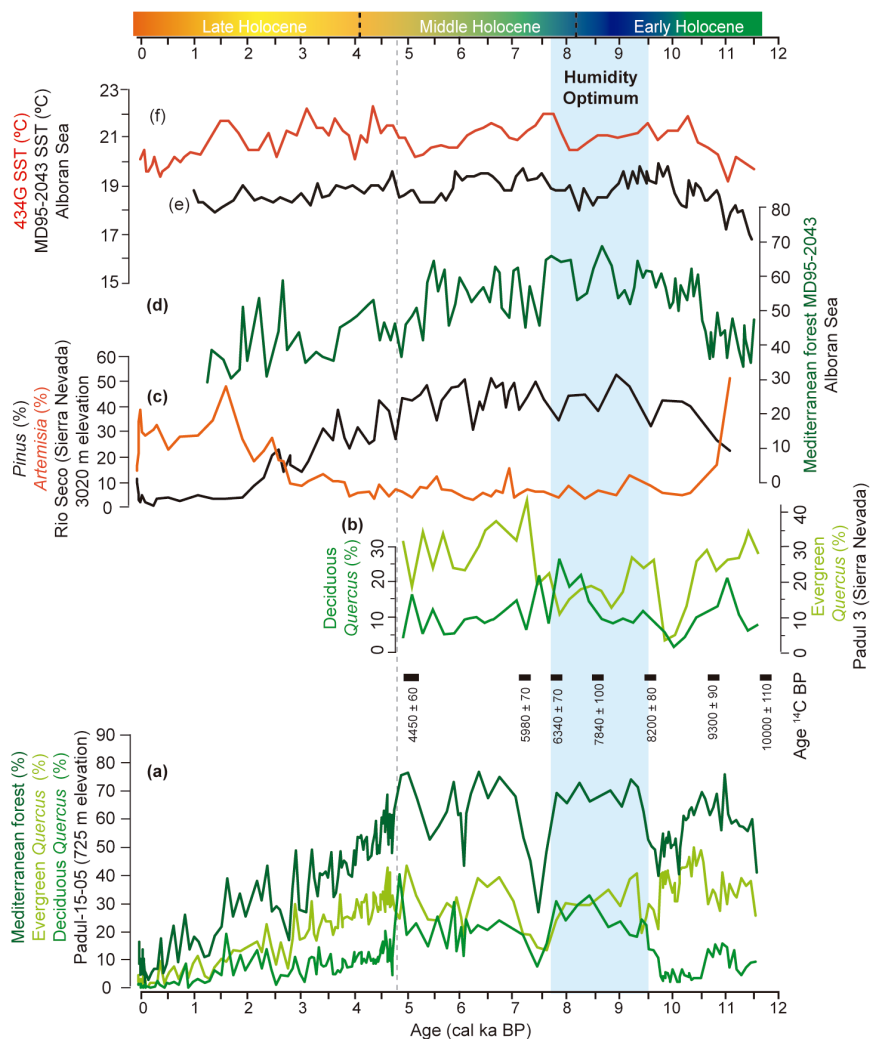


Figure 7. Comparison for the Holocene between different pollen taxa from the Padul-15-05 record with a previously pollen record in the same area and other pollen and temperature proxies from nearby areas in the western Mediterranean region. (a) Deciduous *Quercus*, Evergreen *Quercus* and Mediterranean forest percentages in the Padul-15-05 record, (b) Deciduous *Quercus* and Evergreen *Quercus* in a previously record in the Padul peat bog (Pons and Reille, 1988), (c) Percentage of *Pinus* and *Artemisia* in the nearby Laguna de Rio Seco record, Sierra Nevada (Anderson et al., 2011), (d) Temperate and Mediterranean forest percentage for the MD95-2043 record, Alboran Sea (Fletcher and Sánchez-Goñi, 2008) (e) Alkenone sea surface temperature (SST) reconstruction from the MD95-2043 record, Alboran Sea (Cacho et al., 1999) (f) Alkenone sea surface temperature (SST) reconstruction from the 434G record, Alboran Sea (Rodrigo-Gámiz et al., 2014b). Blue shading represents the humidity optimum during the Holocene in the western Mediterranean region.

4.1.2. Early and Middle Holocene and Humidity optimum

The Early to Middle Holocene (from ~10 to 4.7 cal ka BP) in the Padul-15-05 record is featured by the highest values of Mediterranean forest showing the expansion in mesic components (e.g. deciduous *Quercus*), agreeing with the ideal temperate phase of vegetation transition during interglacial periods (described by Van der Hammen et al., 1971 and reviewed by Tzedakis et al., 2007; Fig. 8). The local Padul wetland environment within this period (~10 to 4.7 cal ka BP) was characterized by generally low water levels, triggering high occurrence of wetland plants, which accumulated in great amounts, generating peat sedimentation probably related with anoxic/reducing conditions and associated geochemical signals (i.e. higher values of TOC, C/N, S and an increase in mid-chain; Figs. 5 and 6). There is an apparent contradiction between the regional vegetation signal indicating high humidity and local sedimentary proxies pointing to low water levels in the area. This contradiction could be explained due to very strong evapotranspiration during Holocene summer insolation maxima (Laskar et al., 2004) even if annual (mostly winter) precipitation was highest (Fig. 6). Low lake levels during the regionally humid Early Holocene have also been observed in other records from the southern Mediterranean area, pointing to the same high-evaporative summer insolation phenomenon (Lamb and van der Kaars, 1995; Reed et al., 2001; Magny et al., 2007).

Despite the overall humid conditions interpreted for the Early and Middle Holocene, millennial-scale climate variability occurred (see section 4.1.4 below) and wettest conditions are observed between ~9.5 to 7.6 cal ka BP in the Padul-15-05 record. This humidity optimum is indicated regionally by the maximum expansion of mesic forest species (deciduous *Quercus*). Our new results from Padul agree with the previously described Holocene climate evolution in the western Mediterranean region, which also show a wet Early and Middle Holocene and a transition to drier conditions in the Late Holocene (Carrión et al., 2010a; Anderson et al., 2011; Fletcher et al., 2013 among others). The maximum in humidity occurred during summer insolation maxima and thus during the warmest Holocene conditions shown by paleoclimate records such as the Greenland ice core record temperature

reconstruction, decrease in the Drift Ice Index in the north Atlantic records, total solar irradiance (TSI) and regionally the SST reconstructions in the Alboran Sea (Cacho et al., 1999; Alley, 2000; Bond et al., 2001; Steinhilber et al., 2009; Rodrigo-Gámiz et al., 2014b; Figs. 7 and 9). Support for the timing of the Holocene humidity optimum recorded in Padul-15-05 comes from a number of paleoclimatic studies from nearby places. For example, previous pollen results from the Padul sedimentary sequence show a similar increase in deciduous *Quercus* and maximum humidity at the same time (Pons and Reille, 1988; Fig. 7). The close by alpine site of Laguna de Rio Seco in Sierra Nevada indicate that the Early and Middle Holocene is characterized by more abundant mesic vegetation and the maximum in algae and aquatic plants, indicating that humid maxima occurred prior to ~7.8 cal ka BP (Anderson et al., 2011). Jimenez-Espejo et al. (2008) in a study in the Algero-Balearic basin described that the end of the Holocene humid conditions occurred between ~7.7 and 7.2 cal ka BP and a synthesis about circum-Mediterranean vegetation change analyses determined that two principal climatic phases occurred during the Early and Middle Holocene, with a more humid phase from 11 to 7.5 cal ka BP and a transition phase from 7 to 5.5 cal ka BP, the later mostly related with the decrease in insolation and the installation of the present climate dynamic (Jalut et al., 2009). Dormoy et al. (2009) also described the maximum in humidity in the Mediterranean region during the Early and Middle Holocene between 9.5 and 7.5 cal ka BP, determined by maximum seasonal anomaly characterized by greatest winter precipitation and minima in precipitation during summer. However, some discrepancies exist about the timing of the mesic maximum within this generally humid period in the Mediterranean region and continental and marine records from southern Iberia and north Africa pointed out that the mesic maximum occurred later on during the Middle Holocene (Lamb and van der Kaars, 1995; Carrión, 2002; Fletcher and Sánchez-Goñi, 2008). Supporting our hypothesis, Anderson et al. (2011) suggested that this difference in timing between montane and subalpine forest development and lower elevation water lake levels could be associated to the different effect that summer insolation maxima and higher seasonality during the Early Holocene provoked in effective precipitation and water levels in the lowland, with higher evaporations rates

during summer, compared to higher elevation areas and alpine lakes with lower summer temperatures and higher snowpack during winter and subsequently high lake level.

The Early Holocene thermal maximum could be explained by maximum orbital-scale summer insolation (Laskar et al., 2004; Figs. 6 and 9). The Early Holocene humidity maximum was likely due to enhanced of fall/winter precipitation, consistent with global climate models predicting that summer insolation maxima favor the land/sea temperature contrast in the Mediterranean thus enhancing the winter rainfall (Meijer and Tuenter, 2007). This occurred at the same time that the Intertropical Convergence Zone was displaced northward (prior to ~6 ka BP) into the Sahara and Arabian desert (Gasse and Roberts, 2004). Arz et al. (2003) and Tzedakis (2007) concluded that summer monsoon did not reach further than the Africa subtropical desert during the Early and Middle Holocene and would not hav a direct influence over the Mediterranean coast.

Sedimentation at that time in the Padul basin is homogeneous peat but the local proxies show some oscillations (see in section 4.1.4).

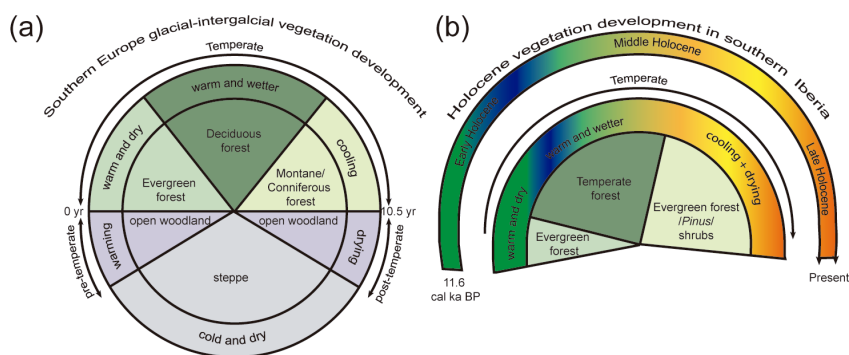


Figure 8. (A) Vegetation succession during an idealized glacial-interglacial cycle in southern Europe with sufficient moisture availability during a precessional period (modified from Tzedakis, 2007). (B) Vegetation succession in southern Iberian since ~11.6 cal ka BP.

4.1.3. End of the humid period and significant environmental change around 4.7 cal ka BP

The Padul-15-05 record shows the most significant climatic change affecting both regional and local environment at ~ 4.7 cal yr BP, right at the Middle to Late Holocene transition. This paleoenvironmental change is regionally depicted by the beginning of a strong decrease in Mediterranean (especially in the deciduous) forest, indicating progressive climate drying conditions, a slight increase in *Pinus*, and an increase in Ericaceae. Similar vegetation changes, with the decline in mesic forest species and the increase in shrubs such as Ericaceae, have previously been recorded in other terrestrial and marine pollen archives from the western Mediterranean region during the transition to the Late Holocene (e.g., Carrión, 2002; Carrión et al., 2003; 2007; 2010b; Fletcher and Sánchez-Goñi, 2008; Gil-Romera et al., 2010) pointing to a regional response to climate aridification and reduction in seasonality (i.e. cooler summers and warmer winters). The timing of this change agrees with Magny et al. (2002) who described the period at 4.5 cal ka BP, as a crucial transition from wetter to drier climate in the Mediterranean region. In addition Jalut et al. (2009), described the aridification process in the Mediterranean region since 5.5 cal ka BP.

This climatic change also locally affected the Padul wetland environment and sedimentation changed drastically from mostly peat (unit 2) to carbonate-rich clays (unit 3) rich in aquatic organisms (charophytes and gastropods; between ~ 4.7 to 1.5 cal ka BP) pointing to an increase in the lake level. This sedimentary change is principally featured in the geochemistry by a decrease in organic content, a decrease in the aquatic plants in the lake (lower values of TOC, C/N and generally decrease in mid-chain index), an increase in Ca and in the palynomorph record by a continuously increase in algae (principally dominated by *Botryococcus*). In addition, a higher terrestrial and detrital input occurred during the aridification trend, observed in the Padul-15-05 by a slight increasing trend in soil erosion (*Glomus*) and clastic input (higher K/Si), most likely due to the decrease in Mediterranean forest in the area.

As discussed above, there seems to be a contradiction between regional proxies, showing increased aridity, and local proxies showing increasing lake levels. This

could be explained due to varied effect of the orbital-scale decrease in summer insolation in both environments. A decrease in summer insolation would trigger a decrease in the sea surface temperature reducing the wind system and precipitation from sea to shore during winter (Marchal et al., 2002) and would also shorten the length of the growing season thus provoking forest depletion. However, decreasing summer insolation would also reduce the seasonality and would lower evapotranspiration during summer, affecting the evaporation/precipitation balance. This along with the continuous groundwater supply in the Padul basin would explain the increasing lake levels in the Padul wetland during the Late Holocene (Fig. 6). Some authors also related this aridification trend with the establishment of the actual atmospheric dynamics with a northward shift of the westerlies -and as consequence a long-term NAO-like positive mode- affecting the western Mediterranean region (Magny et al., 2012). In addition, this climatic shift coincides with the end of the African Humid Period (5.5 ka BP; deMenocal et al., 2000). Shanahan et al. (2015), suggest that the decrease in rainfall at this time shown in the African paleoclimate records (tropical and subtropical Africa) is related with declining in summer insolation and the gradual southward migration of the tropical monsoon.

Within the context of regional progressive aridification, the Late Holocene (*sensu lato*) from Padul could mainly be divided into two phases, a first phase from ~4.7 to 3 cal ka BP characterized by the slight increasing trend in *Botryococcus* and the declining trend in AqP index, and a second phase from ~3 to 1.5 cal ka BP featured by maximum values in *Botryococcus* and a minimum in AqP index (Fig. 6). Relative maxima in Mediterranean forest between ~2.6 and 1.6 cal ka BP, indicating regional humidity, co-occurred with the maximum in *Botryococcus* algae also indicating either high relative lake level and/or more productivity in the lake. High relative humidity in this region is supported by the fact that this mild climatic event occurred during the well-known Iberian Roman Humid Period (IRHP; between 2.6 to 1.6 cal ka BP; (Martín-Puertas et al., 2009).

The aridification trend enhanced around ~1.5 cal ka BP and culminated with a further environmental change to an ephemeral lake (even emerged during the last centuries). This is deduced by the remarkable increase in detritic sedimentation (K/Si;

Fig. 6), probably due to higher soil erosion (increase in *Glomus* type) partially enhanced by human activities in the surroundings of the lake since this time (Ramos-Román et al., in press.), and by a continuous increase in mid-chain, short-chain abundance and wetland plants while *Botryococcus* and other aquatic organisms (especially charophytes) declined. Aquatic plants probably expanded in the Padul wetland area when the water levels dropped. This increasing trend in mid-chain and short-chain abundance started to decline during the last centuries when the wetland became emerged and higher human impact occurred (for more information about human activities see Ramos-Román et al., in press.).

The ~4.7 to Present natural aridification process was interrupted by millennial-scale climate variability with several especially arid events occurring around ~4.7-4, 2.7 and 1.3 cal ka BP (see next section; 4.1.4).

4.1.4. Millennial-scale Holocene climate variability

In addition to the long-term trends observed in the Padul paleoenvironments, likely driven by insolation-related climate changes during the Holocene, the high-resolution multi-proxy record from Padul-15-05 shows millennial-scale vegetation, lake level and sedimentary oscillations that can be related with global climate change and cooling events detected in North Atlantic archives. In this respect, the Padul-15-05 sequence shows arid-cooling climatic events around ~9.6, 8.5, 7.5, 6.5, 5.4, 4.7-4, 2.7 and 1.3 cal ka BP, generally identified in both regional (decreases in the Mediterranean forest suggesting regional cooling and aridity) and local proxies (increases in clays input, short-chain, mid-chain and hygrophyte) and with periodicities of about 2100 and 1100 years. These short-scale climatic changes affected sedimentation and local lake level in the Padul environment, generally with increases in carbonate (charophytes and gastropods) and clastic sedimentation, hygrophytes, short-chain and mid-chain abundances pointing to higher lake levels probably triggered by cooling and less evaporation in the wetland, enhanced erosion due to deforestation and increase in plants adapted to more aquatic wetland environments (Fig. 6). Some of these events are manifested in the Padul-15-05 record

clearly in both regional and local proxies (~9.6, 7.5, 5.4, 4.7-4, 2.7, 1.3 cal ka BP) but some others are more evident in the local signal (for example events at 8.5 and 6.5 cal ka BP), probably indicating that those events were less severe and/or problems recording them sufficiently well in the pollen. During the last ~4.7 cal ka BP, during the establishment of the actual climate dynamics and the decrease in summer insolation, a shallow lake formed and these cold events are also associated with declines in the lake productivity (for example reductions in algae before and after the IRHP; Figs. 6 and 9).

Most of these climatic events have been described in other Mediterranean paleoclimate records, considering the radiocarbon age uncertainties between the different studies. For example, Jalut et al. (2000) also described aridification phases for the western Mediterranean region around ~10.9-9.7, 8.4-7.6 and 5.3-4.2, 4.3-3.4, 2.8-1.7 and 1.3-0.75 cal ka BP, showing that these events were correlated with glacial advance, ^{14}C anomalies, North Atlantic records and paleohydrological changes in European mid-latitudes suggesting that they were a regional response to global climate change. Some arid events around ~9.6-9.5, 8.4-8 and 6-5.5, have been also identified as arid and cool events in a study from the eastern and western Mediterranean region (Dormoy et al., 2009). Fletcher and Zielhofer (2013) detected these rapid climate changes relating these arid periods with high-latitude cooling events around 6-5 and 3.5-2.5 cal ka BP. Recently, Zielhofer et al. (2017) show decrease in western Mediterranean winter rain at 11.4, 10.3, 9.2, 8.2, 7.2, 6.6, 6.0, 5.4, 5.0, 4.4, 3.5, 2.9, 2.2, 1.9, 1.7, 1.5, 1.0, 0.7, and 0.2 cal ka BP. They associate these events during the Early Holocene with Atlantic coolings probably related with meltwater discharges and weakening of the Atlantic overturning circulation. In contrast, after ~5 cal ka BP relating these Atlantic coolings with humid winters and negative NAO conditions evidencing a change in the ocean-atmospheric system in response to the external forcing. In the nearby Sierra Nevada, arid events are detected around 3.8-3.1 and 1.8-0.7 cal ka BP (Laguna de la Mula; Jiménez-Moreno et al., 2013). Cold and arid events detected in the Padul-15-05 record at ~9.6, 8.5, 7.5, 6.5, 5.4, 4.7-4, 2.7 and 1.3 cal ka BP have been also identified in North Atlantic records (Bond events 6, 5, 4, 3, 2, 1; Bond et al., 2001; Fig. 9), which indicate that these events were recorded

at hemispheric scales. The good correspondence with the timing of these cold events with decreases in solar activity recorded by the TSI anomaly during the Holocene could show a link between them (Steinhilber et al., 2009; Fig. 9). This would agree with previous studies showing a strong sun-climate-environment relationship (Zielhofer et al., 2017).

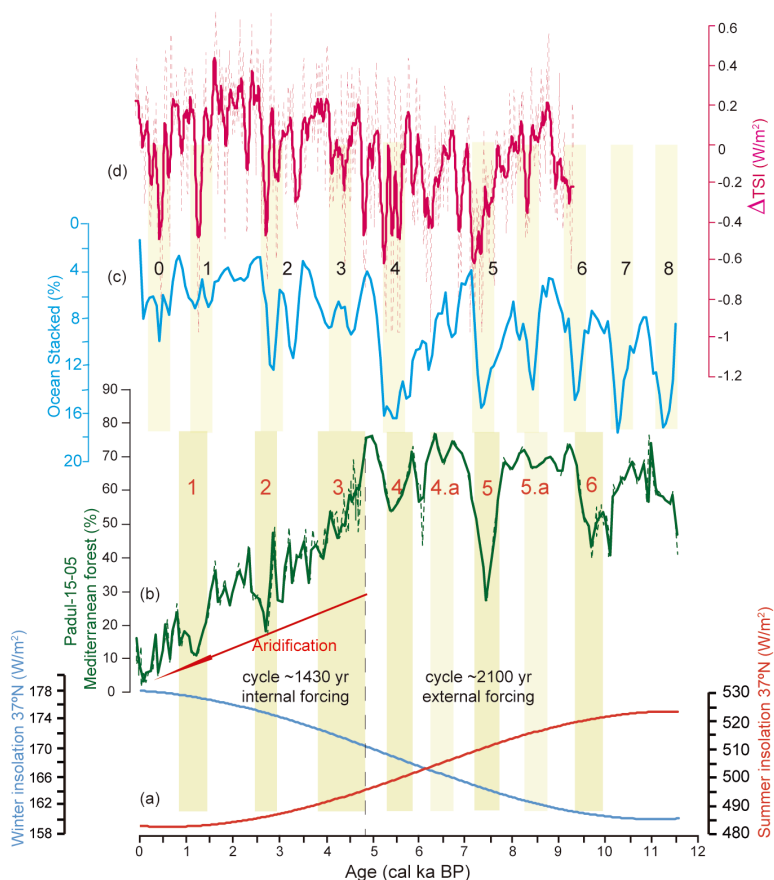


Figure 9. Holocene climate periodicity from the Padul-15-05 record determine by declines in the Mediterranean forest component and comparison with other North Atlantic records. (a) Summer and winter insolation for calculated for 37° N (Laskar et al., 2004), (b) Mediterranean forest taxa (c) Drift Ice Index (reversed) from the North Atlantic (Bond et al., 2001), (d) Total solar irradiance anomaly reconstruction from cosmogenic radionuclide from a Greenland ice core (Steinhilber et al., 2009). Beige shadings represent the decrease in Mediterranean forest component and maximum in cold events related with decrease in total solar irradiance.

4.1.5. Forcing mechanisms of Holocene millennial-scale climate variability in the western Mediterranean region

The time series analysis done on the Mediterranean forest (regional proxy) from the Padul-15-05 record using a wavelet analysis evidence millennial-scale cyclical periodicities during the Early, Middle and Late Holocene. This analysis helps to understand the relationship between the regional paleoenvironmental periodicity in the proxy data from the Padul record and external (i.e. solar activity) and internal (oceanic-atmospheric dynamics) forcings during the Holocene in the western Mediterranean. Cyclicities of around ~2100 yr and ~1100 yr are detected in the Mediterranean forest taxa time series with a statistically strong cyclical pattern during the Early and Middle Holocene (the ~1100 yr cycle is absent in the Late Holocene), and a predominant ~1430 yr cycle between the transition of the Middle-Late Holocene and during the Late Holocene (Supplementary Fig. S4).

Our results are consistent with similar cyclical patterns detected throughout the North Atlantic records and related with solar activity also describing ~2500 and 1000 yr periodicities during the Early Holocene (Debret et al., 2007; 2009). A similar periodicity of about 2300 yr is recognized in the $\Delta^{14}\text{C}$ residual series from the Greenland Ice Sheet record (Mayewski et al., 1997). This periodicity has also been evidenced in sea surface temperatures (SST) reconstructions in the Aegean Sea in the NE Mediterranean related with glacier advance and suggesting a solar modulation (Rohling et al., 2002). The ~1000 yr periodicity is also established as a signal of solar activity in many other records in the Mediterranean and the North Atlantic region (e.g. Debret; 2007; 2009 and references therein). Previous cyclostratigraphic analysis performed in the nearby Sierra Nevada alpine area also described cyclical climatic fluctuations with periodicities around 2200 yr (Jiménez-Espejo et al., 2014). In contrast, other spectral analyses carried out in other records in the North Atlantic and western Mediterranean region detected a periodicity of around ~1500 yr (e.g. Bond et al., 2001; Rodrigo-Gámiz et al., 2014a). This ~1500 yr cycle is also common in other Sierra Nevada records (Jiménez-Espejo et al., 2014; García-Alix et al., 2017) and was interpreted as a solar and atmospheric-oceanic forcing mechanism. In

addition, a cycle of ~800-760 yr has also been detected in the detailed studied of the Late Holocene part of the Padul-15-05 record (Ramos-Román et al., in press.) and in other records in the Sierra Nevada (Ramos-Román et al., 2016). This cycle could be related to the second harmonic of the ~1600-1500 yr cycle. These results show very mixed interpretations with both solar and/or oceanic forcing mechanisms being described to explain cyclicities in the different proxies. Debret et al. (2009) in a non-stationary time series analysis tries to differentiate the different forcing mechanisms for the different cyclicities and also described an intensification of the ~1600 yr period detected in the North Atlantic area (terrestrial and marine records and interpreted of both solar and oceanic origin) in the last 5 cal ka BP. Those authors then interpret this cyclical periodicity change as a shift in dynamics from mostly external (solar) forcing to mostly internal (oceanic) forcing.

According to this, the Holocene results from the Padul-15-05 record evidence that the regional climate variability during the Early and Middle Holocene was due to external forcing (i.e. solar irradiance) and variability during the Late Holocene (since ~4.7 cal ka BP) was dominated by the effect of internal forcing (atmospheric-oceanic dynamic) -established since the NAO system influencing the western Mediterranean region- enhanced since ~5 cal ka BP (Debret et al., 2007; 2009). Fletcher et al. (2013) described a shift in the millennial-scale periodicity since around ~6 cal ka BP related with the establishment of the actual climate system in the western Mediterranean region. The similarities between the millennial-scale oscillations observed in the Padul-15-05 record with the total solar irradiance anomaly (TSI) and cooling events in the North Atlantic region (e.g. Bond et al., 2001; Steinhilber et al., 2009; Fig. 10) support the solar-atmospheric-oceanic link in the Atlantic-western Mediterranean region previously suggested (Debret et al., 2009).

5. Conclusions

Variations in regional and local paleoenvironmental and paleoclimate proxies from the Padul-15-05 core helped us to interpret climate and paleoenvironmental change during the last 11.6 cal ka BP in southern Iberia and the western Mediterranean region. The comparison of our record with other regional and global

oceanic-atmospheric-terrestrial studies aided to comprehend the origin of these paleoenvironmental changes.

The Early and Middle Holocene was characterized by overall humid and warm conditions and a humidity optimum between ~ 9.5 and 7.6 cal yr BP, humid winters and very hot and dry summers and a higher seasonality, occurred in this area due to summer insolation maxima. These interpretations come from the highest occurrence of deciduous tree species and humid conditions in the local environment (higher mid-chain abundance) in the Padul-15-05 core. Summer insolation maxima translated into very high evaporation rates and lowest lake level conditions triggering the abundance of wetland plants and the deposition of peat related with the higher TOC. A transition phase towards drier conditions is recorded in the Middle Holocene between ~ 7.6 and 4.7 cal ka BP through a decrease in deciduous forest and a higher water level variability mainly associated with variations in Ca, K/Si and TOC content. This environmental change was mostly due to a reduction in seasonality and decreasing summer insolation, which also locally triggered less evaporation and the alternation of water level increase within a peatland environment. This climate transition culminated in the Padul area with a significant environmental change at ~ 4.7 cal ka BP, featured by a regional aridification trend that produced a decreasing trend in the Mediterranean forest. Precipitation decreased in the Late Holocene but the decrease in summer insolation locally triggered less evaporation and the development of a shallow water lake environment and a significant sedimentary change characterized by higher values of Ca an increasing trend to increase in clays minerals (K/Si ratio), and the decrease in TOC.

The Padul-15-05 record also shows millennial-scale climate variability with declines in Mediterranean forest showing cool-arid events and variability in the lake level around 9.6 , 8.5 , 7.5 , 6.5 , 5.4 , 4.7 - 4 , 3 , 2.7 and 1.3 cal ka BP, associated with cold events in the North Atlantic records. According to the regional (Mediterranean forest taxa) paleoclimate results from the non-stationary time-series analyses, climate during the Early and Middle Holocene was mostly controlled by external solar forcing with typical periodicities around 1100 and 2100 yrs, and the last ~ 4.7 cal ka BP were

dominated by a more internal oceanic/atmospheric control as periodicities changed towards ~1430 yr in the regional paleoclimate proxy.

We would like to remark the importance of carrying out multi-proxy analyses containing both regional and local signals and a non-stationary time-series analysis in order to clarify the links between terrestrial-oceanic-atmospheric connections in Holocene paleoclimatic studies.

Acknowledgments

This work was supported by the project P11-RNM-7332 funded by Consejería de Economía, Innovación, Ciencia y Empleo de la Junta de Andalucía, the project CGL2013-47038-R funded by Ministerio de Economía y Competitividad of Spain and fondo Europeo de desarrollo regional FEDER and the research group RNM0190 (Junta de Andalucía). M. J. R.-R. acknowledges the PhD funding provided by Consejería de Economía, Innovación, Ciencia y Empleo de la Junta de Andalucía (P11-RNM-7332). J.C. acknowledges the PhD funding provided by Ministerio de Economía y Competitividad (CGL2013-47038-R). J.S.C. acknowledges the support of projects CGL-BOS-2012-34717, CGL-BOS 2015-68604, and Fundación Séneca 19434/PI/14. A.G.-A. was also supported by a Ramón y Cajal Fellowship RYC-2015-18966 of the Spanish Government (Ministerio de Economía y Competitividad). Javier Jaimez (CIC-UGR) is thanked for graciously helping with the coring, the drilling equipment and logistics.

Supplementary Information

Millennial-scale cyclical environment and climate variability during the Holocene in the western Mediterranean region deduced from a new multi-proxy analysis from the Padul record (Sierra Nevada, Spain)

María J. Ramos-Román¹, Gonzalo Jiménez-Moreno¹, Jon Camuera¹, Antonio García-Alix¹, R. Scott Anderson², Francisco J. Jiménez-Espejo³, Dirk Sachse⁴, Jaime L. Toney⁵, José S. Carrión⁶, Cole Webster²

¹ Departamento de Estratigrafía y Paleontología, Universidad de Granada, Spain

² School of Earth Sciences and Environmental Sustainability, Northern Arizona University, USA.

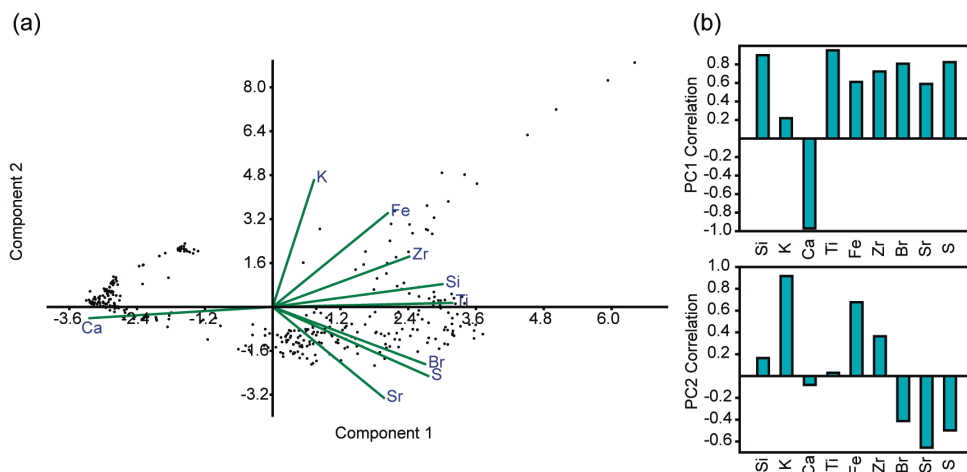
³ Department of Biogeochemistry, Japan Agency for Marine-Earth Science and Technology (JAMSTEC), Japan.

⁴ Helmholtz Centre Potsdam, German Research Centre for Geosciences GFZ, Section 5.1 Geomorphology, Organic Surface Geochemistry Lab., Germany

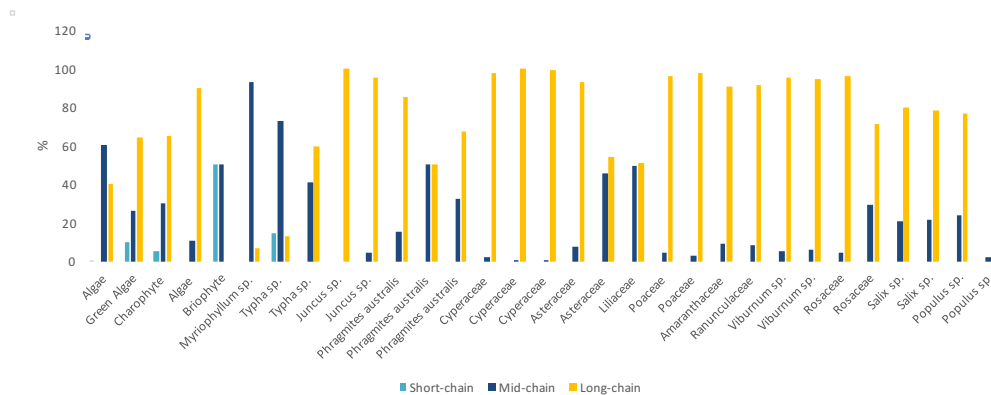
⁵ School of Geographical and Earth Sciences, University of Glasgow, UK

⁶ Departamento de Biología Vegetal, Facultad de Biología, Universidad de Murcia, Murcia, Spain

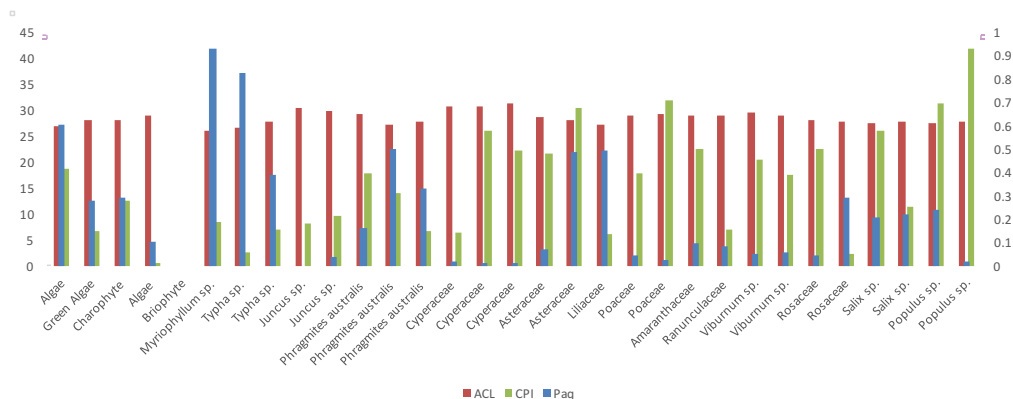
Supplementary Figures



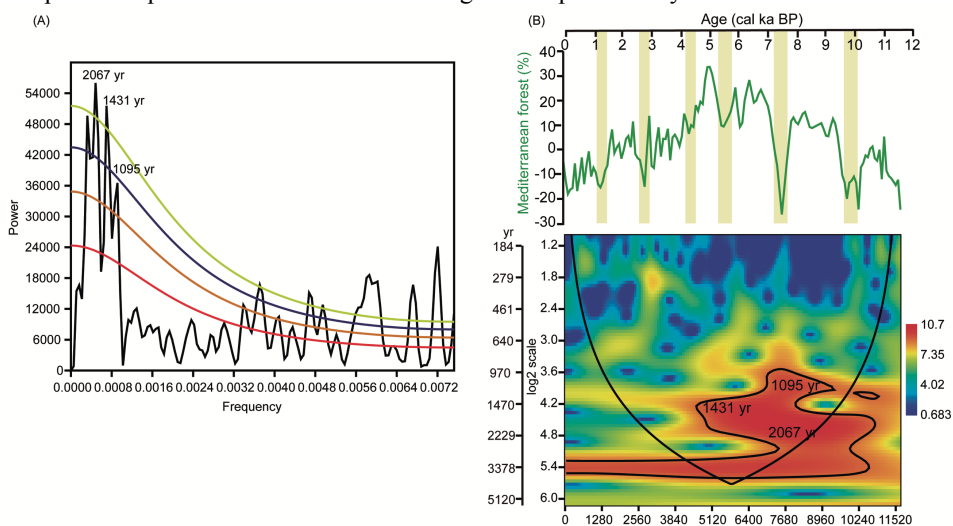
Supplementary Figure S1. X-ray fluorescence (XRF) PCA results from the Padul-15-05 record. (a) Biplot figure and (b) loadings (correlation) of the most significant components; PC1 (above) and PC2 (below). Statistical analysis was performed using Past software (http://palaeo-electronica.org/2001_1/past/issue1_01.htm).



Supplementary Figure S2. *n*-alkane indices [Short-chain, Mid-chain and Long-chain (%)] from the algae, bryophyte and plant samples studies in the surroundings of the present-day Padul lake.



Supplementary Figure S3. *n*-alkane indices (Paq, ACL and CPI) from the algae, bryophyte and plant samples studies in the surroundings of the present-day Padul lake.



Supplementary Figure S4. Wavelet analysis results from the local and regional proxies from Padul-15-05 record. (A) Spectral analysis of Mediterranean forest (%). AR (1) red noise (red line). Confident levels are marked: 80 % (orange line), 90% (blue line) and 95 % (green line) and the significant periodicities above the 80 % confident level are shown. (B) Above. Mediterranean forest taxa (%) detrended and lineally interpolated to 80 yr; shading indicate Mediterranean forest declines with a ~2067 yr of periodicity until ca. 5 cal ka BP and a ~1431 yr of periodicity since ca. 4.7 cal ka BP. Statistical analysis was performed using Past software (http://palaeo-electronica.org/2001_1/past/issue1_01.htm).

Supplementary tables

Supplementary Table S1. X-ray fluorescence (XRF) PCA results from Padul-15-05 record. Eigenvalue, and percentage of variance explained with the different Principal Components. Statistical analysis was performed using Past software (http://palaeo-electronica.org/2001_1/past/issue1_01.htm).

PC	Eigenvalue	% variance
1	5.2735	58.594
2	2.31664	25.74
3	0.575871	6.3986
4	0.327842	3.6427
5	0.213153	2.3684
6	0.168962	1.8774
7	0.077899	0.86554
8	0.0461336	0.5126
9	1.82E-17	2.02E-16

CHAPTER 3

Chapter 3: Holocene climate aridification trend and human impact interrupted by millennial- and centennial-scale climate fluctuations from a new sedimentary record from Padul (Sierra Nevada, southern Iberian Peninsula)

María J. Ramos-Román¹, Gonzalo Jiménez-Moreno¹, Jon Camuera¹, Antonio García-Alix¹, R. Scott Anderson², Francisco J. Jiménez-Espejo³, José S. Carrión⁴

¹ Departamento de Estratigrafía y Paleontología, Universidad de Granada, Spain

² School of Earth Sciences and Environmental Sustainability, Northern Arizona University, USA.

³ Department of Biogeochemistry, Japan Agency for Marine-Earth Science and Technology (JAMSTEC), Japan.

⁴ Departamento de Biología Vegetal, Facultad de Biología, Universidad de Murcia, Murcia, Spain.

Correspondence to: María J. Ramos-Román (mjrr@ugr.es)

Accepted to be published in:

Climate of the Past

. Received 23 August 2017, Accepted 14 December 2017

. Impact factor (JCR): 3.750 (2016)

. Rank: Q1

Abstract

Holocene centennial-scale paleoenvironmental variability has been described in a multiproxy analysis (i.e. lithology, geochemistry, macrofossil and microfossil analyses) of a paleoecological record from the Padul basin in Sierra Nevada, southern Iberian Peninsula. This sequence covers a relevant time interval hitherto unreported in the studies of the Padul sedimentary sequence. The ~4700 yr-long record has preserved proxies of climate variability, with vegetation, lake levels and sedimentological change during the Holocene in one of the most unique and southernmost wetland from Europe. The progressive Middle and Late Holocene trend toward arid conditions identified by numerous authors in the western Mediterranean region, mostly related to a decrease in summer insolation, is also documented in this record, being here also superimposed by centennial-scale variability in humidity. In turn, this record shows centennial-scale climate oscillations in temperature that correlate with well-known climatic events during the Late Holocene in the western Mediterranean region, synchronous with variability in solar and atmospheric dynamics. The multiproxy Padul record first shows a transition from a relatively humid Middle Holocene in the western Mediterranean region to more aridity from ~4700 to ~2800 cal yr BP. A relatively warm and humid period occurred between ~2600 to ~1600 cal yr BP, coinciding with persistent negative NAO conditions and the historic Iberian-Roman Humid Period. Enhanced arid conditions, co-occurring with overall positive NAO conditions and increasing solar activity, are observed between ~1550 to ~450 cal yr BP (~400 to ~1400 CE) and colder and warmer conditions happened during the Dark Ages and Medieval Climate Anomaly, respectively. Slightly wetter conditions took place during the end of the MCA and the first part of the Little Ice Age, which could be related to a change towards negative NAO conditions and minima in solar activity. Time series analysis performed from local (*Botryococcus* and TOC) and regional (Mediterranean forest) signals helped us determining the

relationship between southern Iberian climate evolution, atmospheric, oceanic dynamics and solar activity. Our multiproxy record shows little evidence of human impact in the area until ~1550 cal yr BP, when evidence of agriculture and livestock grazing occurs. Therefore climate is the main forcing mechanism controlling environmental change in the area until relatively recently.

Keywords: Holocene, Padul, peat bog, North Atlantic Oscillation, atmospheric dynamics, southern Iberian Peninsula, Sierra Nevada, western Mediterranean.

1. Introduction

The Mediterranean area is situated in a sensitive region between temperate and subtropical climates making it an important place to study the connections between atmospheric and oceanic dynamics and environmental change. Climate in the western Mediterranean and the southern Iberian Peninsula is influenced by several atmospheric and oceanic dynamics (Alpert et al., 2006), including the North Atlantic Oscillation (NAO) one of the principal atmospheric phenomenon controlling climate in the area (Hurrell, 1995; Moreno et al., 2005). Recent NAO reconstructions in the western Mediterranean relate negative and positive NAO conditions with an increase and decrease, respectively, in winter (effective) precipitation (Trouet et al., 2009; Olsen et al., 2012). Numerous paleoenvironmental studies in the western Mediterranean have detected a link at millennial- and centennial-scales between the oscillations of paleoclimate proxies from sedimentary records with solar variability and atmospheric (i.e., NAO) and/or ocean dynamics during the Holocene (Moreno et al., 2012; Fletcher et al., 2013; Rodrigo-Gámiz et al., 2014a). Very few montane and low altitude lake records in southern Iberia document centennial-scale climate change [see, for example Zoñar Lake (Martín-Puertas et al., 2008)], with most terrestrial records in the western Mediterranean region evidencing only millennial-scale cyclical changes. Therefore, higher-resolution decadal-scale analyses are necessary to analyze the link between solar activity, atmospheric and oceanographic systems with terrestrial environment in this area at shorter (i.e., centennial) time scales.

Sediments from lakes, peat bogs and marine records from the western Mediterranean have documented an aridification trend during the Late Holocene (Jalut et al., 2009; Carrión et al., 2010a; Gil-Romera et al., 2010). This trend, however, was superimposed by shorter-term climate variability, as shown by several recent studies from the region (Carrión, 2002; Martín-Puertas et al., 2008; Fletcher et al., 2013; Jiménez-Moreno et al., 2013a; Ramos-Román et al., 2016). This relationship between climate variability, culture evolution

and human impact during the Late Holocene has also been the subject of recent paleoenvironmental studies (Magny, 2004; Carrión et al., 2007; López-Sáez et al., 2014; Lillios et al., 2016). However, it is still unclear whether climate or human activities have been the main forcing driving environmental change (i.e., deforestation) in this area during this time.

Within the western Mediterranean, Sierra Nevada is the highest and southernmost mountain range in the Iberian Peninsula and thus presents a critical area for paleoenvironmental studies. Most high-resolution studies there have come from high elevation sites. The well-known Padul wetland site is located at the western foot of the Sierra Nevada (Fig. 1) and bears one of the longest continental records in southern Europe, with a sedimentary sequence of ~100 m thick that could represent the last 1 Ma (Ortiz et al., 2004). Several research studies, including radiocarbon dating, geochemistry and pollen analyses, have been carried out on previous cores from Padul, and have documented glacial/interglacial cycles during the Pleistocene and up until the Middle Holocene. However, the Late Holocene section of the Padul sedimentary sequence has never been effectively retrieved and studied (Florschütz et al., 1971; Pons and Reille, 1988; Ortiz et al., 2004). This was due to the location of these previous corings within a current peat mine operation, where the upper (and non-productive) part of the sedimentary sequence was missing.

Here we present a new record from the Padul basin: Padul-15-05, a 42.64 m-long sediment core that, for the first time, contains a continuous record of the Late Holocene (Fig. 2). A high-resolution multi-proxy analysis of the upper 1.15 m, the past ~4700 cal yr BP, has allowed us to determine a complete paleoenvironmental and paleoclimatic record at centennial- and millennial-scales. To accomplish that, we reconstructed changes in the Padul vegetation, sedimentation, climate and human impact during the Holocene throughout the interpretation of the lithology, palynology and geochemistry.

Specifically, the main objective of this paper is to determine environmental variability and climate evolution in the southern Iberian Peninsula and the

western Mediterranean region and their linkages to northern hemisphere climate and solar variability during the latter Holocene. In order to do this, we compared our results with other paleoclimate records from the region and solar activity from the northern hemisphere for the past ~4700 cal yr BP (Bond et al., 2001; Laskar et al., 2004; Steinhilber et al., 2009; Sicre et al., 2016).

2. Regional setting: Padul, climate and vegetation

Padul is located at the foothill of Sierra Nevada, which is a W-E aligned mountain range located in Andalucía (southern Spain; Fig. 1). Climate in this area is Mediterranean, with cool and humid winters and hot/warm summer drought. Sierra Nevada is strongly influenced by thermal and precipitation variations due to the altitudinal gradient (from ca. 700 to more than 3400 m), which control plant taxa distribution in different bioclimatic vegetation belts due to the variability in thermotypes and ombrotypes (Valle Tendero, 2004). According to the climatophilous series classification, Sierra Nevada is divided in four different vegetation belts (Fig. 1). The crioromediterranean vegetation belt, occurring above ~2800 m, is characterized by tundra vegetation and principally composed by species of Poaceae, Asteraceae, Brassicaceae, Gentianaceae, Scrophulariaceae and Plantaginaceae between other herbs, with a number of endemic plants (e.g. *Erigeron frigidus*, *Saxifraga nevadensis*, *Viola crassiuscula*, *Plantago nivalis*). The oromediterranean belt, between ~1900 to ~2800 m, is principally made up of *Pinus sylvestris*, *P. nigra* and *Juniperus* spp. and other shrubs such as species of Fabaceae, Cistaceae and Brassicaceae. The supramediterranean belt, from ~1400 to 1900 m of elevation, bears principally *Quercus pyrenaica*, *Q. faginea* and *Q. rotundifolia* and *Acer opalus* ssp. *granatense* with other trees and shrubs, including members of the Fabaceae, Thymelaeaceae, Cistaceae and *Artemisia* sp. being the most important. The mesomediterranean vegetation belt occurs between ~600 and 1400 m of elevation and is principally characterized by *Quercus rotundifolia*, some shrubs, herbs and plants as *Juniperus* sp., and some species of Fabaceae, Cistaceae and Liliaceae with others (El Aallali et al., 1998; Valle, 2003). The

human impact over this area, especially important during the last millennium, affected the natural vegetation distribution through fire, deforestation, cultivation (i.e., *Olea*) and subsequent reforestation (mostly *Pinus*) (Anderson et al., 2011). The Padul basin is situated in the mesomediterranean vegetation belt at approximately 725 m elevation in the southeastern part of the Granada Basin. In this area and besides the characteristic vegetation at this elevation, nitrophilous communities occur in soils disrupted by livestock, pathways or open forest, normally related with anthropization (Valle, 2003).

This is one of the most seismically active areas in the southern Iberian Peninsula with numerous faults in NW-SE direction, with the Padul fault being one of these active normal faults (Alfaro et al., 2001). It is a small extensional basin approximately 12 km long and covering an area of approximately 45 km², which is bounded by the Padul normal fault. The sedimentary in-filling of the basin consists of Neogene and Quaternary deposits; Upper Miocene conglomerates, calcarenites and marls, and Pliocene and Quaternary alluvial sediments, lacustrine and peat bog deposits (Domingo-García et al., 1983; Sanz de Galdeano et al., 1998; Delgado et al., 2002).

The Padul wetland is endorheic, with a surface of approximately 4 km² placed in the Padul basin that contains a sedimentary sequence characterized mostly by peat accumulation. The basin fill is asymmetric, with thicker sedimentary and peat infill to the northeast (~100 m thick; Florschütz et al., 1971; Domingo-García et al., 1983; Nestares and Torres, 1997) and progressively becoming thinner to the southwest (Alfaro et al., 2001). The main source area of allochthonous sediments in the bog is the Sierra Nevada, which is characterized at higher elevations by Paleozoic siliceous metamorphic rocks (mostly mica-schists and quartzites) from the Nevado-Filabride complex and, at lower elevations and acting as bedrock, by Triassic dolomites, limestones and phyllites from the Alpujarride Complex (Sanz de Galdeano et al. 1998). Geochemistry in the Padul sediments is influenced by detritic materials also primarily from the the Sierra Nevada (Ortiz et al., 2004). Groundwater inputs into the Padul basin come from the Triassic carbonates aquifers (N and S

edge to the basin), the out flow of the Granada Basin (W edge to the basin) and the conglomerate aquifer to the east edge (Castillo Martín et al., 1984; Ortiz et al., 2004). The main water output is by evaporation and evapotranspiration, water wells and by canals (“madres”) that drain the water to the Dúrcal river to the southeast (Castillo Martín et al., 1984). Climate in the Padul area is characterized by a mean annual temperature of 14.4 °C and a mean annual precipitation of 445 mm (<http://www.aemet.es/>). The Padul-15-05 drilling site was located ~50 m south of the present-day Padul lake shore area. This basin area is presently subjected to seasonal water level fluctuations and is principally dominated by *Phragmites australis* (Poaceae). The lake environment is dominated by aquatic and wetland communities with *Chara vulgaris*, *Myriophyllum spicatum*, *Potamogeton pectinatus*, *Potamogetum coloratus*, *Phragmites australis*, *Typha dominguensis*, *Apium nodiflorum*, *Juncus subnodulosus*, *J. bufonius*, *Carex hispida* and *Ranunculus muricatus*, among others (Pérez Raya and López Nieto, 1991). Some sparse riparian trees occur in the northern lake shore, such as *Populus alba*, *Populus nigra*, *Salix* sp., *Ulmus minor* and *Tamarix*. At present *Phragmites australis* is the most abundant plant bordering the lake. Surrounding this area are cultivated crops with cereals, such as *Triticum* spp., as well as *Prunus dulcis* and *Olea europea*.

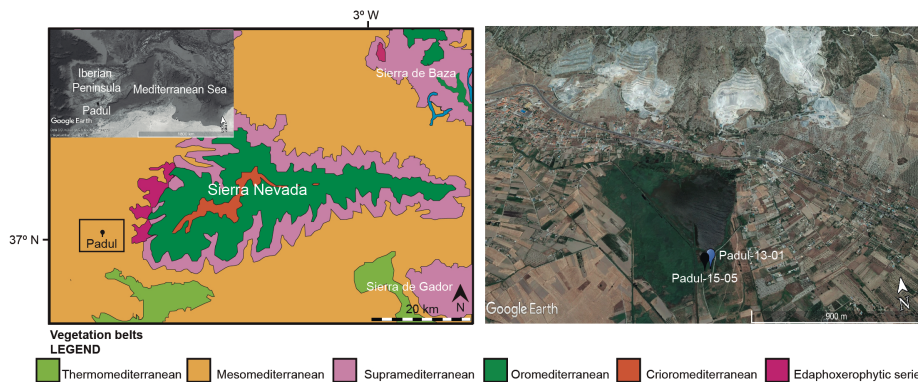


Figure 1. Location of Padul in Sierra Nevada, southern Iberian Peninsula. Panel on the left is the map of the vegetation belts in the Sierra Nevada (Modified from REDIAM. Map of the vegetation series of Andalucía: http://laboratoriorediam.cica.es/VisorGenerico/?tipo=WMS&url=http://www.juntadeandalucia.es/medioambiente/mapwms/REDIAM_Series_Vegetacion_Andalucia?). The inset map is the Google earth image of the Iberian Peninsula in the Mediterranean region. Panel on the right is the Google earth image (<http://www.google.com/earth/index.html>) of Padul peat bog area showing the coring locations.

3. Material and methods

Two sediment cores, Padul-13-01 (37°00'40''N; 3°36'13''W) and Padul-15-05 (37°00'39.77''N; 3°36'14.06''W) with a length of 58.7 cm and 42.64 m, respectively, were collected between 2013 and 2015 from the wetland (Fig. 1). The cores were taken using a Rolatec RL-48-L drilling machine equipped with a hydraulic piston corer from the Scientific Instrumentation Centre of the University of Granada (UGR). The sediment cores were wrapped in film, put in core boxes, transported to UGR and stored in a dark cool room at 4°C.

3.1. Age-depth model (AMS radiocarbon dating)

The core chronology was constrained using fourteen AMS radiocarbon dates from plant remains and organic bulk samples taken from the cores (Table 1). In addition, one sample with gastropods was also submitted for AMS radiocarbon analysis, although it was rejected due to important reservoir effect, that provided a very old date. Thirteen of these samples came from Padul-15-05

with one from the nearby Padul-13-01 (Table 1). We were able to use this date from Padul-13-01 core as there is a very significant correlation between the upper part of Padul-15-05 and Padul-13-01 cores, shown by identical lithological and geochemical changes (Supplementary information 1; Figure S1). The age model for the upper ~3 m minus the upper 21 cm from the surface was built using the R-code package ‘Clam 2.2’ (Blaauw, 2010) employing the calibration curve IntCal 13 (Reimer et al., 2013), a 95 % of confidence range, a smooth spline (type 4) with a 0.20 smoothing value and 1000 iterations (Fig. 2). The chronology of the uppermost 21 cm of the record was built using a linear interpolation between the last radiocarbon date and the top of the record (Present; 2015 CE). Even though the length of the Padul-15-05 core is ~43 m, the studied interval in the work presented here is the uppermost 115 cm of the record that are constrained by seven AMS radiocarbon dates (Fig. 2).

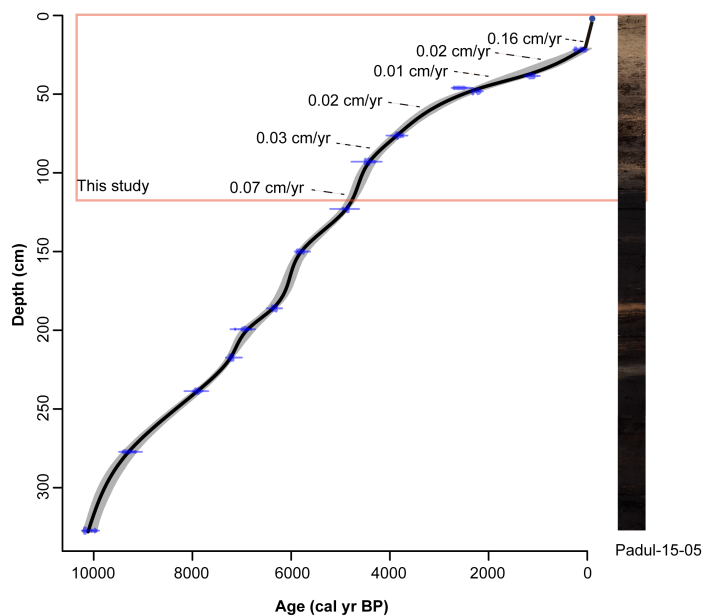


Figure 2. Photo of the Padul-15-05 sediment core with the age-depth model showing the part of the record that was studied here (red rectangle). The sediment accumulation rates (SAR) between individual segments are marked. See the body of the text for the explanation of the age reconstructions.

Table 1. Age data for Padul-15-05 record. All ages were calibrated using R-code package ‘clam 2.2’ employing the calibration curve IntelCal 13 (Reimer et al., 2013) at 95 % of confident range. *Sample number assigned at radiocarbon laboratory.

Laboratory number	Core	Material	Depth (cm)	Age (^{14}C yr BP $\pm 1\sigma$)	Calibrated age (cal yr BP) 95 % confidence interval	Median age (cal yr BP)
Reference ages			0	2015CE	-65	-65
D-AMS 008531	Padul-13-01	Plant remains	21.67	103 \pm 24	23-264	127
Poz-77568	Padul-15-05	Org. bulk sed.	38.46	1205 \pm 30	1014-1239	1130
BETA-437233	Padul-15-05	Plant remains	46.04	2480 \pm 30	2385-2722	2577
Poz-77569	Padul-15-05	Org. bulk sed.	48.21	2255 \pm 30	2158-2344	2251
BETA-415830	Padul-15-05	Shell	71.36	3910 \pm 30	4248-4421	4343
BETA- 437234	Padul-15-05	Plant remains	76.34	3550 \pm 30	3722-3956	3838
BETA-415831	Padul-15-05	Org. bulk sed.	92.94	3960 \pm 30	4297-4519	4431
Poz-74344	Padul-15-05	Plant remains	122.96	4295 \pm 35	4827-4959	4871
BETA-415832	Padul-15-05	Plant remains	150.04	5050 \pm 30	5728-5900	5814
Poz-77571	Padul-15-05	Plant remains	186.08	5530 \pm 40	6281-6402	6341
Poz-74345	Padul-15-05	Plant remains	199.33	6080 \pm 40	6797-7154	6935
BETA-415833	Padul-15-05	Org. bulk sed.	217.36	6270 \pm 30	7162-7262	7212
Poz-77572	Padul-15-05	Org. bulk sed.	238.68	7080 \pm 50	7797-7999	7910
Poz-74347	Padul-15-05	Plant remains	277.24	8290 \pm 40	9138-9426	9293
BETA-415834	Padul-15-05	Plant remains	327.29	8960 \pm 30	9932-10221	10107

3.2. *Lithology, MS, XRF and TOC*

Padul-15-05 core was split longitudinally and was described in the laboratory with respect to lithology and color (Fig. 3). Magnetic susceptibility (MS) was measured with a Bartington MS3 operating with a MS2E sensor. MS measurements (in SI units) were obtained directly from the core surface every 0.5 cm (Fig. 3).

Elemental geochemical composition was measured in an X-Ray fluorescence (XRF) Avaatech core scanner® at the University of Barcelona (Spain). A total of thirty-three chemical elements were measured in the XRF core scanner at 10 mm of spatial resolution, using 10 s count time, 10 kV X-ray voltage and a X-ray current of 650 μA for lighter elements and 35 s count time, 30 kV X-ray voltage, X-ray current of 1700 μA for heavier elements. Thirty-three chemical elements were measured but only the most representative with a major number of counts were considered (Si, K, Ca, Ti, Fe, Zr, Br and Sr). Results for each element are expressed as intensities in counts per second (cps) and normalized (norm.) for the total sum in cps in every measure (Fig. 3).

Total organic carbon (TOC) was analyzed every 2 or 3 cm throughout the core. Samples were previously decalcified with 1:1 HCl in order to eliminate the carbonate fraction. The percentage of organic Carbon (OC %) was measured in an Elemental Analyzer Thermo Scientific Flash 2000 model from the Scientific Instrumentation Centre of the UGR (Spain). Percentage of TOC per gram of sediment was calculated from the percentage of organic carbon (OC %) yielded by the elemental analyzer, and recalculated by the weight of the sample prior to decalcification (Fig. 3).

3.3. *Pollen and NPP*

Samples for pollen analysis (1-3 cm^3) were taken every 1 cm throughout the core, with a total of 103 samples analyzes. Pollen extraction methods followed a modified Faegri and Iversen (1989) methodology. Processing

included the addition of *Lycopodium* spores for calculation of pollen concentration. Sediment was treated with NaOH, HCl, HF and the residue was sieved at 250 μm previous to an acetolysis solution. Counting was performed using a transmitted light microscope at 400 magnifications to an average pollen count of ca. 260 terrestrial pollen grains. Fossil pollen was identified using published keys (Beug, 2004) and modern reference collections at University of Granada (Spain). Pollen counts were transformed to pollen percentages based on the terrestrial pollen sum, excluding aquatics. The palynological zonation was executed by cluster analysis using twelve primary pollen taxa- *Olea*, *Pinus*, deciduous *Quercus*, evergreen *Quercus*, *Pistacia*, Ericaceae, *Artemisia*, Asteroideae, Cichorioideae, Amaranthaceae and Poaceae (Grimm, 1987) (Fig. 4). Non-pollen palynomorphs (NPP) include fungal and algal spores, and thecamoebians (testate amoebae). The NPP percentages were calculated and represented with respect to the terrestrial pollen sum (Fig. 4). Furthermore, some pollen taxa were grouped, according to present-day ecological bases, into Mediterranean forest and xerophytes (Fig. 4). The Mediterranean forest taxa is composed of *Quercus* total, *Olea*, *Phillyrea* and *Pistacia*. The xerophyte group includes *Artemisia*, *Ephedra*, and Amaranthaceae.

4. Results

4.1. Chronology and sedimentation rates

The age-model of the upper 115 cm of Padul-15-05 core (Fig. 2) shows an average sedimentation rate (SAR) of 0.058 cm/yr over last ~4700 cal yr BP, being the age constrained by seven AMS ^{14}C dates (Table 1). However, SARs of individual core segments vary from 0.01 to 0.16 cm/yr (Fig. 2), showing the lowest values between ~51 and 40 cm (from ~2600 to 1350 cal yr BP) and the highest values during the last ~20 cm (last century).

4.2. Lithology, MS, XRF and TOC

The stratigraphy of the upper ~115 cm of the Padul-15-05 sediment core was deduced primarily by visual inspection. However, our visual inspections were supported by comparison with the element geochemical composition (XRF), the MS of the split cores, and TOC (Fig. 3) to determine shifts in sediment facies. The lithology for this sedimentary sequence consists in clays with variable carbonates, siliciclastics and organic content (Fig. 3). We also used a Linear r (Pearson) correlation to calculate the relationship for the XRF data. The correlation for the inorganic geochemical elements determined two different groups of elements that covary (Table 2): Group 1) Si, K, Ti, Fe and Zr with a high positive correlation between them; Group 2) Ca, Br and Sr have negative correlation with Group 1. Based on this, the sequence is subdivided into two principal sedimentary units. The lower ~87 cm of the record is designated to Unit 1, characterized principally by relatively low values of MS and higher values of Ca. The upper ~28 cm of the sequence is designated to Unit 2, in which the mineralogical composition is lower in Ca with higher values of MS in correlation with mostly siliciclastic elements (Si, K, Ti, Fe and Zr).

Within these two units, four different facies can be identified by visual inspection and by the elemental geochemical composition and TOC of the sediments. *Facies 1* (115-110 cm depth, ~4700 to 4650 cal yr BP; and 89-80 cm depth ~4300 to 4000 cal yr BP) are characterized by dark brown organic clays that bear charophytes and macroscopic plant remains. They also have depicted relative higher values of TOC values (Fig. 3). *Facies 2* (110-89 cm depth ~4650 to 4300 cal yr BP; and 80-42 cm depth, ~4000 to 1600 cal yr BP) is composed of brown clays, with the occurrence of gastropods and charophytes. This facies is also characterized by lower TOC values. *Facies 3* (42-28 cm depth, ~1600 to 400 cal yr BP) is characterized by grayish brown clays with the occurrence of gastropods, and lower values of TOC, and an increasing trend in MS and in siliciclastic elements. *Facies 4* (28-0 cm, ~400 cal yr BP to Present)

is made up of light grayish brown clays and features a strong increase in siliciclastic linked to a strong increase in MS.

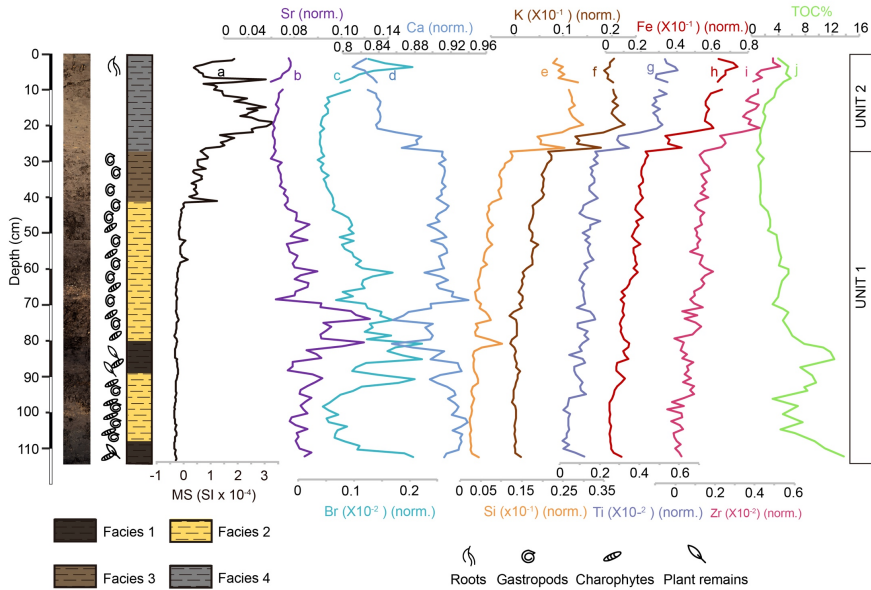


Figure 3. Lithology, facies interpretation with paleontology, magnetic susceptibility (MS), and geochemical (X-ray fluorescence (XRF) and total organic carbon (TOC) data from the Padul-15-05 record. XRF elements are represented normalized by the total counts. (a) Magnetic susceptibility (MS; SI units). (b) Strontium normalized (Sr; norm.). (c) Bromine norm. (Br; norm.). (d) Calcium normalized. (Ca; norm.). (e) Silica normalized (Si; norm.). (f) Potassium normalized (K; norm.). (g) Titanium normalized (Ti; norm.). (h) Iron normalized (Fe; norm.). (i) Zirconium normalized (Zr; norm.). (j) Total organic carbon (TOC %). AMS radiocarbon dates (cal yr BP) are shown on the left.

Table 2. Linear r (Pearson) correlation between geochemical elements from the Padul-15-05 record. Statistical treatment was performed using the Past software (http://palaeo-electronica.org/2001_1/past/issue1_01.htm).

	Si	K	Ca	Ti	Fe	Zr	Br	Sr
Si		8.30E-80	2.87E-34	7.47E-60	3.22E-60	5.29E-44	0.001152	7.79E-09
K	0.98612		7.07E-29	6.05E-60	8.20E-68	1.77E-51	0.00030317	5.38E-12
Ca	-0.88096	-0.84453		6.09E-42	5.81E-39	8.10E-34	0.35819	0.26613
Ti	0.96486	0.96501	-0.91794		1.74E-74	1.12E-57	0.074223	8.88E-07
Fe	0.96546	0.97577	-0.90527	0.98224		2.77E-66	0.051072	3.32E-08
Zr	0.92566	0.94789	-0.8783	0.96109	0.97398		0.054274	7.16E-08
Br	-0.31739	-0.3506	-0.091917	-0.17755	-0.19372	-0.19116		4.03E-18
Sr	-0.53347	-0.61629	0.11113	-0.46426	-0.51386	-0.50295	0.72852	

4.3. Pollen and NPP

Several terrestrial and aquatic pollen taxa were identified but only the most representative taxa are here plotted in the summary pollen diagram (Fig. 4). Selected NPP percentages are also displayed in Figure 4. Four pollen zones (PA) were visually identified with the help of a cluster analysis using the program CONISS (Grimm, 1987). Pollen concentration was higher during Unit 1 with a decreasing trend in the transition to Unit 2 and a later increase during the pollen subzone PA-4b (Fig. 4). Pollen zones are described below:

4.3.1 Zone PA-1 [~4720 to 3400 cal yr BP/ ~2800 to 1450 BCE (115-65 cm)]

Zone 1 is characterized by the abundance of Mediterranean forest species reaching up to ca. 70 %. Another important taxon in this zone is *Pinus*, with average values around 18 %. Herbs are largely represented by Poaceae, averaging around 10 %, and reaching up to ca. 25 %. This pollen zone is subdivided into PA-1a, PA-1b and PA-1c (Fig. 4). The principal characteristic that differentiating PA-1a from PA-1b (boundary at ~4650 cal yr BP/~2700 BCE) is the decrease in Poaceae, the increase in *Pinus*, and the appearance of cf. *Vitis*. The subsequent decrease in Mediterranean forest pollen to average values around 40 %, the increase in *Pinus* to average ~25 % and a progressive increase in Ericaceae to ~6 to 11 %, distinguishes subzones PA-1b and PA-1c (boundary at ca. 3950 cal yr BP).

4.3.2. Zone PA-2 [~3400 to 1550 cal yr BP/~1450 BCE to 400 CE (65-41 cm)]

The main features of this zone are the increase in Ericaceae up to ~16 %, some herbs such as Cichorioideae, became more abundant reaching average percentages of ~7 %. This pollen zone can be subdivided in subzones PA-2a and PA-2b with a boundary at ~2850 cal yr BP (~900 BCE). The principal characteristics that differentiate these subzones is marked by the increasing

trend in Ericaceae and deciduous *Quercus* reaching maximum values of ~30 % and ~20 %, respectively. In addition, the increase in *Botryococcus*, which averages from ~4 to 9 %. Also notable is the expansion of *Mougetia* and *Zygnema* types.

4.3.3 Zone PA-3 [~1550 to 400 cal yr BP/~400 CE to 1550 CE (41-29 cm)]

This zone is distinguished by the continuing decline of Mediterranean forest elements. Cichorioideae reached average values of about 40 %, and is paralleled by the decrease in Ericaceae. A decline in *Botryococcus* and other algal remains is also observed in this zone, although there is an increase in total Thecamoebians from average of <1 % to 10 %. This pollen zone is subdivided in subzones PA-3a and PA-3b at ~1000 cal yr BP (~950 CE). The main features that differentiate these subzones are the increase in *Olea* from subzone PA-3a to PA-3b from average values of ~1 to 5 %. The increasing trend in Poaceae is also a feature in this subzone, as well as the slight increase in Asteroideae at the top. Significant changes are documented in NPP percentages in this subzone with the increase of some fungal remain such as *Tilletia* and *Glomus* type. Furthermore, a decrease in *Botryococcus* and the near disappearance of other algal remains such as *Mougetia* occurred.

4.3.4 Zone PA-4 [~last 400 cal yr BP/ ~ 1550 CE to Present (29-0 cm)]

The main feature in this zone is the significant increase in *Pinus*, reaching maximum values of ~32 %, an increase in Poaceae to ~40 %) and the decrease in Cichorioideae (~44 to 16 %). Other important changes are the nearly total disappearance of some shrubs such as *Pistacia* and a decreasing trend in Ericaceae, as well as a further decline in Mediterranean forest pollen. An increase in wetland pollen taxa, mostly *Typha*, also occurred. A significant increase in xerophytes, mostly Amaranthaceae to ~14 % is also observed in this period. Other herbs such as *Plantago*, Polygonaceae and Convolvulaceae show moderate increases. PA-4 is subdivided into subzones PA-4a and PA-4b (Fig.

4). The top of the record (PA-4b), which corresponds with the last ~120 yr, is differentiated from subzone PA-4a (from ~400 – 120 cal yr BP) by a decline in some herbs such as Cichorioideae. However, an increase in other herbs such as Amaranthaceae and Poaceae occurred. The increase in *Plantago* is also significant during this period. PA-4b also has a noteworthy increase in *Pinus* (from ~14 to 27 %) and a slight increase in *Olea* and evergreen *Quercus* are also characteristic of this subzone. With respect to NPPs, thecamoebians such as *Arcella* type and in the largely coprophilous sordariaceous (Sordariales) spores also increase. This zone also documents the decrease in fresh-water algal spores, in *Botryococcus* concomitant with *Mougeotia* and *Zygnema* type.

4.4. Estimated lake level reconstruction

Different local proxies from the Padul-15-05 record [Si, Ca, TOC, MS, hygrophytes (Cyperaceae and *Typha*), Poaceae and algae (including *Botryococcus*, *Zygnema* types and *Mougeotia*) groups] have been depicted in order to understand the relationship between lithological, geochemical, and palynological variability and the water lake level oscillations. Sediments with higher values of TOC (more algae and hygrophytes) and rich in Ca (related with the occurrence of shells and charophytes remains) most likely characterized a shallow water environment (Unit 1). The continuous decline in *Botryococcus*, the disappearance of charophytes and the progressively increase in detritics (increase in MS and Si values) could be associated with shallower and even ephemeral lake environment (transition from Unit 1 to Unit 2; ~41 to 28 cm). The absence of aquatic remains, almost disappearance of *Botryococcus* and decreasing Ca and a lower TOC and/or a higher input of clastic material (higher MS and Si values) into the lake, could be related with lake level lowering, and even emerged conditions (increase in Poaceae; Unit 2) (Fig. 5).

blue, algae in blue, fungi in brown and thecamoebians in beige. The Mediterranean forest taxa category is composed of *Quercus* total, *Olea*, *Phillyrea* and *Pistacia*. The xerophyte group includes *Artemisia*, *Ephedra*, and Amaranthaceae. PA = Pollen zones.

4.5. Spectral analysis

Spectral analysis was performed on selected pollen and NPP time series (Mediterranean forest and *Botryococcus*), as well as TOC in order to identify millennial- and centennial-scale periodicities. The mean sampling resolution for pollen and NPP is ~50 yr and for geochemical data is ~80 yr. Statistically significant cycles, above the 90, 95 and 99 % of confident levels, were found around 800, 680, 300, 240, 200, 170 (Fig. 7).

5. Discussion

Numerous proxies have been used in this study to interpret the paleoenvironmental and hydrodynamic changes recorded in the Padul sedimentary record during the last 4700 cal yr BP. Palynological analysis (pollen and NPP) is commonly used as a proxy for vegetation and climate change, and lake level variations, as well as human impact and land uses (e.g. Van Geel et al., 1983; Faegri and Iversen, 1990). Disentangling natural vs. anthropogenic effects on the environment in the last millennia is sometimes challenging but can be persuaded using a multi-proxy approach (Roberts et al., 2011; Sadori et al., 2011). In this study, we used the variations between Mediterranean forest taxa, xerophytes and algal communities for paleoclimatic variability and the occurrence of nitrophilous and ruderal plant communities and some NPPs for identifying human influence in the study area. Variations in arboreal pollen (AP, including Mediterranean tree species) have previously been used in previous Sierra Nevada records as a proxy for humidity changes (Jiménez-Moreno and Anderson, 2012; Ramos-Román et al., 2016). The increase or decrease in Mediterranean forest species has been used as a proxy for climate change in other studies in the western Mediterranean region, with greater forest development generally meaning higher humidity (Fletcher et al.,

2013; Fletcher and Sánchez-Goñi, 2008). On the other hand, increases in xerophyte pollen taxa (i.e., *Artemisia*, *Ephedra*, Amaranthaceae) have been used as an indication of aridity in this area (Carrión et al., 2007; Anderson et al., 2011).

The chlorophyceae alga *Botryococcus* sp. has been used as an indicator of freshwater environments, in relatively productive fens, temporary pools, ponds or lakes (Guy-Ohlson, 1992). The high visual and statistical correlation between *Botryococcus* from Padul-15-05 and North Atlantic temperature estimations [Bond et al., 2001; $r = -0.63$; $p < 0.0001$; between ca. 4700 to 1500 cal yr BP and $r = -0.48$; $p < 0.0001$ between 4700 and -65 cal yr BP (the decreasing and very low *Botryococcus* occurrence in the last 1500 cal yr BP makes this correlation moderate)] seems to show that in this case *Botryococcus* is driven by temperature change and would reflect variations in lake productivity (increasing with warmer water temperatures).

Human impact can be investigated using several palynomorphs. Nitrophilous and ruderal pollen taxa, such as *Convolvulus*, *Plantago lanceolata* type, Urticaceae type and *Polygonum avicularis* type, are often proxies for human impact (Riera et al., 2004), and abundant Amaranthaceae has also been used as well (Sadori et al., 2003). Some species of Cichorioideae have been described as nitrophilous taxa (Abel-Schaad and López-Sáez, 2013) and as grazing indicators (Mercuri et al., 2006; Florenzano et al., 2015; Sadori et al., 2016). At the same time, NPP taxa such as some coprophilous fungi, Sordariales and thecamoebians are also used as indicators of anthropization and land use (Van Geel et al., 1989; Riera et al., 2006; Carrión et al., 2007; Ejarque et al., 2015). *Tilletia* a grass-parasitizing fungi has been described as an indicator of grass cultivation in other Iberian records (Carrión et al., 2001a). In this study we follow the example of others (Van Geel et al., 1989; Morellón et al., 2016; Sadori et al., 2016) who used the NPP soil mycorrhizal fungus *Glomus* sp. as a proxy for erosive activity.

The palynological analysis, variations in the lithology, geochemistry and macrofossil remains (gastropod shells and charophytes) from the Padul-15-05

core helped us reconstruct the estimated lake level and the local environment changes in the Padul area and their relationship with regional climate (Fig. 5). Several previous studies on Late Holocene lake records from the Iberian Peninsula show that lithological changes can be used as a proxy for lake level reconstruction (Riera et al., 2004; Morellón et al., 2009; Martín-Puertas et al., 2011). For example, carbonate sediments formed by biogenic remains of gastropods and charophytes are indicative of shallow lake waters (Riera et al., 2004). Furthermore, Van Geel et al. (1983), described occurrences of *Mougeotia* and *Zygnema* type (Zygnemataceae) as typical of shallow water environments. The increase in organic matter accumulation deduced by TOC (and Br) could be considered as characteristic of high productivity (Kalugin et al., 2007) in these shallow water environments. On the other hand, increases in clastic input in lake sediments have been interpreted as due to lowering of lake level and more influence of terrestrial-fluvial deposition in a very shallow/ephemeral lake (Martín-Puertas et al., 2008). Carrión (2002) related the increase in some fungal species and Asteraceae as indicators of seasonal desiccation stages in lakes. Nevertheless, in natural environments with potential interactions with human activities the increase in clastic deposition related with other indications of soil erosion (e.g. *Glomus* sp.) may be assigned to intensification in land use (Morellón et al., 2016; Sadori et al., 2016).

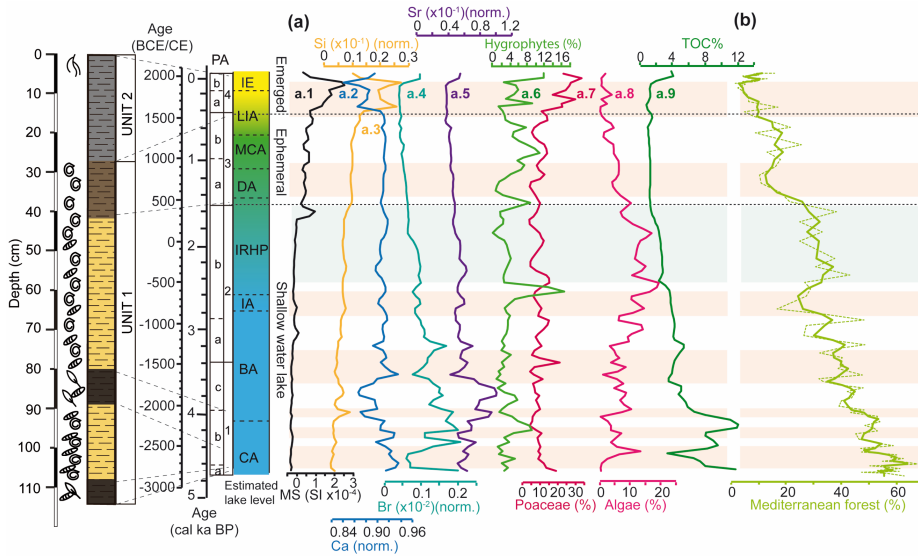


Figure 5. Estimated lake level evolution and regional palynological component from the last ca. 4700 yr based on the synthesis of determinate proxies from the Padul-15-05 record: (a) Proxies used to estimate the water table evolution from the Padul-15-05 record (proxies were resampled at 50 yr (lineal interpolation) using Past software http://palaeo-electronica.org/2001_1/past/issue1_01.htm). [(a.1) Magnetic Susceptibility (MS) in SI; (a.2) Silica normalized (Si; norm.); (a.3) Calcium normalized (Ca; norm.); (a.4) Bromine normalized (Br; norm.); (a.5) Strontium normalized (Sr; norm.); (a.6) Hygrophytes (%); (a.7) Poaceae (%); (a.8) Algae (%) (a.9) Total organic carbon (TOC %)] (b) Mediterranean forest taxa, with a smoothing of three-point in bold. Pink and blue shading indicates Holocene arid and humid regionally events, respectively. See the body of the text for the explanation of the lake level reconstruction. Mediterranean forest smoothing was made using Analseries software (Paillard et al., 1996). PA = Pollen Zones; CA = Copper Age; BA = Bronze Age; IA = Iron Age; IRHP = Iberian Roman Humid Period; DA = Dark Ages; MCA = Medieval Climate Anomaly; LIA = Little Ice Age; IE = Industrial Era.

5.1. Late Holocene aridification trend

Our work confirms the progressive aridification trend that occurred during at least the last ~4700 cal yr BP in the southern Iberian Peninsula, as shown here by the progressive decrease in Mediterranean forest component and the increase in herbs (Figs. 4 and 6). Our lake level interpretations agree with the pollen data, showing an overall decrease during the Late Holocene, from a shallow water table containing relatively abundant organic matter (high TOC, indicating higher productivity), gastropods and charophytes (high Ca values) to

a low-productive ephemeral/emerged environment (high clastic input and MS and decrease in Ca) (Fig. 5). This natural progressive aridification confirmed by the decrease in Mediterranean forest taxa and increase in siliciclastics pointing to a change towards ephemeral (even emerged) environments became more prominent since about 1550 cal yr BP and then enhanced again since ca. 400 cal yr BP to Present. A clear increase in human land use is also observed during the last ca. 1550 cal yr BP (see below), including abundant *Glomus* from erosion, which shows that humans were at least partially responsible for this sedimentary change.

A suite of proxies previous studies supports our conclusions regarding the aridification trend since the Middle Holocene (Carrión, 2002; Carrión et al., 2010; Fletcher and Sánchez-Goñi, 2008; Fletcher et al., 2013; Jiménez-Espejo et al., 2014; Jiménez-Moreno et al., 2015). In the western Mediterranean region the decline in forest development during the Middle and Late Holocene is related with a decrease in summer insolation (Jiménez-Moreno and Anderson, 2012; Fletcher et al., 2013), which may have decreased winter rainfall as a consequence of a northward shift of the westerlies - a long-term enhanced positive NAO trend – which induced drier conditions in this area since 6000 cal yr BP (Magny et al., 2012). Furthermore, the decrease in summer insolation would produce a progressive cooling, with a reduction in the length of the growing season as well as a decrease in the sea-surface temperature (Marchal et al., 2002), generating a decrease in the land-sea contrast that would be reflected in a reduction of the wind system and a reduced precipitation gradient from sea to shore during the fall-winter season. The aridification trend can clearly be seen in the nearby alpine records from the Sierra Nevada, where there was little influence by human activity (Anderson et al., 2011; Jiménez-Moreno and Anderson, 2012; Jiménez-Moreno et al., 2013a; Ramos-Román et al., 2016).

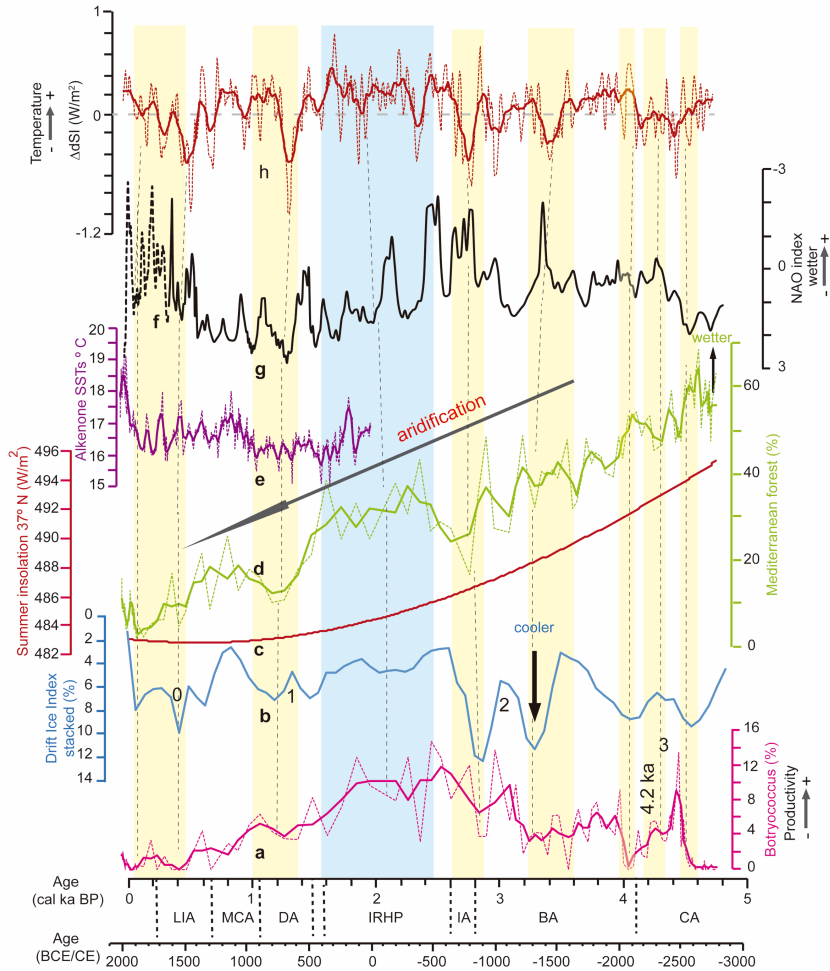


Figure 6. Comparison of the last ca. 4700 yr between different pollen taxa from the Padul-15-05 record, summer insolation for the Sierra Nevada latitude, eastern Mediterranean humidity and North Atlantic temperature. (a) *Botryococcus* from the Padul-15-05 record, with a smoothing of three-point in bold (this study). (b) Drift Ice Index (reversed) from the North Atlantic (Bond et al., 2001). (c) Summer insolation calculated for 37° N (Laskar et al., 2004). (d) Mediterranean forest taxa from the Padul-15-05 record, with a smoothing of three-point in bold (this study). (e) Alkenone-SSTs from the Gulf of Lion (Sicre et al., 2016), with a smoothing of four-point in bold. (f) North Atlantic Oscillation (NAO) index from a climate proxy reconstruction from Morocco and Scotland (Trouet et al., 2009). (g) North Atlantic Oscillation (NAO) index (reversed) from a climate proxy reconstruction from Greenland (Olsen et al., 2012). (h) Total solar irradiance reconstruction from cosmogenic radionuclide from a Greenland ice core (Steinhilber et al., 2009), with a smoothing of twenty-one-point in bold. Note that the magnitude of the different curves is not in the same scale. Yellow and blue shading correspond with arid (and cold) and humid (and warm) periods, respectively. Grey dash lines show a tentative correlation between arid and cold conditions and the

decrease in the Mediterranean forest and *Botryococcus*. Mediterranean forest, *Botryococcus* and solar irradiance smoothing was made using Analyseries software (Paillard et al., 1996), Alkenone-SSTs smoothing was made using Past software (http://palaeo-electronica.org/2001_1/past/issue1_01.htm). A linear r (Pearson) correlation was calculated between *Botryococcus* (detrended) and Drift Ice Index (Bond et al., 2001; $r = -0.63$; $p < 0.0001$; between ca. 4700 to 1500 cal ka BP – $r = -0.48$; $p < 0.0001$ between 4700 and -65 cal yr BP). Previously, the data were detrended (only in *Botryococcus*), resampled at 70-yr (linear interpolation) in order to obtain equally spaced time series and smoothed to three-point average. CA = Copper Age; BA = Bronze Age; IA = Iron Age; IRHP = Iberian Roman Humid Period; DA = Dark Ages; MCA = Medieval Climate Anomaly; LIA = Little Ice Age; IE = Industrial Era.

5.2. Millennial- and centennial-scale climate variability in the Padul area during the Late Holocene

The multi-proxy paleoclimate record from Padul-15-05 shows an overall aridification trend. However, this trend seems to be modulated by millennial- and centennial-scale climatic variability.

5.2.1 Aridity pulses around 4200 (4500, 4300 and 4000 cal yr BP) and around 3000 cal yr BP (3300 and 2800 cal yr BP)

Marked aridity pulses are registered in the Padul-15-05 record around 4200 and 3000 cal yr BP (Unit 1; PA-1 and PA-2a; Figs. 5 and 6). These arid pulses are mostly evidenced in this record by declines in Mediterranean forest taxa, as well as lake level drops and/or cooling evidenced by a decrease in organic component as TOC and the decrease in *Botryococcus* algae. However, a discrepancy between the local and regional occurs between 3000-2800 cal yr BP, with an increase in the estimated lake level and a decrease in the Mediterranean forest during the late Bronze Age until the early Iron Age (Figs. 5 and 6). The disagreement could be due to deforestation by humans during a very active period of mining in the area observed as a peak in lead pollution in the alpine records from Sierra Nevada (García-Alix et al., 2013). The aridity pulses agree regionally with recent studies carried out at higher elevation in the Sierra Nevada, a decrease in AP percentage in Borreguil de la Caldera record around 4000-3500 cal yr BP (Ramos-Román et al., 2016), high

percentage of non-arboreal pollen around 3400 cal ka BP in Zoñar lake [Southern Córdoba Natural Reserve; (Martín-Puertas et al., 2008)], and lake desiccation at ca. 4100 and 2900 cal yr BP in Lake Siles (Carrión et al., 2007). Jalut et al. (2009) compared paleoclimatic records from different lakes in the western Mediterranean region and also suggested a dry phase between 4300 to 3400 cal yr BP, synchronous with this aridification phase. Furthermore, in the eastern Mediterranean basin other pollen studies show a decrease in arboreal pollen concentration toward more open landscapes around 4 cal ka BP (Magri, 1999).

Significant climatic changes also occurred in the Northern Hemisphere at those times and polar cooling and tropical aridity are observed at ~4200-3800 and 3500-2500 cal yr BP; (Mayewski et al., 2004), cold events in the North Atlantic [cold event 3 and 2; (Bond et al., 2001)], decrease in solar irradiance (Steinhilber et al., 2009) and humidity decreases in the eastern Mediterranean area at 4200 cal yr BP (Bar-Matthews et al., 2003) that could be related with global scale climate variability (Fig. 6). These generally dry phases between 4.5 and 2.8 in Padul-15-05 are generally in agreement with persistent positive NAO conditions during this time (Olsen et al., 2012).

The high-resolution Padul-15-05 record shows that climatic crises such as the essentially global event at ~4200 cal yr BP (Booth et al., 2005), are actually multiple events in climate variability at centennial-scales (i.e., ca. 4500, 4300, 4000 cal yr BP).

5.2.2 Iberian-Roman Humid Period (~2600 to 1600 cal yr BP)

High relative humidity is recorded in the Padul-15-05 record between ~2600 and 1600 cal yr BP, synchronous with the well-known Iberian-Roman Humid Period (IRHP; between 2600 and 1600 cal yr BP; (Martín-Puertas et al., 2009). This is interpreted in our record due to an increase in the Mediterranean forest species at that time (Unit 1; PA-2b; Figs. 6). In addition, there is a simultaneous increase in *Botryococcus* algae, which is probably related to higher productivity during warmer conditions and relatively higher water level.

A minimum in sedimentary rates at this time is also recorded, probably related with lower detritic input caused by less erosion due to afforestation and probably also related to the decrease in TOC due to less organic accumulation in the sediment. Evidence of a wetter climate around this period has also been shown in several alpine records from Sierra Nevada. For example, in the Laguna de la Mula core (Jiménez-Moreno et al. 2013) an increase in deciduous *Quercus* is correlated with the maximum in algae between 2500 to 1850 cal yr BP, also evidencing the most humid period of the Late Holocene. A geochemical study from the Laguna de Río Seco (also in Sierra Nevada) also evidenced humid conditions around 2200 cal yr BP by the decrease in Saharan dust input and the increase in detritic sedimentation into the lake suggesting higher rainfall (Jiménez-Espejo et al., 2014). In addition, Ramos-Román et al. (2016) showed an increase in AP in the Borreguil de la Caldera record around 2200 cal yr BP, suggesting an increase in humidity at that time.

Other records from the Iberian Peninsula also show this pattern to wetter conditions during the IRHP. For example, high lake levels are recorded in Zoñar Lake in southern Spain between 2460 to 1600 cal yr BP, only interrupted by a relatively arid pulse between 2140 and 1800 cal yr BP (Martín-Puertas et al., 2009). An increase in rainfall is described in the central region of the Iberian Peninsula in a study from the Tablas de Daimiel National Park between 2100 and 1680 cal yr BP (Gil García et al., 2007). Deeper lake levels at around 2650 to 1580 cal yr BP, also interrupted by an short arid event at ca. 2125-1790 cal yr BP, were observed to the north, in the Iberian Range (Currás et al., 2012). The fact that the Padul-15-05 record also shows a relatively arid-cold event between 2150-2050 cal yr BP, just in the middle of this relative humid-warm period, seems to point to a common feature of centennial-scale climatic variability in many western Mediterranean and North Atlantic records (Fig. 6). Humid climate conditions at around 2500 cal yr BP are also interpreted in previous studies from lake level reconstructions from Central Europe (Magny, 2004). Increases in temperate deciduous forest are also observed in marine records from the Alboran Sea around 2600 to 2300 cal yr BP, also pointing to

high relative humidity (Combourieu-Nebout et al., 2009). Overall humid conditions between 2600 and 1600 cal yr BP seem to agree with predominant negative NAO reconstructions at that time, which would translate into greater winter (and thus more effective) precipitation in the area triggering greater development of forest species in the area.

Generally warm conditions are interpreted between 1900 and 1700 cal yr BP in the Mediterranean Sea, with high sea surface temperatures (SSTs), and in the North Atlantic area, with the decrease in Drift Ice Index. In addition, persistent positive solar irradiance occurred at that time. The increase in *Botryococcus* algae reaching maxima during the IRHP also seems to point to very productive and perhaps warmer conditions in the Padul area (Fig. 6). There seems to be a short lag of about 200 years between maximum in *Botryococcus* and maximum in Mediterranean forest. This could be due to different speed of reaction to climate change, with algae (short life cycle, blooming if conditions are favorable) responding faster than forest (tree development takes decades). An alternative explanation could be that they might be responding to different forcings, with regional signal (forest) mostly conditioned by precipitation and local (algae) also conditioned by temperature (productivity).

5.2.3 DA and MCA (~1550 cal yr BP to 600 cal yr BP)

Enhanced aridity occurred right after the IRHP in the Padul area. This is deduced in the Padul-15-05 record by a significant forest decline, with a prominent decrease in Mediterranean forest elements, an increase in herbs (Unit 1; PA-3; Figs. 4 and 6). In addition, our evidence suggests a transition from a shallow lake to a more ephemeral wetland. This is suggested by the disappearance of charophytes, a significant decrease in algae component and higher Si and MS and lower TOC values (Unit 1; Figs. 5). Humans probably also contributed to enhancing erosion in the area during this last ~1550 cal yr BP. The significant change during the transition from Unit 1 to Unit 2 with a decrease in the pollen concentration and the increase in Cichoroideae could be due to enhanced pollen degradation as Cichoroideae have been found to be very

resistant to pollen deterioration (Bottema, 1975). However, the occurrence of other pollen taxa (e.g. *Quercus*, Ericaceae, *Pinus*, Poaceae, *Olea*) showing climatic trends and increasing between ca. 1500-400 cal yr BP and a decrease in Cichoroideae in the last ~400 cal yr BP, when an increase in clastic material occurred, do not entirely support a preservation issue (see section of Human activity; 5.4).

This phase could be separated into two different periods. The first period occurred between ~1550 cal yr BP and 1100 cal yr BP (~400 to 900 CE) and is characterized by a decreasing trend in Mediterranean forest and *Botryococcus* taxa. This period corresponds with the Dark Ages [from ca. 500 to 900 CE; (Moreno et al., 2012)]. Correlation between the decline in Mediterranean forest, the increase in the Drift Ice Index in the North Atlantic record (cold event 1; Bond et al., 2001), the decline in SSTs in the Mediterranean Sea and maxima in positive NAO reconstructions suggests drier and colder conditions during this time (Fig. 6). Other Mediterranean and central-European records agree with our climate interpretations, for example, a decrease in forest pollen types is shown in a marine record from the Alboran Sea (Fletcher et al., 2013) and a decrease in lake levels is also observed in Central Europe (Magny et al., 2004) pointing to aridity during the DA. Evidences of aridity during the DA have been shown too in the Mediterranean part of the Iberian Peninsula, for instance, cold and arid conditions were suggested in the northern Betic Range by the increase in xerophytic herbs around 1450 and 750 cal yr BP (Carrión et al., 2001b) and in southeastern Spain by a forest decline in lacustrine deposits around 1620 and 1160 cal yr BP (Carrión et al., 2003). Arid and colder conditions during the Dark Ages (around 1680 to 1000 cal yr BP) are also suggested for the central part of the Iberian Peninsula using a multiproxy study of a sediment record from the Tablas de Daimiel Lake (Gil García et al., 2007).

A second period that we could differentiate occurred around 1100 to 600 cal yr BP/900 to 1350 CE, during the well-known MCA (900 to 1300 CE after Moreno et al., 2012). During this period the Padul-15-05 record shows a slight increasing trend in the Mediterranean forest taxa with respect to the DA, but

the decrease in *Botryococcus* and the increase in herbs still point to overall arid conditions. This change could be related to an increase in temperature, favoring the development of temperate forest species, and would agree with inferred increasing temperatures in the North Atlantic areas, as well as the increase in solar irradiance and the increase in SSTs in the Mediterranean Sea (Fig. 6). This hypothesis would agree with the reconstruction of persistent positive NAO and overall warm conditions during the MCA in the western Mediterranean (see synthesis in Moreno et al., 2012). A similar pattern of increasing xerophytic vegetation during the MCA is observed in alpine peat bogs and lakes in the Sierra Nevada (Anderson et al., 2011; Jiménez-Moreno et al., 2013; Ramos-Román et al., 2016) and arid conditions are shown to occur during the MCA in southern and eastern Iberian Peninsula deduced by increases in salinity and lower lake levels (Martín-Puertas et al., 2011; Corella et al., 2013). However, humid conditions have been reconstructed for the northwestern of the Iberian Peninsula at this time (Lebreiro et al., 2006; Moreno et al., 2012), as well as northern Europe (Martín-Puertas et al., 2008). The different pattern of precipitation between northwestern Iberia / northern Europe and the Mediterranean area is undoubtedly a function of the NAO precipitation dipole (Trouet et al., 2009).

5.2.4 The last ~600 cal yr BP: LIA (~600 to 100 cal yr BP/~1350 to 1850 CE) and IE (~100 cal yr BP to Present/~1850 CE-Present)

Two climatically distinct periods can be distinguished during the last ~600 years (end of PA-3b to PA-4; Fig. 4) in the area. However, the climatic signal is more difficult to interpret due to a higher human impact at that time. The first phase around 600-500 cal yr BP was characterized as increasing relative humidity by the decrease in xerophytes and the increase in Mediterranean forest taxa and *Botryococcus* after a period of decrease during the DA and MCA, corresponding to the LIA. The second phase is characterized here by the decrease in the Mediterranean forest around 300-100 cal yr BP, pointing to a return to more arid conditions during the last part of the LIA (Figs. 5 and 6). This climatic pattern agrees with an increase in precipitation by the transition from positive to negative NAO mode and from warmer to cooler conditions in the North Atlantic area during the first phase of the LIA and a second phase characterized by cooler (cold event 0; Bond et al., 2001) and drier conditions (Fig. 6). A stronger variability in the SSTs is described in the Mediterranean Sea during the LIA (Fig. 6). Mayewski et al. (2004) described a period of climate variability during the Holocene at this time (600 to 150 cal yr BP) suggesting a polar cooling but more humid in some parts of the tropics. Regionally, Morellón et al., (2011) also described a phase of more humid conditions between 1530 to 1750 CE (420 to 200 cal yr BP) in a lake sediment record from NE Spain. An alternation between wetter to drier periods during the LIA are also shown in the nearby alpine record from Borreguil de la Caldera in the Sierra Nevada mountain range (Ramos-Román et al., 2016).

The environmental transition from ephemeral, observed in the last ca. 1550 cal yr BP (Unit 1; Fig. 5), to emerged conditions occur in the last ca. 400 cal yr BP. This is shown by the highest MS and Si values, enhance sedimentation rates and the increase in wetland plants and the stronger decrease in Ca and organic components (TOC) in the sediments in the uppermost part of the Padul-15-05 record (Unit 2; Figs. 3 and 5).

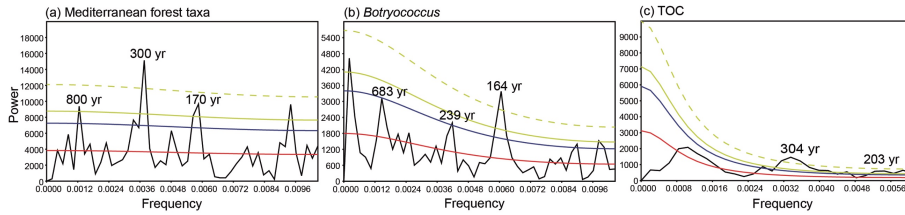


Figure 7. Spectral analysis of (a) Mediterranean forest taxa and (b) *Botryococcus* (mean sampling space = 47 yr) and (c) TOC (mean sampling space = 78 yr) from the Padul-15-05. The significant periodicities above confident level are shown. Confidence level 90 % (blue line), 95 % (green line), 99 % (green dash line) and AR (1) red noise (red line). Spectral analysis was made with Past software (http://palaeo-electronica.org/2001_1/past/issue1_01.htm).

5.3. Centennial-scale variability

Time series analysis has become important in determining the recurrent periodicity of cyclical oscillations in paleoenvironmental sequences (e.g. Fletcher et al., 2013; Jiménez-Espejo et al., 2014; Rodrigo-Gámiz et al., 2014a; Ramos-Román et al., 2016). This analysis also assists in understanding possible relationships between the paleoenvironmental proxy data and the potential triggers of the observed cyclical changes: i.e., solar activity, atmospheric, oceanic dynamics and climate evolution during the Holocene. The cyclostratigraphic analysis on the pollen (Mediterranean forest; regional signal), algae (*Botryococcus*; local signal) and TOC (local signal) times series from the Padul-15-05 record evidence centennial-scale cyclical patterns with periodicities around ~800, 680, 300, 240, 200 and 170 years above the 90 % confidence levels (Fig. 7).

Previous cyclostratigraphic analysis in Holocene western Mediterranean records suggest cyclical climatic oscillations with periodicities around 1500 and 1750 yr (Fletcher et al., 2013; Jiménez-Espejo et al., 2014; Rodrigo-Gámiz et al., 2014a). Other North Atlantic and Mediterranean records also present cyclicities in their paleoclimatic proxies of ca. 1600 yr (Bond et al., 2001; Debret et al., 2007; Rodrigo-Gámiz et al., 2014a). However, this cycle is absent from the cyclostratigraphic analysis in the Padul-15-05 record (Fig. 7). In contrast, the spectral analysis performed in the Mediterranean forest time series

from Padul record, pointing to cyclical hydrological changes, shows a significant ~800 yr cycle that could be related to solar variability (Damon and Sonett, 1991) or could be the second harmonic of the ca. ~1600 yr oceanic-related cycle (Debret et al., 2009). A very similar periodicity of ca. 760 yr is detected in the *Pinus* forest taxa, also pointing to humidity variability, from the alpine Sierra Nevada site of Borreguil de la Caldera and seems to show that this is a common feature of cyclical paleoclimatic oscillation in the area.

A significant ~680 cycle is shown in the *Botryococcus* time series most likely suggesting recurrent centennial-scale changes in temperature (productivity) and water availability. A similar cycle is shown in the *Artemisia* signal in an alpine record from Sierra Nevada (Ramos-Román et al., 2016). This cycle around ~650 yr is also observed in a marine record from the Alboran Sea, and was interpreted as the secondary harmonic of the 1300 yr cycle that those authors related with cyclic thermohaline circulation and sea surface temperature changes (Rodrigo-Gámiz et al., 2014a).

A statistically significant ~300 yr cycle is shown in the Mediterranean forest taxa and TOC from the Padul-15-05 record suggesting shorter-scale variability in water availability. This cycle is also observed in the cyclical *Pinus* pollen data from Borreguil de la Caldera at higher elevations in the Sierra Nevada (Ramos-Román et al., 2016). This cycle could be principally related to NAO variability as observed by Olsen et al. (2012), which follows variations in humidity observed in the Padul-15-05 record. NAO variability also regulates modern precipitation in the area.

The *Botryococcus* and TOC time series shows variability with a periodicity around ~240, 200 and 164 yrs. Sonett and Suess, (1984) described a significant cycle in solar activity around ~208 yr (Suess solar cycle), which could have triggered our ~200 cyclicity. The observed ~240 yr periodicity in the Padul-15-05 record could be either related to variations in solar activity or due to the mixed effect of the solar together with the ~300 yr NAO-interpreted cycle and could point to a solar origin of the centennial-scale NAO variations as suggested by previously published research (Lukianova and Alekseev, 2004;

Zanchettin et al., 2008). Finally, a significant ~170 yr cycle has been observed in both the Mediterranean forest taxa and *Botryococcus* times series from the Padul-15-05 record. A similar cycle (between 168-174 yr) was also described in the alpine pollen record from Borreguil de la Caldera in Sierra Nevada (Ramos-Román et al., 2016), which shows that it is a significant cyclical pattern in climate, probably precipitation, in the area. This cycle could be related to the previously described ~170 yr cycle in the NAO index (Olsen et al., 2012), which would agree with the hypothesis of the NAO controlling millennial- and centennial-scale environmental variability during the Late Holocene in the area (Ramos-Román et al., 2016; García-Alix et al., 2017).

5.4. Human activity

Humans probably had an impact in the area since Prehistoric times, however, the Padul-15-05 multiproxy record shows a more significant human impact during the last ca. 1550 cal yr BP, which intensified in the last ~500 years (since 1450 CE to Present). This is deduced by, a significant increase in nitrophilous plant taxa such as Cichorioideae, Convolvulaceae, Polygonaceae and *Plantago* and the increase in some NPP such as *Tilletia*, coprophilous fungi and thecamoebians (Unit 2; PA-4; Fig. 4). Most of these pollen taxa and NPPs are described in other southern Iberian paleoenvironmental records as indicators of land uses, for instance, *Tilletia* and covarying nitrophilous plants have been described as indicators of farming (e.g. Carrión et al., 2001a). Thecamoebians also show a similar trend and have also been detected in other areas being related to nutrient enrichment as consequences of livestock (Fig. 8). The stronger increase in Cichorioideae have also been described as indicators of animal grazing in areas subjected to intense use of the territory (Mercuri et al., 2006). Interestingly, these taxa began to decline around ca. 400 cal yr BP (~1550 CE), coinciding with the higher increase in detritic material into the basin. We could then interpret this increase in Cichorioideae as greater in livestock activity in the surroundings of the lake during this period, which is supported by the increase in these other proxies related with animal husbandry.

Climatically, this event coincides with the start of persistent negative NAO conditions in the area (Trouet et al., 2009), which could have further triggered more rainfall and more detritic input into the basin. Bellin et al. (2011) in a study from the Betic Cordillera (southern Iberian Peninsula) demonstrate that soil erosion increase in years with higher rainfall and this could be intensified by human impact. Nevertheless, in a study in the southeastern part of the Iberian Peninsula (Bellin et al., 2013) suggested that major soil erosion could have occurred by the abandonment of agricultural activities in the mountain areas as well as the abandonment of irrigated terrace systems during the Christian Reconquest. Enhanced soil erosion at this time is also supported by the increase in *Glomus* type (Figs. 4 and 8).

An important change in the sedimentation in the environment is observed during the last ca. 400 cal yr BP marked by the stronger increase in MS and Si values. This higher increase in detritics occurred during an increase in other plants related with human and land uses such as Polygonaceae, Amaranthaceae, Convolvulaceae, *Plantago*, Apiaceae and Cannabaceae-Urticaceae type (Land Use Plants; Fig. 8). This was probably related to drainage canals in the Padul wetland in the late XVIII century for cultivation purposes (Villegas Molina, 1967). The increase in wetland vegetation and higher values of Poaceae could be due to cultivation of cereals or by an increase in the population of *Phragmites australis* (also a Poaceae), very abundant in the Padul lake margins at present due to the increase in drained land surface. The uppermost part (last ca. 100 cal yr BP) of the pollen record from Padul-15-05 shows an increasing trend in some arboreal taxa at that time, including Mediterranean forest, *Olea* and *Pinus* (Fig. 4). This change is most likely of human origin and generated by the increase in *Olea* cultivation in the last two centuries, also observed in many records from higher elevation sites from Sierra Nevada, and *Pinus* and other Mediterranean species reforestation in the 20th century (Anderson et al., 2011; Jiménez-Moreno and Anderson, 2012; Jiménez-Moreno et al., 2013; Ramos-Román et al., 2016). Preliminary charcoal data show maxima in charcoal particle sedimentation coinciding with maxima in forest (fuel) during

the Early and Middle Holocene humid and warmest maxima and do not show any increase in the last millennia, supporting our conclusions about little human impact in the area until very recent (Webster, pers. comm.). This agrees with previous studies on the area showing that Mediterranean fire regimes today are mostly conditioned by fuel load variations (Jiménez-Moreno et al., 2013; Ramos-Román et al., 2016).

6. Conclusions

Our multiproxy analysis from the Padul-15-05 sequence has provided a detailed climate reconstruction for the last 4700 ca yr BP for the Padul area and the western Mediterranean. This study, supported by the comparison with other Mediterranean and North Atlantic records suggests a link between vegetation, atmospheric dynamics and insolation and solar activity during the Late Holocene. A climatic aridification trend occurred during the Late Holocene in the Sierra Nevada and the western Mediterranean, probably linked with an orbital-scale declining trend in summer insolation. This long-term trend is modulated by centennial-scale climate variability as shown by the pollen (Mediterranean forest taxa), algae (*Botryococcus*) and sedimentary and geochemical data in the Padul record. These events can be correlated with regional and global scale climate variability. Cold and arid pulses identified in this study around the 4200 and 3000 cal yr BP are synchronous with cold events recorded in the North Atlantic and decreases in precipitation in the Mediterranean area, probably linked to persistent positive NAO mode. Moreover, one of the most important humid and warmer periods during the Late Holocene in the Padul area coincides in time with the well-known IRHP, characterized by warm and humid conditions in the Mediterranean and North Atlantic regions and overall negative NAO conditions. A drastic decline in Mediterranean forest taxa, trending towards an open landscape and pointing to

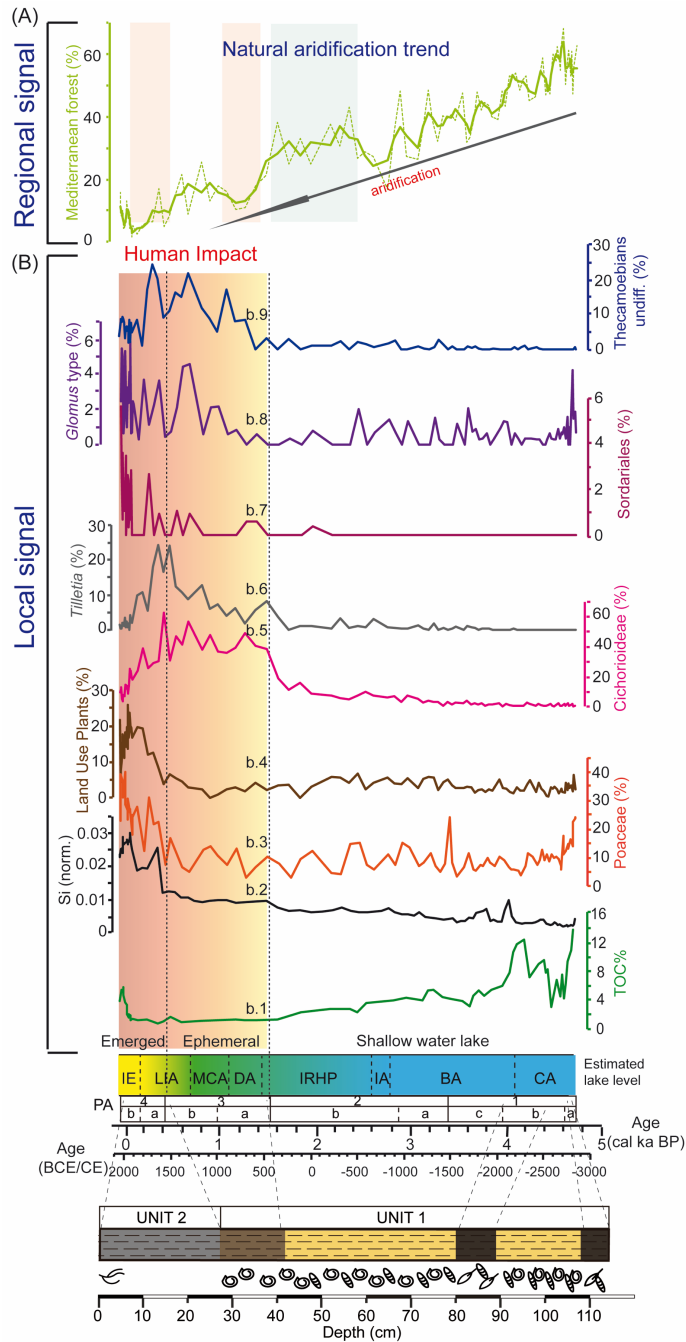


Figure 8. Comparison of the last ca. 4700 yr between regional climatic proxies and local human activity indicators from the Padul-15-05 record. (A) Mediterranean forest taxa, with a smoothing of three-point in bold. (B) Local human activities indicators [(b.1) Total organic carbon (TOC %), soil erosion indicator; (b.2) Si normalized (Si, norm.), soil erosion indicator; (b.3) Poaceae (%), lake drained and/or cultivars indicator; (b.4) Land Use Plants (%), cultivar indicator; (b.5) Cichorioideae (%),

livestock occurrence indicator; (b.6) *Tilletia* (%), farming indicator; (b.7) Sordariales (%), livestock indicator; (b.8) *Glomus* type, soil erosion, (b.9) Thecamoebians undiff. (%), livestock indicator]. Degraded yellow to red shading correspond with the time when we have evidence of human shaping the environment since ca. 1550 cal yr BP to Present. Previously to that period there is a lack of clear evidences of human impact in the area. Land use plants is composed by Polygonaceae, Amaranthaceae, Convolvulaceae, *Plantago*, Apiaceae and Cannabaceae-Urticaceae type.

colder conditions with enhanced aridity, occurred in two steps (DA and end of the LIA) during the last ~1550 cal yr BP. However, this trend was slightly superimposed by a more arid but warmer event coinciding with the MCA and a cold but wetter event during the first part of the LIA. Besides natural climatic and environmental variability, strong evidences exists for intense human activities in the area during the last ~1550 years. This suggests that the natural aridification trend during the Late Holocene, which produced a progressive decrease in the Mediterranean forest taxa in the Padul area, could have been intensified by human activities, notably in the last centuries.

Furthermore, time series analyses done in the Padul-15-05 record show centennial-scale changes in the environment and climate that are coincident with the periodicities observed in solar, oceanic and NAO reconstructions and could show a close cause-and-effect linkage between them.

Acknowledgements

This work was supported by the project P11-RNM-7332 funded by Consejería de Economía, Innovación, Ciencia y Empleo de la Junta de Andalucía, the project CGL2013-47038-R funded by Ministerio de Economía y Competitividad of Spain and fondo Europeo de desarrollo regional FEDER and the research group RNM0190 (Junta de Andalucía). M. J. R.-R. acknowledges the PhD funding provided by Consejería de Economía, Innovación, Ciencia y Empleo de la Junta de Andalucía (P11-RNM-7332). J.C. acknowledges the PhD funding provided by Ministerio de Economía y Competitividad (CGL2013-47038-R). A.G.-A. was also supported by a Ramón y Cajal Fellowship RYC-2015-18966 of the Spanish Government (Ministerio de Economía y Competitividad). Javier Jaimez (CIC-UGR) is thanked for graciously helping with the coring, the drilling equipment and logistics. We also would like to thanks to Graciela Gil-Romera, Laura Sadori and an anonymous reviewer for their comments and suggestions which improved the manuscript.

Supplementary Information

Holocene climate aridification trend and human impact interrupted by millennial- and centennial-scale climate fluctuations from a new sedimentary record from Padul (Sierra Nevada, southern Iberian Peninsula)

María J. Ramos-Román¹, Gonzalo Jiménez-Moreno¹, Jon Camuera¹, Antonio García-Alix¹, R. Scott Anderson², Francisco J. Jiménez-Espejo³, José S. Carrión⁴

¹ Departamento de Estratigrafía y Paleontología, Universidad de Granada, Spain. *mjrr@ugr.es*

² School of Earth Sciences and Environmental Sustainability, Northern Arizona University, USA.

³ Department of Biogeochemistry, Japan Agency for Marine-Earth Science and Technology (JAMSTEC), Japan.

⁴ Departamento de Biología Vegetal, Facultad de Biología, Universidad de Murcia, Murcia, Spain.

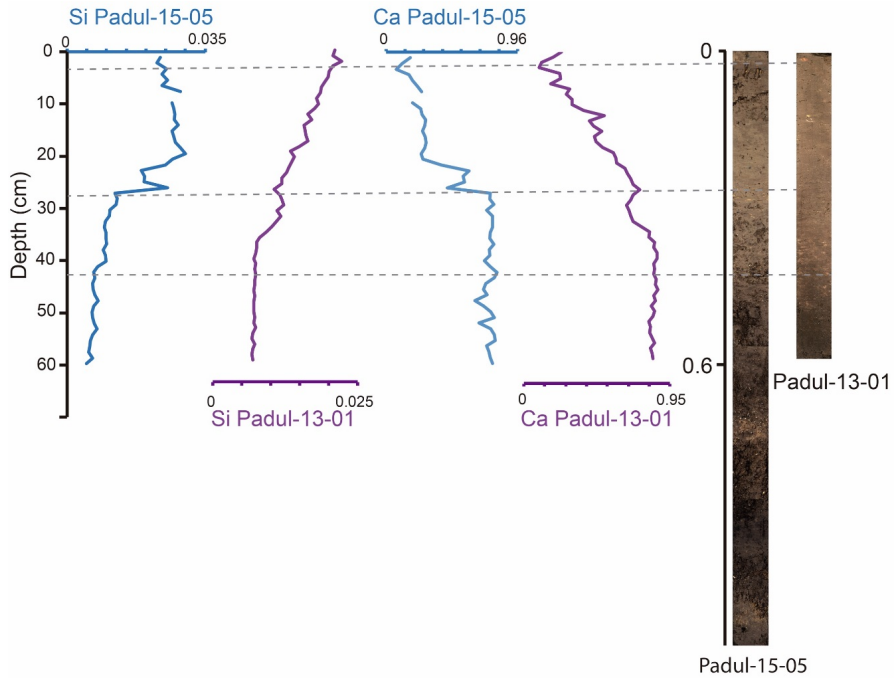


Figure S1: Lithological and geochemical comparison between the upper part of the Padul-15-05 and the Padul-13-01 records.

CHAPTER 4

Chapter 4: Centennial-scale vegetation and North Atlantic Oscillation changes during the Late Holocene in the southern Iberia

M.J. Ramos-Román¹, G. Jiménez-Moreno¹, R.S. Anderson², A. García-Alix³, J.L. Toney³, F.J. Jiménez-Espejo⁴, J.S. Carrión⁵

¹ Departamento de Estratigrafía y Paleontología, Universidad de Granada, Granada, Spain

² School of Earth Sciences and Environmental Sustainability, Northern Arizona University, Flagstaff, AZ, USA

³ School of Geographical and Earth Sciences, University of Glasgow, UK

⁴ Department of Biogeochemistry, Japan Agency for Marine-Earth Science and Technology (JAMSTEC), Yokosuka, Japan

⁵ Departamento de Biología Vegetal, Facultad de Biología, Universidad de Murcia, Murcia, Spain

Published in:

Quaternary Science Reviews, 143 (2016), 84–95

<http://dx.doi.org/10.1016/j.quascirev.2016.05.007>

. Received 4 December 2015; Accepted 9 May 2016

. Impact factor (JCR): 4.797 (2016)

. Rank: Q1

Abstract

High-resolution pollen analysis, charcoal, non-pollen palynomorphs and magnetic susceptibility have been analyzed in the sediment record of a peat bog in Sierra Nevada in southern Iberia. The study of these proxies provided the reconstruction of vegetation, climate, fire and human activity of the last ~4500 cal yr BP. A progressive trend towards aridification during the late Holocene is observed in this record. This trend is interrupted by millennial- and centennial-scale variability of relatively more humid and arid periods. Arid conditions are recorded between ~4000 to 3100 cal yr BP, being characterized by a decline in arboreal pollen and with a spike in magnetic susceptibility. This is followed by a relatively humid period from ~3100 to 1600 cal yr BP, coinciding partially with the Iberian-Roman Humid Period, and is indicated by the increase of *Pinus* and the decrease in xerophytic taxa. The last 1500 cal yr BP are characterized by several centennial-scale climatic oscillations. Generally arid conditions from ~450 to 1300 CE, depicted by a decrease in *Pinus* and an increase in *Artemisia*, comprise the Dark Ages and the Medieval Climate Anomaly. Since ~1300 to 1850 CE pronounced oscillations occur between relatively humid and arid conditions. Four periods depicted by relatively higher *Pinus* coinciding with the beginning and end of the Little Ice Age are interrupted by three arid events characterized by an increase in *Artemisia*. These alternating arid and humid shifts could be explained by centennial-scale changes in the North Atlantic Oscillation and solar activity.

Keywords: Holocene, Southern Iberia, Pollen analysis, Fire, North Atlantic Oscillation, Solar activity

1. Introduction

Recent studies have demonstrated a response of terrestrial vegetation, atmosphere and ocean environments to changes in solar radiation (Jiménez-Moreno et al., 2008, 2013b; Fletcher et al., 2013). Occurring at the boundary between temperate, subtropical and tropical climate regimes the Mediterranean region is a key area in our attempt to understand the interactions between these environments (Alpert et al., 2006). Numerous global paleoclimate proxy records for the Holocene show that weak changes in solar activity triggered climatic variability not only at millennial-scales (e.g. Bond et al., 1997), but also at centennial- and decadal-scales (e.g. Bond et al., 2001; Bard et al., 2006). In addition, one of the main mechanisms influencing present climate in the Mediterranean region is the North Atlantic Oscillation (NAO) and many studies have attempted to relate atmospheric dynamics of the NAO with environmental change in this area (e.g. Lionello and Sanna, 2005). In the last years a variety of multiproxy records have been used for the reconstruction of past NAO conditions (e.g. D'Arrigo et al., 1993; Trouet et al., 2009; Olsen et al., 2012; Baker et al., 2015). These show that positive NAO conditions triggered a decrease in precipitation in the western Mediterranean area, while wetter conditions occurred during negative NAO phases.

Holocene sediment records from lakes, peat bogs and marine environments from the western Mediterranean have been very informative in relating records of vegetation, fire activity and human impact to climate change. Several high-resolution multiproxy lake records from northern and central Iberia have documented centennial-scale paleoclimate evolution for the last millennia (e.g. Martín-Puertas et al., 2011; Currás et al., 2012; Moreno et al., 2012; Corella et al., 2013). Most of the Holocene paleoclimate reconstructions in the southern Iberian Peninsula come from lake and peat deposits at low and montane altitudes, as well as from marine cores (Carrión, 2002; Carrión et al., 2001b, 2003, 2007, 2010a, Martín-Puertas et al., 2008, 2010; Nieto-Moreno et al., 2011; Moreno et al., 2012; Jiménez-Moreno et al., 2015). Studies at higher

elevations are scarcer and mostly come from lake and peat bog sedimentary deposits from the Sierra Nevada range (Anderson et al., 2011; Jiménez-Moreno and Anderson, 2012; García-Alix et al., 2012a, 2013; Jiménez-Moreno et al., 2013a). These studies have provided a strong record of Holocene vegetation, fire, human impact and climate evolution at millennial- and centennial-scales. Currently this region lacks high-resolution records of change that can capture decadal-scale variations such as the NAO.

Within the region, Sierra Nevada has been a key location for paleoecological studies, due to its high elevation records for southern Europe and its sensitive alpine wetland environments (Anderson et al., 2011). Previous records from the range showed that humans influenced these alpine environments during the late Holocene, especially in the last millennium, with increases in pasturing, cultivars and *Pinus* reforestation. However, human impact in these alpine environments is minimal compared to other sites at lower elevations in the area (Anderson et al., 2011; Jiménez-Moreno and Anderson, 2012; Jiménez-Moreno et al., 2013a). Although numerous studies have suggested that the Mediterranean vegetation evolution during the Holocene was largely due to human impact (Reille and Pons, 1992; Pons and Quézel, 1998). Jalut et al., (2009) considered climate change to be a more important determining factor. Others have suggested that we are still far from understanding the correlation between vegetation, fire, climate and human activity, because of the importance of ecological factors in shaping the timing of vegetation responses to disturbances (Carrión et al., 2007).

In this paper we present a multi-proxy high-resolution study from Borreguil de la Caldera (BdlC), a peat bog that records the last ~4500 cal yr BP of vegetation, fire, human impact, and climate history from the Sierra Nevada in southern Spain. The main focus of this study is to elucidate the relationship between vegetation and fire activity with solar cyclicality and atmospheric dynamics. High-resolution studies such as the one here from Borreguil de la Caldera, with ca. 30-yr resolution for the last 1500 yr BP and ca. 120-yr

resolution between approximately 4450 to 1600 cal yr BP, allow us to detect changes in the NAO through time and its impact on the environment. In addition, we also comment on the record of human impact in the Sierra Nevada during the late Holocene.

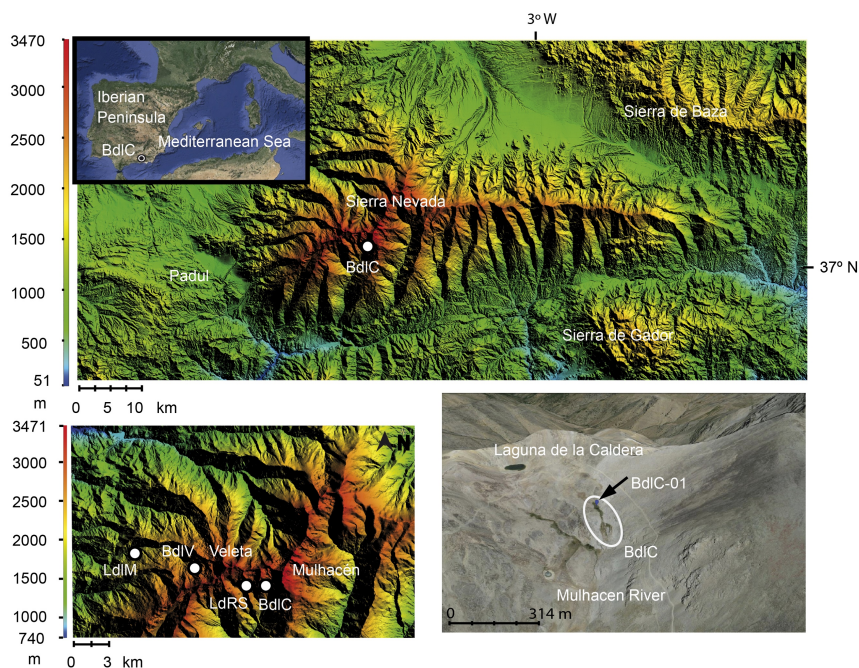


Figure 1. Location of the Borreguil de la Caldera (BdlC) in Sierra Nevada southern Iberian Peninsula, Mediterranean region. Panel on below left is the general location of BdlC, showing the major peaks in the mountain range, and other previously studied wetlands: BdlV = Borreguil de la Virgen peat bog (Jiménez-Moreno and Anderson 2012); LdRS = Laguna de Rio Seco (Anderson et al., 2011); LdIM = Laguna de la Mula (Jiménez-Moreno et al., 2013b). Panel on below right shows the location of BdlC respect to the upper elevation Laguna de la Caldera and the location of the BdlC-01 where the core was taken.

1.1. Sierra Nevada: climate and vegetation

Sierra Nevada is a W-E aligned mountain range located in southern Spain. The range is one of the southernmost European areas to be glaciated during the Late Pleistocene (Schulte, 2002). The postglacial melting of cirque glaciers allowed the formation of lakes and wetlands. These formed on the metamorphic bedrock located at elevations between 2600 to 3100 m asl. Some of these lakes

have filled sediments and have transitioned to small peat bogs (Castillo Martín, 2009). Bedrock is Permotriassic and Paleozoic metamorphic rocks mostly characterized by micashists (Martín Martín et al., 2010).

In the Sierra Nevada Range, the mean annual temperature at 2500 m asl is 4.5 °C, and the mean temperature during the snow free months is 10 ± 6 °C, but could occasionally reach 21 °C. Annual precipitation is 700 mm/yr, seasonally concentrated between October and April, mostly as snow (Oliva et al., 2009). Situated between a temperate humid climate to the north and at subtropical, arid climate to the south, its location proximal to the last-glacial coastal shelves and its high-altitude make this area a particular vegetation hotspot in southern Europe (Carrión et al., 2008; Anderson et al., 2011; González-Sampériz et al., 2010; Jiménez-Moreno and Anderson, 2012; Jiménez-Moreno et al., 2013a). Sierra Nevada is one of the most important centers of plant diversity in the western Mediterranean region. With more than 2100 vascular taxa (species and subspecies) catalogued, it accounts for nearly 30% of the entire vascular flora of the Iberian Peninsula (Blanca, 1996; 2002). Due to the altitudinal gradient of Sierra Nevada (from 900 to more than 3400 m) this mountain range is strongly influenced by thermal and precipitation gradients allowing well-characterized vegetation belts (Valle et al., 2003). The crioromediterranean vegetation belt characterized principally by *Festuca clementei*, *Hormatophylla purpurea*, *Erigeron frigidus*, *Saxifraga nevadensis*, *Viola crassiuscula*, and *Linaria glacialis* is the highest in the area and occurs above ~2800 m. The oromediterranean belt, between ~1900 to 2800 m, bears *Pinus sylvestris*, *Pinus nigra*, *Juniperus hemisphaerica*, *Juniperus sabina*, *Juniperus communis* subsp. *nana*, *Genista versicolor*, *Cytisus oromediterraneus*, *Hormatophylla spinosa*, *Prunus prostrata*, *Deschampsia iberica* and *Astragalus sempervirens* subsp. *nevadensis* as the most representative species. The supramediterranean belt, from approximately 1400 to 1900 m of elevation principally includes *Quercus pyrenaica*, *Quercus faginea*, *Quercus rotundifolia*, *Acer opalus* subsp. *granatense*, *Fraxinus angustifolia*, *Sorbus torminalis*, *Adenocarpus*

decorticans, *Helleborus foetidus*, *Daphne gnidium*, *Clematis flammula*, *Cistus laurifolius*, *Berberis hispanicus*, *Festuca scariosa* and *Artemisia glutinosa*. The mesomediterranean between ~600 and 1400 m of elevation are characterized by *Quercus rotundifolia*, *Retama sphaerocarpa*, *Paeonia coriacea*, *Juniperus oxycedrus*, *Rubia peregrina*, *Asparagus acutifolius*, *D. gnidium*, *Ulex parviflorus*, *Genista umbellata*, *Cistus albidus* and *Cistus laurifolius* (El Aallali et al., 1998; Valle, 2003). The human impact over this area affected the vegetation distribution especially during the last millennium. The most important examples of human disturbance in the area are the *Olea* increase for cultivation at relatively low elevations and *Pinus* reforestation (Anderson et al., 2011; Jiménez-Moreno and Anderson 2012; Jiménez-Moreno et al., 2013a).

1.2. Borreguil de la Caldera (BdlC)

This bog presently occurs above treeline, in the crioromediterranean vegetation belt (Valle, 2003). In Sierra Nevada small bogs such as this one are locally known as “Borreguiles”, which are installed on cirque basin environments with constant moisture characterized by tundra-like vegetation with Cyperaceae as the most representative species. Other secondary species are represented by *Nardus stricta*, *Festuca iberica*, *Leontodon microcephalus*, *Luzula hispanica*, *Ranunculus demissus*, *Sagina saginoides* subsp. *nevadensis*, *Campanula herminii*, *Saxifraga stellaris* subsp. *alpigena*, *Veronica turbicola*, *Sedum anglicum* subsp. *melanantherum*, *Festuca rivularis* and some species of briophytes. Around this peat bog other plant species occur, such as *Armeria splendens*, *Agrostis nevadensis*, *Ranunculus acetosellifolius*, *Plantago nivalis* and *Lepidium stylatum* (Molero-Mesa et al., 1992). BdlC formed part of those high-elevation wetland areas; it is a small peat bog located at 37° 03' 02" N and 3° 19' 24" W in the south face of Sierra Nevada at ~2992 m elevation (Fig. 1). It is situated right below Laguna de la Caldera, another cirque-lake basin located in the upper drainage part of the Mulhacen River. The peat bog area is 0.17 ha. The surface of the drainage basin is 62 ha and includes the Mulhacen

(3479 m asl), the highest peak of the Iberian Peninsula. The area is snow-free approximately between July and October.

2. Methods

Two sediment cores, BdlC-01 and BdlC-02, were recovered in September 2013 from the center of the BdlC basin. Cores were taken with a Livingstone square-rod piston corer. The length for BdlC-01 and BdlC-02 was 56 and 51 cm, respectively. BdlC-02 was taken ca. 50 cm apart from BdlC-01. BdlC-01 was the longest core and it was used for this study.

The split sediment core BdlC-01 was described in the laboratory with respect to lithology and color (Fig. 2). Magnetic susceptibility (MS), a measure of the tendency of sediment to carry a magnetic charge (Snowball and Sandgren, 2001), was measured with a Bartington MS2E meter in SI units. MS measurements were obtained directly from the core surface every 0.5 cm for the entire length of the core (Fig. 2). Five calibrated AMS radiocarbon dates were used to constrain the core chronology. Material used for the AMS datings was peat.

Radiocarbon dates were converted to calendar year before present (cal yr BP) using the IntCal13 curve (Reimer et al., 2013) with Calib 7.1 (<http://calib.qub.ac.uk/calib/>) (Table 1). The age model for BdlC-01 was built using a constant variance model following Heegaard et al., (2005). Calculations of the expected ages and their 95% confidence intervals were made using the software package R (Development Core Team, 2013) employing the functions Cagedepth.r Cagenew.r (Heegaard et al., 2005) (Fig. 2). The sedimentary accumulation rate (SAR) was calculated based on the linear interpolation between radiocarbon dates (Fig. 2).

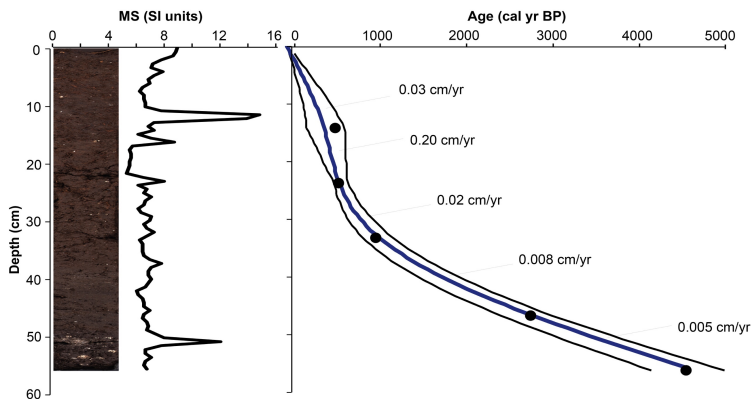


Figure 2. Photo of core BdIC-01, along with the magnetic susceptibility (MS) profile and age-depth model. Sedimentary rates (SAR) are marked. Thin black lines show the 95% confidence intervals. See body of text for explanation of age model construction.

Samples for pollen analysis (1 cm^3) were taken every 0.5 cm throughout the core (Fig. 3). Pollen extraction methods followed a modified Faegri and Iversen, (1989) methodology. Processing included the addition of *Lycopodium* spores for calculation of pollen concentration. Sediment was treated with NaOH, HCl, HF and the residue was sieved at $250 \mu\text{m}$ previous to an acetolysis solution. Counting was performed using a transmitted light microscope at $400\times$ magnification to a minimum pollen count of 300 terrestrial pollen grains. Fossil pollen was identified using published keys (Beug, 1961) and modern reference collections at University of Granada (Spain). Pollen concentration is a measure of pollen density [grains per cm^3 of sample sediment (gr/cm^3); Fig. 3]. The raw counts were transformed to pollen percentages based on the terrestrial sum, not including Cyperaceae (Fig. 3). The pollen zonation was executed by cluster analysis using eight different pollen taxa- *Pinus*, *Olea*, *Artemisia*, Poaceae, Caryophyllaceae, Cichorioideae, *Quercus* total and Other Asteraceae (CONISS; Grimm, 1987). Non-pollen palynomorphs (NPP) were found in the pollen slides including fungal spores, thecamoebians, algal spores and microzoological remains. The NPP percentages were calculated and represented with respect to the total pollen sum (Fig. 3). Tree pollen taxa were grouped in

arboreal pollen (AP). In addition, we calculated the Cyperaceae/Poaceae ratio (C/P ratio) (Fig. 4). This ratio has previously been used as an indicator of wet and dry conditions in bog areas (e.g., Turney et al., 2004). A cyclostratigraphic analysis was performed in the BdlC-01 pollen time series. We used the REDFIT software (Schulz and Mudelsee, 2002) on the unevenly spaced pollen time series in order to identify cyclical changes in the vegetation through spectral peaks registered at different frequencies throughout the studied core.

Samples for macrocharcoal analysis (1 cm^3) were taken every 0.5 cm through the core (Fig. 3), following the methodology described in Whitlock and Anderson, (2003). In order to deflocculate the sediments, the samples were soaked in a solution of ca. 10% sodium hexametaphosphate and distilled water for two to five days. Samples were washed and sieved into a set with mesh size of 125 and 250 μm . Each subsample was counted using a stereomicroscope to 10-70x magnifications.

Table 1. Age data for BdlC-01. All ages were calibrated using IntCal13 curve (Reimer et al., 2013) with Calib 7.1 (<http://calib.qub.ac.uk/calib/>). *Sample number assigned at radiocarbon laboratory; DirectAMS= Accium BioSciences, Seattle, Washington.

Laboratory number ^a	Depth (cm)	Dating method (AMS)	Age (14C cal yr BP \pm 1 σ)	Calibrated age (cal yr BP) 2 σ range	Median age (cal yr BP)
Reference ages	0	Present	AD2013	-63	-63
DirectAMS-004385	13.7	¹⁴ C	388+24	327-507	469
DirectAMS-004386	23.2	¹⁴ C	474+26	500-537	517
DirectAMS-004387	36.8	¹⁴ C	1036+31	915-1049	950
DirectAMS-004388	46.4	¹⁴ C	2563+30	2505-2754	2725
DirectAMS-004389	56	¹⁴ C	4066+29	4438-4798	4551

3. Results

3.1. Chronology and sedimentary rates

The age-depth model (Fig. 2) shows that the BdlC-01 record covers the last 4500 cal yr BP. SARs between 0.008 and 0.02 cm/yr occurred from ~23 cm to the core bottom. SAR increased to ~0.03 cm/yr between ~13 cm to the core top. The highest SAR of 0.20 cm/yr occurred right above ~ 23 to 13 cm [about 550 to 350 cal yr BP].

3.2. Lithology and magnetic susceptibility

The BdlC-01 record mostly consists of peat sediments but thin layers of clay occur at about 52 to 51 cm, coinciding with a MS spike (Fig. 2). MS data show minimum values around 20 to 17 cm, corresponding to a more fibrous peat at that depth. MS spikes again at ~12 cm but visually we could not observe any significant lithological change.

3.3. Pollen, NPP and charcoal

A total of fifty-four pollen taxa were identified but only the most representative (taxa higher than 1%) were plotted in the pollen diagram (Fig. 3). NPP and charcoal are also displayed in Figure 3. Four pollen zones (Fig. 3) were visually identified with the help of cluster analysis using the program CONISS (Grimm, 1987). Pollen preservation was good and concentration was high from ~50,000 to 3,500,000 grains/cc. Charcoal concentration varied from 0 to 8 particles/cc.

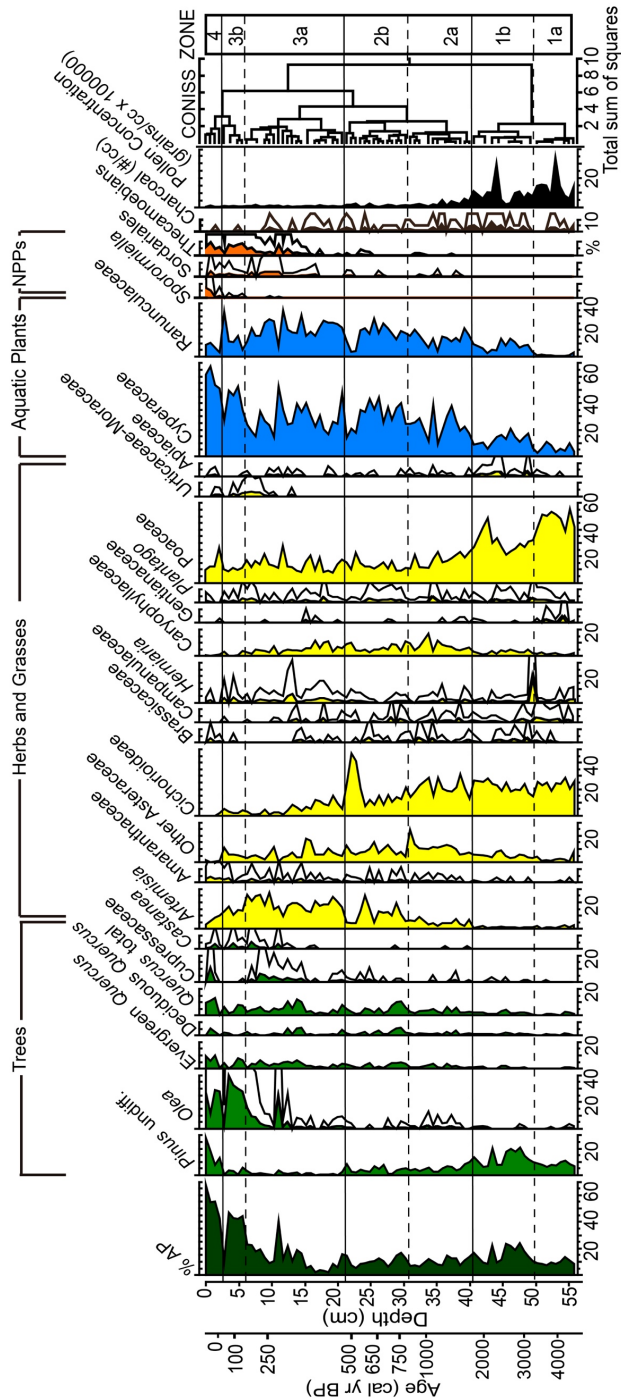


Figure 3. Pollen and non-pollen palynomorphs (NPPs) percentage of selected taxa and charcoal concentration in the BdIC-01 core. Pollen percentage was calculated with respect to the total pollen sum, excluding Cyperaceae. NPP percentages were calculated

with respect to the total pollen sum. Tree taxa are shown in green, herbs and grasses in yellow, aquatic plant in blue and NPPs in orange. Charcoal concentration (number of particles/cc = #/cc), pollen concentration (grains/cc) and pollen zonation are shown on the right. Silhouette shows exaggeration of pollen percentage X5.

Pollen zones are described below:

3.3.1. Zone BdlC- 1 [~4500 to 1740 cal yr BP/~2600 to 200 BCE (56-40 cm)]

Zone 1 is principally characterized by the abundance of herbs and grasses such as Poaceae, with an average occurrence around 37% and Cichorioideae of ca. 22%. Other herbs such as Amaranthaceae, Caryophyllaceae, Gentianaceae and Campanulaceae also occur but with lower abundances in this zone. The AP is mainly composed of *Pinus*, with average values around 11% but there are some important peaks around 20%. Although tree pollen is dominated by *Pinus* other tree taxa occur in lesser concentrations, with *Quercus* total (ca. 2%), *Olea* (< 1%) and *Betula* (ca. 1%; not plotted in the diagram due to very low percentage) as the most representative. This pollen zone is subdivided into zones subzone-1a and subzone-1b (Fig. 3). The main characteristics that differentiate subzone 1a from 1b (at ca. 3000 cal yr BP/ca. 1050 cal BC) are the decline in Poaceae from ca. 55 to 25% and the increase in *Pinus* from ca. 10 to 20%. Other Asteraceae and Caryophyllaceae also slightly increase ca. 3-7% and ca. 2-5%, respectively. Wetland plants such as Cyperaceae also occur and show a considerable increase (from ca. 8% to 15%) between subzone 1a/1b. Charcoal particles are rare, but show a slight increase in subzone 1b (Fig. 3).

3.3.2. Zone BdlC- 2 [~1740 to 500 cal yr BP/ ~200 BCE-1450 CE (40-21 cm)]

The decline in Poaceae to values around 15% and the decrease in *Pinus* averaging around 5% are the most important features in this zone. *Artemisia*, other Asteraceae and, most notably, Cupressaceae become more abundant in zone 2, while Caryophyllaceae also increases. Arboreal pollen decreases remarkably, with a decline in *Pinus*, however an increase in *Quercus* total (to

ca. 5%) occurred. The transition between subzone 2a/b (boundary at ~760 cal yr BP/1200 CE) is remarkable, with a prominent increase in *Artemisia* and *Quercus* total, but on the other hand, a slight decline in other Asteraceae, Caryophyllaceae and Cichorioideae. Wetland pollen shows a considerable increase, with Cyperaceae (averaging ca. 30%) and Ranunculaceae (averaging ca. 15%). Fungal remains are also present; coprophilous fungi such as Sordariales and thecamoebians show their first occurrence in this zone. The number of charcoal particles declines.

3.3.3. Zone Bd1C- 3 [~500 cal yr BP to 50 cal yr BP/~1450 to 1900 CE (21-2.5 cm depth)]

The main feature in zone 3 is the major expansion of *Artemisia*, reaching maximum values (to ca. 40%), and the decrease in *Pinus* (to ca. 2%). A noteworthy drop in Cichorioideae (to ca. 7%) and the slight increase in evergreen *Quercus*, Cupressaceae and *Castanea* also characterize this zone. The disappearance of *Betula* and the first occurrence of *Juglans*, *Cerealia*, *Vitis* (not plotted in the diagram due to very low percentage) and Urticaceae-Moraceae are also remarkable. The subzone 3a/b (~160 cal yr BP/~1790 CE) transition is marked by an increase in arboreal pollen mostly produced by a high increase in *Olea*, reaching maximum values (ca. 40%) at around 60 cal yr BP (1890 CE). Wetland pollen remain abundant. This zone documents a prominent increase in coprophilous fungi (*Sporormiella* and Sordariales); thecamoebians are very abundant too, showing maxima. Charcoal particles show a decrease in zone 3 in relation with the zone 2. This decrease is stronger in the end of the subzone 3b.

3.3.4. Zone BdlC- 4 [1900 CE to present (2.5 to 0 cm depth)]

Zone 4 shows the expansion of tree species with respect to zone 3, especially in *Pinus* (maximum around 30%) and evergreen *Quercus* (to ca. 10%). *Olea* remains very important in the assemblage with a very slight decline in values than in the previous subzone 3b but with two punctually stronger decreases around 1900 and 1980 CE. With respect to herbs, *Artemisia*, other Asteraceae and Caryophyllaceae show a decrease and Cichorioideae even disappeared. However slight increases in Amaranthaceae occurred. *Castanea*, *Juglans* and Urticaceae-Moraceae pollen disappeared at the end of the zone. Maximum values of the wetland plant Cyperaceae (ca. 60%) is observed in this zone. Thecamoebians show an increase in this zone and dung fungi continue to increase, with particular incidence for *Sporormiella* and Sordariales. Charcoal occurrence is insignificant.

3.4. Spectral Analysis

Spectral analysis was performed on the *Pinus* and *Artemisia* time-series in order to identify the presence of cyclical periodicities in the BdlC-01 record (Fig. 5). Centennial-scale cycles with periodicities around ca. 750, 650, 300, 200, 170 and 140 yr (above the 80 % confidence level) were obtained.

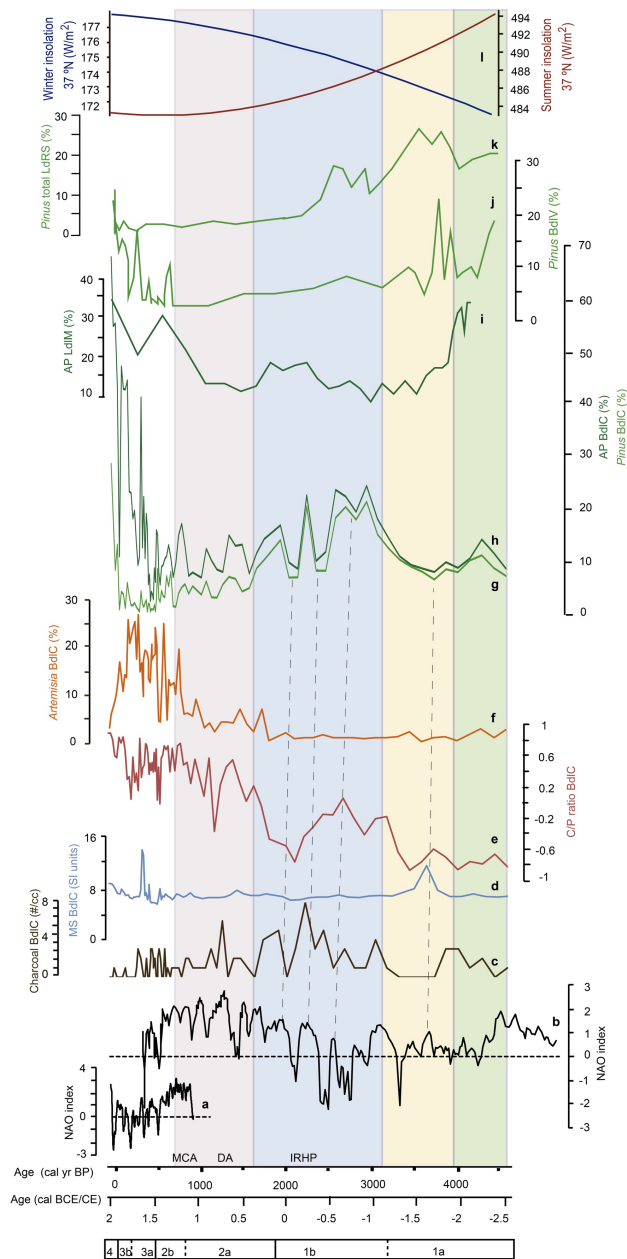


Figure 4. Comparison of different pollen taxa from the last 4500 yr from the BdlC and other pollen records from other Sierra Nevada lakes and peat bogs, North Atlantic Oscillation (NAO) reconstructions and insolation curve. (a) NAO index from a climate proxy reconstruction from Morocco and Scotland (Trouet et al., 2009). (b) NAO index from a climate proxy reconstruction from Greenland (Olsen et al., 2012). (c) BdlC charcoal record. (d) BdlC Magnetic Susceptibility (MS) record. (e) Cyperaceae/Poaceae (C/P) ratio from the BdlC record. (f) *Artemisia* percentage from

the BdlC record. (g) *Pinus* percentage from the BdlC record. (h) Arboreal pollen (AP) percentage from the BdlC record. (i) AP percentage from LdlM record (Jiménez-Moreno et al., 2013), Sierra Nevada. (j) *Pinus* percentage from BdlV record (Jiménez-Moreno and Anderson, 2012), Sierra Nevada. (k) *Pinus* percentage from LdRS (Anderson et al., 2011), Sierra Nevada. (l) Winter [left] and summer [right] insolation calculated for 37° N (Laskar et al., 2004). IRHP = Iberian-Roman Humid Period, DA = Dark Ages, MCA = Medieval Climatic Anomaly. Dashed black lines show a tentative correlation between the *Pinus* record (g) and the NAO reconstruction (b). Color vertical bars highlight discussed climate variability. The green bar represents a relative humid period, the yellow bar an arid period, the blue bar a humid period corresponding with the IRHP and the gray bar a generally arid period.

4. Discussion

One of the main goals of this study is to analyze the relationship of vegetation changes from the BdlC bog in the Sierra Nevada with atmospheric variations in the area and the possible links with solar variability. Integration of pollen, NPP and charcoal data are important in reconstructing the paleoclimatic and palaeoenvironmental history in this climatically sensitive region. In this study we compared our record with other local and more distant paleoclimate records, NAO reconstructions, insolation and solar output for the past 4500 cal yr BP (Bard et al., 2000; Laskar et al., 2004; Trouet et al., 2009; Olsen et al., 2012; Figs. 4 and 6). This allowed us to determine regional- and global-scale paleoclimate interpretations and inferences about the origin of these cyclic climate variations. Below we show that the BdlC Sierra Nevada alpine pollen record supports the hypothesis of a coupling between solar activity, North Atlantic atmospheric activity and environmental changes in the western Mediterranean during the Holocene.

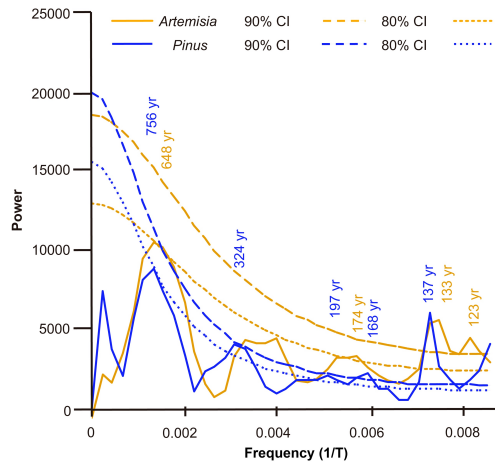


Figure 5. Spectral analysis of *Pinus* and *Artemisia* from the BdlC-01 record. Confidence levels (CI) are marked (80 and 90 %) and the significant periodicities above 80% of confident level are shown. A number of overlapping (50%) segments (n_{seg}) of 3 and a rectangular window were used. Spectral analysis was made using Past (http://palaeo-electronica.org/2001_1/past/issue1_01.htm).

4.1. Proxy interpretation

Variations in AP have previously been used in the Sierra Nevada as a proxy for humidity changes (Jiménez-Moreno et al., 2013a; Fig. 4). *Pinus* dominates the AP pollen sum throughout much of the Holocene in the Sierra Nevada region and this is the reason we pay special attention to this pollen taxa. *Pinus nigra* and *Pinus sylvestris* occur at present in the Sierra Nevada oromediterranean vegetation belt, between 1600-2100 m asl (Carrión et al., 2002) and 1600-2200 m asl (Castro et al., 2004), respectively. Pollen sedimentation studies show that in locations where *Pinus* is present, its percentage is approximately 50-60% of the total pollen sum (Andrade Olalla et al., 1994). This is confirmed in the Sierra Nevada by an ongoing moss polster analysis carried out in an altitudinal transect (Ramos-Román, in prep.). The pollen results show that where pine forest occurs the *Pinus* percentage is around 40-70 % and in places above the treeline it is around 20-30%. In the BdlC-01 record *Pinus* percentage is between 10-30%, which suggests that *Pinus* forest never occurred at such high-elevation in the Sierra Nevada during the late

Holocene and that these pollen grains come from lower elevations (Anderson et al., 2011).

On the other hand, increases in xerophyte pollen (e.g., *Artemisia*) have been used as an indication of aridity in the Mediterranean region (Carrión et al., 2001b, 2007, 2010a; Anderson et al., 2011; Jiménez-Moreno and Anderson, 2012; Jiménez-Moreno et al., 2013a). In this study we also used xerophyte pollen to elucidate climatic shifts. In addition, the widely-used Cyperaceae – Poaceae pollen ratio (C/P ratio; Cour et al., 1999; Turney et al., 2004; Mensing et al., 2008) was used as a paleoclimate proxy to record the local vegetation response to fluctuations between wetter and drier bog conditions. Alternating high pollen percentages of Cyperaceae and Poaceae suggest that the bog frequently changed between wetter (high C/P ratio) and drier (low C/P ratio) states (Jiménez-Moreno et al., 2008).

Charcoal analysis is based on the accumulation of charcoal particles in sedimentary basins during or following a fire event. Gaussian models suggest that particles smaller than 100 µm travel well beyond 100 m and only very small particles can travel long distances (Whitlock and Anderson, 2003). The charcoal particles that we quantified were >100 µm, between 250 and 125 µm, suggesting a local source of charcoal. However Anderson et al. (2011) suggest that during the Holocene in this alpine area in the Sierra Nevada, charcoal particles probably came from fires at lower elevation.

4.2. Aridification trend during the late Holocene

Our data document an increasing trend in dryness in this area during the past 4500 cal yr BP (Fig. 4) as shown by the progressive decrease in natural forest species and the increase in xerophytes such as *Artemisia*. This agrees with previous paleoclimatic studies in the western Mediterranean, which document a progressive aridification trend since ~7000 cal yr BP (Carrión, 2002; Fletcher and Sánchez-Goñi, 2008; Jalut et al., 2009; Carrión et al., 2010a; Anderson et al., 2011; Jiménez-Moreno and Anderson, 2012; Jiménez-Moreno

et al., 2015). Jiménez-Moreno et al. (2012, 2015) suggested that semi-desert expansion and Mediterranean forest decline during the late Holocene in this area could be explained by decreasing summer insolation (Laskar et al., 2004; Fig. 4). Reduced summer insolation could have produced lower sea-surface temperatures (Marchal et al., 2002), generating a decrease in the land–sea contrast that would be reflected in a reduction of the wind system and a reduced precipitation gradient from sea to shore during the fall–winter season. Also, a reorganization of the general atmospheric circulation with a northward shift of the westerlies – a long-term enhanced positive NAO trend – has been interpreted, inducing drier conditions in this area (Magny et al., 2012). Declining summer insolation at these latitudes would have negatively affected the growing season due to cooling, producing further forest decline (Fletcher et al., 2007).

An interesting feature in the BdlC-01 record is the increasing trend in wetland plants (Cyperaceae) and the decrease in grasses (Poaceae) during the late Holocene (see C/P ratio; Fig. 4). Although this contrasts with the aridification trend discussed above, we suggest that this may be explained by two local processes. First, the decrease in summer insolation could have caused wetland and aquatic plants to have greater surface runoff water availability for longer in the summer, due to greater persistence of snowbanks upstream and a meltwater more slowly, providing a better local environment for Cyperaceae. Second, the progressive sediment infilling of the basin could have created a broader bog surface profile producing a greater surface wetland environment for Cyperaceae expansion. This increase in wetland plants during the late Holocene is in agreement with an increase in Cyperaceae pollen in the nearby record of Borreguil de la Virgen (Jiménez-Moreno and Anderson, 2012). García-Alix et al. (2012), who studied the geochemistry from this site explained this change as the transition from a lacustrine to a full bog environment [an increase in C/N ratios and a decrease in Carbon isotopes ($\delta^{13}\text{C}$)].

4.3. Millennial-scale environment and climate change

Previous paleoecological records are available from other alpine wetlands from the Sierra Nevada (Anderson et al., 2011; Jiménez-Moreno and Anderson, 2012; Jiménez-Moreno et al., 2013a). The BdIC improves on the late Holocene record of paleoenvironmental and paleoclimates through high-resolution analysis of pollen and other proxies. Our high-resolution analysis here shows that the late Holocene progressive aridification trend is climatically more complex than originally demonstrated (Fig. 4).

4.3.1. Arid interval between ~4000 and ~3100 cal yr BP

The pollen record from BdIC-01 begins with a relatively small peak in *Pinus* between 4500 and 4200 pointing to relatively humid climate but a trend to arid conditions occurred later on, starting around 4000 cal yr BP. This relatively dry period comprises part of the pollen subzone-1a and is mainly distinguished by the lowest percentage in AP, very low abundance of *Pinus* and very low occurrence of charcoal particles. The C/P ratio also shows a decreasing trend, indicating a drier bog environment. A lithological change towards clay sedimentation and a spike in MS at ~3600 cal yr BP (around 51-52 cm) is also observed at this time (Fig. 2). Drier conditions could have triggered less vegetal productivity in the bog and/or more erosion in the drainage area producing more detritic sedimentation. Our results agree with previous studies in the area and arid conditions at this time are well documented in changes in paleoecological and geochemical proxies in the Laguna de la Mula, Sierra Nevada (Jiménez-Moreno et al., 2013a) and in several other marine records from Alboran Sea (synthesized in Fletcher et al., 2013; Martín-Puertas et al., 2010) and terrestrial sites such as Zoñar Lake (synthesized in Martín-Puertas et al., 2010). Oliva et al. (2009) shows the occurrence of solifluction landforms between 2500 and 3000 m asl in the Sierra Nevada around 3400 cal yr BP, which they explained as cold and/or wet periods. Cold and arid conditions are inferred during this period in the western Mediterranean

Sea (M3; Frigola et al., 2007) and higher Saharan dust input (Zr/Al ratio; Jimenez-Espejo et al., 2014). Aridity in the western Mediterranean area could be explained by multi-decadal persistence of positive NAO conditions at this time (Olsen et al., 2012).

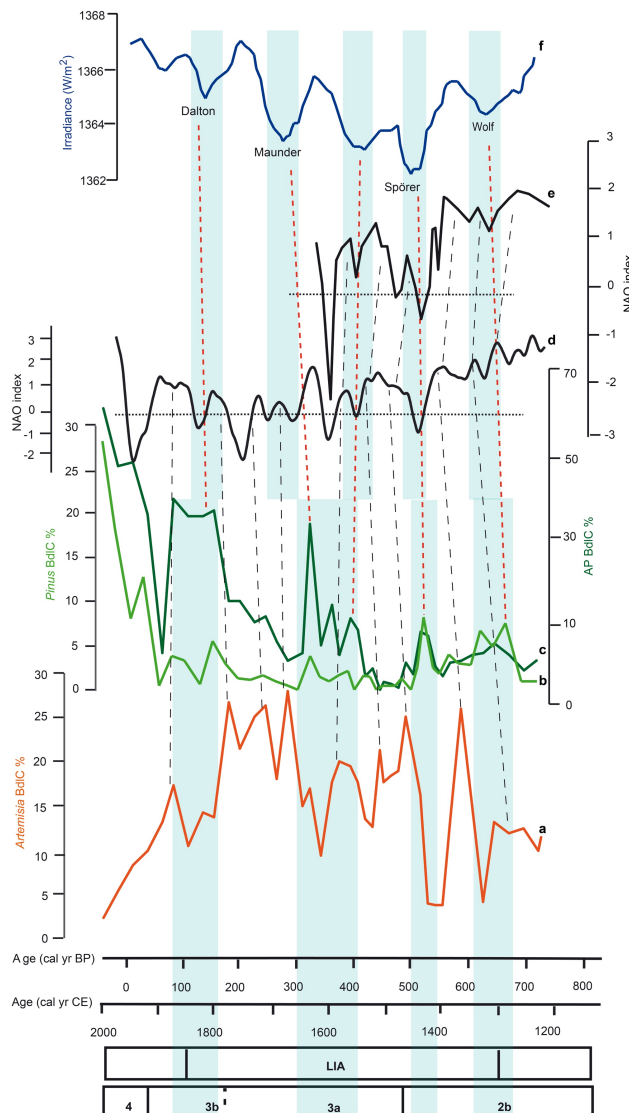


Figure 6. Comparison of different pollen taxa from the last 700 yr from the BdlC record, NAO reconstruction and solar irradiance curve. (a) *Artemisia* percentage from the BdlC record. (b) *Pinus* percentage from the BdlC record. (c) Arboreal pollen (AP) percentage from the BdlC record. (d) North Atlantic Oscillation (NAO) index from a

climate proxy reconstruction from Morocco and Scotland (Trouet et al., 2009). (e) North Atlantic Oscillation (NAO) index from a climate proxy reconstruction from Greenland (Olsen et al., 2012). (f) Reconstruction of the total solar irradiance (Bard et al., 2000). Dashed black lines are a tentative correlation between *Artemisia* record (a) and NAO reconstruction (d, e). Dashed red lines show a tentative correlation between the *Pinus* record (b) and solar activity (f).

4.3.2. Humid period between ~3100 and ~1600 cal yr BP

Probably the most humid period during the late Holocene in southern Iberia occurred during the well-known Iberian-Roman Humid Period (IRHP) (Martín-Puertas et al., 2009). The BdlC record shows maxima in humid conditions at this time (zone-1b) through maximum values of AP (mostly *Pinus*) previously to recent human reforestation and a decrease in xerophytic plants with a minimum in *Artemisia* (BdlC-1b pollen zone; Fig. 4). This is in agreement with other western Mediterranean paleoclimate records such as Zoñar Lake (Martín-Puertas et al., 2009), a marine core of Alboran Sea (Martín-Puertas et al., 2010) and the Laguna de la Mula in the Sierra Nevada (Jiménez-Moreno et al., 2013a). NAO reconstructions show the most negative phases during this period (Olsen et al., 2012; Baker et al., 2015; Fig. 4), which could explain high winter precipitation, the main source of moisture in this area. The smaller-scale variability observed in the pollen record, with two relative minima in AP during this generally-humid period, could also be due to oscillations in the NAO, observed in the Olsen et al. (2012) reconstruction, further supporting the link between vegetation changes and the NAO cyclical phases. This variability is shown in AP and C/P ratios from BdlC. A first gradual transition phase from an arid period between ca. 3100 and 2800 cal yr BP is observed in the increase in AP and C/P ratio. The most humid period is observed between ca. 2800 to 2400 cal yr BP, with the maximum in AP and a high increase in C/P ratio. A relative arid period is interpreted between ca. 2400 to 1900 cal yr BP by a general decrease in AP (even though there is a peak in AP at approximately 2200 cal yr BP) and C/P ratio. A relative humid interval occurred between ca. 1900 and 1600 cal yr BP, depicted by the increase in AP and C/P ratios. Other

studies in southern Iberia show variability in humidity during the IRHP. The most humid period from 2500 to 2140 cal yr BP, an arid period between 2140 to 1800 cal yr BP and a relative humid period from 1800 to 1600 cal yr BP are also observed in the record from Zoñar Lake (Martín-Puertas et al., 2009) and a very similar variability is showed in the record of Somolinos Lake (Currás et al., 2012).

The maximum macrocharcoal concentration registered in BdIC-01 coincided in time with the wettest period in the record (Figs. 3 and 4). The comparison with another records from the Sierra Nevada (Anderson et al., 2011; Jiménez-Moreno et al., 2013a) and other studies in close mountain ranges and marine records in the western Mediterranean region (Sierra de Gador [Carrión et al., 2003], Sierra de Baza [Carrión et al., 2007], Alborán Sea [Daniau et al., 2007] and Djamila, northern Morocco [Linstädter and Zielhofer, 2010]) also show an increase in fire activity during this period. This suggests that higher fire activity at this time could have been related to the presence of abundant fuel load (Daniau et al., 2007; Linstädter and Zielhofer, 2010; Jiménez-Moreno et al., 2013a). Nevertheless, two different records in Sierra de Cazorla show a reverse trend in fire activity during this period (Carrión et al., 2001b; Carrión et al., 2002), which may be due to different characteristics in fire regimes related with precipitation (Linstädter and Zielhofer, 2010; Jiménez-Moreno et al., 2013a). For example, in typically arid and semiarid environments in the Mediterranean area fuel load limits fire regimes. However, in the less arid Mediterranean environments with a mean annual precipitation above 500-700 mm the factor for fire recurrence could have been moisture. We suggest that this could explain the different fire recurrences during this period in one of the Sierra de Cazorla records (Siles lake; Carrión et al., 2002) with an annual precipitation average of 800-1000 mm. However in the other record from the Sierra de Cazorla (Villaverde lake; Carrión et al., 2001a) a lesser annual precipitation average of around 225 mm is recorded and it is not possible to apply this hypothesis but another of the many factors controlling fire in the

area. Gil-Romera et al., (2010) summarized pollen and charcoal records from southeastern Spain and showed that differences in fire regimes could be explained by variations in climate, vegetation, altitude and human activity.

4.3.3. Most Recent 1500 cal yr BP: Dark Ages, Medieval Climate Anomaly and Little Ice Age

The most recent 1500 years in the BdIC record are characterized by several centennial-scale environmental and climatic oscillations (Fig. 6). First, a generally arid period (coinciding with the majority of zone-2) occurred between ca. 1500 to 660 cal yr BP (ca. 450 to 1300 CE), depicted by a progressive decrease in *Pinus* (and AP in general) and an increase in *Artemisia*. This period comprises the Dark Ages (DA) and the Medieval Climate Anomaly (MCA), between 500 to 900 CE and 900 to 1300 CE, respectively (Moreno et al., 2012). Previous studies show overall arid conditions and persistently positive NAO (low winter precipitation) during this time, supporting our results. For example, tree-ring and speleothem analyses from Morocco and Scotland (Trouet et al., 2009; Wassenburg et al., 2013; Baker et al., 2015) and a multiproxy geochemical record from a small lake in Greenland (Olsen et al., 2012) all show a strong correlation among different paleoclimate proxies with positive NAO during that time. This also agrees with more regional marine and terrestrial studies from the Iberian Peninsula. Vegetation evolution through the MCA in central and eastern Iberia shows a general decrease in AP, principally in mesophytic taxa, and an increase in more xerophytic and heliophytic vegetation (Moreno et al., 2008; Morellón et al., 2011; Rull et al., 2011; Moreno et al., 2012; Corella et al., 2013) also suggesting aridity. Further, Moreno et al. (2012) reviewed paleoclimate proxies for the MCA from the Iberian Peninsula and showed a general decline in lake levels in northeast and southeast Iberia (Martín-Puertas et al., 2010; Morellón et al., 2011) with major Saharan eolian input in the westernmost part of the Mediterranean Sea (Nieto-Moreno et al., 2011).

The last ca. 700 cal yr BP (between 1300 CE and present) are characterized by rapid and pronounced centennial-scale oscillations (Fig. 6). Four periods depicted by relatively higher *Pinus* (and AP) and centered at ca. 1300, 1410, 1550-1620 and 1810 CE occurred, most likely indicating enhanced humid conditions. The first and last of these humid periods coincided with the beginning and end of the Little Ice Age (LIA; from ca. 1300 to 1850 CE). It is worth noting that charcoal peaks occurred immediately after these humid periods, supporting the hypothesis of the availability of fuel conditioning fire activity discussed above (Figs. 3 and 4). Continuing with our reasoning above, wetter climatic conditions during the LIA period are probably related to negative NAO conditions, which produces a general increase in winter precipitation in the area (Trouet et al., 2009; Fig. 6). These alternate with three arid events are also observed during the LIA, perhaps related to cyclical changes in NAO states as previously observed in Trouet et al. (2009) (Fig. 6). The strong visual covariation between these humid-to-arid events, NAO states and solar activity (sunspots) observed in the last few centuries (Bard et al., 2000) could indicate a strong coupling between changes in solar activity, atmospheric variations and vegetation changes here. Low solar activity during the Wolf, Spörer, Maunder and Dalton minima could have triggered persistent negative NAO conditions, enhancing winter precipitation in the area that would produce increases in forest species (i.e., *Pinus*) and decreases in *Artemisia* (Fig. 8). Morellón et al. (2011) also observed increases in *Pinus nigra* and *P. sylvestris* as well as higher lake levels in a montane lake in the Pre-Pyrenees (northeastern Spain) coinciding in time with minima in solar activity. The increase in *Pinus* during the last century (zone-4) is more difficult to interpret due to the major influence of human activity in the area that could have modified the landscape (see section below).

4.4. Centennial-scale vegetation, solar and atmospheric changes

Previous Holocene studies suggest that small variations in solar activity

could have produced changes in the atmospheric dynamics at millennial-, centennial- and decadal-scales (e.g., Bard et al., 2000; Bond et al., 2001; Hu et al., 2003; Martin-Puertas et al., 2012). Times series analysis on the BdIC-01 record reveals centennial-scale periodicities around ca. 750, 650, 300, 200, 170, 140 and 120 years above the 80% confidence level (Fig. 5). Some of these periodicities are very similar to well-known atmospheric variations (e.g. NAO) and solar cycles, suggesting a link between changes in the vegetation and thus climate in this area, mostly conditioned by NAO modes, with solar activity. The 650-yr cycle could be in relation with the 650-yr cycle shown in a record from the East Alboran Sea basin (Rodrigo-Gámiz et al., 2014a) related with North Atlantic thermohaline circulation and sea surface temperatures. With respect to the 300-yr cycle, Bond et al. (2001) found a similar cycle of ca. 300 yr in the ice rafting debris record, this cycle is also shown in the NAO reconstruction (Olsen et al., 2012). The 200-yr period could be linked with the 208-yr Suess cycle (Damon and Sonett, 1991). The 170-yr cycle shows similar periodicities with the NAO reconstruction (Olsen et al., 2012). Other pollen records also point to a relationship between vegetation changes and the solar-climate activity and some similar centennial-scale cycles at 197, 212, 222, 292 and 750 yr are shown in an alpine bog record from New Mexico (Jiménez-Moreno et al., 2008), coinciding with the BdIC-01 record at ca. 200, 300 and 750 yr periodicities. Therefore, these studies show similar millennial- and centennial-scale changes in vegetation related with solar and North Atlantic atmospheric oscillations that could be of hemispheric-scale.

4.5. Human impact

Evidences of human impact in the BdIC record began to appear prior to the Industrial Era, notably since ca. 1500 CE (zones BdIC-3 and BdIC-4). Coprophilous fungi such as Sordariales are first recovered from sediments beginning about 1500 years ago, but strongly increase in abundance and frequency in the last ~400 years contemporaneous with the appearance of *Sporormiella* (Fig. 7). This trend correlates with other locations in Sierra Nevada, specifically with the BdIV and LdRS records, where *Sporormiella* consistently occurs during the last 500 yr (Jiménez-Moreno and Anderson, 2012) and 1000 yr (Anderson et al., 2011), respectively. This increase is probably due to the introduction of livestock and grazing at high elevation in the Sierra Nevada (Anderson et al., 2011; Jiménez-Moreno and Anderson, 2012). Nearly contemporaneously, an increase in thecamoebians occurred in the BdIC record (Fig. 7). A similar occurrence in the BdIV record over the last 150 cal yr BP was interpreted by Jiménez-Moreno and Anderson (2012) as being due to a nutrient enrichment of the wetland by livestock that frequented the bogs.

The most recent centuries witnessed an increase in AP, principally from *Pinus* and *Olea* pollen (Figs. 4 and 7) in the BdIC-01 record. Anderson et al. (2011) suggested the increase in *Olea* paralleled an increase in olive oil production in the last century. The same pattern identified in the BdIV (Jiménez-Moreno and Anderson, 2012) and LdlM (Jiménez-Moreno et al., 2013a) records shows this is a regional event. The increase in *Pinus* is associated with *Pinus sylvestris* plantation (Anderson et al., 2011). This reforestation commenced in the middle of the 20th century to reverse human deforestation in the preceding centuries (Valbuena-Carabaña et al., 2010).

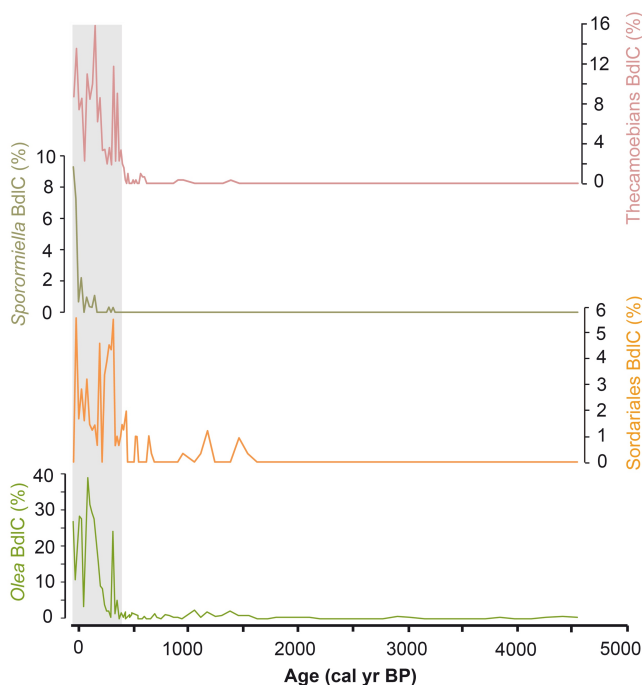


Figure 7. Comparison of pollen and non-pollen palynomorphs (NPPs) for the last 4500 cal yr BP from the BdlC-01 core considered to be related to human activities. Note the exponential increase in the taxa in the last 400 cal yr BP: *Olea* pollen, Sordariales, *Sporormiella* and thecamoebians. The gray vertical bar represents evidences of human impact in the last 400 cal yr BP.

5. Conclusions

The details recorded in the BdlC cores help to clarify the potential relationship between environmental changes in the western Mediterranean, atmospheric dynamics of the NAO and solar activity variations during the late Holocene. The overall climatic reconstructions using pollen, charcoal and NPP from the BdlC-01 record confirms previous evidence of an increasingly arid trend in climate during the late Holocene. However, our high-resolution multi-proxy analysis of the BdlC record provides a greater understanding of centennial- to decadal-scale climate change, recording rapid oscillation between relatively arid and humid intervals in this area during key-periods of the late Holocene such as the IRHP, MCA and LIA. This strong relationship is further supported in this record by correlation of these centennial-scale

humidity shifts at very similar times, and with amplitudes and periodicities coinciding with previously published Mediterranean regional records, NAO reconstructions and with evidence of solar activity variations. This study has then allowed us to associate persistently positive NAO conditions with drier periods and negative NAO conditions with wetter climate in the Mediterranean region. Further, our study documents that fire activity during the late Holocene in our region is probably connected with vegetation fuel load, also in agreement with other studies in the western Mediterranean, demonstrating that climate is a crucial factor in fire dynamics. Although anthropogenic impact is evident in the last centuries in the Sierra Nevada, our work demonstrates that, overall, climate is the most important trigger for vegetation change.

Acknowledgements

The support for the present study derives from the project P11-RNM 7332 funded by Consejería de Economía, Innovación, Ciencia y Empleo de la Junta de Andalucía, the project CGL2013-47038-R funded by Ministerio de Economía y Competitividad of Spain and Fondo Europeo de Desarrollo Regional FEDER and the research group RNM0190 (Junta de Andalucía). M.J.R.-R. acknowledges the PhD funding provided by Consejería de Economía, Innovación, Ciencia y Empleo de la Junta de Andalucía (P11-RNM 7332). Charcoal analysis was completed while M.J.R.-R. was a resident scholar at Northern Arizona. A.G.-A. was supported by a Marie Curie Intra-European Fellowship of the 7th Framework Programme for Research, Technological Development and Demonstration (European Commission). We would also like to thank two anonymous reviewers and the editor (Neil Roberts) for their valuable suggestions.

CHAPTER 5

Chapter 5: Alpine bogs of southern Spain show human-induced environmental change superimposed on long-term natural variations

Antonio García-Alix^{1,2}, Francisco J. Jiménez-Espejo³, Jaime L. Toney¹, Gonzalo Jiménez-Moreno², María J. Ramos-Román², R. Scott Anderson⁴, Patricia Ruano^{5,6}, Ignasi Queralt⁷, Antonio Delgado Huertas⁶, and Junichiro Kuroda³

¹ School of Geographical and Earth Sciences, University of Glasgow, UK.

² Departamento de Estratigrafía y Paleontología, Universidad de Granada, Granada, Spain.

³ Department of Biogeochemistry (JAMSTEC), Yokosuka, Japan.

⁴ School of Earth Sciences and Environmental Sustainability, Northern Arizona University, Flagstaff, AZ, USA.

⁵ Departamento de Geodinámica, Universidad de Granada, Granada, Spain.

⁶ Instituto Andaluz de Ciencias de la Tierra (IACT), CISC-UGR, Armilla, Spain.

⁷ Institute of Environmental Assessment and Water Research (IDAEA), CSIC, Barcelona, Spain.

Published in:

Scientific Reports, 7 (1), 7439

DOI:10.1038/s41598-017-07854-w

. Received 5 October 2016; Accepted 5 July 2017

. Impact factor (JCR): 4.259 (2016)

. Rank: Q1

Abstract

Recent studies have proved that high elevation environments, especially remote wetlands, are exceptional ecological sensors of global change. For example, European glaciers have retreated during the 20th century while the Sierra Nevada National Park in southern Spain witnessed the first complete disappearance of modern glaciers in Europe. Given that the effects of climatic fluctuations on local ecosystems are complex in these sensitive alpine areas, it is crucial to identify their long-term natural trends, ecological thresholds, and responses to human impact. In this study, the geochemical records from two adjacent alpine bogs in the protected Sierra Nevada National Park reveal different sensitivities and long-term environmental responses, despite similar natural forcings, such as solar radiation and the North Atlantic Oscillation, during the late Holocene. After the Industrial Revolution both bogs registered an independent, abrupt and enhanced response to the anthropogenic forcing, at the same time that the last glaciers disappeared. The different response recorded at each site suggests that the National Park and land managers of similar regions need to consider landscape and environmental evolution in addition to changing climate to fully understand implications of climate and human influence.

1. Introduction

Mountainous areas in the Mediterranean region are among the most vulnerable in Europe, and have been severely affected by recent climate and human-induced environmental changes with regard to water resources, temperature gradients, sensitive species, and soil fertility (Schröter et al., 2005; Regato and Salman, 2008). Alpine systems here function as ‘sky islands’, because plant communities are often patchy, occur over narrow elevational bands and are highly susceptible to environmental and climate stressors. The lack of ecosystem connectivity leaves plant communities and plant species (many of which are endemic) highly vulnerable to extinction (Blanca, 2001; Regato and Salman, 2008), because they cannot respond via latitudinal redistribution, but shift altitudinally (Thomas et al., 2006; Menéndez et al., 2014).

The long-term natural environmental evolution in the western Mediterranean region follows an aridification and desertification trend during the late Holocene (deMenocal et al., 2000; Carrión et al., 2003). This signal has been influenced and even boosted by human impact, especially in the last centuries (Carrión et al., 2003; García-Alix et al., 2013). So far, the increased rate and magnitude of recent changes have had significant economic and social consequences, such as crop destruction, human migrations, or conflicts between farmers and herders (Kepner et al., 2006). However, exactly how these recent fluctuations will manifest in additional environmental changes is still largely unknown, so longer-term records that demonstrate how current changes fit into the historical context are needed. These longer-term records will help in understanding future change, where climatic forecasts for the mountains of the Mediterranean region are not optimistic, and point toward a marked temperature increase and precipitation decrease (López-Moreno et al., 2011), which are likely to accelerate environmental degradation.

The highest elevation environments in the Sierra Nevada of southern Iberia (~3000 masl) have experienced little direct impact from human activities for centuries. Although these areas are actively protected today due to their environmental richness, and are part of the Natural Park and Biosphere Reserve of

Sierra Nevada (Gómez-Ortiz et al., 2010), they have recorded indirect influence of human activities such as reforestation and atmospheric pollution (Anderson et al., 2011; García-Alix et al., 2013). Wetlands in this alpine area are mainly oligotrophic, since their catchment basins consist of bare mica-schist bedrock with sparse soil development. Consequently, their biogeochemistry is highly influenced by allocthonous atmospheric inputs that supply important nutrients rather than by local sources (Morales-Baquero et al., 2006; Pulido-Villena et al., 2006). All of these features make these remote alpine environments outstanding ecological observatories of climate change (Catalan et al., 2013) that allow the identification of the signatures of both natural and human-induced environmental changes (Morales-Baquero et al., 2006; Anderson et al., 2011; García-Alix et al., 2013; Jiménez-Espejo et al., 2014). In particular, our previous research from sedimentary archives of these wetlands shows a possible increase in the rate of environmental change during the last century (García-Alix et al., 2012a; Jiménez-Espejo et al., 2014), in agreement with the sharp precipitation decrease and temperature increase, as well as an increase in industrial activities and changes in land use in the western Mediterranean region (Rogora et al., 2003; López-Moreno et al., 2011; Oliva and Gómez-Ortiz, 2012). Clear evidence of these changes include the final melting of the Little Ice Age (LIA) Corral del Veleta Glacier (the southernmost glacier in Europe) in the 1920s (Grunewald and Scheithauer, 2010) and the gradual permafrost reduction in recent decades (Gómez-Ortiz et al., 2014). In this paper we identify the oscillations and trends of natural and anthropogenically-induced ecosystem changes by comparing two adjacent Holocene records from high elevation wetlands in the Sierra Nevada: Borreguil de la Virgen (BdlV: 37° 03' 15'' N; 3° 22' 40'' W) and Borreguil de la Caldera (BdlC: 37° 03' 02'' N; 3° 19' 24'' W) (Fig. 1). The sediments mainly consist of clays and peat in both sites, but the sedimentary record is longer in BdlV (165cm, ~8.5 cal ky BP) (Jiménez-Moreno and Anderson, 2012) than in BdlC (56cm, ~4.5 cal ky BP) (Ramos-Román et al., 2016). The sedimentary records along with the age models of both sites are depicted in Supplementary Fig. S1. The Holocene pollen record in both sites (Jiménez-Moreno and Anderson, 2012; Ramos-Román et al., 2016), along with the

organic data from bulk sediment (carbon and nitrogen) in BdIV (García-Alix et al., 2012a) have provided a strong framework to design the present study. The outcomes of this work can be used to set up strategies to minimise the impact of present abrupt climate changes in sensitive areas and to identify other potentially vulnerable high-elevation sites.

The selected high-elevation peat bogs (called “borreguiles”) have similar areas (~0.18 hectares in BdIV and ~0.17 hectares in BdIC) and elevation (2945 masl in BdIV and 2992 masl in BdIC), but the catchment basins and valley orientations are different (Fig. 1). The catchment basin of BdIV is ~30 hectares, and it is located in the north-west-facing Dílar River Valley. However, the catchment basin of BdIC, which is nearly twice the size, ~62 hectares, is located in the south-facing glacially carved Poqueira River Valley. Most of the alpine catchment basins in the Sierra Nevada area are small and non-vegetated, with plant growth limited to the bog surface and immediate surrounding wetland during the ice-free season (from ~April to ~October) (Valle, 2003). The small size of the catchment basins and peatland areas as well as the effect of the steep topography, imply that our records not only register the environmental evolution of the peatland areas, but could also be influenced by their catchment basins.

Vegetation in Sierra Nevada is distributed in elevationally-determined belts, controlled by the amount of precipitation and seasonal temperature gradients (Anderson et al., 2011). The present treeline occurs at ~2550 masl and the selected records are located in the tundra-like vegetation belt with open herbaceous grasslands (above ~2900 masl) (Valle, 2003; Anderson et al., 2011). Peatland vegetation mainly consists of Poaceae and Cyperaceae, as well as non-vascular plants (bryophytes), even though there are also some less abundant plant taxa (Valle, 2003; Pérez-Luque et al., 2015). The studied sites are mostly ombrotrophic terrestrial peatlands, since the primary hydrological input to both bogs is from direct precipitation (rain or snow). However, BdIC has a small spring upstream that is fed through groundwater seepage from Laguna de la Caldera, located at the head of the catchment basin at ~3030 masl (Fig. 1c).

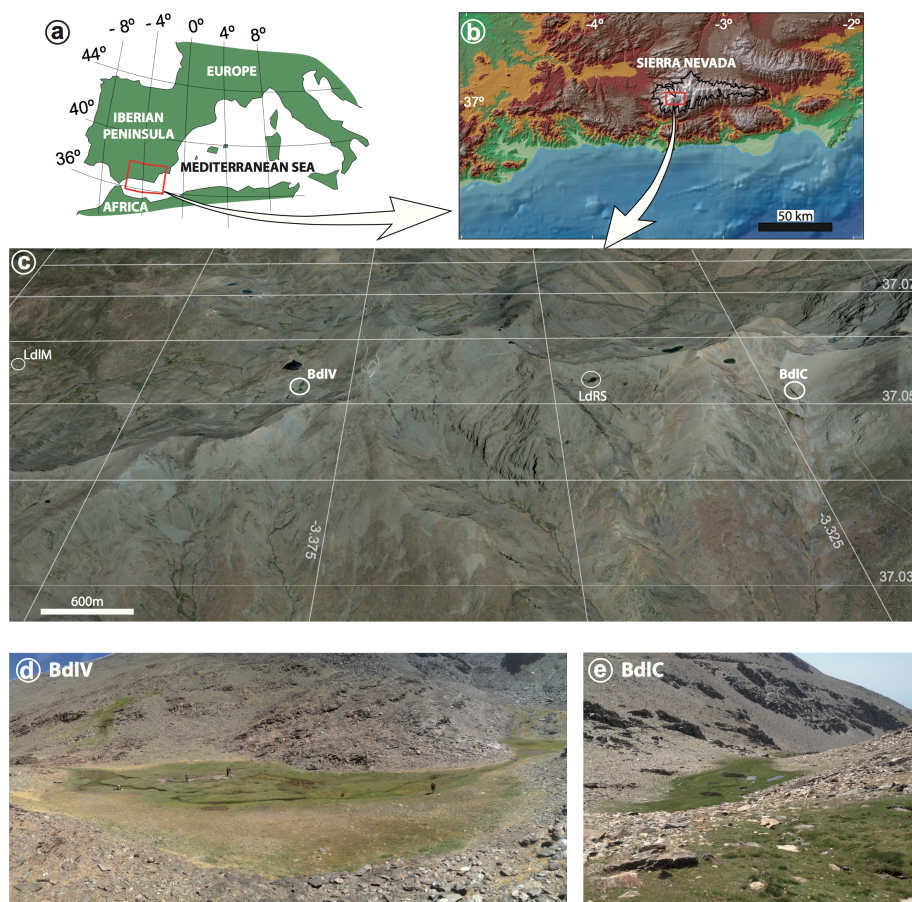


Figure 1. Geographical setting. (a) Location of the studied area in the western Mediterranean, (b) the relief of Sierra Nevada (black line, National Park limit), and (c) the location of studied sedimentary records, including the sampling areas for vegetation and soils, Laguna de la Mula (LdIM), Borreguil de la Virgen (BdIV), Laguna de Río Seco (LdRS), and Borreguil de la Caldera site (BdIC), (d) Borreguil de la Virgen area and (e) Borreguil de la Caldera area. Data source and software: (a) map created by P. Ruano using Adobe Illustrator [5.5] (<https://www.adobe.com/>), (b) data from Suttle Radar Tomography Mission (SRTM-90: <http://www2.jpl.nasa.gov/srtm/>) (USGS, 2006) plotted by means of ArcMap [10.1] (<http://www.esri.com/software/arcgis/arcgis-for-desktop>), (c) map from Google Earth Pro [7.1.5.1557] (<https://www.google.es/earth/download/gep/agree.html>) using the data provided by Google 2016 and DigitalGlobe 2016, and (d-e) pictures from G. Jiménez-Moreno.

2. Results

Recent plant and soil biomarkers. One way to detect changes in vegetation and vegetation belts through time is by analysis of *n*-alkanes from plant leaf waxes.

Investigation of the distribution of different chain lengths in modern plant species (Ficken et al., 2000; Bush and McInerney, 2013) can be applied to interpretations of past vegetation, environmental and landscape changes (Schefuß et al., 2003). Our modern plant and soil survey in the extreme Sierra Nevada environments (Fig. 1c) shows that the distance plants occur from a water source, such as wetlands, controls the length of *n*-alkanes carbon chains. In particular, plants that are in or near the water pools show a stronger predominance of the shorter carbon chains. This relationship is expressed by different *n*-alkane indices, such as average chain length (ACL), carbon preference index (CPI), and proportion of aquatics (P_{aq}) in the studied sites (Table 1; Supplementary Fig. S2). ACL values and the most abundant *n*-alkane are usually lower in areas closer to the water pools. Opposite trends have been found in the P_{aq} . CPI values are higher than 3, which indicate that diagenesis and thermal alteration have not occurred (Bush and McInerney, 2013). Analysis of modern plant CPI values show that the lowest values are recorded in algae/moss/peat samples, as expected (Table 1; Supplementary Fig. S2).

Organic geochemistry in the sedimentary records. Leaf wax biomarkers (*n*-alkanes) and organic proxies from bulk sediments, such as carbon to nitrogen atomic ratio (C/N), hydrogen to carbon atomic ratio (H/C), total organic carbon (TOC), total nitrogen (TN), as well as carbon and nitrogen isotopes ($\delta^{13}\text{C}$ and $\delta^{15}\text{N}$), are useful tools to understand the origin of the organic matter and the biogeochemical cycles of past environments (Meyers, 2003). Leaf wax extractions from both sedimentary records released enough *n*-alkane concentrations to develop high-quality paleoenvironmental reconstructions (Supplementary Fig. S3). Bulk sediment organic variables were also analysed in BdlC. Previously published bulk sediment organic data from BdlV (García-Alix et al., 2012a) will be also used in the environmental models in order to compare similar variables in both studied sites (Supplementary Figs. S4, S5). Principal Components Analyses (PCA) were performed using the same variables in both cores: ACL, P_{aq} , CPI, C/N, TOC, TN, $\delta^{13}\text{C}$, and $\delta^{15}\text{N}$, to identify the different factors (components) that have driven the environmental responses at each site (Fig. 2; Supplementary Figs. S6-S8; Supplementary Tables S1-S3). A major shift

in environmental parameters, deduced from pollen, algae, and geochemical records, occurred in BdlV at around 5500-5000 cal yr BP, during the transition from an early-middle Holocene lake to a bog (García-Alix et al., 2012a; Jiménez-Moreno and Anderson, 2012) (Supplementary Fig. S5). So, another PCA was performed for the BdlV-bog stage (last 5000 yrs) to compare the bog stages in both areas (Supplementary Fig. S8; Supplementary Table S3). We will focus on the latter in the discussion, because it is more comparable to BdlC.

The PCA analysis yielded three significant components (Supplementary Fig. S6-S8; Supplementary Tables S1-S3). The first principal component (PC1) describes 42% of the total variance for BdlC and 56.5% for BdlV-bog. The main positive loadings for PC1 are ACL-CPI-TOC in BdlV-bog, and ACL-CPI-C/N in BdlC, while the main negative component is P_{aq} in both sites. C/N also has a large positive loading in PC1 for both sites. As previously described, P_{aq} , ACL, CPI, and C/N are related to the source of organic matter (aquatic/terrestrial), so PC1 reflects the kind of inputs: terrestrial vs aquatic, which we interpret as representing the water availability of the site.

The second principal component (PC2) explains 25% of the total variance for BdlC and 19% for BdlV-bog. The main loadings (positive) for the PC2 are TOC and TN. These variables primarily represent the concentration of organic matter in the sediment (Meyers, 2003), which mostly depends on the terrestrial and aquatic primary productivity and their accumulation rates in the studied sites.

The third principal component (PC3) only describes 14.4% of the total variance in BdlC, and 10.6% in BdlV-bog stage. PC3 in BdlC is mainly related to the isotopes in the bulk sediments and inversely related to wetland plant/algal proxies (low C/N, high TN) (Cloern et al., 2002; Meyers, 2003), and slightly related to the P_{aq} . These relationships suggest that PC3 is likely related to the isotopic enrichment that usually occurs when there is either high aquatic activity/productivity in the water pools and/or C and N limitation (Meyers, 2003). The main loadings in PC3 BdlV-bog are C/N (positive) and TN (negative), related to higher presence of terrestrial vascular plant relative to algal inputs, which mainly depends on the water and nutrient availability.

Table 1. Summary of the *n*-alkane indices (CPI, ACL, and P_{aq}) from the studied plant, algae and peat samples at different distance from the water pools in Sierra Nevada (see more details in Supplementary Fig. S2).

Distance from the main water pool	<i>n</i> -alkane indices		
	CPI	ACL	P_{aq}
Far	22.0±10.4	30.2±1.0	0.02±0.02
Intermediate	13.6±8.6	29.8±0.4	0.10±0.03
Near/in	6.5±2.5	28.7±0.5	0.32±0.12

Inorganic geochemistry. Concentrations of various metals and elements were measured in the core. For instance, mercury (Hg) is often input to lakes via eolian processes and is typically sourced from industrial and urban emissions (Selin, 2009; Guédron et al., 2016). Hg content of the sedimentary record of BdIC is constant ($\sim 55.9 \pm 8.9$ ppb) before ~ 170 cal yr BP, but there is an abrupt increase (to ~ 99.1 ppb) since that time, and a generally increasing trend until present, reaching more than 160 ppb (Fig. 3c; Supplementary Fig. S4). In addition, this alpine area is located in the free troposphere, making this location highly sensitive to Saharan uplifted aerosols injected in the troposphere (Bozzano et al., 2002; Mladenov et al., 2010). Certain elemental ratios such as Zr/Th or Zr/Al have been successfully used as a proxy of the source of the aeolian input in Sierra Nevada (Jiménez-Espejo et al., 2014) and western Mediterranean (Rodrigo-Gámiz et al., 2015), as Zr is characteristic of North African rocks, soils, and aerosols (Moreno et al., 2006). This African Zr signal has also been recorded in summer aerosols at ~ 3000 masl in Sierra Nevada, where Zr concentrations of 27.7 ± 3.8 ppm were registered in 2008 AD (Supplementary Table S4). BdIC core shows an increasing trend in the Zr/Al record from ~ 3500 cal yr BP until the end of the Medieval Climate Anomaly (MCA), ~ 700 cal yr BP. Since then, there is a fluctuating decreasing trend until the 20th century (Fig. 2n; Supplementary Fig. S4).

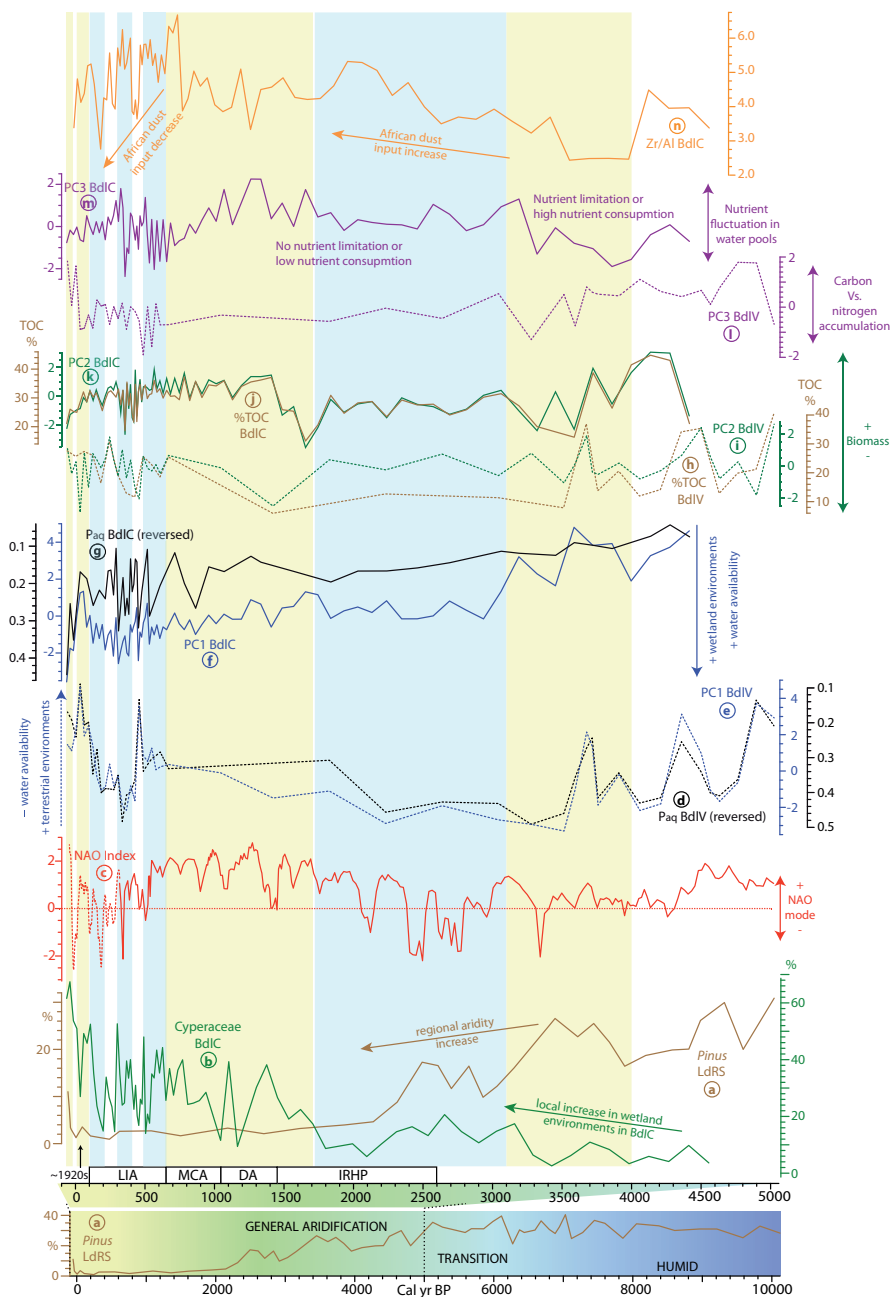


Figure 2. Comparison of humidity trends along with different productivity features and African dust input fluctuations during the middle-to-late Holocene in the studied records, including: (a) general trends of humidity in the studied region along with *Pinus* pollen record of LdRS (Anderson et al., 2011; García-Alix et al., 2012a; Jiménez-Espejo et al., 2014; Jiménez-Moreno et al., 2013a; Jiménez-Moreno and Anderson, 2012; Ramos-Román et al., 2016) (blue colour: humid periods; yellow colours: dry periods), (b) local wetland development at BdlC deduced from *Cyperaceae* pollen (Ramos-Román et al., 2016), (c)

middle-to-late Holocene NAO index reconstruction: solid line (Olsen et al., 2012) and dotted line (Trouet et al., 2009), (d-g) water availability evolution in both cores (PC1s and P_{aq}), (h-k) biomass accumulation/production in both cores (PC2s and %TOC), (l) terrestrial / algal inputs in the bog (PC3 of BdlV), (m) isotopic fluctuations caused by nutrient availability in aquatic environments (PC3 of BdlC), and (n) aeolian dust input fluctuations in BdlC (Zr/Al). Acronyms: LIA: Little Ice Age; MCA; Medieval Climatic Anomaly; DA: Dark Ages; IRHP: Ibero-Roman Humid Period.

Cyclostratigraphy. Time-series analysis is used to identify important cyclical changes within sediment records. Spectral analyses performed on the multiple proxies at our sites indicate several cycles exist at both cores above the 90%, 95% and 99% confidence threshold (Supplementary Figs. S9, S10; Supplementary Table S5). The most significant cycles at BdlC are ~1500 years for productivity proxies (TOC, TN and TOH) and ~250-200 years for water availability/nutrient proxies ($\delta^{13}C$ and $\delta^{15}N$, CPI, ACL and P_{aq}). The spectral analysis on the BdlV-bog data shows the most significant cycles are at ~650 and ~520 years for several productivity and aquatic/terrestrial proxies, and ~400, ~350-300, and ~250-year cycles mainly in aquatic/terrestrial inputs (CPI and ACL). The 200-250, and 400-year cycles are typically related to solar-activity (Stuiver et al., 1995), and the others (e.g., 170 or 300-year cycles) have been linked with the North Atlantic Oscillation (NAO) (Olsen et al., 2012) (Supplementary Table S5). We are aware that the periodicity of the highest frequency cycles (i.e. 113 -150 years) might be too short for the resolution of the core data in certain intervals. Although these highest frequency cycles at least double the mean sample spacing for each proxy (Supplementary Figs. S9-10) and are over the confidence threshold of 90%, we prefer not to include them in the discussion.

3. Discussion

Bog origin and evolution. Electrical resistivity tomography (ERT) profiles support different origins for each bog (Supplementary Fig. S11). BdlV initially was a lake in a glacial depression during the early Holocene, evolving into a wetland/peatland in the middle-to-late Holocene (García-Alix et al., 2012a), ~5100-5000 cal yr BP (Supplementary Fig. S5). BdlC probably had no lacustrine phase, because it exists on a slope. We suggest that this bog stage at both sites resulted from transition to more

arid conditions (deMenocal et al., 2000; Carrión et al., 2007; Anderson et al., 2011) generated by the demise of the African Humid Period in the western Mediterranean (Thomas et al., 2006). For BdlV, higher evaporation rates may have precipitated the transition from a small lake to a bog, while increased side slope erosion rates at BdlC valley caused sediment deposition and initial bog substrate formation at this time. At both sites, developing bogs with important biomass production were dominated mainly by vascular terrestrial plants until ~3600 cal yr BP. Evidence for this exists in the high PC1 values: high C/N (>20), ACL, CPI, and low P_{aq} , as well as for the high TN and specially TOC content, the main components of PC2 related to primary production (Fig. 2; Supplementary Figs. S4, S5). Thus, predominantly terrestrial conditions are interpreted, especially at BdlC, probably boosted by the high summer insolation (Fletcher et al., 2007). The biomass development in the extreme environments of alpine Sierra Nevada is at present enhanced by warm temperatures or shorter cold seasons, which provide more ice-free surfaces during longer times and greater soil development (Oliva and Gómez-Ortiz, 2012). High PC2 and TOC values, especially at BdlC, were also recorded throughout the MCA, the last pre-industrial warm era in Europe (Mann et al., 2009) (Fig. 2h-k).

After this primary peatland stage (after ~3600 cal yr BP), the general long-trends of the PC1s of BdlC and BdlV-bog during the late Holocene up until ~600-500 cal yr BP tend to be opposite, suggesting different local responses to the same regional climatic oscillations (Fig. 2a-g). The geochemical record of BdlV-bog suggests a shift toward increased aridity and/or a terrestrial environment in this bog through time (Fig. 2d-e; Supplementary Figs. S5), in agreement with the local wetland signal of Cyperaceae pollen at this site, especially during the last millennium (Jiménez-Moreno and Anderson, 2012). Similar aridity trends deduced from regional pollen data, such as *Pinus* and *Artemisia* are depicted in Sierra Nevada (Anderson et al., 2011; Jiménez-Moreno and Anderson, 2012; Ramos-Román et al., 2016) (Fig. 2a) following the general climatic evolution of the western Mediterranean region during the late Holocene (deMenocal et al., 2000; Trouet et al., 2009; Anderson et al., 2011). NAO cycles have been identified by means of spectral analyses in the main loadings of PC1

in BdIV (Supplementary Table S5). This fact along with the moderate-to-high correlation between the NAO index and PC1 in BdIV in different simulations (ranging from $r=0.45$ to $r=0.69$ and $p<0.01$ in 6 out of the 8 developed simulations: Supplementary Table 6), suggest that the water availability variations in BdIV-bog record might have been influenced by NAO fluctuations (Trouet et al., 2009; Olsen et al., 2012) (Fig. 2c-e). However, the geochemical record of BdIC points toward greater water availability and/or higher development of aquatic environments at this site during the late Holocene (gradual P_{aq} increase and C/N-ACL-CPI decrease). The local signal of Cyperaceae pollen in BdIC (Ramos-Román et al., 2016) also confirms this gradual development of local aquatic environments (wetland areas) (Fig. 2b,f-g). The difference in response during this period between both peatlands suggests that, at least for the BdIC record, local conditions may have overridden the regional pattern. For BdIC, local response toward more aquatic conditions during the late Holocene could be related to the increase in the wetland area as a consequence of the progressive infilling of the basin (Ramos-Román et al., 2016), and it might be also boosted by the Caldera Lake output (as groundwater seepage) (Fig. 1c-d), acting as “water availability buffer” in this site, and preventing or masking the NAO influence and the effect of the general climate evolution in the western Mediterranean. This different response between both adjacent sites also points out the potential problems on single-site studies.

During the last 600 years both PC1s and PC2s (TN and TOC) show fluctuating conditions (Figs. 2d-k), especially during the LIA. While these oscillations are mostly abrupt during this last part of the records, we cannot conclude whether this variability is only caused by the resolution of the records. Although the LIA affected both bogs, BdIV registered the main oscillations, as expected. More humid environments occurred during abrupt and extreme negative NAO excursions at around ~340 and 180 cal yr BP (Trouet et al., 2009) (Figs. 2c-e). This potential NAO effect along with the drastic fluctuations in the solar irradiance during the LIA (Bard et al., 2000) might have given rise to the alternation of periods of longer ice-free conditions vs. periods of longer snow/ice surface cover (changes in the seasonality and precipitation),

affecting biomass production proxies, mainly TOC and TN in PC2s (Fig. 2h-k) during this period.

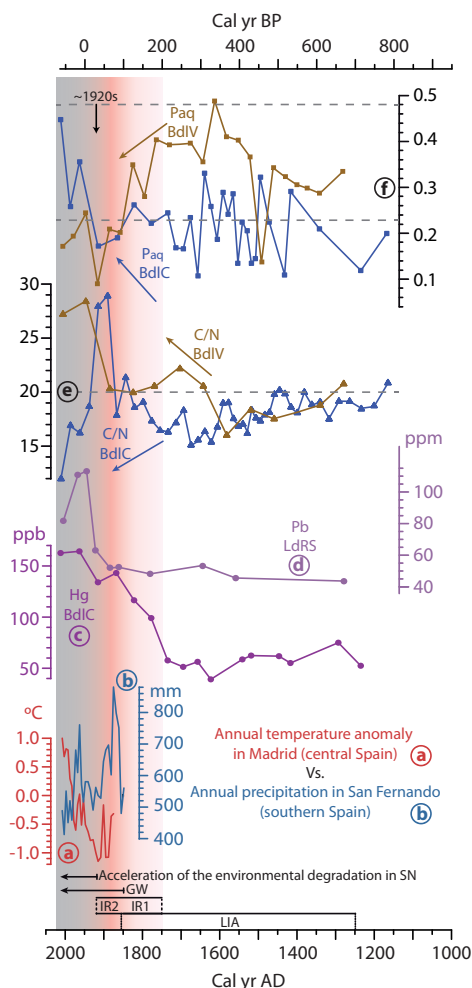


Figure 3. Environmental evolution in Sierra Nevada during the last ~800 years. (a) Longest temperature anomaly record in Spain (Madrid, central Spain) (Jiménez et al., 2015), (b) longest precipitation record in Spain (San Fernando, Cádiz, southern Spain) (Jiménez et al., 2015), (c, d) indirect human impact in the studied area during the last hundred years: (c) record of the atmospheric Hg pollution in BdlC (this work), and (d) atmospheric Pb pollution in LdRS (García-Alix et al., 2013), (e) C/N and (f) Paq and fluctuations at BdlC and BdlIV. Acronyms: LIA: Little Ice Age; IR1: First Industrial Revolution; IR2: Second Industrial Revolution; GW: Recent Global Warming. P_{aq} thresholds: terrestrial plants < 0.23 > emergent aquatic plant > 0.48 submerged/floating plants (Ficken et al., 2000). C/N thresholds: algae < 10 > terrestrial and aquatic vascular plants+algae < 20 > terrestrial vascular plants (Cloern et al., 2002; Meyers, 2003).

Allochthonous inputs in the study area. The NW Sahara region has been a persistent source of aeolian input during the Holocene (Rodrigo-Gámiz et al., 2015), but the development of commercial agriculture in the Sahel area (~200 years ago) has largely influenced the aerosol composition in the western Mediterranean (Mulitza et al., 2010). The aeolian inputs to our study area can be estimated by measuring the atmospheric Zr deposition (Jiménez-Espejo et al., 2014; Rodrigo-Gámiz et al., 2015). Saharan aerosols collected at ~3000 masl in the study area of Sierra Nevada confirms this hypothesis (Supplementary Table S4). The Zr/Al ratio in BdIC suggests a continuous increase in the N African dust inputs into the area after ~4000 cal yr BP, reaching its maximum value around the end of the MCA. After the MCA, these aeolian inputs have been decreasing (with some oscillations) until present (Fig. 2n). According to our simulations, the whole trend of this proxy shows moderate correlations with the NAO index (Supplementary Table S6). However, this correlation declines during the last ~300 years, pointing to a change in aeolian input features likely caused by either recent major variations in Saharan dust composition (Mulitza et al., 2010; Armitage et al., 2015), a higher local dust contribution (Morales-Baquero and Pérez-Martínez, 2016), or some combination.

Allochthonous inputs of phosphorus, calcium, or nitrogen, which are partially ruled by seasonal Saharan dust dynamics (Morales-Baquero et al., 2006; Pulido-Villena et al., 2006), are particularly important at Laguna de la Caldera (upstream of BdIC), which is strongly limited by phosphorus (Morales-Baquero et al., 2006). In that way, phosphorus and calcium cycles in Sierra Nevada reached maximum values during the dry season (Morales-Baquero et al., 2006; Pulido-Villena et al., 2006), and especially during positive NAO index periods (Moulin et al., 1997), but there is no important correlation between Saharan dust episodes and nitrogen deposition in this region (Morales-Baquero and Pérez-Martínez, 2016), as it is mainly controlled by rainfall (Morales-Baquero et al., 2006; Morales-Baquero and Pérez-Martínez, 2016). Similar scenarios are expected in the past; however, this nutrient effect on the water pools cannot be observed during the middle-to-late Holocene transition since terrestrial vascular plants are the main source of organic matter in both sedimentary

records (Supplementary Figs. S4, S5). After this stage (after ~3500 cal yr BP), the main loadings of PC3 ($\delta^{13}\text{C}$ and $\delta^{15}\text{N}$) displayed negative correlations against the aeolian proxy Zr/Al in BdlC (Supplementary Table 6). In these oligotrophic alpine aquatic environments, $\delta^{13}\text{C}$ and $\delta^{15}\text{N}$ values in primary production are mainly influenced by the dissolved inorganic nitrogen (DIN) and dissolved inorganic carbon (DIC) in the water pools, which mainly depends on allochthonous inputs (Pulido-Villena et al., 2005; Morales-Baquero et al., 2006). The inverse correlation between Zr/Al and $\delta^{13}\text{C}$ might be interpreted as Saharan aeolian influence, as Sahara aerosol are carbonate-rich (Guieu et al., 2002) and might influence the water DIC. On the other hand, the inverse correlation between Zr/Al and $\delta^{15}\text{N}$ is weaker because the nitrogen source in atmospheric depositions is more heterogeneous (dry or wet atmospheric deposition) (Morales-Baquero et al., 2006) (Supplementary Table 6).

Pre-industrial environmental variability: natural cycles and trends.

Environmental changes deduced from marine core pollen data during the middle-to-late Holocene oscillated with a periodicity of ~1750 yr in the western Mediterranean (Fletcher et al., 2013). Although the BdlC record is too short, this oscillation has not been noted in Sierra Nevada from the longer LdRS (Jiménez-Espejo et al., 2014) or BdlV records either. This may be because biomass/productivity is also affected not only by precipitation variability, as in low altitude sites (Fletcher et al., 2013), but also by temperature seasonality (i.e. length of snow-free season) and nutrient input. Solar cycles and their harmonics are mainly evident in all BdlC geochemical proxies in this study and the previously published pollen record (Ramos-Román et al., 2016), showing that solar forcing probably influenced locally the environments, at least at centennial scales (Supplementary Table S5). Our data suggest that summer solar irradiance controls biomass development and water availability by modulation of the ice melting/ice-free surfaces and warm summer temperatures. Runoff proxies, related to the dynamic of ice and/or snow melt processes, are also affected by solar cycles (i.e. ~1500-yr cycle) in the nearby record of LdRS (Jiménez-Espejo et al., 2014). In addition, we identified statistically significant high frequency cycles in the proxies

from BdlC that could be related to solar cycles such as the Suess cycle (~208 years) (Supplementary Table S5).

The general trend of the geochemical record of BdlC points towards greater expansion of wetland environment (more water availability), in agreement with the general increase in the Cyperaceae pollen record at the site (Ramos-Román et al., 2016) (Fig. 2b,f-g). The water availability here is likely influenced by the buffering effect of Laguna de la Caldera higher up in the catchment basin, which contributes to a subdued response to the NAO relative to the BdlV site. NAO-like cycles are mainly found in the carbon and nitrogen isotopic composition, which are primarily related to the nutrient input/consumption in the BdlC bog (Supplementary Table S5). BdlV record, however, is bound to be influenced by medium frequency NAO-derived cycles (i.e. 650, 520, 300-year cycles) due to the general trend toward drier conditions, agreeing with the regional patterns (Anderson et al., 2011; García-Alix et al., 2012a; Jiménez-Moreno and Anderson, 2012; Jiménez-Moreno et al., 2013a; Jiménez-Espejo et al., 2014; Ramos-Román et al., 2016) (Fig. 2a,d-e). In addition, there is an important influence of the solar cycles in BdlV record (i.e. 400 or 250-year cycle), especially in productivity proxies (i.e. TOC or $\delta^{15}\text{N}$). Therefore, according to these results, NAO-like cycles seem to control the humidity fluctuation in the area (largely a winter effect), which is also in agreement with the NAO-PC1 correlation in BdlV (Supplementary Table 6), and solar cycles could have regulated the seasonality by modulation of the ice/snow-free surface and temperature during the vegetation-growing season (largely a summer effect).

Human impact and disruption of natural biogeochemical cycles. Although our study sites are located at high elevation in the protected Sierra Nevada National Park, where direct anthropogenic impact has been minimal, the indirect human impact affecting temperature and precipitation regimes in the region has been significant during the last century (IPCC, 2013; Oliva and Gómez-Ortiz, 2012). Furthermore, industrial and mining activities at lower elevations have left their footprint in this alpine area, especially as heavy metals (Pb and Hg) in sedimentary records from LdRS (García-Alix et al., 2013) and BdlC, respectively (Fig. 3c,d). These Sierra

Nevada records show an increase in the Hg concentration at the end of 18th century (BdlC), following by a rise in the Pb concentration at the beginning of the 20th century (~1910-1920 AD) (García-Alix et al., 2013) (Fig. 3c,d). Naturally-occurring concentrations of these metals are extremely low in this alpine region, and their primary source has been atmospheric pollution, at least for Pb (García-Alix et al., 2013). Although the main source of the atmospheric Hg pollution is industrial and urban emissions (Selin, 2009; Guédron et al., 2016), emissions from local cinnabar (HgS) mining and melting activities at lower elevations in Sierra Nevada appear to have contributed greatly to the local mercury atmospheric pollution, especially during the 18th and 19th centuries. Local mining started between the 17th and 18th centuries, reaching a peak from ~1885 to ~1930 AD, ending in 1957 (Sánchez-Hita, 2008) (Fig. 3c). Contrary to the LdRS record, in which the Pb content decreased at around 1970 AD with the use of unleaded fuels (García-Alix et al., 2013), Hg content at BdlC has only stabilised and does not show any significant decrease despite major legal regulations on the industrial use and mining of mercury (Selin, 2009) (Fig. 3c,d). These persistently high Hg values are related to the increase in industrial activities and fossil fuels, especially coal burning (Selin, 2009). If this situation continues in the near future, it might be a risk for this protected region, as biological activities can transform mercury into toxic methylmercury in anaerobic wetlands (Selin, 2009), which would be the case for saturated peat bogs, such as BdlC.

The timing of the industrial development in the area, evidenced by heavy metal records, is coincident with the beginning of abrupt fluctuations in the water resources in both peatland records during the last hundred years. PC1 in BdlC shows a drastic increase in P_{aq} and a decrease in C/N, which points towards more humid environments (Fig. 3e,f). This trend is opposite to the general climatic trends in the western Mediterranean (IPCC, 2013) towards drier conditions (Pérez-Luque et al., 2015) (Fig. 2a). The general trend of PC1 and PC3 from the BdlV-bog, and more specifically the P_{aq} decreases and C/N increases, show a abrupt reduction in the humid environment during the last hundred years until present (Fig. 2l, 3e,f). These changes also agree with a lesser NAO influence in the water availability (PC1) of BdlV

(Supplementary Table S6) in the last ca. two centuries.

In addition to this amplification of the natural trends during the last ~100-150 years, an important abrupt dry event and development of more terrestrial conditions occurred in the region at ~1920 AD (Fig. 3b,e-f). This arid event was dramatically recorded in both areas, and is coeval with prevalent NAO positive conditions (Trouet et al., 2009). The biomass proxies (PC2s) also show significant changes around this time (Fig 2h-k): (1) the biomass decrease trend is enhanced in BdIC after ~1920 AD, agreeing with an abrupt decrease in TOC and C/N, and an increase in the P_{aq} and H/C (the latter is also related to algal production), and (2) it had an abrupt and occasional decrease in BdIV, followed by a drastic increase (more terrestrial environments) (Figs. 2h-k, 3e-f; Supplementary Figs. S4, S5). All those proxies point towards an important change in the effective precipitation, seasonality, and temperature at the beginning of the 20th century, in agreement with instrumental meteorological data in Spain (Jiménez et al., 2015) (Figs. 3a-b,e-f), reducing the amount of ice/snow on the surface. Coincidentally, this event occurs at the timing of the industrial development of the region at the end of the Second Industrial Revolution (Technological Revolution) in Europe (Landes, 1969), pointed out by the beginning of the last sharp increase in heavy metal atmospheric pollution caused by human activities (Fig. 3). Similar evolution of the mercury atmospheric pollution during the first part of the 20th century has been identified in the French Alps (Guédron et al., 2016). This mixture of both natural and human pressure might have been the trigger of the Veleta Glacier melting at the beginning of the 20th century, the last glacier in southern Iberia. This was the first signal of human-induced environmental degradation in Sierra Nevada in the 20th century, pointing at the fact that the natural tolerance threshold in this climate-sensitive area was exceeded.

The trend of consumption of C and N in aquatic environments (PC3) during the last ca. two centuries was also atypical in the BdIC record. Apparently, the important development of algae (C/N and H/C increases) and aquatic environments (P_{aq} increase) at the end of this record did not have any explicit response on PC3, and no enrichment in nitrogen or carbon isotopes was detected (Fig. 2f-g,m; Supplementary

Fig. S4). This might have been caused by a change in the source/composition of the nutrient inputs into the area, i.e. increase in local aerosol sources triggered by recent changes in the land use, which could have contributed to dust atmospheric content even during the periods of low Saharan dust inputs (Morales-Baquero and Pérez-Martínez, 2016). The correlation between the aeolian Zr/Al ratio in BdIC and the NAO index during the last ~300 years seems to be lower (Supplementary Table S6), suggesting changes in the large-scale atmospheric-controlled dynamics that delivered nutrients in this area. These recent variations in the aeolian source (Mulitza et al., 2010), along with the major anthropogenic disruption on the nitrogen cycle during the last century (Galloway et al., 2004), might have influenced the composition of the nutrient deposition in our sites, comparing with the late Holocene natural trends, as it has been observed in other mountain wetland areas, such as it is the case of the Alps (Rogora et al., 2003).

4. Conclusions

Unexpected and almost opposite local environmental responses between two nearby alpine bogs during the late Holocene show that the ecosystem development and its response to climate changes is a complex mechanism, even in the same region, and that these responses are highly influenced by the landscape and the environmental evolution of the area. In addition, these opposite environmental responses were amplified during the last centuries. This abrupt amplification at both sites is coincident with regional industrial development, evidenced by the increased heavy metal atmospheric deposition in the study area, as well as the melting and eventual disappearance of the Veleta Glacier at the beginning of the 20th century. Spectral analyses performed on the multiple proxies indicate several cycles exist at both locations that can be explained by a different resilience and sensitivity to climate variations between the peatlands. Anthropogenic influences also appear to moderate the influence of solar and atmospheric cycles in the environments. The obtained paleoenvironmental records indicate that present day ecosystems were settled in the last century after perennial ice disappeared. This means that this former glaciated area

will suffer drastic changes and higher vulnerability to climate variations and human-induced environmental pressure if the current climatic trends continue, and can be used as a mirror for endangered still-glaciated areas in Europe.

5. Methods

Site and sampling description. A 56 cm long core was extracted from Borreguil de la Caldera (BdlC 13-01) in 2013 with a Livingstone piston corer. Eighty-two samples for organic analyses in bulk sediment, fifty samples for biomarkers, and eleven samples for inorganic (mercury) analyses were obtained. The age model is based on five calibrated AMS ages (Ramos-Román et al., 2016) (Supplementary Fig. S1). A 165 cm long core was extracted from Borreguil de la Virgen (BdlV 06-01) in 2006. Ninety-three samples for biomarker analyses were collected. Organic data from bulk sediment of the same record (TOC, C/N, $\delta^{13}\text{C}$ and $\delta^{15}\text{N}$) were previously published (García-Alix et al., 2012a). The age model is based on nine calibrated AMS radiocarbon dates (Jiménez-Moreno and Anderson, 2012) (Supplementary Fig. S1).

Fifty plant, peat, and soil samples were taken at different distance from the main water pool(s) in several wetlands of Sierra Nevada for biomarker analyses: LdRS (Laguna de Rio Seco, south face, 3020 masl), BdlC (Borreguil de la Caldera, south face 2992 masl), BdlV (Borreguil de la Virgen, north face, 2945 masl), and LdlM (Laguna de la Mula, north face, 2497 masl).

Three high elevation aerosol samples were collected in 2008 by means of 16 MTX1 ARS 1010 automatic deposition sampler in Sierra Nevada (S Spain) at the Sierra Nevada Observatory station (osn: 2896 masl) and the Sierra Nevada Veleta station (vsn: 3000 masl).

Organic Geochemistry. To track the source of the organic matter in the sediments several proxies have been studied in bulk sediment samples: total organic carbon (TOC), total nitrogen content (TN), atomic C/N ratio, atomic H/C ratio, and carbon and nitrogen isotopes. Three indices of leaf wax biomarkers (*n*-alkanes), assessing

the length of the carbon chain length, are used to constrain the source of organic matter and the water availability in the environments: 1) the average chain length (ACL), which is the measurement of the weighted average of the carbon chain lengths; 2) the carbon preference index CPI, which shows the relative abundance of odd vs. even carbon chains, where values lower than 2 point towards even *n*-alkane preference (diagenetic alteration or algae/bacteria influence), and higher than 2, towards odd preference (terrestrial plant source, and thermal immaturity of the source rock) (Bush and McInerney, 2013); and 3) the portion aquatic (P_{aq}), the ratio between typical aquatic *n*-alkanes and terrestrial ones, which is an useful index to identify aquatic or terrestrial plant sources (water availability) in sedimentary records (Ficken et al., 2000).

Freeze dried samples from BdIC were decalcified with 1:1 HCl in order to eliminate the carbonate fraction for the organic analyses of bulk sediments. Carbon, nitrogen, and hydrogen content of the decalcified samples were analysed in an elemental analyser Thermo Scientific Flash 2000 at the Centro de Instrumentación Científica (University of Granada). Carbon and nitrogen isotopes ($\delta^{13}C$ and $\delta^{15}N$) were measured simultaneously by means of a continuous flow Isoprime IRMS with a coupled Eurovector EA at the Centro de Instrumentación Científica (University of Granada). Certified Elemental Microanalysis standards were used: Sorgo Flour Standard ($\delta^{13}C$: -13.68‰ and $\delta^{15}N$: 1.58‰), Wheat Flour Standard ($\delta^{13}C$: -27.1‰ and $\delta^{15}N$: 2.85‰), and Casein Standard ($\delta^{13}C$: -26.98‰ and $\delta^{15}N$: 5.94‰), calibrated to the international standards IAEA-CH-6 and IAEA-N1. Isotopic results are expressed in δ notation, using the standard PDB (carbon) and AIR (nitrogen). The atomic C/N ratio has been used in this paper. The calculated precision was better than $\pm 0.1\%$ for $\delta^{13}C$ and $\delta^{15}N$.

The total lipid extract from BdIC and BdIV freeze-dried samples was obtained with a 3:1 DCM:methanol solution. After the separation of the neutral and acid fractions by means of aminopropyl-silica gel chromatography using 1:1 DCM:isopropanol and ether with 4% acetic acid respectively, the *n*-alkanes were recovered in the first neutral fraction eluted with hexane through a 230-400 mesh/35-

70 micron silica-gel chromatographic column. The *n*-alkanes were analysed using a GC-FID (Shimadzu 2010) and a GC-MS (Shimadzu OP2010-Plus Mass Spectrometer interfaced with a Shimadzu 2010 GC). To check the reproducibility of the measurements and to quantify the *n*-alkane content, a mixture of *n*-alkanes (C₁₆, C₁₈, C₁₉, C₂₀, C₂₃, C₂₅, C₂₆; C₂₈; C₃₀, C₃₂, C₃₇) was measured every five samples. The standard reproducibility was better than 97%.

Inorganic Geochemistry. The potential detrital and aeolian input in the bogs is studied by means of the Zr content in the samples. It has commonly been used as a proxy for aeolian input in different regions, including Saharan dust inputs in the western Mediterranean (Moreno et al., 2006; Jiménez-Espejo et al., 2014; Rodrigo-Gámiz et al., 2015). Three high elevation aerosol samples were also selected to check their Zr content. Firstly, they were weighed and digested with HNO₃-HF mixture at 120 °C overnight. After drying down, each sample was treated with HNO₃ several times. Samples were re-dissolved in a diluted HNO₃, and trace element compositions were measured by external calibration method with an ICP_MS NEXION 300D quadrupole inductive coupled plasma-mass spectrometry (ICP-MS) at the Centro de Instrumentación Científica (University of Granada, Spain). Procedural blank was nearly negligible for all elements presented in this study.

An Avaatech X-Ray fluorescence (XRF) core Scanner was used to obtain high-resolution Zr/Al profiles in the BdIC core at the XRF-Core Scanner Laboratory (University of Barcelona, Spain). Two runs of analyses were performed: one at 10 s count times, 10 kV X-ray voltage, and 650 mA X-ray current for lighter elements (Al), and another one at 35 s count time, 30 kV X-ray voltage, and 1700 mA X-ray current for heavier elements (Zr). Among all the obtained signals, we have focused on the Zr/Al ratio, as it is the most relevant one for the purpose of this paper. Results were expressed in intensities (counts per second, cps) and normalized for the total sum in cps in every measure.

Total mercury concentrations in 11 samples from the uppermost 26 cm of BdIC were determined to track the potential heavy metal pollution at high elevation. They

were analysed by means of an Advanced Mercury Analyser (LECO AMA-254) with an absolute mass detection limit of 0.01 ng of Hg (Diez et al., 2007). Samples were combusted in an oxygen-rich atmosphere (99.5%) and the evolved gasses were transported via an oxygen carrier gas through specific catalytic compounds to a gold-plated ceramic, which collects the mercury in vapour. The amalgamator was heated up to approx. 700°C to release mercury to the detection system. The working range was between 0.05 ng and 500 ng. In this study, samples of peat bog and quality control materials with masses of 20 mg to 100 mg were inserted into the AMA-254 spectrometer in a nickel boat, dried at 120°C for 50 s, combusted in the oxygen atmosphere at 700°C for 150 s and after 45 s of waiting (the time needed for cleaning of the system) the next sample was introduced. The entire analytical procedure was validated by analysing certified reference material DORM-3 (Fish tissue, NRCC, Canada) at the beginning and end of each set of samples, ensuring that the instrument remained calibrated during the analytical routine.

Statistics. Statistical treatment of the data was performed by means of PAST free software (Hammer et al., 2001). Data were normalised subtracting the mean and dividing by the standard deviation to conduct the Principal Component Analyses (PCA). Spectral analyses have also been carried out with PAST and the REDFIT module. The time series has been fitted to an AR(1) red noise model, and 90%, 95%, and 99% confidence levels were chosen. The selected cycles range from around 1/3 of the total time interval (~1500 yr), in the case of the lowest frequency cycles, to at least two times the estimated time represented for the most usual sampling interval (mean sample spacing), which depends on the site and the studied variables (supplementary figures S9 and S10) (Jiménez-Espejo et al., 2014).

Acknowledgements

This study was supported by the project P11-RNM 7332 of the “Junta de Andalucía”, the projects CGL2013-47038-R and CGL2015-67130-C2-1-R of the “Ministerio de Economía y Competitividad of Spain and Fondo Europeo de Desarrollo Regional FEDER” and the research group RNM0190 and RNM309 (Junta de Andalucía). A.G.-A. was also supported by a Marie Curie Intra-European Fellowship of the 7th Framework Programme for Research, Technological Development and Demonstration of the European Commission (NAOSIPUK. Grant Number: PIEF-GA-2012-623027) and by a Ramón y Cajal Fellowship RYC-2015-18966 of the Spanish Government (Ministerio de Economía y Competitividad). J.L.T. was also supported by a Small Research Grant by the Carnegie Trust for the Universities of Scotland and hosted the NAOSIPUK project (PIEF-GA-2012-623027). M. J. R-R acknowledges the PhD funding provided by Consejería de Economía, Innovación, Ciencia y Empleo de la Junta de Andalucía (P11-RNM 7332). We would like to thank to Dr. I.M. Sánchez Almazo (CIC- University of Granada), A. Cochrane, J. McGourlay, S. Pauchet (University of Glasgow), and Dr. S. Diez (IDAEA-CSIC) for their help preparing and analysing the organic and inorganic samples, as well as to Dr. I. Reche (University of Granada) for the aerosol samples from Sierra Nevada. Authors would also like to thank the journal editor K.H. Knorr and two anonymous reviewers for their comments improving the manuscript.

Author Contributions

Conceived the idea A.G.-A., F.J.J.-E. Analysed the samples: A.G.-A., F.J.J.-E., J.L.T., P.R., I.Q. Data discussion: A.G.-A., F.J.J.-E., J.L.T., G.J.M., M.J.R.R., R.S.A., P.R., I.Q., A.D.H., J.K. Wrote this work with contributions from all authors: A.G.-A., F.J.J.-E., G.J.M

Additional information

Supplementary Information accompanies this paper at <http://www.nature.com/>

srep

Competing financial interests: The authors declare no competing financial interests.

Supplementary Information

**Alpine bogs of southern Spain show human-induced environmental change
superimposed on long-term natural variations**

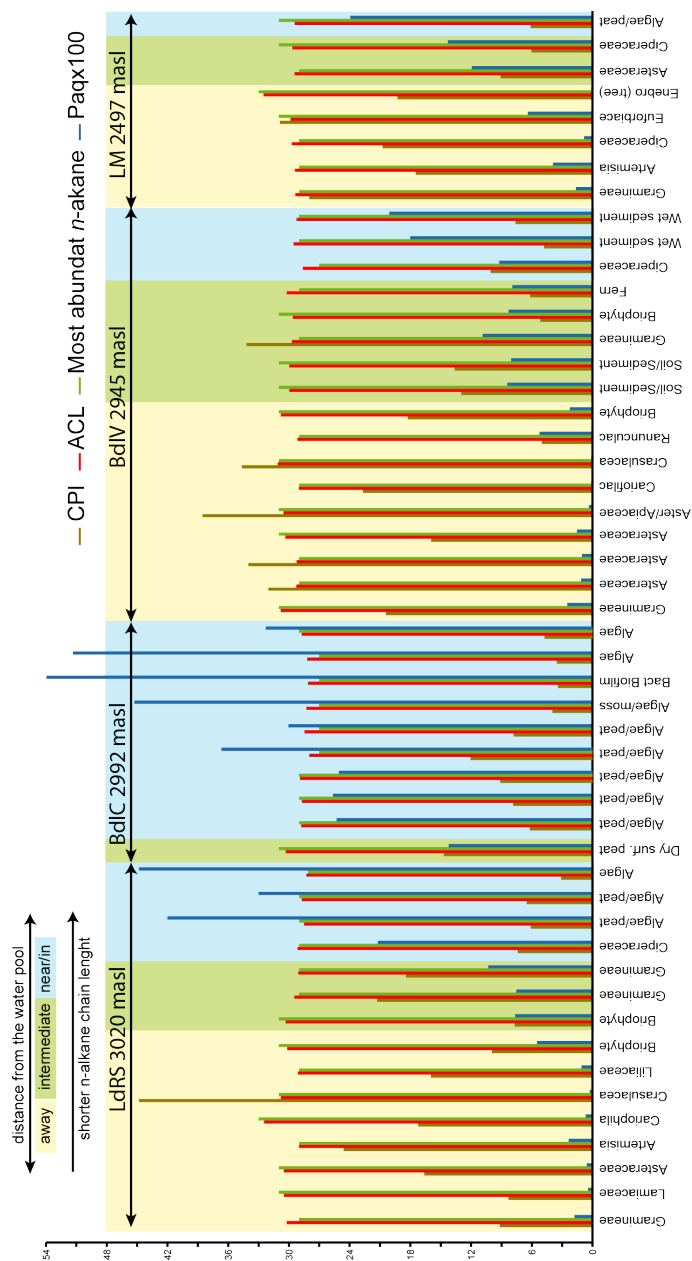
Antonio García-Alix, Francisco J. Jiménez-Espejo, Jaime L. Toney, Gonzalo
Jiménez-Moreno, María J. Ramos-Román, R. Scott Anderson, Patricia Ruano,
Ignasi Queralt, Antonio Delgado Huertas, and Junichiro Kuroda

The supplementary material file includes:

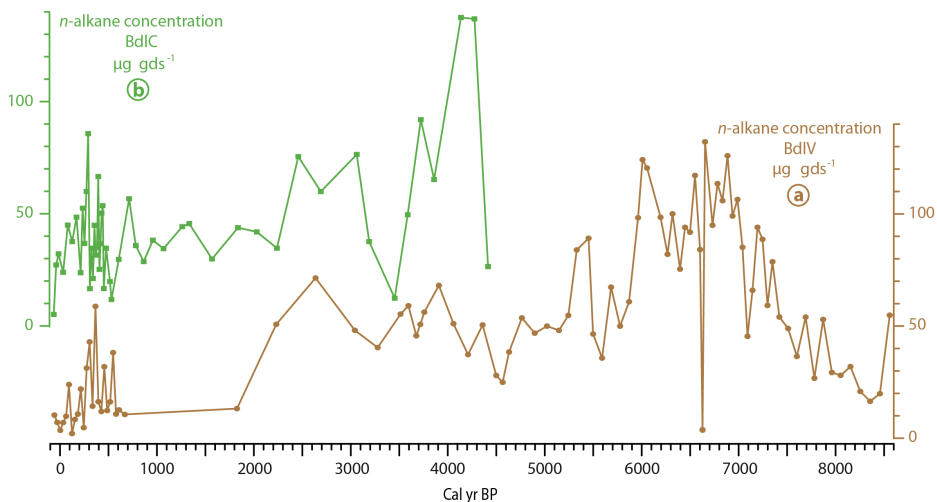
Supplementary Figures S1 – S9

Supplementary Tables S1 – S4

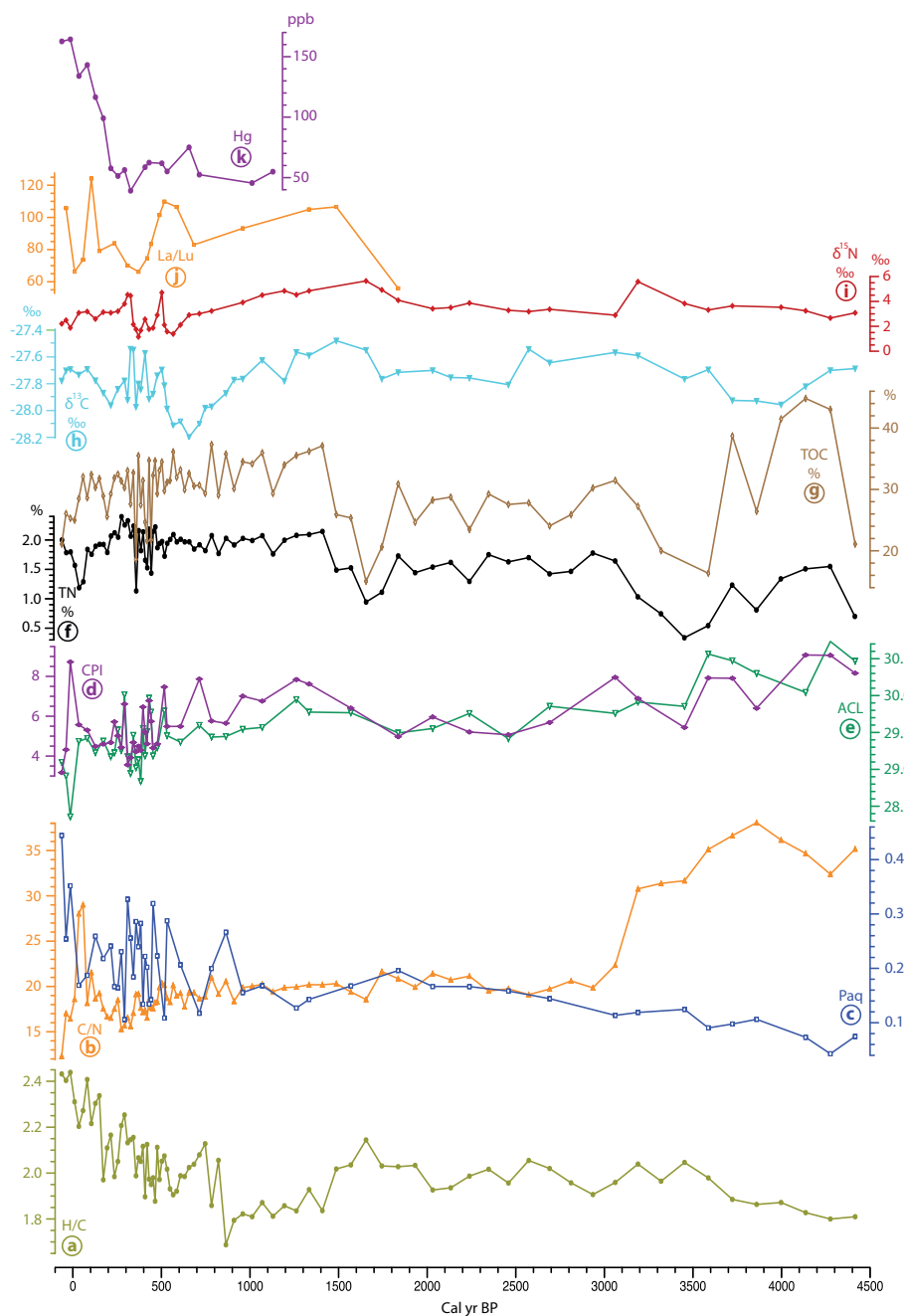
Supplementary Figures



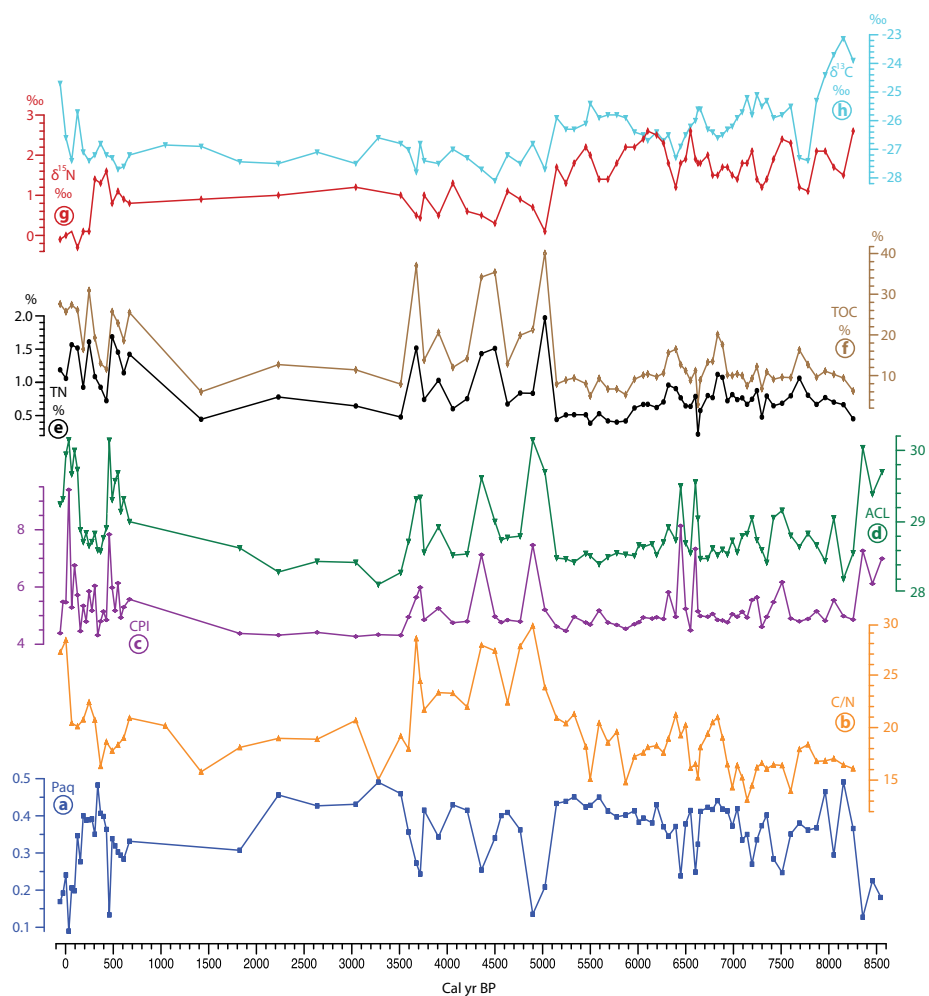
Supplementary Figure S1. Biomarker results in recent plants and soils. *n*-alkane indices (CPI, ACL, Paq, and the most important *n*-alkane in each sample) from the studied plant, algae, and peat samples at different distance from the water pools at four different sites in Sierra Nevada.



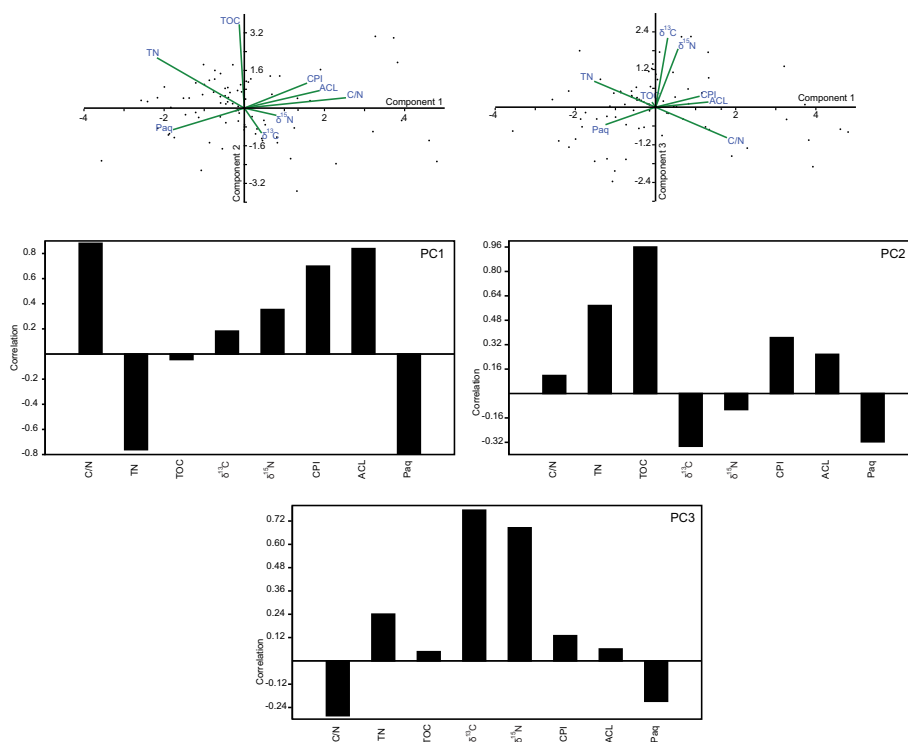
Supplementary Figure S2. *n*-alkane concentration in the studied records. *n*-alkane concentrations in microgram of sediment per gram of dry sample ($\mu\text{g gds}^{-1}$) from (a) BdIV and (b) BdIC. The highest *n*-alkane concentration in BdIV occurred from ~ 7000 to ~ 6000 cal yr BP, with values usually higher than $100 \mu\text{g gds}^{-1}$ (gds = gram of dry sediment). Subsequently, values generally fluctuated between 25 and $89 \mu\text{g gds}^{-1}$ until ~ 2200 cal yr BP. Similar fluctuations occurred in BdIC from ~ 4500 to 2200 cal yr BP, but with higher *n*-alkane concentrations, ranging from 12 to $137 \mu\text{g gds}^{-1}$. The concentrations are more constant in BdIC until the Little Ice Age (LIA). During the Little Ice Age (LIA) higher fluctuations occurred in both records, which subsequently declined (BdIC: $5\text{--}45 \mu\text{g gds}^{-1}$ and BdIV: $2\text{--}24 \mu\text{g gds}^{-1}$).



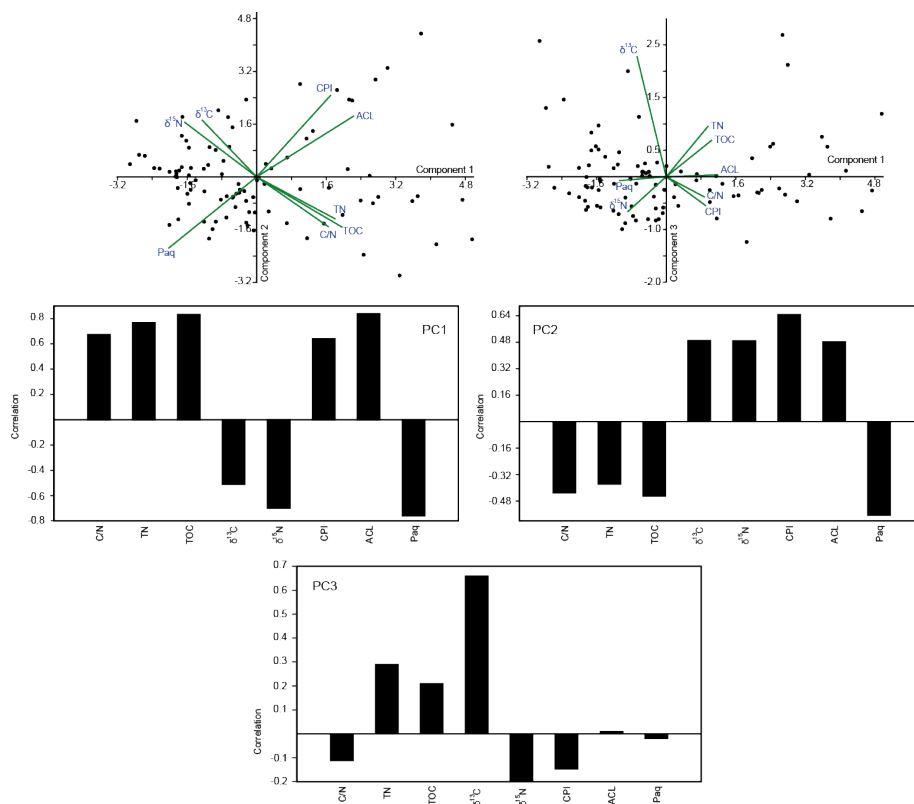
Supplementary Figure S3. Organic proxies studied from the BdlC record during the middle-to-late Holocene: (a) atomic hydrogen – carbon ratio (H/C), (b) atomic carbon – nitrogen ratio (C/N), (c) portion aquatic (P_{aq}), (d) carbon preference index (CPI), (e) average chain length (ACL), (f) total nitrogen content (TN%), (g) total organic carbon (TOC%), (h) carbon isotopic composition of the bulk organic matter ($\delta^{13}\text{C}$), (i) nitrogen isotopic composition of the bulk organic matter ($\delta^{15}\text{N}$), (j) La/Lu ratio, and (k) Hg concentration (ppb).



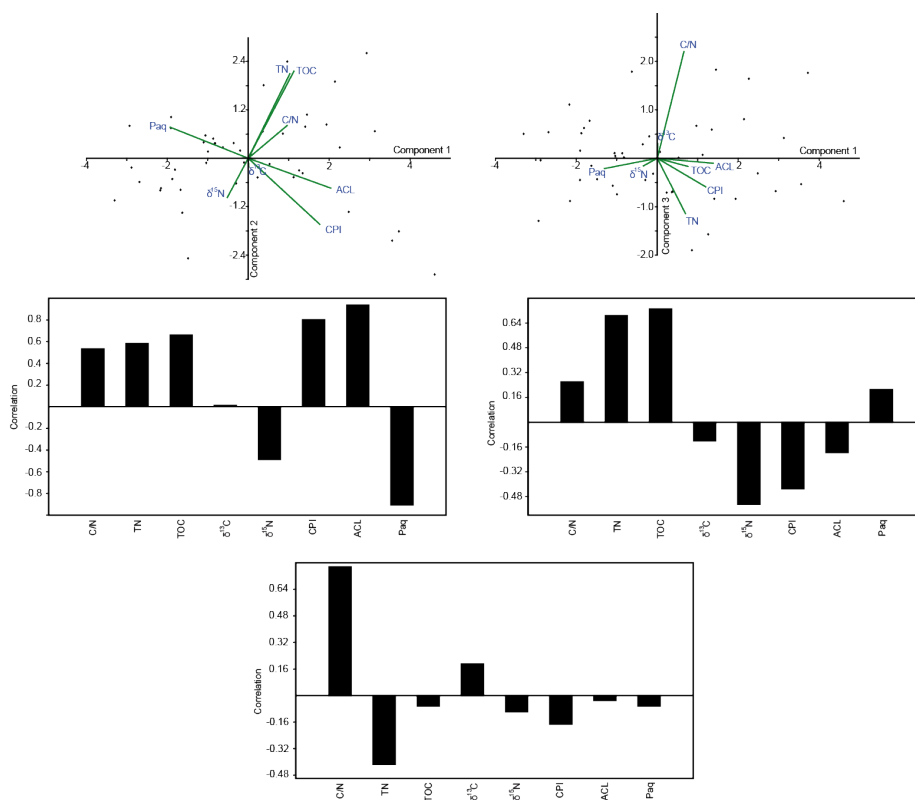
Supplementary Figure S4. Organic proxies studied from the BdlV record during the Holocene: (a) portion aquatic (P_{aq}), (b) atomic carbon – nitrogen ratio (C/N) (García-Alix et al., 2012a), (c) carbon preference index (CPI), (d) average chain length (ACL), (e) total nitrogen content (TN%), (f) total organic carbon (TOC%)¹, (g) nitrogen isotopic composition of the bulk organic matter ($\delta^{15}\text{N}$)¹, and (h) carbon isotopic composition of the bulk organic matter ($\delta^{13}\text{C}$) (García-Alix et al., 2012a).



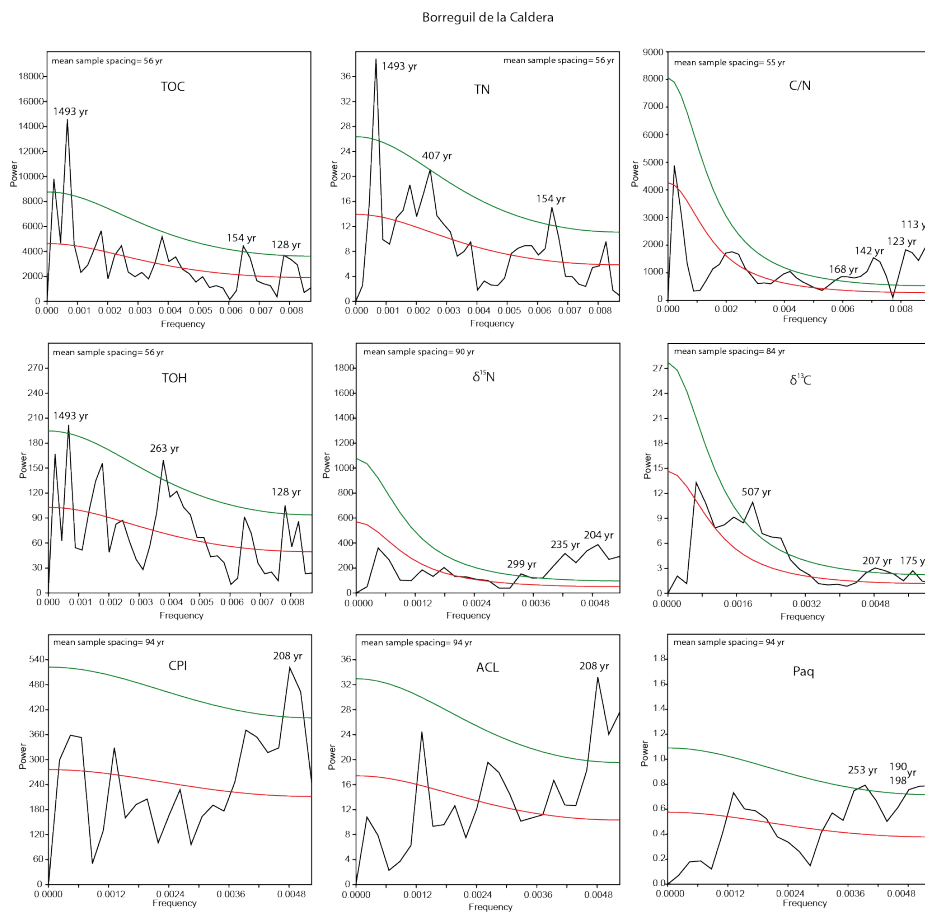
Supplementary Figure S5. Organic PCA results from Borreguil de la Caldera. Used indices ACL, P_{aq}, CPI, C/N, TOC, TN, δ¹³C, and δ¹⁵N. Biplot figure and loadings (correlation) of the most important PCs: PC1, PC2, and PC3 in BdIC record.



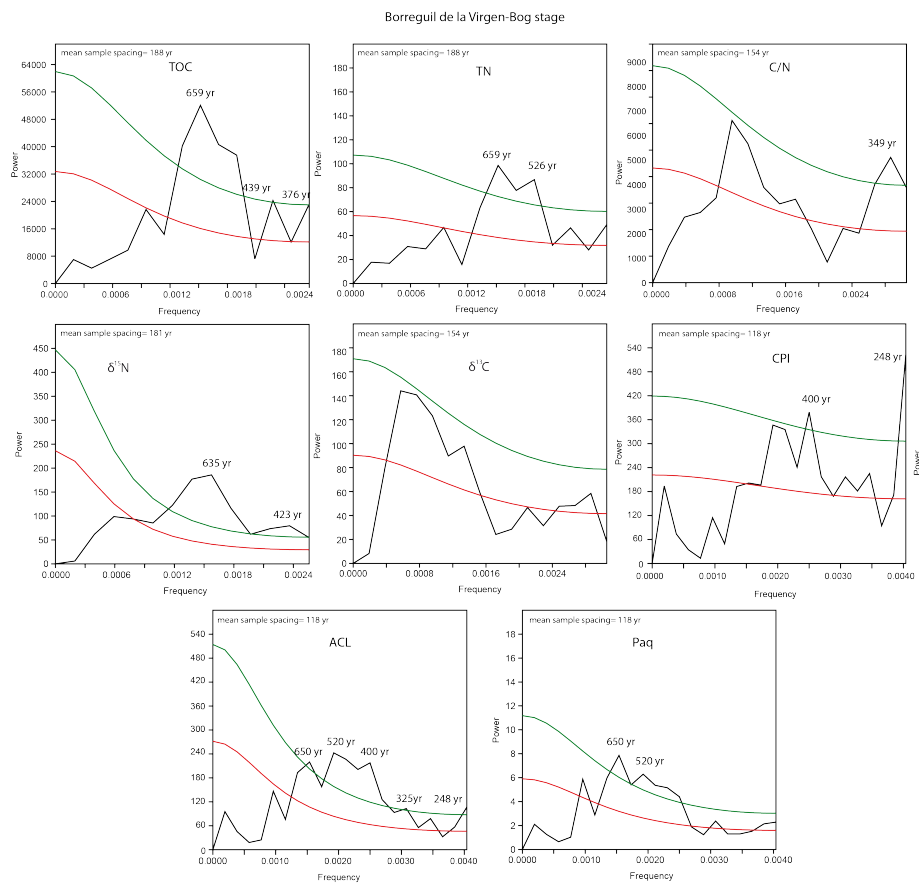
Supplementary Figure S6. Organic PCA Results from Borreguil de la Virgen (whole record). Used indices ACL, P_{aq} , CPI, C/N, TOC, TN, $\delta^{13}\text{C}$, and $\delta^{15}\text{N}$. Biplot figure and loadings (correlation) of the most important PCs: PC1, PC2, and PC3 in BdlV record.



Supplementary Figure S7. Organic PCA Results. Borreguil de la Virgen (last 5000 years). Used indices ACL, P_{aq} , CPI, C/N, TOC, TN, $\delta^{13}\text{C}$, and $\delta^{15}\text{N}$. Biplot figure and loadings (correlation) of the most important PCs: PC1, PC2, and PC3 in BdIV-bog record.



Supplementary Figure S8. Spectral analyses of the organic proxies of BdIC. Red line: AR(1) red noise, green line: 90 % confidence threshold.



Supplementary Figure S9. Spectral analyses of the organic proxies of BdIV-bog stage. Red line: AR(1) red noise, green line: 90 % confidence threshold.

Supplementary Tables

BdIC PCs	Eigenvalue	% Variance	Cumulative variance
1	2.6	41.9	
2	1.5	25.0	66.9
3	0.9	14.4	81.3
4	0.4	7.0	88.3
5	0.4	6.0	94.4
6	0.2	3.5	97.9
7	0.1	1.5	99.4
8	0.0	0.6	100.0

Supplementary Table S1. Organic PCA Results from Borreguil de la Caldera. Eigenvalue, and percentage of variance explained with the different Principal Components in BdIC record.

BdIV-w PCs	Eigenvalue	% variance	Cumulative variance
1	3.6	52.3	52.3
2	1.7	25.4	77.7
3	0.5	7.5	85.2
4	0.5	6.7	91.9
5	0.3	3.8	95.7
6	0.2	3.2	98.9
7	0.1	1.0	4.2
8	0.0	0.1	100.0

Supplementary Table S2. Organic PCA Results from Borreguil de la Virgen (whole record). Eigenvalue, and percentage of variance explained with the different Principal Components in BdIV whole record.

BdIV-b PCs	Eigenvalue	% variance	Cumulative variance
1	3.8	56.6	
2	1.3	19.0	75.5
3	0.7	10.6	86.2
4	0.4	6.7	92.9
5	0.2	3.6	96.5
6	0.1	1.9	98.4
7	0.1	1.3	3.3
8	0.0	0.2	100.0

Supplementary Table S3. Organic PCA Results from Borreguil de la Virgen (last 5000 years). Eigenvalue, and percentage of variance explained with the different Principal Components in BdIV-bog record.

Site	Proxy	Cycles (years)											
		~1500	~650	~520	~400	~350	~300	~250	~200	~170	~150	~130	~113
BdIC	TOC	X									X	X	
	TN	X			X						X	X	
	C/N									X	X	X	X
	TOH	X						X				X	
	$\delta^{15}\text{N}$						X	X	X				
	$\delta^{13}\text{C}$			X					X	X			
	CPI								X				
	ACL								X				
	Paq							X	X				
BdIV bog stage	TOC		X		X								
	TN		X	X									
	C/N					X							
	$\delta^{15}\text{N}$		X		X								
	$\delta^{13}\text{C}$												
	CPI				X			X					
	ACL		X	X	X	X	X						
	Paq		X	X									
Forcing	S/ A-O/ Or	S/ NAT/ NAO	S/ NAO	S	S/ NAO	NAO	S	S: Suess	NAO	S: Gleissberg band			

Supplementary Table S4. Summary of the cycles obtained from the spectral analyses from BdIC and BdIV (bog stage) records. Acronyms: S, Solar; A-O; Atmosphere-Ocean circulation; Orbital forcing; NAT: North Atlantic thermohaline circulation; NAO, North Atlantic Oscillation. The 150, 130, and 113-year cycles, likely Gleissberg cycles, have been identified as solar cycles. They have a characteristic frequency between 60 and 150 years during the middle and late Holocene (Ma, 2009). Nevertheless, Gleissberg cycles are only clear at BdIC, which also preserved a ~1500-year cycle, not present at BdIV. This ~1500-year cycle is quite common in marine and terrestrial records in the north hemisphere, and its origin is quite controverted: solar, atmospheric-ocean circulation, or orbital modulation (Bond et al., 1993; Jiménez-Espejo et al., 2014), or even a mixture of the 1000- and 2000-year solar cycles (Obrochta et al., 2012). The Suess (or de Vries) cycle at 208 year (Sonett et al., 1991; Stuiver and Braziunas, 1993), related to solar fluctuations, is one of the most important cycle identified in Holocene records (Stuiver and Braziunas, 1993), and can affect lacustrine paleoproductivity and summer temperatures, such as in some records of Alaska (Hu et al., 2003b; Wiles et al., 2004). The 170 and 300-year cycles are related to NAO fluctuations (Olsen et al., 2012). The 250-year cycle has been identified as a solar cycle during the last 2000 years (Vaquero et al., 2002). The 350-year cycle has been recently described as solar forced (Steinhilber et al., 2012; Summerhayes, 2015), that could also influence the NAO

cycles (Lamy et al., 2006). Obtained *~400-year cycle* can be considered a solar cycle, and has impact in the late Holocene humidity from north America to China (Wu et al., 2009; Yu and Ito, 1999). The *~520-year cycle* can correspond to the *~500-530-year solar activity cycle* (Stuiver et al., 1995). Those changes in solar irradiance induce NAO anomalies (Lamy et al., 2006; Xu et al., 2014). It has also been related to warm/cold fluctuations during the middle/late Holocene in East Asia (Xu et al., 2014), and variations in the North Atlantic circulation patterns (Chapman and Shackleton, 2000). *650-year cycle* has been recognised in the storminess frequency, seasonal sea-ice development, and cooling trends at high latitudes in the Northern Hemisphere, in agreement with solar radiation fluctuations (Berner et al., 2011; SARNTHEIN et al., 2003). Those variations at high latitudes could be linked with NAO variations (Bader et al., 2011). It has been also proposed as a secondary harmonic of the *1300-year cycle* (Rodrigo-Gámiz et al., 2014a) related to North Atlantic thermohaline circulation and/or sea surface temperatures (Rodrigo-Gámiz et al., 2014a). This is the first mention of the 650-year cycle in continental records, so a mechanism connecting terrestrial and marine environments, such as the NAO, should drive this cycle.

CHAPTER 6

Chapter 6: Concluding Remarks. Climate evolution and human impact in Sierra Nevada based on vegetation reconstruction dynamics

Outline

The objective of this concluding remarks is to summarize, integrating and making a comparison of the results and the main conclusions obtained in the previous chapters (that focused specifically on each of the two sites studied) with the purpose of showing the goals that this doctoral thesis study have achieved, contributing to the paleoclimate and paleoenvironmental knowledge in Sierra Nevada, the Iberian Peninsula and the Mediterranean region.

1. Long-term Holocene vegetation dynamics, environmental variability and climate change during in Sierra Nevada

Anderson et al. (2011) suggest that differences in altitudinal vegetation gradient, geomorphological changes and human perturbation on the landscape could be important parameters to be considered when making paleoclimatic reconstructions. Below we show a pollen comparison between different vegetation belts from Sierra Nevada in order to find links between vegetation dynamics, climate, atmospheric-oceanic and solar dynamics and human impact in this area.

1.1. The warm and dry earliest Holocene (from ~11.6 to 10 cal ka BP)

A transition period from glacial to interglacial conditions occurred from ~11.6 to 10 cal ka BP. Marine records from the Alboran Sea show a trend to increasing sea surface temperatures (Cacho et al., 1999; Rodrigo-Gámiz et al., 2014b). The sedimentary record from Laguna de Rio Seco [LdRS; 3020 asl; Anderson et al. (2011)] shows a steppe vegetation depicting higher values of *Artemisia* ~50% (Fig. 1), indicating arid conditions. At lower altitude in the mesomediterranean vegetation belt the Padul-15-05 sedimentary sequence shows the expansion of Mediterranean

forest (reaching average values of around ~55%; Fig. 1), mainly composed of evergreen *Quercus* (note the lower values of deciduous *Quercus*) suggesting warmer but still dry conditions in Sierra Nevada after the cold and dry Younger Dryas. These results agree with the increase in *Quercus* forest in the previously published pollen record from Padul (Pons and Reille, 1988). This increase in oak forest is also observed in the cave site of Carihuela in Granada within the supramediterranean vegetation belt (Carrión et al., 1999; Fernández et al., 2007) and a clear dominance in the Middle Atlas mountains (Lamb and van der Kaars, 1995).

1.2. The warm and humid Early and Middle Holocene (from ~10 to 4.7 cal ka BP)

The abundance of oak forest at lower altitude and *Pinus* at higher altitude (averaging values around 65 % and 45 %, respectively; Fig. 1), suggests wetter conditions during the Early and Middle Holocene (between ~10 and 4.7 cal ka BP). The LdRS record also detected an increase in mesic component (i.e., *Betula*; Anderson et al., 2011), although in this record the Holocene climatic optimum is mainly characterized by *Pinus maxima*, which could be explained by the difference in altitude with respect to Padul being the subalpine forest (oromediterranean vegetation belt) mostly characterized by *Pinus*. Other studies in southern Iberia also described humid conditions during the Early and Middle Holocene (Carrión, 2002; Carrión et al., 2001b; 2010b). Despite this generally wetter Early and Middle Holocene, a humidity optimum is observed around ~9.5 to 7.6 cal ka BP, detected by the higher average values of deciduous *Quercus* (Fig. 2). Agreeing with our results other regional studies also described humid conditions during this period (Fletcher and Sánchez-Goñi et al., 2008; Dormoy et al., 2009; Jalut et al., 2009). This humidity maximum could be explained due to summer insolation maxima, which favored the land/sea contrast enhancing winter rainfall in the Mediterranean (Meijer and Tuenter, 2007).

Within this period the local environment of Padul was characterized by a low water level due to very strong evapotranspiration during the Holocene insolation maxima (Laskar et al., 2004), lower water levels during the Early Holocene were also

detected in the Mediterranean area (Lamb and van der Kaars, 1995; Magny et al., 2007). However, Anderson et al. (2011) interpreted higher water level in the alpine area of Sierra Nevada, suggesting lake levels there being mostly controlled by lower summer temperatures and higher snowpack during winter at that time.

Rapid abrupt climatic events occurred during the generally humid Early and Middle Holocene. This millennial-scale climatic oscillations are discussed later in section 3.3.

1.3. The Late Holocene abrupt shift toward cooler and more arid conditions (last ~4.7 cal ka BP)

An abrupt climatic shift toward probably cooler and more arid conditions occurred since ~4.7 cal ka BP, determined by the strong decreasing trend in Mediterranean forest, mainly in deciduous *Quercus*, and the increase in scrubs and the subsequent increase in herbs (Fig. 1). *Pinus* reduction at higher altitude (LdRS) occurred at the same time as *Pinus* increased at lower elevations (Padul), which points to an altitudinal displacement of this species probably due to climate cooling and/or drying (Fig. 2). The expansion of *Ericaceae* at lower elevation could be explained by the decrease in thermal seasonality during the Late Holocene, as has previously been interpreted in the Mediterranean region (Fletcher and Sánchez-Goñi et al., 2008). In the alpine environment this aridification process is deduced by the increase in *Artemisia* that start to increase at the same time that *Cichorioideae* at lower altitude (Fig. 3). However, stronger values of *Chiroideae* has also been associated with enhanced human activities in the Padul area since 1.5 cal ka BP (see section 3.4.). A suite of proxies of previous studies supports our conclusions pointing to aridification process during the Late Holocene in the Mediterranean (e.g. Carrión, 2002; Carrión et al., 2003; 2007; Jalut et al., 2009; Gil-Romera et al., 2010). This climatic shift is related with a reorganization of the general atmospheric circulation reflecting an orbital climatic shift - enhancing a positive NAO trend- by reduced in summer insolation (Magny et al., 2002; 2012). In addition, the orbital-scale decrease in summer insolation would trigger a decrease in sea surface temperature generating a

decrease in the land-sea contrast (Marchal et al., 2002), reducing precipitation during winter provoking forest depletion. On the contrary, the local environment in the Padul area show an increase in water level during this climatic change which is also related with the decrease in summer insolation affecting the evaporation/precipitation balance and increasing the lake level (Fig. 2). In the BdlC an increasing trend in wetland plants also occurred, which could be explained by two local processes: (1) the decrease in summer insolation (as explained before) and/or (2) geomorphological conditions of the basin (see in Chapter 4 and 5).

The high-resolution pollen studies for the Late Holocene show that the progressive aridification trend is climatically more complex, showing arid and humid periods superimposed on this long-term climate process.

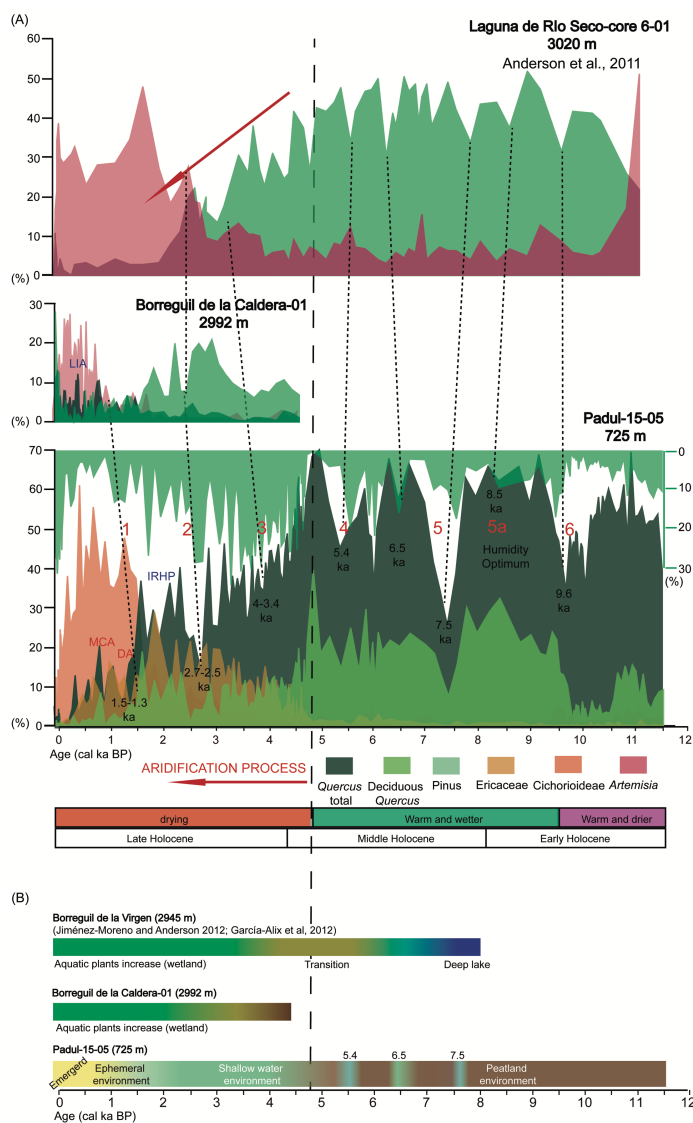


Figure 1. Vegetation dynamics and water level reconstruction in different altitudinal vegetation belts in Sierra Nevada. (A) Laguna de Rio Seco (LRS; 3020 m asl) pollen reconstruction (Anderson et al., 2011), Borreguil de la Caldera (BdlC-01; 2992 m asl) and Padul-15-05 (725 m asl) pollen reconstructions. (B) Peat bog/wetland development and lake level reconstruction from Borreguil de la Virgen (BdlV; 2945 m asl; Jiménez-Moreno and Anderson 2012; García-Alix et al., 2012a), Borreguil de la Caldera (BdlC-01) and Padul-15-05. Dashed lines show correlations between Padul-15-05 and LdRS pollen records indicating forest responses to abrupt climatic events. Numbers 1, 2, 3, 4, 5, 5a and 6 corresponds with cool events in the North Atlantic region (Bond et al., 2001).

2. Millennial-scale paleoenvironmental and climate variability during the Holocene in Sierra Nevada

The long-term climate evolution during the Holocene in Sierra Nevada was interrupted by millennial-scale climate oscillations, mainly determined by abrupt regional vegetation shifts. In this sense, the Sierra Nevada records show temperature/aridity pulses related with global climatic change associated with cool events in the North Atlantic region (Bond et al., 2001). These events are manifested by decrease in forest occurring suggesting arid conditions ~9.6, 8.5, 7.5, 6.5, 5.4, 4-3.4, 2.7-2.5, 1.5-1.3, 0.3-01 cal ka BP (Figs. 1 and 2). Curiously, during this short-scale climatic events, while *Pinus* (at higher altitude) and *Quercus* (at lower altitude) decreased, an increase in *Pinus* occurred in the Padul record, suggesting a displacement of the oromediterranean vegetation belt (where *Pinus* occur today) to lower altitudes during colder conditions. These abrupt coolings and arid events also affected sedimentation and local lake levels in the Padul environment pointing to higher lake level probably triggered by less evaporation in the wetland during coolings (Fig. 2). These oscillations could be related with cool events detected in the North Atlantic region and the decrease in solar irradiance (Bond et al., 2001; Steinhilber et al., 2009; see Chapter 2). These events are detected in our records with a periodicity of around ~2100 yr (and probably its second ~1000 yr-harmonic) during the Early and Middle Holocene and a predominant ~1400-1200 yr between the transition of the Middle-Late Holocene and during the Late Holocene. These results suggest that this abrupt climate variability during the Early and Middle Holocene was due to an external forcing (i.e. solar irradiance) and during the Late Holocene by internal forcing (i.e. atmospheric-oceanic dynamic) as previously suggested by Debret et al. (2007; 2009).

2.1. Iberian-Roman Humid period

The most humid period during the Late Holocene in southern Iberia probably occurred during the Iberian-Roman Humid period (IRHP from 2.6 to 1.6 cal ka BP; Martín-Puertas et al., 2009). The BdIC and LdlM alpine records show maxima in

Pinus (previous to human reforestation) and maxima in *Quercus*, respectively, between ~3.1 and 1.6 cal ka BP (Fig. 2). This humid period could be divided in two phases, as was previously indicated by Jiménez-Moreno et al. (2013a). Our results indicated that between ~3.1 and 2.6 cal ka BP humid but cooler conditions occurred, related with higher values of evergreen *Quercus*. (2) Between ~2.6 and 1.6 cal ka BP, an increase in deciduous *Quercus* occurred at lower and higher altitude showing maximum values during the Late Holocene, suggesting us humid but warmer conditions than in the previous phase (Figs. 2 and 3). Support for our results is the link between vegetation changes and the NAO reconstructions showing the most persistent negative phase and thus humidity within this period (Olsen et al., 2012). The forest variability observed within this humid period would also agree with the oscillations observed in the NAO reconstruction (see Chapters 3 and 4 related to this matter). In addition, these cooler and warmer periods could be supported by the temperature variability recorded in the North Atlantic record (Fig. 2; Bond et al., 2001; see IRD curve in Chapter 2).

2.2. The last ~1.5 cal ka BP: Dark ages, Medieval Climate Anomaly and the Little Ice Age

The last ~1.5 cal ka BP in the high-resolution pollen analyses from the sedimentary sequences studied in this thesis are characterized by several centennial-scale environmental and climatic oscillations (Fig. 2). Generally arid conditions occurred after the IRHP, indicated by stronger decrease in forest and the increase in herbs between 1.5-1.3 cal ka BP (Figs. 1 and 2). This is deduced in the BdIC record by the increase in *Artemisia* and in the Padul-15-05 record by the increase in Cichorioideae (probably enhanced by human perturbation during this period). This period could be subdivided in three phases corresponding with historical epochs. (1) A first phase, corresponding with the Dark Ages (DA; from ~1.4 to 1 cal ka BP/~500 to 900 CE; Moreno et al., 2012) is characterized by a progressive decrease in forest after the IRHP suggesting drier and probably cooler conditions. (2) A second phase, corresponding with the Medieval Climate Anomaly (MCA; from ~1 to 0.6 cal ka BP/~900 to 1300 CE; Moreno et al., 2012) was still arid but probably warmer phase

determined by the slight increase *Quercus* (mainly composed by evergreen *Quercus*; Figs. 1 and 2). Previous studies support our results showing persistent positive NAO conditions during the MCA (Trouet et al. 2009; Moreno et al., 2012). (3) A third phase would correspond with the Little Ice Age (LIA; ~0.6 cal ka BP/~1300 CE) in which could be appreciated a rapid and pronounced centennial-scale oscillation (partially due to higher-resolution) between warmer and cooler conditions within this overall arid period, also related with NAO oscillations (Trouet et al., 2009) and solar activity (Fig. 2; Bard et al., 2000). Wetter climatic conditions within the LIA, observed by a relative decrease in herbs and increase in trees, are probably related to negative NAO conditions and could have been triggered by minima in solar activity (Fig. 2). Some of these arid periods as the DA and the second part of the LIA are related with global cooling events (see previous section 1.2).

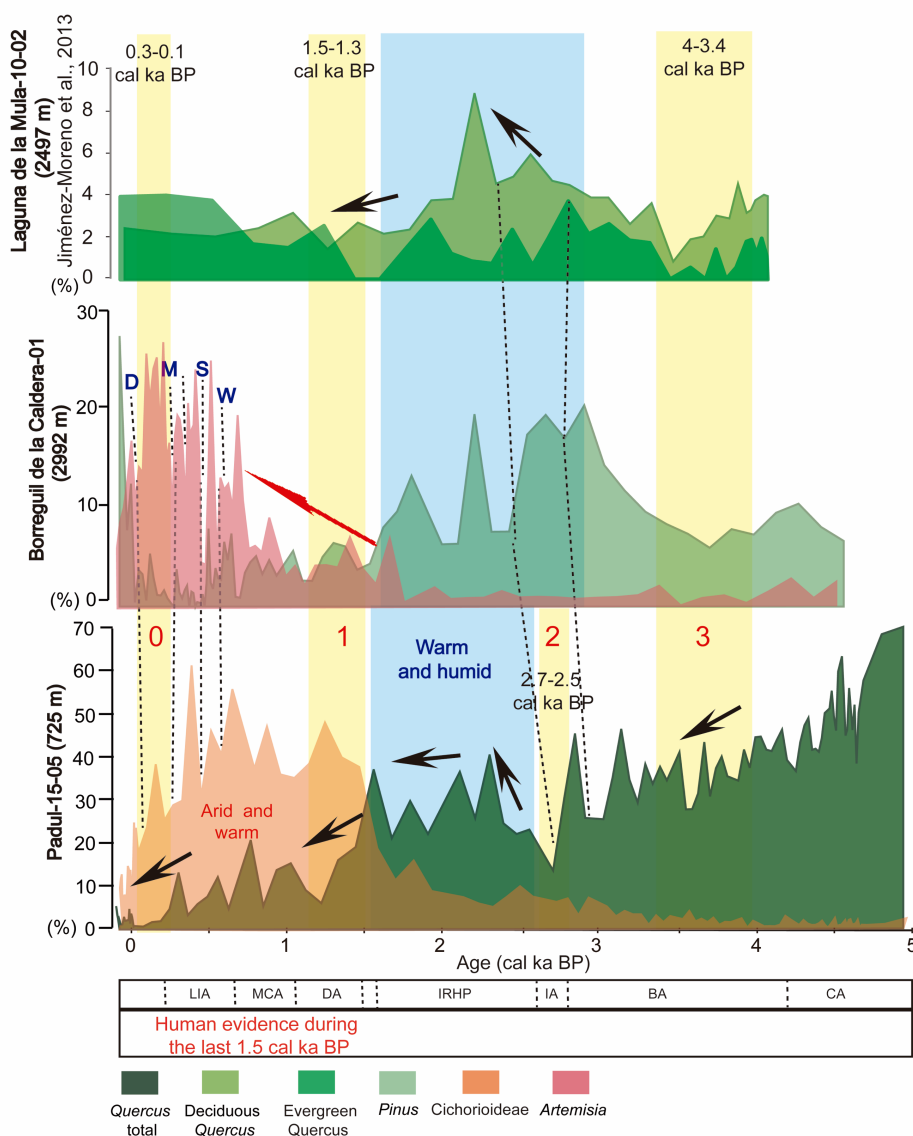


Figure 2. Summary of vegetation variability in the alpine and montane areas of Sierra Nevada (crioromediterranean and mesomediterranean vegetation belts). (Below) *Quercus* and Cichorioideae pollen data from the Padul-15-05 record (725 m asl). (Middle) *Pinus* and *Artemisia* pollen data from the Borreguil de la Caldera-01 sequence (BdIC-01; 2992 m asl) and (above) deciduous *Quercus* from Laguna de la Mula (LdIM; 2497 m asl; Jiménez-Moreno et al., 2013a). Yellow and blue shadings correspond with arid (cold) events and humid (warm) periods, respectively. Dash lines show the correlation between Padul-15-05 pollen record and BdIC-01 and LdIM-10-02 indicating responses in vegetation to abrupt climatic events. D = Dalton, M = Maunder, S = Spörer, W = Wolf (solar minima; Bard et al., 2000). LIA = Little Ice Age, MCA = Medieval Climate Anomaly, DA = Dark Ages, IRHP = Iberian-Roman Humid Period, IA = Iron Ages, BA = Bronze Age, CA = Cooper Age. Numbers 0, 1, 2 and 3 corresponds with cool events in the North Atlantic region (Bond et al., 2001).

3. Human Impact

Evidence of human impact at lower elevation (Padul, 725 m asl) in Sierra Nevada began to be significant in the last 1.5 cal ka BP. This is deduced by the increase in plants related with cultivation (e.g. nitrophilous plants related with land uses) and the increase in some NPPs as *Tilletia*, Sordariales and Thecamoebians, probably associated with farming and/or animal husbandry (Fig. 3). The significant increase in Cichoriodeae, previously related with the natural climatic trend to aridification, could have been enhanced by a greater livestock in the area, supported by the link with other proxies related with animal husbandry (i.e. Thecamoebians, Sordariales). However, in the high elevation alpine environments, evidences seem to be less clear until very recent and coprophilous fungi such as *Sporormiella* and Sordariales began to occur consistently in the last ~400 yr (Fig. 3), probably related with the introduced of livestock and grazing at in Sierra Nevada (Anderson et al., 2011).

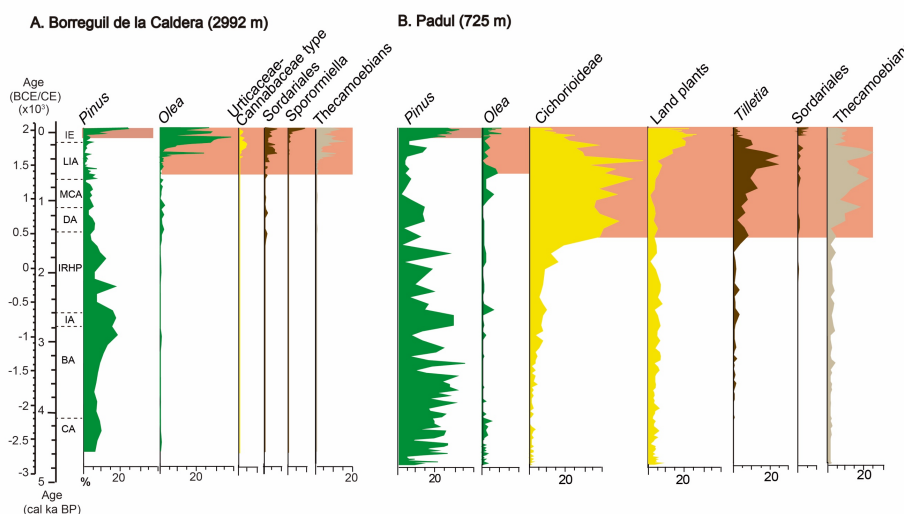


Figure 3. Comparison of selected pollen and non-pollen palynomorphs (NPPs) for the last ~4.7 cal ka BP from BdIC-01 (A) and Padul-15-05 (B) records considered to be related to human activities. Tree taxa are showing in green, herbs and plants in yellow, fungi in brown and thecamoebians in beige. Red bars highlight are showing the evidence of human impact in the BdIC-01 and Padul-15-05 records during the last ca. 4.7 cal ka yr. Proxies interpretation: *Sporormiella*, Sordariales and Thecamoebians (livestock indicator), *Olea* and *Tilletia* (cultivar indicator), Land Use Plants (cultivar indicator). Land Use Plants is composed by Polygonaceae, Amaranthaceae, Convolvulaceae, *Plantago*, Apiaceae and Cannabaceae-Urticaceae type.

A recent increase in *Olea* began to be noticeable in the last ~250 yr (1750 CE; Figs. 3 and 4). At the lower elevation Padul sequence *Olea* has been found in very small amounts, reaching maximum values of ~10 %, probably only recording the local cultivation of this tree species at this altitude. Curiously, higher values of *Olea* are recorded in the higher elevation sites (reaching maximum values of ~40 %). Moss polsters analysis done on an altitudinal transect in Sierra Nevada also show high percentages of *Olea* at high elevation (reaching values of around ~30 % at 2707 m asl; Ramos-Román, in prep.). At present, most of the *Olea* cultivations are located under 700 m of elevation as this is a thermophilous species (Galán et al., 2005). Anderson et al. (2011) suggested that *Olea* pollen travelled uphill towards higher elevation sites – probably recording higher concentration of this pollen taxa in the alpine environments. The significant increase in *Olea* in the studied records during the last 100 yr (~1920 CE; Fig. 4) corresponds to the great increase in olive oil production in southern Spain beginning in the 1920s (Bull, 1936). The significant increase in *Pinus* during the last century (Fig. 4) has been associated with reforestation of *P. sylvestris* trees that commenced in the Sierra Nevada since the middle of the 20th century to combat erosion (Anderson et al., 2011). Finally, global climatic events could have also conditioned changes in the agricultural practices or affected cultivations, this is suggested here by the decrease in *Olea* recorded during the second half of the LIA, when cooler conditions were previously interpreted (see section 3.3).

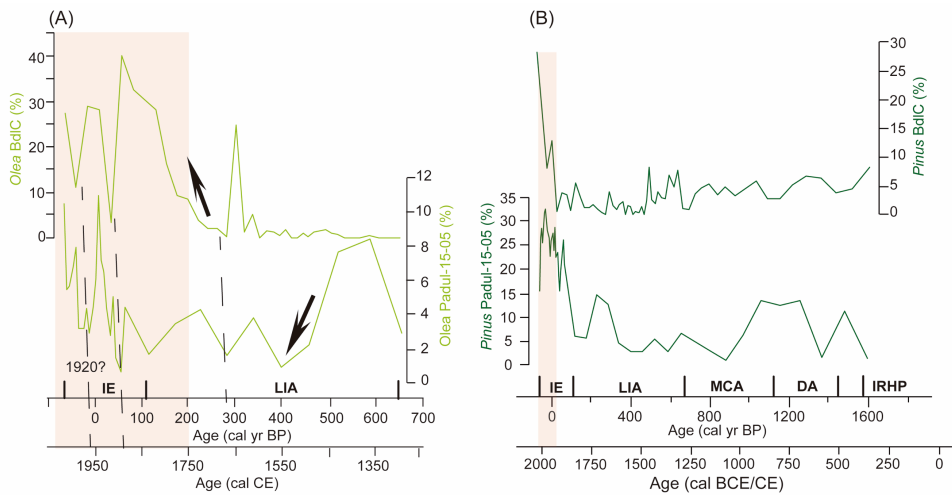


Fig. 4. *Olea* (left) and *Pinus* (right) pollen records from BdlC and Padul. Note the increase and the variability in *Olea* in the last ~250 yr and the increase in *Pinus* in the last century.

CHAPTER 7

Conclusions

The high-resolution multi-proxy analysis (pollen, charcoal, sedimentological and geochemical analysis) of two sedimentary sequences from the high-elevation Borreguil de la Cadera and low-elevation Padul sites in the Sierra Nevada mountain area permitted obtaining the following conclusions:

1. The multi-proxy analyses show paleoenvironmental variability in Sierra Nevada related with orbital- and suborbital-scale climate changes.
2. Warming characterized the earliest part of the Holocene in southern Iberia after the lateglacial period and the time between ~11.6 to 9.5 cal ka BP was characterized by the presence of evergreen forest in the mesomediterranean vegetation belt. This type of Mediterranean-adapted forest would show vegetal adaptation to the climate conditions at that time, with maxima in summer insolation and higher seasonality - higher summer temperatures and lower temperatures in winter. This climatic condition triggered high summer evaporation and low lake levels, recorded with the establishment of abundant reed vegetation and peatland environment in the Padul area.
3. The second part of the Early Holocene (*sensu lato*), from around 9.5 to 7.6 cal ka BP, featured the expansion of deciduous *Quercus* in montane areas reflecting the Holocene climatic optimum and maxima in moisture availability in the regional environment. Although persistent high summer insolation and thus evaporation precluded the rise of local lake levels.
4. The Middle Holocene between 7.6 and 4.7 cal ka BP was characterized by higher arboreal component, with Mediterranean forest mainly dominated by evergreen taxa. A decrease in summer insolation and a reduction in seasonality occurred during this period, allowing water table to rise periodically and producing the intercalation between peats and shallow water lake sediments in Padul.

5. The Late Holocene is characterized in Sierra Nevada by an aridification trend observed in the records by the decrease in the Mediterranean (at low elevation) and pine (at high elevations) forests and the increase in scrubs and herbs. This was mainly related with the decrease in summer insolation, triggering a decrease in winter precipitations and the establishment of the actual climate system dominated by persistent positive NAO. On the other hand, lake levels in Padul and perhaps in BdIC show a significant increase since 4.7 cal ka BP. This apparent contradiction could be explained by the decreasing summer insolation, which would also reduce the seasonality and would lower evapotranspiration during summer, affecting the evaporation/precipitation balance and increasing lake levels in the area.
6. Superimposed on the general climatic and environmental long-term trends during the Holocene is millennial-scale variability, recorded in the studied records through several abrupt decreases in forest pointing to arid events at ~9.7, 8.5, 7.5, 6.5, 5.4, 4.2, 2.7 and 1.3 cal ka BP. These environmental changes occurred at times coinciding with well-known decreases in temperatures in the north Atlantic region (Bond events) and with decreases in solar irradiance, which point to the same hemispheric-scale most likely solar-induced climatic trigger. Relatively wet periods are also recorded, being also related with this millennial-scale climate variability and a humid period is recorded between 2.6-1.6 cal ka BP coinciding with the historical IRHP. The especially high-resolution record from Borreguil de la Caldera also permitted recording centennial-scale climatic oscillations during historical periods such as the well-known DA, MCA and LIA, also linked with atmospheric (NAO) variability.
7. The evidence of human impact on the environment in the area began to be evident in the studied records in the Late Holocene and being especially intense in the last ~1.5 cal ka BP. Direct anthropic evidences in the alpine ecosystems from the Sierra Nevada are shown during the last centuries by signs of grazing, with little impact in the environment. In the lower elevation Padul area, a higher signal of

anthropic influence is detected since the last ~1.5 cal ka BP, enhancing the aridification trend in the local environment by enhanced soil erosion, agriculture and animal husbandry. Although anthropogenic impact occurred in the Sierra Nevada area, our studies demonstrate that climate was the main forcing driving vegetation change (i.e. deforestation) process in southern Iberia and the western Mediterranean region at least until the last centuries.

Conclusiones

El análisis multi-proxy a alta resolución (polen, carbón, análisis sedimentológico y geoquímico) de dos secuencias sedimentarias de Sierra Nevada, Borreguil de la cadera situada a elevada altitud y Padul a baja altitud, permitió obtener las siguientes conclusiones:

1. El análisis multi-proxy muestra una variabilidad paleoambiental en Sierra Nevada relacionada con cambios climáticos a escala orbital y suborbital.
2. Una fase de calentamiento definió la parte más temprana del Holoceno en el sur de Iberia después del período tardiglaciario y entre ~11.6 a 9.5 cal ka BP fue característica la presencia de bosque perenne en el cinturón de vegetación mesomediterránea. Este tipo de bosque adaptado al Mediterráneo, muestra la adaptación de la vegetación a las condiciones climáticas de ese momento, determinadas por un máximo en la insolación de verano y una mayor estacionalidad - temperaturas más altas de verano y temperaturas más bajas en invierno. Esta condición climática desencadenó una alta evaporación de verano y bajos niveles de lagos, registrados con el establecimiento de abundante vegetación de carrizo y el ambiente de turbera en el área de Padul.
3. La segunda parte del Holoceno temprano (*sensu lato*), desde 9.5 a 7.6 cal ka BP, fue caracterizada por la expansión del bosque de *Quercus* caduco en áreas montañosas, reflejando el óptimo climático Holoceno y el máximo de humedad en el ambiente regional. Aunque la persistente insolación de verano y consecuente evaporación impidió el desarrollo de lagos locales.
4. El Holoceno medio entre 7.6 y 4.7 cal ka BP fue caracterizado por un elevado componente arbóreo, con el bosque Mediterráneo principalmente dominado por bosque perenne. Un descenso en la insolación y reducción de la estacionalidad ocurren durante este periodo, permitiendo periódicos ascensos del nivel del lago

y produciendo la intercalación entre sedimentos de turbera y lago somero en Padul.

5. El Holoceno tardío es caracterizado en Sierra Nevada por un proceso de aridificación, observado en los registros por el descenso del bosque Mediterráneo (a baja altitud) y pino (a elevada altitud) así como el incremento de arbustos y hierbas. Esto está principalmente relacionado con el descenso en la insolación de verano, desencadenando un descenso en la precipitación de invierno y el establecimiento del actual sistema climático dominado por una persistente NAO positiva. Por otro lado, los niveles de lagos en Padul y, quizás en Borreguil de la Caldera, mostraron un significativo incremento durante los últimos 4.7 cal ka BP. Esta aparente contradicción puede ser explicada por el descenso de la insolación de verano, lo que también reduciría la estacionalidad y la evaporación durante el verano, afectando al balance evaporación/precipitación e incrementando el nivel de los lagos en esta área.
6. Superpuesto a las tendencias generales climáticas y ambientales a largo plazo durante el Holoceno, se encuentra la variabilidad a escala milenaria, registrada en las secuencias estudiadas a través de varias disminuciones abruptas del bosque apuntando a eventos áridos ~9.7, 8.5, 7.5, 6.5, 5.4, 4.2, 2.7 y 1.3 cal ka BP. Estos cambios ambientales ocurrieron coincidiendo con descensos en las temperaturas en la región del Atlántico norte (eventos de Bond) y con disminuciones en la irradiancia solar, que indican a escala hemisférica un cambio climático probablemente desencadenado por inducción solar. También se registran períodos relativamente húmedos, que están relacionados con esta variabilidad climática a escala milenaria, registrándose un período húmedo entre 2.6-1.6 cal ka BP coincidiendo con el histórico IRHP. La secuencia de alta resolución del Borreguil de la Caldera permitió registrar oscilaciones climáticas a escala centenaria durante periodos históricos como el conocido DA, MCA y LIA, también relacionados con la variabilidad atmosférica (NAO).

7. La evidencia del impacto humano sobre el medio ambiente en el área de estudio comenzó a ser notoria en los registros estudiados durante el Holoceno Tardío, y fue especialmente intensa en los últimos ~ 1.5 cal ka BP. Las evidencias antrópicas directas en los ecosistemas alpinos de Sierra Nevada, se registran durante los últimos siglos por signos de pastoreo, con poco impacto en el medio ambiente. En el área de Padul, a menor altitud, se detecta una mayor señal de influencia antrópica en los últimos ~ 1.5 cal ka BP, favoreciendo la tendencia de aridificación en el ambiente local mediante el aumento de la erosión del suelo, la agricultura y la cría de animales. Aunque el impacto antropogénico ocurrió en el área de Sierra Nevada, nuestros estudios demuestran que el clima fue el principal factor que forzó el proceso de cambio de vegetación (es decir, la deforestación) en el sur de Iberia y la región mediterránea occidental, al menos hasta los últimos siglos.

Future Perspectives

The study carried out in the present PhD thesis may be contemplated as a first stage for the knowledge of vegetation, climate variability and human impact in Sierra Nevada ecosystems and the southern Iberia Peninsula. More questions arise with the increasing number of paleoenvironmental studies in the area, principally related with the timing and physical forcings of the environmental variability (e.g. precipitation vs. temperature) and human effects on the ecosystems. This study shows that the response of the vegetation and environment varies depending on elevation gradients, geomorphological context and anthropic influence. One way of removing the interfering human impact from the climate signal conditioning environmental change is to study older periods previous to human spread, such as the last interglacial period (Eemian or MIS5e). The last interglacial is also recorded in the Padul-15-05 sediment core. The high resolution study of the last interglacial period, comparable or even warmer than today, will allow us to draw conclusions about how ecosystems vary when temperatures and / or drought increase in this region.

This study also shows a relationship between environmental (i.e., vegetation) change and NAO variability at millennial- and centennial-scales. One way of improving our knowledge on how NAO variability affected the Sierra Nevada environments is to estimate past rainfall in this semi-arid environments, where the forest is mainly controlled by water availability, with the study tree growth (Douglass, 1914). A dendrochronological study done on native high-elevation tree species (i.e., *Pinus sylvestris*, *P. nigra*) could thus help us understanding the NAO-precipitation (and effective precipitation) relationship.

References

- Abel-Schaad, D., López-Sáez, J.A., 2013. Vegetation changes in relation to fire history and human activities at the Peña Negra mire (Bejar Range, Iberian Central Mountain System, Spain) during the past 4,000 years. *Veg. Hist. Archaeobotany* 22, 199–214. <https://doi.org/10.1007/s00334-012-0368-9>
- Ahn, J., Brook, E.J., 2008. Atmospheric CO₂ and Climate on Millennial Time Scales During the Last Glacial Period. *Science* 322, 83. <https://doi.org/10.1126/science.1160832>
- Alfaro, P., Galinod-Zaldívar, J., Jabaloy, A., López-Garrido, A.C., Sanz de Galdeano, C., 2001. Evidence for the activity and paleoseismicity of the Padul fault (Betic Cordillera, Southern Spain) [Evidencias de actividad y paleoseismicidad de la falla de Padul (Cordillera Bética, sur de España)]. *Acta Geol. Hisp.* 36, 283–297.
- Alley, R., Clark, P., Keigwin, L., Webb, R., 2000. Making sense of millennial-scale climate change. *Mech. Glob. Clim. Change Millenn. Time Scales* 385–394.
- Alpert, P., Baldi, M., Ilani, R., Krichak, S., Price, C., Rodó, X., Saaroni, H., Ziv, B., Kishcha, P., Barkan, J., Mariotti, A., Xoplaki, E., 2006. Chapter 2 Relations between climate variability in the Mediterranean region and the tropics: ENSO, South Asian and African monsoons, hurricanes and Saharan dust. *Dev. Earth Environ. Sci.* 4, 149–177. [https://doi.org/10.1016/S1571-9197\(06\)80005-4](https://doi.org/10.1016/S1571-9197(06)80005-4)
- Anderson, R.S., 1990. Holocene Forest Development and Paleoclimates Within the Central Sierra Nevada, California. *J. Ecol.* 78, 470–489. <https://doi.org/10.2307/2261125>
- Anderson, R.S., Jiménez-Moreno, G., Carrión, J.S., Pérez-Martínez, C., 2011. Postglacial history of alpine vegetation, fire, and climate from Laguna de Río Seco, Sierra Nevada, southern Spain. *Quat. Sci. Rev.* 30, 1615–1629. <https://doi.org/10.1016/j.quascirev.2011.03.005>
- Andrade Olalla, A., Valdeolmillos, A., Ruiz Zapata, B., 1994. Modern pollen spectra and contemporary vegetation in the Paramera mountain range (Avila, Spain). *Mod. Pollen Rain Foss. Pollen Spectra* 82, 129–139. [https://doi.org/10.1016/0034-6667\(94\)90024-8](https://doi.org/10.1016/0034-6667(94)90024-8)
- Aranbarri, J., González-Sampériz, P., Valero-Garcés, B., Moreno, A., Gil-Romera, G., Sevilla-Callejo, M., García-Prieto, E., Rita, F.D., Mata, M.P., Morellón, M., Magri, D., Rodríguez-Lázaro, J., Carrión, J.S., 2014. Rapid climatic changes and resilient vegetation during the Lateglacial and Holocene in a continental region of south-western Europe. *Glob. Planet. Change* 114, 50–65. <https://doi.org/10.1016/j.gloplacha.2014.01.003>
- Armitage, S.J., Bristow, C.S., Drake, N.A., 2015. West African monsoon dynamics inferred from abrupt fluctuations of Lake Mega-Chad. *Proc. Natl. Acad. Sci.* 112, 8543–8548. <https://doi.org/10.1073/pnas.1417655112>
- Arz, H.W., Lamy, F., Pätzold, J., Müller, P.J., Prins, M., 2003. Mediterranean Moisture Source for an Early-Holocene Humid Period in the Northern Red Sea. *Science* 300, 118. <https://doi.org/10.1126/science.1080325>

- Bader, J., Mesquita, M.D.S., Hodges, K.I., Keenlyside, N., Østerhus, S., Miles, M., 2011. A review on Northern Hemisphere sea-ice, storminess and the North Atlantic Oscillation: Observations and projected changes. *Atmospheric Res.* 101, 809–834. <https://doi.org/10.1016/j.atmosres.2011.04.007>
- Baker, A., C. Hellstrom, J., Kelly, B.F.J., Mariethoz, G., Trouet, V., 2015. A composite annual-resolution stalagmite record of North Atlantic climate over the last three millennia 5, 10307.
- Bard, E., Raisbeck, G., Yiou, F., Jouzel, J., 2000. Solar irradiance during the last 1200 years based on cosmogenic nuclides. *Tellus B* 52, 985–992. <https://doi.org/10.1034/j.1600-0889.2000.d01-7.x>
- Bard, F., Casano, L., Mallabiabarrena, A., Wallace, E., Saito, K., Kitayama, H., Guizzunti, G., Hu, Y., Wendler, F., DasGupta, R., Perrimon, N., Malhotra, V., 2006. Functional genomics reveals genes involved in protein secretion and Golgi organization. *Nature* 439, 604–607. <https://doi.org/10.1038/nature04377>
- Bar-Matthews, M., Ayalon, A., Gilmour, M., Matthews, A., Hawkesworth, C.J., 2003. Sea–land oxygen isotopic relationships from planktonic foraminifera and speleothems in the Eastern Mediterranean region and their implication for paleorainfall during interglacial intervals. *Geochim. Cosmochim. Acta* 67, 3181–3199. [https://doi.org/10.1016/S0016-7037\(02\)01031-1](https://doi.org/10.1016/S0016-7037(02)01031-1)
- Battarbee, R.W., Thompson, R., Catalan, J., Grytnes, J.-A., Birks, H.J.B., 2002. Climate variability and ecosystem dynamics of remote alpine and arctic lakes: the MOLAR project. *J. Paleolimnol.* 28, 1–6. <https://doi.org/10.1023/A:1020342316326>
- Bellin, N., Vanacker, V., De Baets, S., 2013. Anthropogenic and climatic impact on Holocene sediment dynamics in SE Spain: A review. *Quat. Int.* 308–309, 112–129. <https://doi.org/10.1016/j.quaint.2013.03.015>
- Bellin, N., Vanacker, V., van Wesemael, B., Solé-Benet, A., Bakker, M.M., 2011. Natural and anthropogenic controls on soil erosion in the internal betic Cordillera (southeast Spain). *Catena* 87, 190–200. <https://doi.org/10.1016/j.catena.2011.05.022>
- Berger, A., 1988. Milankovitch Theory and climate. *Rev. Geophys.* 26, 624–657. <https://doi.org/10.1029/RG026i004p00624>
- Berger, A., 1980. The Milankovitch astronomical theory of paleoclimates: A modern review. *Vistas Astron.* 24, 103–122. [https://doi.org/10.1016/0083-6656\(80\)90026-4](https://doi.org/10.1016/0083-6656(80)90026-4)
- Berner, K.S., Koç, N., Godtlibsen, F., Divine, D., 2011. Holocene climate variability of the Norwegian Atlantic Current during high and low solar insolation forcing. *Paleoceanography* 26, n/a-n/a. <https://doi.org/10.1029/2010PA002002>
- Beug, H.-J., 2004. Leitfaden der Pollenbestimmung für Mitteleuropa und angrenzende Gebiete. *Fisch. Stuttg.* 61.
- Beug, H.-J., 1961. Leitfaden der Pollenbestimmung für Mitteleuropa und angrenzende Gebiete. *Fisch. Stuttg.* 61.
- Blaauw, M., 2010. Methods and code for ‘classical’ age-modelling of radiocarbon sequences. *Quat. Geochronol.* 5, 512–518. <https://doi.org/10.1016/j.quageo.2010.01.002>

- Blanca, G., 2001. Flora amenazada y endémica de Sierra Nevada. 401 (Consejería de Medio Ambiente de la Junta de Andalucía and University of Granada, 2001).
- Blanca, G., 1996. Diversidad y protección de la flora vascular de Sierra Nevada (Granada, España). *Sierra Nev. Conserv. Desarro. Sosten.* 2, 245-269.
- Blanca, G., López, M., Lorite, J., Martínez, M., Molero, J., Quintas, S., Ruiz, M., Varo, M., Vidal, S., 2002. Flora amenazada y endémica de Sierra Nevada. Univ. Granada Cons. Medio Ambiente Junta Anda- Lucía Granada 410.
- Bojariu, R., Gimeno, L., 2003. The role of snow cover fluctuations in multiannual NAO persistence. *Geophys. Res. Lett.* 30.
- Bond, G., Broecker, W., Johnsen, S., McManus, J., Labeyrie, L., Jouzel, J., Bonani, G., 1993. Correlations between climate records from North Atlantic sediments and Greenland ice. *Nature* 365, 143–147. <https://doi.org/10.1038/365143a0>
- Bond, G., Kromer, B., Beer, J., Muscheler, R., Evans, M.N., Showers, W., Hoffmann, S., Lotti-Bond, R., Hajdas, I., Bonani, G., 2001. Persistent Solar Influence on North Atlantic Climate During the Holocene. *Science* 294, 2130. <https://doi.org/10.1126/science.1065680>
- Bond, G., Showers, W., Cheseby, M., Lotti, R., Almasi, P., deMenocal, P., Priore, P., Cullen, H., Hajdas, I., Bonani, G., 1997. A Pervasive Millennial-Scale Cycle in North Atlantic Holocene and Glacial Climates. *Science* 278, 1257. <https://doi.org/10.1126/science.278.5341.1257>
- Booth, R.K., Jackson, S.T., Forman, S.L., Kutzbach, J.E., E. A. Bettis, I., Kreigs, J., Wright, D.K., 2005. A severe centennial-scale drought in midcontinental North America 4200 years ago and apparent global linkages. *The Holocene* 15, 321–328. <https://doi.org/10.1191/0959683605hl825ft>
- Bottema, S., 1975. The interpretation of pollen spectra from prehistoric settlements (with special attention of Liguliflorae). *Palaeohistoria* 17, 17–35.
- Bozzano, G., Kuhlmann, H., Alonso, B., 2002. Storminess control over African dust input to the Moroccan Atlantic margin (NW Africa) at the time of maxima boreal summer insolation: a record of the last 220 kyr. *Palaeogeogr. Palaeoclimatol. Palaeoecol.* 183, 155–168.
- Broecker, W.S., 1992. Upset for Milankovitch theory. *Nature* 359, 779.
- Bull, W.E., 1936. The olive industry of Spain. *Econ. Geogr.* 12, 136–154.
- Bush, R.T., McInerney, F.A., 2013. Leaf wax n-alkane distributions in and across modern plants: Implications for paleoecology and chemotaxonomy. *Geochim. Cosmochim. Acta* 117, 161–179. <https://doi.org/10.1016/j.gca.2013.04.016>
- Cacho, I., Grimalt, J.O., Canals, M., Sbaiffi, L., Shackleton, N.J., Schönfeld, J., Zahn, R., 2001. Variability of the western Mediterranean Sea surface temperature during the last 25,000 years and its connection with the Northern Hemisphere climatic changes. *Paleoceanography* 16, 40–52. <https://doi.org/10.1029/2000PA000502>
- Cacho, I., Grimalt, J.O., Pelejero, C., Canals, M., Sierro, F.J., Flores, J.A., Shackleton, N., 1999. Dansgaard-Oeschger and Heinrich event imprints in Alboran Sea paleotemperatures. *Paleoceanography* 14, 698–705. <https://doi.org/10.1029/1999PA900044>
- Carrasco Duarte, M., 1999. Padul. Padul: Editación del autor.

- Carrión, J., Van Geel, B., 1999. Fine-resolution Upper Weichselian and Holocene palynological record from Navarrés (Valencia, Spain) and a discussion about factors of Mediterranean forest succession. *Rev. Palaeobot. Palynol.* 106, 209–236.
- Carrión, J.S., 2002. Patterns and processes of Late Quaternary environmental change in a montane region of southwestern Europe. *Quat. Sci. Rev.* 21, 2047–2066. [https://doi.org/10.1016/S0277-3791\(02\)00010-0](https://doi.org/10.1016/S0277-3791(02)00010-0)
- Carrión, J.S., Andrade, A., Bennett, K.D., Navarro, C., Munuera, M., 2001a. Crossing forest thresholds: inertia and collapse in a Holocene sequence from south-central Spain. *The Holocene* 11, 635–653. <https://doi.org/10.1191/09596830195672>
- Carrión, J.S., Fernández, S., González-Sampériz, P., Gil-Romera, G., Badal, E., Carrión-Marco, Y., López-Merino, L., López-Sáez, J.A., Fierro, E., Burjachs, F., 2010b. Expected trends and surprises in the Lateglacial and Holocene vegetation history of the Iberian Peninsula and Balearic Islands. *Rev. Palaeobot. Palynol.* 162, 458–475. <http://dx.doi.org/10.1016/j.revpalbo.2009.12.007>
- Carrión, J.S., Fernández, S., Jiménez-Moreno, G., Fauquette, S., Gil-Romera, G., González-Sampériz, P., Finlayson, C., 2010a. The historical origins of aridity and vegetation degradation in southeastern Spain. *J. Arid Environ.* 74, 731–736. <https://doi.org/10.1016/j.jaridenv.2008.11.014>
- Carrión, J.S., Finlayson, C., Fernández, S., Finlayson, G., Allué, E., López-Sáez, J.A., López-García, P., Gil-Romera, G., Bailey, G., González-Sampériz, P., 2008. A coastal reservoir of biodiversity for Upper Pleistocene human populations: palaeoecological investigations in Gorham's Cave (Gibraltar) in the context of the Iberian Peninsula. *Coast. Shelf Mediterr. Corridor Refug. Hum. Popul. Pleistocene* 27, 2118–2135. <https://doi.org/10.1016/j.quascirev.2008.08.016>
- Carrión, J.S., Fuentes, N., González-Sampériz, P., Quirante, L.S., Finlayson, J.C., Fernández, S., Andrade, A., 2007. Holocene environmental change in a montane region of southern Europe with a long history of human settlement. *Quat. Sci. Rev.* 26, 1455–1475. <https://doi.org/10.1016/j.quascirev.2007.03.013>
- Carrión, J.S., Munuera, M., Dupré, M., Andrade, A., 2001b. Abrupt vegetation changes in the Segura Mountains of southern Spain throughout the Holocene. *J. Ecol.* 89, 783–797. <https://doi.org/10.1046/j.0022-0477.2001.00601.x>
- Carrión, J.S., Munuera, M., Navarro, C., Burjachs, F., Dupré, M., Walker, M.J., 1999. The palaeoecological potential of pollen records in caves: the case of Mediterranean Spain. *Quat. Sci. Rev.* 18, 1061–1073. [https://doi.org/10.1016/S0277-3791\(98\)00002-X](https://doi.org/10.1016/S0277-3791(98)00002-X)
- Carrión, J.S., Sánchez-Gómez, P., Mota, J.F., Yll, R., Chaín, C., 2003. Holocene vegetation dynamics, fire and grazing in the Sierra de Gádor, southern Spain. *Holocene* 13, 839–849. <https://doi.org/10.1191/0959683603hl662rp>
- Castillo Martín, A., 2009. *Lagunas de Sierra Nevada*. Editor. Univ. Granada Granada.

- Castillo Martín, A., Benavente Herrera, J., Fernández Rubio, R., Pulido Bosch, A., 1984. Evolución y ámbito hidrogeológico de la laguna de Padul (Granada). *Las Zonas Húmedas En Andal. Monogr. DGMA-MOPU*.
- Castro, J., Zamora, R., Hódar, J.A., Gómez, J.M., 2004. Seedling establishment of a boreal tree species (*Pinus sylvestris*) at its southernmost distribution limit: consequences of being in a marginal Mediterranean habitat. *J. Ecol.* 92, 266–277. <https://doi.org/10.1111/j.0022-0477.2004.00870.x>
- Catalan, J., Pla-Rabés, S., Wolfe, A.P., Smol, J.P., Rühland, K.M., Anderson, N.J., Kopáček, J., Stuchlík, E., Schmidt, R., Koinig, K.A., Camarero, L., Flower, R.J., Heiri, O., Kamenik, C., Korhola, A., Leavitt, P.R., Psenner, R., Renberg, I., 2013. Global change revealed by palaeolimnological records from remote lakes: a review. *J. Paleolimnol.* 49, 513–535. <https://doi.org/10.1007/s10933-013-9681-2>
- Chapman, M.R., Shackleton, N.J., 2000. Evidence of 550-year and 1000-year cyclicities in North Atlantic circulation patterns during the Holocene. *The Holocene* 10, 287–291. <https://doi.org/10.1191/095968300671253196>
- Chapman, S.J., 2001. Sulphur Forms in Open and Afforested Areas of Two Scottish Peatlands. *Water. Air. Soil Pollut.* 128, 23–39. <https://doi.org/10.1023/A:1010365924019>
- Cheddadi, R., Yu, G., Guiot, J., Harrison, S.P., Prentice, I.C., 1997. The climate of Europe 6000 years ago. *Clim. Dyn.* 13, 1–9. <https://doi.org/10.1007/s003820050148>
- Clausing, A., 1999. Palaeoenvironmental significance of the green alga *Botryococcus* in the lacustrine rotliegend (upper carboniferous - lower permian). *Historical Biology* 13, 221–234. doi:10.1080/08912969909386582
- Cloern, J.E., Canuel, E.A., Harris, D., 2002. Stable carbon and nitrogen isotope composition of aquatic and terrestrial plants of the San Francisco Bay estuarine system. *Limnol. Oceanogr.* 47, 713–729. <https://doi.org/10.4319/lo.2002.47.3.0713>
- Combourieu-Nebout, N., Peyron, O., Dormoy, I., Desprat, S., Beaudouin, C., Kotthoff, U., Marret, F., 2009. Rapid climatic variability in the west Mediterranean during the last 25 000 years from high resolution pollen data. *Clim Past* 5, 503–521. <https://doi.org/10.5194/cp-5-503-2009>
- Corella, J.P., Stefanova, V., El Anjoumi, A., Rico, E., Giralt, S., Moreno, A., Plata-Montero, A., Valero-Garcés, B.L., 2013. A 2500-year multi-proxy reconstruction of climate change and human activities in northern Spain: The Lake Arreo record. *Palaeogeogr. Palaeoclimatol. Palaeoecol.* 386, 555–568. <https://doi.org/10.1016/j.palaeo.2013.06.022>
- Cortés Sánchez, M., Jiménez Espejo, F.J., Simón Vallejo, M.D., Gibaja Bao, J.F., Carvalho, A.F., Martínez-Ruiz, F., Gamiz, M.R., Flores, J.-A., Paytan, A., López Sáez, J.A., Peña-Chocarro, L., Carrión, J.S., Morales Muñoz, A., Roselló Izquierdo, E., Riquelme Cantal, J.A., Dean, R.M., Salgueiro, E., Martínez Sánchez, R.M., De la Rubia de Gracia, J.J., Lozano Francisco, M.C., Vera Peláez, J.L., Rodríguez, L.L., Bicho, N.F., 2012. The Mesolithic–Neolithic

- transition in southern Iberia. *Quat. Res.* 77, 221–234. <https://doi.org/10.1016/j.yqres.2011.12.003>
- Cour, P., Zheng, Z., Duzer, D., Calleja, M., Yao, Z., 1999. Vegetational and climatic significance of modern pollen rain in northwestern Tibet. *Rev. Palaeobot. Palynol.* 104, 183–204. [https://doi.org/10.1016/S0034-6667\(98\)00062-1](https://doi.org/10.1016/S0034-6667(98)00062-1)
- Cranwell, P., Eglinton, G., Robinson, N., 1987. Lipids of aquatic organisms as potential contributors to lacustrine sediments—II. *Org. Geochem.* 11, 513–527.
- Cranwell, P.A., 1984. Lipid geochemistry of sediments from Upton Broad, a small productive lake. *Org. Geochem.* 7, 25–37. [https://doi.org/10.1016/0146-6380\(84\)90134-7](https://doi.org/10.1016/0146-6380(84)90134-7)
- Currás, A., Zamora, L., Reed, J.M., García-Soto, E., Ferrero, S., Armengol, X., Mezquita-Joanes, F., Marqués, M.A., Riera, S., Julià, R., 2012. Climate change and human impact in central Spain during Roman times: High-resolution multiproxy analysis of a tufa lake record (Somolinos, 1280m asl). *Catena* 89, 31–53. <https://doi.org/10.1016/j.catena.2011.09.009>
- Damon, P.E., Sonett, C.P., 1991. Solar and terrestrial components of the atmospheric C-14 variation spectrum. In: Sonett, C.P., Giampapa, M.S., Matthews, M.S. (Eds.), *The Sun in Time*. University of Arizona Press, Tucson, AZ, USA.
- Daniau, A.-L., Sánchez-Goñi, M.F., Beaufort, L., Laggoun-Défarge, F., Loutre, M.-F., Duprat, J., 2007. Dansgaard–Oeschger climatic variability revealed by fire emissions in southwestern Iberia. *Quat. Sci. Rev.* 26, 1369–1383. <https://doi.org/10.1016/j.quascirev.2007.02.005>
- Dansgaard, W., 1987. Ice core evidence of abrupt climatic changes, in: *Abrupt Climatic Change*. Springer, pp. 223–233.
- Dansgaard, W., Johnsen, S.J., Clausen, H.B., Dahl-Jensen, D., Gundestrup, N.S., Hammer, C.U., Hvidberg, C.S., Steffensen, J.P., Sveinbjornsdottir, A.E., Jouzel, J., Bond, G., 1993. Evidence for general instability of past climate from a 250-kyr ice-core record. *Nature* 364, 218–220. <https://doi.org/10.1038/364218a0>
- D'Arrigo, R.D., Cook, E.R., Jacoby, G.C., Briffa, K.R., 1993. Nao and sea surface temperature signatures in tree-ring records from the North Atlantic sector. *Quat. Sci. Rev.* 12, 431–440. [https://doi.org/10.1016/S0277-3791\(05\)80007-1](https://doi.org/10.1016/S0277-3791(05)80007-1)
- Davis, J.C., Sampson, R.J., 1986. *Statistics and data analysis in geology*. Wiley New York et al.
- Debret, M., Bout-Roumazeilles, V., Grousset, F., Desmet, M., McManus, J.F., Massei, N., Sebag, D., Petit, J.-R., Copard, Y., Trentesaux, A., 2007a. The origin of the 1500-year climate cycles in Holocene North-Atlantic records. *Clim Past* 3, 569–575. <https://doi.org/10.5194/cp-3-569-2007>
- Debret, M., Bout-Roumazeilles, V., Grousset, F., Desmet, M., McManus, J.F., Massei, N., Sebag, D., Petit, J.-R., Copard, Y., Trentesaux, A., 2007b. The origin of the 1500-year climate cycles in holocene north-atlantic records. *Clim. Past* 3, 569–575.
- Debret, M., Sebag, D., Crosta, X., Massei, N., Petit, J.-R., Chapron, E., Bout-Roumazeilles, V., 2009. Evidence from wavelet analysis for a mid-Holocene

- transition in global climate forcing. *Quat. Sci. Rev.* 28, 2675–2688. <https://doi.org/10.1016/j.quascirev.2009.06.005>
- Delgado, J., Alfaro, P., Galindo-Zaldivar, J., Jabaloy, A., Lopez Garrido, A., Sanz de Galdeano, C., 2002. Structure of the Padul-Nigüelas basin (S Spain) from H/V ratios of ambient noise: application of the method to study peat and coarse sediments. *Pure Appl. Geophys.* 159, 2733–2749.
- deMenocal, P., Ortiz, J., Guilderson, T., Sarnthein, M., 2000. Coherent High- and Low-Latitude Climate Variability During the Holocene Warm Period. *Science* 288, 2198–2202. <https://doi.org/10.1126/science.288.5474.2198>
- Denton, G.H., Broecker, W.S., 2008. Wobbly ocean conveyor circulation during the Holocene? *Quat. Sci. Rev.* 27, 1939–1950. <https://doi.org/10.1016/j.quascirev.2008.08.008>
- Diez, S., Montuori, P., Querol, X., Bayona, J.M., 2007. Total mercury in the hair of children by combustion atomic absorption spectrometry (Comb-AAS). *J. Anal. Toxicol.* 31, 144–149.
- Domingo-García, M., Fernández-Rubio, R., Lopez, J., González, C., 1983. Aportación al conocimiento de la Neotectónica de la Depresión del Padul (Granada). *Tecniterrae* 53, 6–16.
- Dormoy, I., Peyron, O., Combourieu Nebout, N., Goring, S., Kotthoff, U., Magny, M., Pross, J., 2009. Terrestrial climate variability and seasonality changes in the Mediterranean region between 15 000 and 4000 years BP deduced from marine pollen records. *Clim Past* 5, 615–632. <https://doi.org/10.5194/cp-5-615-2009>
- Douglas, M.S.V., Smol, J.P., Blake, W., 1994. Marked Post-18th Century Environmental Change in High-Arctic Ecosystems. *Science* 266, 416. <https://doi.org/10.1126/science.266.5184.416>
- Douglass, A.E., 1914. A Method of Estimating Rainfall by the Growth of Trees. *Bull. Am. Geogr. Soc.* 46, 321–335. <https://doi.org/10.2307/201814>
- Ejarque, A., Anderson, R.S., Simms, A.R., Gentry, B.J., 2015. Prehistoric fires and the shaping of colonial transported landscapes in southern California: A paleoenvironmental study at Dune Pond, Santa Barbara County. *Quat. Sci. Rev.* 112, 181–196. <https://doi.org/10.1016/j.quascirev.2015.01.017>
- El Aallali, A., Nieto, J.M.L., Raya, F.A.P., Mesa, J.M., 1998. Estudio de la vegetación forestal en la vertiente sur de Sierra Nevada (Alpujarra Alta granadina). *Itineraria Geobot.* 387–402.
- Faegri, K., Iversen, J., 1989. *Textbook of Pollen Analysis*. Wiley, New York.
- Feijtel, T.C., Salingar, Y., Hordijk, C.A., Sweerts, J.P.R.A., Van Breemen, N., Cappenberg, T.E., 1989. Sulfur cycling in a dutch moorland pool under elevated atmospheric S-deposition. *Water. Air. Soil Pollut.* 44, 215–234. <https://doi.org/10.1007/BF00279256>
- Fernández, S., Fuentes, N., Carrión, J.S., González-Sampériz, P., Montoya, E., Gil, G., Vega-Toscano, G., Riquelme, J.A., 2007. The Holocene and Upper Pleistocene pollen sequence of Carihuela Cave, southern Spain. *Geobios* 40, 75–90. <https://doi.org/10.1016/j.geobios.2006.01.004>

- Ficken, K.J., Li, B., Swain, D., Eglinton, G., 2000. An n-alkane proxy for the sedimentary input of submerged/floating freshwater aquatic macrophytes. *Org. Geochem.* 31, 745–749.
- Fletcher, W.J., Boski, T., Moura, D., 2007. Palynological evidence for environmental and climatic change in the lower Guadiana valley, Portugal, during the last 13 000 years. *The Holocene* 17, 481–494. <https://doi.org/10.1177/0959683607077027>
- Fletcher, W.J., Debret, M., Goñi, M.F.S., 2013a. Mid-Holocene emergence of a low-frequency millennial oscillation in western Mediterranean climate: Implications for past dynamics of the North Atlantic atmospheric westerlies. *The Holocene* 23, 153–166. <https://doi.org/10.1177/0959683612460783>
- Fletcher, W.J., Debret, M., Sánchez-Goñi, M.F., 2013b. Mid-Holocene emergence of a low-frequency millennial oscillation in western Mediterranean climate: Implications for past dynamics of the North Atlantic atmospheric westerlies. *The Holocene* 23, 153–166. <https://doi.org/10.1177/0959683612460783>
- Fletcher, W.J., Sánchez Goñi, M.F., Allen, J.R.M., Cheddadi, R., Combourieu-Nebout, N., Huntley, B., Lawson, I., Londeix, L., Magri, D., Margari, V., Müller, U.C., Naughton, F., Novenko, E., Roucoux, K., Tzedakis, P.C., 2010. Millennial-scale variability during the last glacial in vegetation records from Europe. *Veg. Response Millenn.-Scale Var. Last Glacial* 29, 2839–2864. <https://doi.org/10.1016/j.quascirev.2009.11.015>
- Fletcher, W.J., Sánchez-Goñi, M.F., 2008. Orbital- and sub-orbital-scale climate impacts on vegetation of the western Mediterranean basin over the last 48,000 yr. *Quat. Res.* 70, 451–464. <https://doi.org/10.1016/j.yqres.2008.07.002>
- Fletcher, W.J., Zielhofer, C., 2013. Fragility of Western Mediterranean landscapes during Holocene Rapid Climate Changes. *Long-Term Degrad. Fragile Landsc. Syst.* 103, 16–29. <https://doi.org/10.1016/j.catena.2011.05.001>
- Florenzano, A., Marignani, M., Rosati, L., Fascetti, S., Mercuri, A.M., 2015. Are Cichorieae an indicator of open habitats and pastoralism in current and past vegetation studies? *Plant Biosyst. - Int. J. Deal. Asp. Plant Biol.* 149, 154–165. <https://doi.org/10.1080/11263504.2014.998311>
- Florschütz, F., Amor, J.M., Wijmstra, T.A., 1971. Palynology of a thick quaternary succession in southern Spain. *Palaeogeogr. Palaeoclimatol. Palaeoecol.* 10, 233–264. [http://dx.doi.org/10.1016/0031-0182\(71\)90049-6](http://dx.doi.org/10.1016/0031-0182(71)90049-6)
- Frigola, J., Moreno, A., Cacho, I., Canals, M., Sierro, F.J., Flores, J.A., Grimalt, J.O., Hodell, D.A., Curtis, J.H., 2007. Holocene climate variability in the western Mediterranean region from a deepwater sediment record. *Paleoceanography* 22, n/a-n/a. <https://doi.org/10.1029/2006PA001307>
- Galán, C., García-Mozo, H., Vázquez, L., Ruiz, L., De La Guardia, C.D., Trigo, M., 2005. Heat requirement for the onset of the *Olea europaea* L. pollen season in several sites in Andalusia and the effect of the expected future climate change. *Int. J. Biometeorol.* 49, 184–188.
- Galloway, J.N., Dentener, F.J., Capone, D.G., Boyer, E.W., Howarth, R.W., Seitzinger, S.P., Asner, G.P., Cleveland, C.C., Green, P.A., Holland, E.A., Karl, D.M., Michaels, A.F., Porter, J.H., Townsend, A.R., Vöosmarty, C.J.,

2004. Nitrogen Cycles: Past, Present, and Future. *Biogeochemistry* 70, 153–226. <https://doi.org/10.1007/s10533-004-0370-0>
- García-Alix, A., Delgado Huertas, A., Martín Suárez, E., 2012b. Unravelling the Late Pleistocene habitat of the southernmost woolly mammoths in Europe. *Quat. Sci. Rev.* 32, 75–85. <https://doi.org/10.1016/j.quascirev.2011.11.007>
- García-Alix, A., Jimenez-Espejo, F.J., Lozano, J.A., Jiménez-Moreno, G., Martínez-Ruiz, F., Sanjuán, L.G., Jiménez, G.A., Alfonso, E.G., Ruiz-Puertas, G., Anderson, R.S., 2013. Anthropogenic impact and lead pollution throughout the Holocene in Southern Iberia. *Sci. Total Environ.* 449, 451–460. <https://doi.org/10.1016/j.scitotenv.2013.01.081>
- García-Alix, A., Jiménez-Espejo, F.J., Toney, J.L., Jiménez-Moreno, G., Ramos-Román, M.J., Anderson, R.S., Ruano, P., Queralt, I., Delgado Huertas, A., Kuroda, J., 2017. Alpine bogs of southern Spain show human-induced environmental change superimposed on long-term natural variations. *Sci. Rep.* 7, 7439. <https://doi.org/10.1038/s41598-017-07854-w>
- García-Alix, A., Jiménez-Moreno, G., Anderson, R.S., Jiménez Espejo, F.J., Delgado Huertas, A., 2012a. Holocene environmental change in southern Spain deduced from the isotopic record of a high-elevation wetland in Sierra Nevada. *J. Paleolimnol.* 48, 471–484. <https://doi.org/10.1007/s10933-012-9625-2>
- Gasse, F., Roberts, C.N., 2004. Late Quaternary Hydrologic Changes in the Arid and Semiarid Belt of Northern Africa, in: Diaz, H.F., Bradley, R.S. (Eds.), *The Hadley Circulation: Present, Past and Future*. Springer Netherlands, Dordrecht, pp. 313–345. https://doi.org/10.1007/978-1-4020-2944-8_12
- Gelpi, E., Schneider, H., Mann, J., Oró, J., 1970. Hydrocarbons of geochemical significance in microscopic algae. *Phytochemistry* 9, 603–612. [https://doi.org/10.1016/S0031-9422\(00\)85700-3](https://doi.org/10.1016/S0031-9422(00)85700-3)
- Gil García, M.J., Ruiz Zapata, M.B., Santisteban, J.I., Mediavilla, R., López-Pamo, E., Dabrio, C.J., 2007. Late holocene environments in Las Tablas de Daimiel (south central Iberian peninsula, Spain). *Veg. Hist. Archaeobotany* 16, 241–250. <https://doi.org/10.1007/s00334-006-0047-9>
- Gil-Romera, G., Carrión, J.S., Pausas, J.G., Sevilla-Callejo, M., Lamb, H.F., Fernández, S., Burjachs, F., 2010. Holocene fire activity and vegetation response in South-Eastern Iberia. *Quat. Sci. Rev.* 29, 1082–1092. <https://doi.org/10.1016/j.quascirev.2010.01.006>
- Giorgi, F., 2006. Climate change hot-spots. *Geophys. Res. Lett.* 33, n/a-n/a. <https://doi.org/10.1029/2006GL025734>
- Giorgi, F., Lionello, P., 2008. Climate change projections for the Mediterranean region. *Mediterr. Clim. Trends Var. Change* 63, 90–104. <https://doi.org/10.1016/j.gloplacha.2007.09.005>
- Gómez-Ortiz, A., Oliva, M., Salvador-Franch, F., Salvà-Catarineu, M., Palacios, D., de Sanjosé-Blasco, J., Tanarro-García, L.M., Galindo-Zaldívar, J., de Galdeano, C.S., 2014. Degradation of buried ice and permafrost in the Veleta cirque (Sierra Nevada, Spain) from 2006 to 2013 as a response to recent climate trends. *Solid Earth* 5, 979.

- Gómez-Ortiz, A., Oliva-Franganillo, M., Salvà-Catarineu, M., Salvador-Franch, F., 2010. El paisaje como valor patrimonial en los espacios protegidos: el caso del Parque Nacional de Sierra Nevada (España). *Scr. Nova Rev. Electrónica Geogr. Cienc. Soc.* 2010 Vol XIV Num 346 P 1-12.
- Gómez-Ortiz, A., Schulte, L., Salvador Franch, F.S., Palacios Estremera, D., Sanjosé Blasco, J., Atkinson Gordo, A., 2004. Deglaciación reciente de Sierra Nevada. Repercusiones morfológicas, nuevos datos y perspectivas de estudio futuro. *Cuad. Investig. Geográfica* 30, 147–168.
- González-Sampériz, P., Leroy, S.A.G., Carrión, J.S., Fernández, S., García-Antón, M., Gil-García, M.J., Uzquiano, P., Valero-Garcés, B., Figueiral, I., 2010. Steppes, savannahs, forests and phytodiversity reservoirs during the Pleistocene in the Iberian Peninsula. *Iber. Floras Time Land Divers. Surviv.* 162, 427–457. <https://doi.org/10.1016/j.revpalbo.2010.03.009>
- González-Sampériz, P., Utrilla, P., Mazo, C., Valero-Garcés, B., Sopena, M., Morellón, M., Sebastián, M., Moreno, A., Martínez-Bea, M., 2009. Patterns of human occupation during the early Holocene in the Central Ebro Basin (NE Spain) in response to the 8.2 ka climatic event. *Quat. Res.* 71, 121–132. <https://doi.org/10.1016/j.yqres.2008.10.006>
- González-Sampériz, P., Valero-Garcés, B.L., Moreno, A., Jalut, G., García-Ruiz, J.M., Martí-Bono, C., Delgado-Huertas, A., Navas, A., Otto, T., Dedoubat, J.J., 2006. Climate variability in the Spanish Pyrenees during the last 30,000 yr revealed by the El Portalet sequence. *Quat. Res.* 66, 38–52. <https://doi.org/10.1016/j.yqres.2006.02.004>
- Grimm, E.C., 1987. CONISS: a FORTRAN 77 program for stratigraphically constrained cluster analysis by the method of incremental sum of squares. *Comput. Geosci.* 13, 13–35. [http://dx.doi.org/10.1016/0098-3004\(87\)90022-7](http://dx.doi.org/10.1016/0098-3004(87)90022-7)
- Grootes, P.M., Stuiver, M., White, J.W.C., Johnsen, S., Jouzel, J., 1993. Comparison of oxygen isotope records from the GISP2 and GRIP Greenland ice cores. *Nature* 366, 552.
- Grunewald, K., Scheithauer, J., 2010. Europe's southernmost glaciers: response and adaptation to climate change. *J. Glaciol.* 56, 129–142.
- Guédron, S., Amouroux, D., Sabatier, P., Desplanque, C., Deville, A.-L., Barre, J., Feng, C., Guiter, F., Arnaud, F., Reyss, J.L., Charlet, L., 2016. A hundred year record of industrial and urban development in French Alps combining Hg accumulation rates and isotope composition in sediment archives from Lake Luitel. *Chem. Geol.* 431, 10–19. <https://doi.org/10.1016/j.chemgeo.2016.03.016>
- Guiou, C., Loÿe-Pilot, M.-D., Ridame, C., Thomas, C., 2002. Chemical characterization of the Saharan dust end-member: Some biogeochemical implications for the western Mediterranean Sea. *J. Geophys. Res. Atmospheres* 107, ACH 5-1. <https://doi.org/10.1029/2001JD000582>
- Guy-Ohlson, D., 1992. Botryococcus as an aid in the interpretation of palaeoenvironment and depositional processes. *Rev. Palaeobot. Palynol.* 71, 1–15. [http://dx.doi.org/10.1016/0034-6667\(92\)90155-A](http://dx.doi.org/10.1016/0034-6667(92)90155-A)

- Hammer, Ø., Harper, D., Ryan, P., 2001. Paleontological statistics software: Package for education and data analysis. *Palaeontol. Electron.*
- Haylock, M.R., Hofstra, N., Klein Tank, A.M.G., Klok, E.J., Jones, P.D., New, M., 2008. A European daily high-resolution gridded data set of surface temperature and precipitation for 1950–2006. *J. Geophys. Res. Atmospheres* 113, n/a–n/a. <https://doi.org/10.1029/2008JD010201>
- Heegaard, E., Birks, H.J.B., Telford, R.J., 2005. Relationships between calibrated ages and depth in stratigraphical sequences: an estimation procedure by mixed-effect regression. *The Holocene* 15, 612–618. <https://doi.org/10.1191/0959683605hl836rr>
- Hernández Bermejo, J.E., Shinz Ollero, H., 1984. El análisis de semejanza aplicado al estudio de barreras y fronteras biogeográficas: Su aplicación a la corologla y endemoflora ibéricas. *Anales Jardín Botánico Madrid* 40, 421–432.
- Hu, F.S., Kaufman, D., Yoneji, S., Nelson, D., Shemesh, A., Huang, Y., Tian, J., Bond, G., Clegg, B., Brown, T., 2003a. Cyclic Variation and Solar Forcing of Holocene Climate in the Alaskan Subarctic. *Science* 301, 1890. <https://doi.org/10.1126/science.1088568>
- Hu, F.S., Kaufman, D., Yoneji, S., Nelson, D., Shemesh, A., Huang, Y., Tian, J., Bond, G., Clegg, B., Brown, T., 2003b. Cyclic Variation and Solar Forcing of Holocene Climate in the Alaskan Subarctic. *Science* 301, 1890. <https://doi.org/10.1126/science.1088568>
- Hudon, C., 2004. Shift in wetland plant composition and biomass following low-level episodes in the St. Lawrence River: looking into the future. *Can. J. Fish. Aquat. Sci.* 61, 603–617. <https://doi.org/10.1139/f04-031>
- Huntley, B., Prentice, I.C., 1988. July Temperatures in Europe from Pollen Data, 6000 Years Before Present. *Science* 241, 687–690. <https://doi.org/10.1126/science.241.4866.687>
- Hurrell, J.W., 1995. Decadal Trends in the North Atlantic Oscillation: Regional Temperatures and Precipitation. *Science* 269, 676. <https://doi.org/10.1126/science.269.5224.676>
- IPCC, 2013, 2013. Climate change 2013: the physical science basis: Working Group I contribution to the Fifth assessment report of the Intergovernmental Panel on Climate Change. Cambridge University Press.
- Jalut, G., Dedoubat, J.J., Fontugne, M., Otto, T., 2009. Holocene circum-Mediterranean vegetation changes: Climate forcing and human impact. *Quat. Int.* 200, 4–18. <https://doi.org/10.1016/j.quaint.2008.03.012>
- Jalut, G., Esteban Amat, A., Bonnet, L., Gauquelin, T., Fontugne, M., 2000. Holocene climatic changes in the Western Mediterranean, from south-east France to south-east Spain. *Palaeogeogr. Palaeoclimatol. Palaeoecol.* 160, 255–290. [https://doi.org/10.1016/S0031-0182\(00\)00075-4](https://doi.org/10.1016/S0031-0182(00)00075-4)
- Jiménez, L., Romero-Viana, L., Conde-Porcuna, J.M., Pérez-Martínez, C., 2015. Sedimentary photosynthetic pigments as indicators of climate and watershed perturbations in an alpine lake in southern Spain. *Limnetica* 34, 439–454.
- Jiménez-Espejo, F.J., García-Alix, A., Jiménez-Moreno, G., Rodrigo-Gámiz, M., Anderson, R.S., Rodríguez-Tovar, F.J., Martínez-Ruiz, F., Giral, S., Delgado

- Huertas, A., Pardo-Igúzquiza, E., 2014. Saharan aeolian input and effective humidity variations over western Europe during the Holocene from a high altitude record. *Chem. Geol.* 374–375, 1–12. <https://doi.org/10.1016/j.chemgeo.2014.03.001>
- Jiménez-Espejo, F.J., Martínez-Ruiz, F., Finlayson, C., Paytan, A., Sakamoto, T., Ortega-Huertas, M., Finlayson, G., Iijima, K., Gallego-Torres, D., Fa, D., 2007. Climate forcing and Neanderthal extinction in Southern Iberia: insights from a multiproxy marine record. *Quat. Sci. Rev.* 26, 836–852. <https://doi.org/10.1016/j.quascirev.2006.12.013>
- Jimenez-Espejo, F.J., Martínez-Ruiz, F., Rogerson, M., González-Donoso, J.M., Romero, O.E., Linares, D., Sakamoto, T., Gallego-Torres, D., Rueda Ruiz, J.L., Ortega-Huertas, M., Perez Claros, J.A., 2008. Detrital input, productivity fluctuations, and water mass circulation in the westernmost Mediterranean Sea since the Last Glacial Maximum. *Geochem. Geophys. Geosystems* 9, n/a-n/a. <https://doi.org/10.1029/2008GC002096>
- Jiménez-Moreno, G., Anderson, R.S., 2012a. Holocene vegetation and climate change recorded in alpine bog sediments from the Borreguiles de la Virgen, Sierra Nevada, southern Spain. *Quat. Res.* 77, 44–53. <https://doi.org/10.1016/j.yqres.2011.09.006>
- Jiménez-Moreno, G., Burjachs, F., Expósito, I., Oms, O., Carrancho, Á., Villalaín, J.J., Agustí, J., Campeny, G., Gómez de Soler, B., van der Made, J., 2013b. Late Pliocene vegetation and orbital-scale climate changes from the western Mediterranean area. *Glob. Planet. Change* 108, 15–28. <https://doi.org/10.1016/j.gloplacha.2013.05.012>
- Jiménez-Moreno, G., Fawcett, P.J., Scott Anderson, R., 2008. Millennial- and centennial-scale vegetation and climate changes during the late Pleistocene and Holocene from northern New Mexico (USA). *Quat. Sci. Rev.* 27, 1442–1452. <https://doi.org/10.1016/j.quascirev.2008.04.004>
- Jiménez-Moreno, G., García-Alix, A., Hernández-Corbalán, M.D., Anderson, R.S., Delgado-Huertas, A., 2013a. Vegetation, fire, climate and human disturbance history in the southwestern Mediterranean area during the late Holocene. *Quat. Res.* 79, 110–122. <https://doi.org/10.1016/j.yqres.2012.11.008>
- Jiménez-Moreno, G., Rodríguez-Ramírez, A., Pérez-Asensio, J.N., Carrión, J.S., López-Sáez, J.A., Villarías-Robles, J.J.R., Celestino-Pérez, S., Cerrillo-Cuenca, E., León, Á., Contreras, C., 2015. Impact of late-Holocene aridification trend, climate variability and geodynamic control on the environment from a coastal area in SW Spain. *Holocene* 25, 607–617. <https://doi.org/10.1177/0959683614565955>
- Johnsen, S.J., Clausen, H.B., Dansgaard, W., Fuhrer, K., Gundestrup, N., Hammer, C.U., Iversen, P., Jouzel, J., Stauffer, B., steffensen, J.P., 1992. Irregular glacial interstadials recorded in a new Greenland ice core. *Nature* 359, 311–313. <https://doi.org/10.1038/359311a0>
- Kalugin, I., Daryin, A., Smolyaninova, L., Andreev, A., Diekmann, B., Khlystov, O., 2007. 800-yr-long records of annual air temperature and precipitation over

- southern Siberia inferred from Teletskoye Lake sediments. *Quat. Res.* 67, 400–410. <https://doi.org/10.1016/j.yqres.2007.01.007>
- Kaushal, S., Binford, M.W., 1999. Relationship between C:N ratios of lake sediments, organic matter sources, and historical deforestation in Lake Pleasant, Massachusetts, USA. *J. Paleolimnol.* 22, 439–442. <https://doi.org/10.1023/A:1008027028029>
- Kepner, W.G., Rubio, J.L., Mouat, D.A., Pedrazzini, F., 2006. Desertification in the Mediterranean Region. A Security Issue. Springer Netherlands.
- Lamb, H.F., van der Kaars, S., 1995. Vegetational response to Holocene climatic change: pollen and palaeolimnological data from the Middle Atlas, Morocco. *The Holocene* 5, 400–408. <https://doi.org/10.1177/095968369500500402>
- Lamy, F., Arz, H.W., Bond, G.C., Bahr, A., Pätzold, J., 2006. Multicentennial-scale hydrological changes in the Black Sea and northern Red Sea during the Holocene and the Arctic/North Atlantic Oscillation. *Paleoceanography* 21, n/a-n/a. <https://doi.org/10.1029/2005PA001184>
- Landes, D.S., 1969. The unbound Prometheus: technological change and industrial development in Western Europe from 1750 to the present. 566 (Cambridge University Press, 1969).
- Laskar, J., Robutel, P., Joutel, F., Gastineau, M., Correia, A.C.M., Levrard, B., 2004. A long-term numerical solution for the insolation quantities of the Earth. *A&A* 428, 261–285. <https://doi.org/10.1051/0004-6361:20041335>
- Lebreiro, S.M., Francés, G., Abrantes, F.F.G., Diz, P., Bartels-Jónsdóttir, H.B., Stroynowski, Z.N., Gil, I.M., Pena, L.D., Rodrigues, T., Jones, P.D., Nombela, M.A., Alejo, I., Briffa, K.R., Harris, I., Grimalt, J.O., 2006. Climate change and coastal hydrographic response along the Atlantic Iberian margin (Tagus Prodelta and Muros Ría) during the last two millennia. *Holocene* 16, 1003–1015. <https://doi.org/10.1177/095968360606hl990rp>
- Lillios, K.T., Blanco-González, A., Drake, B.L., López-Sáez, J.A., 2016. Mid-late Holocene climate, demography, and cultural dynamics in Iberia: A multi-proxy approach. *Quat. Sci. Rev.* 135, 138–153. <https://doi.org/10.1016/j.quascirev.2016.01.011>
- Linstädter, A., Zielhofer, C., 2010. Regional fire history shows abrupt responses of Mediterranean ecosystems to centennial-scale climate change (Olea–Pistacia woodlands, NE Morocco). *J. Arid Environ.* 74, 101–110. <https://doi.org/10.1016/j.jaridenv.2009.07.006>
- Lionello, P., Malanotte-Rizzoli, P., Boscolo, R., 2006. Mediterranean climate variability. Elsevier.
- Lionello, P., Sanna, A., 2005. Mediterranean wave climate variability and its links with NAO and Indian Monsoon. *Clim. Dyn.* 25, 611–623.
- Lisiecki, L.E., Raymo, M.E., 2005. A Pliocene-Pleistocene stack of 57 globally distributed benthic $\delta^{18}\text{O}$ records. *Paleoceanography* 20, n/a-n/a. <https://doi.org/10.1029/2004PA001071>
- López-Buendía, A.M., Whateley, M.K.G., Bastida, J., Urquiola, M.M., 2007. Origins of mineral matter in peat marsh and peat bog deposits, Spain. *Int. J. Coal Geol.* 71, 246–262.

- López-Moreno, J.I., Vicente-Serrano, S.M., Morán-Tejeda, E., Lorenzo-Lacruz, J., Kenawy, A., Beniston, M., 2011. Effects of the North Atlantic Oscillation (NAO) on combined temperature and precipitation winter modes in the Mediterranean mountains: Observed relationships and projections for the 21st century. *Glob. Planet. Change* 77, 62–76. <https://doi.org/10.1016/j.gloplacha.2011.03.003>
- López-Sáez, J.A., Abel-Schaad, D., Pérez-Díaz, S., Blanco-González, A., Alba-Sánchez, F., Dorado, M., Ruiz-Zapata, B., Gil-García, M.J., Gómez-González, C., Franco-Múgica, F., 2014. Vegetation history, climate and human impact in the Spanish Central System over the last 9000 years. *Quat. Int.* 353, 98–122. <https://doi.org/10.1016/j.quaint.2013.06.034>
- Lukianova, R., Alekseev, G., 2004. Long-Term Correlation Between the Nao and Solar Activity. *Sol. Phys.* 224, 445–454. <https://doi.org/10.1007/s11207-005-4974-x>
- Ma, L.H., 2009. Gleissberg cycle of solar activity over the last 7000years. *New Astron.* 14, 1–3. <https://doi.org/10.1016/j.newast.2008.04.001>
- Magny, M., 2004. Holocene climate variability as reflected by mid-European lake-level fluctuations and its probable impact on prehistoric human settlements. *Quat. Int.* 113, 65–79. [https://doi.org/10.1016/S1040-6182\(03\)00080-6](https://doi.org/10.1016/S1040-6182(03)00080-6)
- Magny, M., Beaulieu, J.-L. de, Drescher-Schneider, R., Vanni re, B., Walter-Simonnet, A.-V., Miras, Y., Millet, L., Bossuet, G., Peyron, O., Brugiapaglia, E., Leroux, A., 2007. Holocene climate changes in the central Mediterranean as recorded by lake-level fluctuations at Lake Accesa (Tuscany, Italy). *Quat. Sci. Rev.* 26, 1736–1758. <http://dx.doi.org/10.1016/j.quascirev.2007.04.014>
- Magny, M., B geot, C., Guiot, J., Peyron, O., 2003. Contrasting patterns of hydrological changes in Europe in response to Holocene climate cooling phases. *Quat. Sci. Rev.* 22, 1589–1596. [https://doi.org/10.1016/S0277-3791\(03\)00131-8](https://doi.org/10.1016/S0277-3791(03)00131-8)
- Magny, M., Miramont, C., Sivan, O., 2002. Assessment of the impact of climate and anthropogenic factors on Holocene Mediterranean vegetation in Europe on the basis of palaeohydrological records. *Palaeogeogr. Palaeoclimatol. Palaeoecol.* 186, 47–59. [https://doi.org/10.1016/S0031-0182\(02\)00442-X](https://doi.org/10.1016/S0031-0182(02)00442-X)
- Magny, M., Peyron, O., Sadori, L., Ortu, E., Zanchetta, G., Vanni re, B., Tinner, W., 2012. Contrasting patterns of precipitation seasonality during the Holocene in the south- and north-central Mediterranean. *J. Quat. Sci.* 27, 290–296. <https://doi.org/10.1002/jqs.1543>
- Magny, M., Vanni re, B., Calo, C., Millet, L., Leroux, A., Peyron, O., Zanchetta, G., La Mantia, T., and Tinner, W.: Holocene hydrological changes in southwestern Mediterranean as recorded by lake-level fluctuations at Lago Preola, a coastal lake in southern Sicily, Italy, *Quaternary Sci. Rev.*, 30, 2459–2475, 2011
- Magri, D., 1999. Late Quaternary vegetation history at Lagaccione near Lago di Bolsena (central Italy). *Rev. Palaeobot. Palynol.* 106, 171–208. [https://doi.org/10.1016/S0034-6667\(99\)00006-8](https://doi.org/10.1016/S0034-6667(99)00006-8)

- Mann, M.E., Zhang, Z., Rutherford, S., Bradley, R.S., Hughes, M.K., Shindell, D., Ammann, C., Faluvegi, G., Ni, F., 2009. Global Signatures and Dynamical Origins of the Little Ice Age and Medieval Climate Anomaly. *Science* 326, 1256. <https://doi.org/10.1126/science.1177303>
- Marchal, O., Cacho, I., Stocker, T.F., Grimalt, J.O., Calvo, E., Martrat, B., Shackleton, N., Vautravers, M., Cortijo, E., Van Kreveld, S., Andersson, C., Koç, N., Chapman, M., Saffi, L., Duplessy, J.-C., Sarnthein, M., Turon, J.-L., Duprat, J., Jansen, E., 2002. Apparent long-term cooling of the sea surface in the northeast Atlantic and Mediterranean during the Holocene. *Quat. Sci. Rev.* 21, 455–483. [https://doi.org/10.1016/S0277-3791\(01\)00105-6](https://doi.org/10.1016/S0277-3791(01)00105-6)
- Martín Martín, J., Braga Alarcón, J., Gómez Pugnaire, M., 2010. Geological Routes of Sierra Nevada. *Reg. Minist. Environ. Junta Andal.*
- Martín-Puertas, C., Jiménez-Espejo, F., Martínez-Ruiz, F., Nieto-Moreno, V., Rodrigo, M., Mata, M.P., Valero-Garcés, B.L., 2010. Late Holocene climate variability in the southwestern Mediterranean region: an integrated marine and terrestrial geochemical approach. *Clim Past* 6, 807–816. <https://doi.org/10.5194/cp-6-807-2010>
- Martín-Puertas, C., Matthes, K., Brauer, A., Muscheler, R., Hansen, F., Petrick, C., Aldahan, A., Possnert, G., Van Geel, B., 2012. Regional atmospheric circulation shifts induced by a grand solar minimum. *Nat. Geosci.* 5, 397.
- Martín-Puertas, C., Valero-Garcés, B.L., Brauer, A., Mata, M.P., Delgado-Huertas, A., Dulski, P., 2009. The Iberian-Roman Humid Period (2600-1600 cal yr BP) in the Zoñar Lake varve record (Andalucía, southern Spain). *Quat. Res.* 71, 108–120. <https://doi.org/10.1016/j.yqres.2008.10.004>
- Martín-Puertas, C., Valero-Garcés, B.L., Mata, M.P., González-Sampériz, P., Bao, R., Moreno, A., Stefanova, V., 2008. Arid and humid phases in southern Spain during the last 4000 years: the Zoñar Lake record, Córdoba. *The Holocene* 18, 907–921. <https://doi.org/10.1177/0959683608093533>
- Martín-Puertas, C., Valero-Garcés, B.L., Mata, M.P., Moreno, A., Giralt, S., Martínez-Ruiz, F., Jiménez-Espejo, F., 2011. Geochemical processes in a Mediterranean Lake: A high-resolution study of the last 4,000 years in Zoñar Lake, southern Spain. *J. Paleolimnol.* 46, 405–421. <https://doi.org/10.1007/s10933-009-9373-0>
- Mayewski, P.A., Meeker, L.D., Twickler, M.S., Whitlow, S., Yang, Q., Lyons, W.B., Prentice, M., 1997. Major features and forcing of high-latitude northern hemisphere atmospheric circulation using a 110,000-year-long glaciochemical series. *J. Geophys. Res. Oceans* 102, 26345–26366. <https://doi.org/10.1029/96JC03365>
- Mayewski, P.A., Rohling, E.E., Stager, J.C., Karlén, W., Maasch, K.A., Meeker, L.D., Meyerson, E.A., Gasse, F., Kreveld, S. van, Holmgren, K., Lee-Thorp, J., Rosqvist, G., Rack, F., Staubwasser, M., Schneider, R.R., Steig, E.J., 2004. Holocene climate variability. *Quat. Res.* 62, 243–255. <https://doi.org/10.1016/j.yqres.2004.07.001>

- Meehl, G.A., Tebaldi, C., 2004. More Intense, More Frequent, and Longer Lasting Heat Waves in the 21st Century. *Science* 305, 994. <https://doi.org/10.1126/science.1098704>
- Meijer, P.T., Tuenter, E., 2007. The effect of precession-induced changes in the Mediterranean freshwater budget on circulation at shallow and intermediate depth. *J. Mar. Syst.* 68, 349–365. <https://doi.org/10.1016/j.jmarsys.2007.01.006>
- Menéndez Amor, J., Florschütz, F., 1964. Results of the preliminary palynological investigation of samples from a 50 m boring in southern Spain. *Bol. Real Soc. Esp. Hist. Nat. Sección Geológica* 62, 251–255.
- Menéndez, R., González-Megías, A., Jay-Robert, P., Marqués-Ferrando, R., 2014. Climate change and elevational range shifts: evidence from dung beetles in two European mountain ranges. *Glob. Ecol. Biogeogr.* 23, 646–657. <https://doi.org/10.1111/geb.12142>
- Mensing, S., Smith, J., Burkle Norman, K., Allan, M., 2008. Extended drought in the Great Basin of western North America in the last two millennia reconstructed from pollen records. *22nd Pac. Clim. Workshop* 188, 79–89. <https://doi.org/10.1016/j.quaint.2007.06.009>
- Mercuri, A.M., Accorsi, C.A., Mazzanti, M.B., Bosi, G., Cardarelli, A., Labate, D., Marchesini, M., Grandi, G.T., 2006. Economy and environment of Bronze Age settlements – Terramaras – on the Po Plain (Northern Italy): first results from the archaeobotanical research at the Terramara di Montale. *Veg. Hist. Archaeobotany* 16, 43. <https://doi.org/10.1007/s00334-006-0034-1>
- Mercuri, A.M., Sadori, L., Uzquiano Ollero, P., 2011. Mediterranean and north-African cultural adaptations to mid-Holocene environmental and climatic changes. *The Holocene* 21, 189–206. <https://doi.org/10.1177/0959683610377532>
- Meyers, P.A., 2003. Applications of organic geochemistry to paleolimnological reconstructions: a summary of examples from the Laurentian Great Lakes. *Org. Geochem.* 34, 261–289. [https://doi.org/10.1016/S0146-6380\(02\)00168-7](https://doi.org/10.1016/S0146-6380(02)00168-7)
- Meyers, P.A., 1994. Preservation of elemental and isotopic source identification of sedimentary organic matter. *Chem. Geol.* 114, 289–302. [https://doi.org/10.1016/0009-2541\(94\)90059-0](https://doi.org/10.1016/0009-2541(94)90059-0)
- Meyers, P.A., Lallier-vergés, E., 1999. Lacustrine Sedimentary Organic Matter Records of Late Quaternary Paleoclimates. *J. Paleolimnol.* 21, 345–372. <https://doi.org/10.1023/A:1008073732192>
- Milankovitch, M., 1941. Canon of insolation and the ice-age problem. *Royal Serbian Sciences Special Publication. Section of Mathematical and Natural Sciences* 33, 633.
- Mladenov, N., Reche, I., Olmo, F.J., Lyamani, H., Alados-Arboledas, L., 2010. Relationships between spectroscopic properties of high-altitude organic aerosols and Sun photometry from ground-based remote sensing. *J. Geophys. Res. Biogeosciences* 115, n/a-n/a. <https://doi.org/10.1029/2009JG000991>

- Molero-Mesa, J., Pérez-Raya, F., Valle-Tendero, F., 1992. Vegetación. Vegetación climática. Parq. Nat. Sierra Nev. Paisaje Fauna Flora E Itiner. Rueda Madr. 107–130.
- Morales-Baquero, R., Pérez-Martínez, C., 2016. Saharan versus local influence on atmospheric aerosol deposition in the southern Iberian Peninsula: Significance for N and P inputs. *Glob. Biogeochem. Cycles* 30, 501–513. <https://doi.org/10.1002/2015GB005254>
- Morales-Baquero, R., Pulido-Villena, E., Reche, I., 2006. Atmospheric inputs of phosphorus and nitrogen to the southwest Mediterranean region: Biogeochemical responses of high mountain lakes. *Limnol. Oceanogr.* 51, 830–837. <https://doi.org/10.4319/lo.2006.51.2.0830>
- Morellón, M., Anselmetti, F.S., Ariztegui, D., Brushulli, B., Sinopoli, G., Wagner, B., Sadori, L., Gilli, A., Pambuku, A., 2016. Human–climate interactions in the central Mediterranean region during the last millennia: The laminated record of Lake Butrint (Albania). *Spec. Issue Mediterr. Holocene Clim. Environ. Hum. Soc.* 136, 134–152. <https://doi.org/10.1016/j.quascirev.2015.10.043>
- Morellón, M., Valero-Garcés, B., González-Sampériz, P., Vegas-Vilarrúbia, T., Rubio, E., Rieradevall, M., Delgado-Huertas, A., Mata, P., Romero, Ó., Engstrom, D.R., López-Vicente, M., Navas, A., Soto, J., 2011. Climate changes and human activities recorded in the sediments of Lake Estanya (NE Spain) during the Medieval Warm Period and Little Ice Age. *J. Paleolimnol.* 46, 423–452. <https://doi.org/10.1007/s10933-009-9346-3>
- Morellón, M., Valero-Garcés, B., Vegas-Vilarrúbia, T., González-Sampériz, P., Romero, Ó., Delgado-Huertas, A., Mata, P., Moreno, A., Rico, M., Corella, J.P., 2009. Lateglacial and Holocene palaeohydrology in the western Mediterranean region: The Lake Estanya record (NE Spain). *Quat. Sci. Rev.* 28, 2582–2599. <https://doi.org/10.1016/j.quascirev.2009.05.014>
- Moreno, A., Cacho, I., Canals, M., Grimalt, J.O., Sánchez-Goñi, M.F., Shackleton, N., Sierro, F.J., 2005. Links between marine and atmospheric processes oscillating on a millennial time-scale. A multi-proxy study of the last 50,000 yr from the Alboran Sea (Western Mediterranean Sea). *Quat. Sci. Rev.* 24, 1623–1636. <https://doi.org/10.1016/j.quascirev.2004.06.018>
- Moreno, A., López-Merino, L., Leira, M., Marco-Barba, J., González-Sampériz, P., Valero-Garcés, B.L., López-Sáez, J.A., Santos, L., Mata, P., Ito, E., 2011. Revealing the last 13,500 years of environmental history from the multiproxy record of a mountain lake (Lago Enol, northern Iberian Peninsula). *Journal of Paleolimnology* 46, 327–349. doi:10.1007/s10933-009-9387-7
- Moreno, A., Pérez, A., Frigola, J., Nieto-Moreno, V., Rodrigo-Gámiz, M., Martrat, B., González-Sampériz, P., Morellón, M., Martín-Puertas, C., Corella, J.P., Belmonte, Á., Sancho, C., Cacho, I., Herrera, G., Canals, M., Grimalt, J.O., Jiménez-Espejo, F., Martínez-Ruiz, F., Vegas-Vilarrúbia, T., Valero-Garcés, B.L., 2012. The Medieval Climate Anomaly in the Iberian Peninsula reconstructed from marine and lake records. *Quat. Sci. Rev.* 43, 16–32. <https://doi.org/10.1016/j.quascirev.2012.04.007>

- Moreno, A., Valero-Garcés, B.L., González-Sampériz, P., Rico, M., 2008. Flood response to rainfall variability during the last 2000 years inferred from the Taravilla Lake record (Central Iberian Range, Spain). *J. Paleolimnol.* 40, 943–961. <https://doi.org/10.1007/s10933-008-9209-3>
- Moreno, T., Querol, X., Castillo, S., Alastuey, A., Cuevas, E., Herrmann, L., Mounkaila, M., Elvira, J., Gibbons, W., 2006. Geochemical variations in aeolian mineral particles from the Sahara–Sahel Dust Corridor. *Chemosphere* 65, 261–270. <https://doi.org/10.1016/j.chemosphere.2006.02.052>
- Moro, M.J., Domingo, F., López, G., 2004. Seasonal transpiration pattern of *Phragmites australis* in a wetland of semi-arid Spain. *Hydrol. Process.* 18, 213–227. <https://doi.org/10.1002/hyp.1371>
- Moulin, C., Lambert, C.E., Dulac, F., Dayan, U., 1997. Control of atmospheric export of dust from North Africa by the North Atlantic Oscillation. *Nature* 387, 691–694.
- Mulitza, S., Heslop, D., Pittauerova, D., Fischer, H.W., Meyer, I., Stuut, J.-B., Zabel, M., Mollenhauer, G., Collins, J.A., Kuhnert, H., Schulz, M., 2010. Increase in African dust flux at the onset of commercial agriculture in the Sahel region. *Nature* 466, 226–228. <https://doi.org/10.1038/nature09213>
- Nestares, T., Torres, T. de, 1997. Un nuevo sondeo de investigación paleoambiental del Pleistoceno y Holoceno en la turbera del Padul (Granada, Andalucía). *Geogaceta* 23, 99–102.
- Nieto-Moreno, V., Martínez-Ruiz, F., Giralt, S., Jiménez-Espejo, F., Gallego-Torres, D., Rodrigo-Gámiz, M., García-Orellana, J., Ortega-Huertas, M., De Lange, G., 2011. Tracking climate variability in the western Mediterranean during the Late Holocene: a multiproxy approach. *Clim. Past* 7, 1395.
- Obrochta, S.P., Miyahara, H., Yokoyama, Y., Crowley, T.J., 2012. A re-examination of evidence for the North Atlantic “1500-year cycle” at Site 609. *Quat. Sci. Rev.* 55, 23–33. <https://doi.org/10.1016/j.quascirev.2012.08.008>
- Ogura, K., Machihara, T., Takada, H., 1990. Diagenesis of biomarkers in Biwa Lake sediments over 1 million years. *Org. Geochem.* 16, 805–813.
- Oliva, M., Gómez-Ortiz, A., 2012. Late-Holocene environmental dynamics and climate variability in a Mediterranean high mountain environment (Sierra Nevada, Spain) inferred from lake sediments and historical sources. *The Holocene* 22, 915–927. <https://doi.org/10.1177/0959683611434235>
- Oliva, M., Schulte, L., Ortiz, A.G., 2009. Morphometry and Late Holocene activity of solifluction landforms in the Sierra Nevada, Southern Spain. *Permafrost. Periglac. Process.* 20, 369–382.
- Olsen, J., Anderson, N.J., Knudsen, M.F., 2012. Variability of the North Atlantic Oscillation over the past 5,200 years. *Nat. Geosci.* 5, 808–812. <https://doi.org/10.1038/ngeo1589>
- Ortiz, J.E., Torres, T., Delgado, A., Julià, R., Lucini, M., Llamas, F.J., Reyes, E., Soler, V., Valle, M., 2004. The palaeoenvironmental and palaeohydrological evolution of Padul Peat Bog (Granada, Spain) over one million years, from elemental, isotopic and molecular organic geochemical proxies. *Org. Geochem.* 35, 1243–1260. <https://doi.org/10.1016/j.orggeochem.2004.05.013>

- Ortiz, J.E., Torres, T., Delgado, A., Llamas, J.F., Soler, V., Valle, M., Julià, R., Moreno, L., Díaz-Bautista, A., 2010. Palaeoenvironmental changes in the Padul Basin (Granada, Spain) over the last 1Ma based on the biomarker content. *Palaeogeogr. Palaeoclimatol. Palaeoecol.* 298, 286–299. <https://doi.org/10.1016/j.palaeo.2010.10.003>
- Paillard, D., Labeyrie, L., Yiou, P., 1996. Macintosh Program performs time-series analysis. *Eos Trans. Am. Geophys. Union* 77, 379–379. <https://doi.org/10.1029/96EO00259>
- Pérez Raya, F., López Nieto, J., 1991. Vegetación acuática y helofítica de la depresión de Padul (Granada). *Acta Bot Malacit.* 16, 373–389.
- Pérez-Luque, A.J., Sánchez-Rojas, C.P., Zamora, R., Pérez-Pérez, R., Bonet, F.J., 2015. Dataset of Phenology of Mediterranean high-mountain meadows flora (Sierra Nevada, Spain). *PhytoKeys* 89–107. <https://doi.org/10.3897/phytokeys.46.9116>
- Pérez-Sanz, A., González-Sampériz, P., Moreno, A., Valero-Garcés, B., Gil-Romera, G., Rieradevall, M., Tarrats, P., Lasheras-Álvarez, L., Morellón, M., Belmonte, A., Sancho, C., Sevilla-Callejo, M., Navas, A., 2013. Holocene climate variability, vegetation dynamics and fire regime in the central Pyrenees: the Basa de la Mora sequence (NE Spain). *Quat. Sci. Rev.* 73, 149–169. <https://doi.org/10.1016/j.quascirev.2013.05.010>
- Peyron, O., Magny, M., Goring, S., Joannin, S., de Beaulieu, J.-L., Brugiapaglia, E., Sadori, L., Garfi, G., Kouli, K., Ioakim, C., Combourieu-Nebout, N., 2013. Contrasting patterns of climatic changes during the Holocene across the Italian Peninsula reconstructed from pollen data. *Clim Past* 9, 1233–1252. <https://doi.org/10.5194/cp-9-1233-2013>
- Pons, A., Quétel, P., 1998. À propos de la mise en place du climat méditerranéen. *Comptes Rendus Académie Sci. - Ser. IIA - Earth Planet. Sci.* 327, 755–760. [https://doi.org/10.1016/S1251-8050\(99\)80047-0](https://doi.org/10.1016/S1251-8050(99)80047-0)
- Pons, A., Reille, M., 1988. The holocene- and upper pleistocene pollen record from Padul (Granada, Spain): A new study. *Palaeogeogr. Palaeoclimatol.*
- Pulido-Villena, E., Reche, I., Morales-Baquero, R., 2006. Significance of atmospheric inputs of calcium over the southwestern Mediterranean region: High mountain lakes as tools for detection. *Glob. Biogeochem. Cycles* 20, n/a-n/a. <https://doi.org/10.1029/2005GB002662>
- Pulido-Villena, E., Reche, I., Morales-Baquero, R., 2005. Food web reliance on allochthonous carbon in two high mountain lakes with contrasting catchments: a stable isotope approach. *Can. J. Fish. Aquat. Sci.* 62, 2640–2648. <https://doi.org/10.1139/f05-169>
- Ramos-Román, M.J., Jiménez-Moreno, G., Anderson, R.S., García-Alix, A., Toney, J.L., Jiménez-Espejo, F.J., Carrión, J.S., 2016. Centennial-scale vegetation and North Atlantic Oscillation changes during the Late Holocene in the southern Iberia. *Quat. Sci. Rev.* 143, 84–95. <https://doi.org/10.1016/j.quascirev.2016.05.007>
- Ramos-Román, M.J., Jiménez-Moreno, G., Camuera, J., García-Alix, A., Anderson, R.S., Jiménez-Espejo, F.J., Carrión, J.S. Holocene climate aridification trend

- and human impact interrupted by millennial- and centennial-scale climate fluctuations from a new sedimentary record from Padul (Sierra Nevada, southern Iberian Peninsula). *Clim Past Discuss* 2017, 1–36. <https://doi.org/10.5194/cp-2017-104>. In press.
- Reed, J.M., Stevenson, A.C., Juggins, S., 2001. A multi-proxy record of Holocene climatic change in southwestern Spain: the Laguna de Medina, Cádiz. *The Holocene* 11, 707–719. <https://doi.org/10.1191/09596830195735>
- Regato, P., Salman, R., 2008. Mediterranean Mountains in a Changing World. 88 (International Union for Conservation of Nature, 2008).
- Reille, M., Pons, A., 1992. The ecological significance of sclerophyllous oak forests in the western part of the Mediterranean basin: a note on pollen analytical data, in: *Quercus Ilex L. Ecosystems: Function, Dynamics and Management*. Springer, pp. 13–17.
- Reimer, P.J., Bard, E., Bayliss, A., Beck, J.W., Blackwell, P.G., Ramsey, C.B., Buck, C.E., Cheng, H., Edwards, R.L., Friedrich, M., Grootes, P.M., Guilderson, T.P., Haflidason, H., Hajdas, I., Hatté, C., Heaton, T.J., Hoffmann, D.L., Hogg, A.G., Hughen, K.A., Kaiser, K.F., Kromer, B., Manning, S.W., Niu, M., Reimer, R.W., Richards, D.A., Scott, E.M., Southon, J.R., Staff, R.A., Turney, C.S.M., van der Plicht, J., 2013. IntCal13 and Marine13 Radiocarbon Age Calibration Curves 0–50,000 Years cal BP. *Radiocarbon* 55, 1869–1887. https://doi.org/10.2458/azu_js_rc.55.16947
- Riera, S., López-Sáez, J.A., Julià, R., 2006. Lake responses to historical land use changes in northern Spain: The contribution of non-pollen palynomorphs in a multiproxy study. *Rev. Palaeobot. Palynol.* 141, 127–137. <https://doi.org/10.1016/j.revpalbo.2006.03.014>
- Riera, S., Wansard, G., Julià, R., 2004. 2000-year environmental history of a karstic lake in the Mediterranean Pre-Pyrenees: the Estanya lakes (Spain). *Catena* 55, 293–324. [https://doi.org/10.1016/S0341-8162\(03\)00107-3](https://doi.org/10.1016/S0341-8162(03)00107-3)
- Roberts, N., Brayshaw, D., Kuzucuoğlu, C., Perez, R., Sadori, L., 2011. The mid-Holocene climatic transition in the Mediterranean: Causes and consequences. *The Holocene* 21, 3–13. <https://doi.org/10.1177/0959683610388058>
- Rodrigo-Gámiz, M., Martínez-Ruiz, F., Chiaradia, M., Jiménez-Espejo, F.J., Ariztegui, D., 2015. Radiogenic isotopes for deciphering terrigenous input provenance in the western Mediterranean. *Chem. Geol.* 410, 237–250. <https://doi.org/10.1016/j.chemgeo.2015.06.004>
- Rodrigo-Gámiz, M., Martínez-Ruiz, F., Rampen, S.W., Schouten, S., Sinninghe Damsté, J.S., February 1, 2014b. Sea surface temperature variations in the western Mediterranean Sea over the last 20 kyr: A dual-organic proxy (UK'37 and LDI) approach. *Paleoceanography* 29, 87–98. <https://doi.org/10.1002/2013PA002466>
- Rodrigo-Gámiz, M., Martínez-Ruiz, F., Rodríguez-Tovar, F.J., Jiménez-Espejo, F.J., Pardo-Igúzquiza, E., 2014a. Millennial- to centennial-scale climate periodicities and forcing mechanisms in the westernmost Mediterranean for the past 20,000 yr. *Quat. Res.* 81, 78–93. <https://doi.org/10.1016/j.yqres.2013.10.009>

- Rogora, M., Marchetto, A., Mosello, R., 2003. Modelling the effects of atmospheric sulphur and nitrogen deposition on selected lakes and streams of the Central Alps (Italy). *Hydrol. Earth Syst. Sci. Discuss.* 7, 540–551.
- Rohling, E., Mayewski, P., Abu-Zied, R., Casford, J., Hayes, A., 2002. Holocene atmosphere-ocean interactions: records from Greenland and the Aegean Sea. *Clim. Dyn.* 18, 587–593. <https://doi.org/10.1007/s00382-001-0194-8>
- Rull, V., González-Sampériz, P., Corella, J.P., Morellón, M., Giralt, S., 2011. Vegetation changes in the southern Pyrenean flank during the last millennium in relation to climate and human activities: the Montcortès lacustrine record. *J. Paleolimnol.* 46, 387–404. <https://doi.org/10.1007/s10933-010-9444-2>
- Sachse, D., Radke, J., Gleixner, G., 2006. δD values of individual n-alkanes from terrestrial plants along a climatic gradient – Implications for the sedimentary biomarker record. *Org. Geochem.* 37, 469–483. <https://doi.org/10.1016/j.orggeochem.2005.12.003>
- Sadori, L., Giraudi, C., Masi, A., Magny, M., Ortu, E., Zanchetta, G., Izdebski, A., 2016. Climate, environment and society in southern Italy during the last 2000 years. A review of the environmental, historical and archaeological evidence. *Spec. Issue Mediterr. Holocene Clim. Environ. Hum. Soc.* 136, 173–188. <https://doi.org/10.1016/j.quascirev.2015.09.020>
- Sadori, L., Jahns, S., Peyron, O., 2011. Mid-Holocene vegetation history of the central Mediterranean. *The Holocene* 21, 117–129. <https://doi.org/10.1177/0959683610377530>
- Sánchez Goñi, M., Cacho, I., Turon, J., Guiot, J., Sierro, F., Peyrouquet, J., Grimalt, J., Shackleton, N., 2002. Synchronicity between marine and terrestrial responses to millennial scale climatic variability during the last glacial period in the Mediterranean region. *Clim. Dyn.* 19, 95–105. <https://doi.org/10.1007/s00382-001-0212-x>
- Sánchez-Goñi, M.F.S., Hannon, G.E., 1999. High-altitude vegetational pattern on the Iberian Mountain Chain (north-central Spain) during the Holocene. *The Holocene* 9, 39–57. <https://doi.org/10.1191/095968399671230625>
- Sánchez-Hita, A., 2008. El patrimonio histórico de La Alpujarra y Río Nacimiento. Granada ADR Alpujarra.
- Sanz de Galdeano, C., El Hamdouni, R., Chacón, J., 1998. Neotectónica de la fosa del Padul y del Valle de Lecrín. *Itiner. Geomorfológicos Por Andal. Orient. Publicacions Univ. Barc. Barc.* 65–81.
- Sardans, J., Peñuelas, J., 2004. Increasing drought decreases phosphorus availability in an evergreen Mediterranean forest. *Plant Soil* 267, 367–377. <https://doi.org/10.1007/s11104-005-0172-8>
- Sarnthein, M., Van kreveld, S., Erlenkeuser, H., Grootes, P.M., Kucera, M., Pflaumann, U., Schulz, M., 2003. Centennial-to-millennial-scale periodicities of Holocene climate and sediment injections off the western Barents shelf, 75°N. *Boreas* 32, 447–461. <https://doi.org/10.1111/j.1502-3885.2003.tb01227.x>
- Schefeuf, E., Rاتمeyer, V., Stuut, J.-B.W., Jansen, J.H.F., Sinninghe Damsté, J.S., 2003. Carbon isotope analyses of n-alkanes in dust from the lower atmosphere

- over the central eastern Atlantic. *Geochim. Cosmochim. Acta* 67, 1757–1767. [https://doi.org/10.1016/S0016-7037\(02\)01414-X](https://doi.org/10.1016/S0016-7037(02)01414-X)
- Schröter, D., Cramer, W., Leemans, R., Prentice, I.C., Araújo, M.B., Arnell, N.W., Bondeau, A., Bugmann, H., Carter, T.R., Gracia, C.A., de la Vega-Leinert, A.C., Erhard, M., Ewert, F., Glendining, M., House, J.I., Kankaanpää, S., Klein, R.J.T., Lavorel, S., Lindner, M., Metzger, M.J., Meyer, J., Mitchell, T.D., Reginster, I., Rounsevell, M., Sabaté, S., Sitch, S., Smith, B., Smith, J., Smith, P., Sykes, M.T., Thonicke, K., Thuiller, W., Tuck, G., Zaehle, S., Zierl, B., 2005. Ecosystem Service Supply and Vulnerability to Global Change in Europe. *Science* 310, 1333. <https://doi.org/10.1126/science.1115233>
- Schulte, L., 2002. Climatic and human influence on river systems and glacier fluctuations in southeast Spain since the Last Glacial Maximum. *Quat. Int.* 93, 85–100.
- Schulz, M., Mudelsee, M., 2002. REDFIT: estimating red-noise spectra directly from unevenly spaced paleoclimatic time series. *Comput. Geosci.* 28, 421–426. [https://doi.org/10.1016/S0098-3004\(01\)00044-9](https://doi.org/10.1016/S0098-3004(01)00044-9)
- Schulz, M., Prange, M., Klocker, A., 2007. Low-frequency oscillations of the Atlantic Ocean meridional overturning circulation in a coupled climate model. *Clim Past* 3, 97–107. <https://doi.org/10.5194/cp-3-97-2007>
- Seierstad, I.A., Bader, J., 2009. Impact of a projected future Arctic sea ice reduction on extratropical storminess and the NAO. *Clim. Dyn.* 33, 937.
- Selin, N.E., 2009. Global Biogeochemical Cycling of Mercury: A Review. *Annu. Rev. Environ. Resour.* 34, 43–63. <https://doi.org/10.1146/annurev.enviro.051308.084314>
- Shackleton, N.J., 2000. The 100,000-Year Ice-Age Cycle Identified and Found to Lag Temperature, Carbon Dioxide, and Orbital Eccentricity. *Science* 289, 1897. <https://doi.org/10.1126/science.289.5486.1897>
- Shanahan, T.M., McKay, N.P., Hughen, K.A., Overpeck, J.T., Otto-Bliesner, B., Heil, C.W., King, J., Scholz, C.A., Peck, J., 2015. The time-transgressive termination of the African Humid Period. *Nat. Geosci.* 8, 140.
- Sicre, M.-A., Jalali, B., Martrat, B., Schmidt, S., Bassetti, M.-A., Kallel, N., 2016. Sea surface temperature variability in the North Western Mediterranean Sea (Gulf of Lion) during the Common Era. *Earth Planet. Sci. Lett.* 456, 124–133. <http://dx.doi.org/10.1016/j.epsl.2016.09.032>
- Smol, J.P., Wolfé, A.P., Birks, H.J.B., Douglas, M.S.V., Jones, V.J., Korhola, A., Pienitz, R., Rühland, K., Sorvari, S., Antoniades, D., Brooks, S.J., Fallu, M.-A., Hughes, M., Keatley, B.E., Laing, T.E., Michelutti, N., Nazarova, L., Nyman, M., Paterson, A.M., Perren, B., Quinlan, R., Rautio, M., Saulnier-Talbot, É., Siitonen, S., Solovieva, N., Weckström, J., 2005. Climate-driven regime shifts in the biological communities of arctic lakes. *Proc. Natl. Acad. Sci. U. S. A.* 102, 4397–4402. <https://doi.org/10.1073/pnas.0500245102>
- Snowball, I., Sandgren, P., 2001. Application of mineral magnetic techniques to paleolimnology. *Dev. Paleoenviron. Res. Track-Ing Environ. Change Using Lake Sediments Phys. Geochem. Methods* 2, 217–237.
- Sonett, C.P., Giampapa, M.S., Matthews, M.S., 1991. The Sun in time.

- Sonett, C.P., Suess, H.E., 1984. Correlation of bristlecone pine ring widths with atmospheric ^{14}C variations: a climate-Sun relation. *Nature* 307, 141–143. <https://doi.org/10.1038/307141a0>
- Steinhilber, F., Abreu, J.A., Beer, J., Brunner, I., Christl, M., Fischer, H., Heikkilä, U., Kubik, P.W., Mann, M., McCracken, K.G., Miller, H., Miyahara, H., Oerter, H., Wilhelms, F., 2012. 9,400 years of cosmic radiation and solar activity from ice cores and tree rings. *Proc. Natl. Acad. Sci.* 109, 5967–5971. <https://doi.org/10.1073/pnas.1118965109>
- Steinhilber, F., Beer, J., Fröhlich, C., 2009. Total solar irradiance during the Holocene. *Geophys. Res. Lett.* 36, n/a–n/a. <https://doi.org/10.1029/2009GL040142>
- Strong, C., Magnusdottir, G., Stern, H., 2009. Observed Feedback between Winter Sea Ice and the North Atlantic Oscillation. *J. Clim.* 22, 6021. <https://doi.org/10.1175/2009JCLI3100.1>
- Stuiver, M., Braziunas, T.F., 1993. Sun, ocean, climate and atmospheric $^{14}\text{CO}_2$: an evaluation of causal and spectral relationships. *The Holocene* 3, 289–305. <https://doi.org/10.1177/095968369300300401>
- Stuiver, M., Grootes, P.M., Braziunas, T.F., 1995. The GISP2 $\delta^{18}\text{O}$ Climate Record of the Past 16,500 Years and the Role of the Sun, Ocean, and Volcanoes. *Quat. Res.* 44, 341–354. <https://doi.org/10.1006/qres.1995.1079>
- Stuiver, M., Reimer, P.J., Braziunas, T.F., 1998. High-Precision Radiocarbon Age Calibration for Terrestrial and Marine Samples. *Radiocarbon* 40, 1127–1151. <https://doi.org/10.1017/S0033822200019172>
- Summerhayes, C.P., 2015. *Earth's Climate Evolution*. John Wiley & Sons.
- Talbot, M., 1988. The origins of lacustrine oil source rocks: evidence from the lakes of tropical Africa. *Geol. Soc. Lond. Spec. Publ.* 40, 29–43.
- Talbot, M.R., Livingstone, D.A., 1989. Hydrogen index and carbon isotopes of lacustrine organic matter as lake level indicators. *Phaneroz. Rec. Lacustrine Basins Their Environ.* 70, 121–137. [https://doi.org/10.1016/0031-0182\(89\)90084-9](https://doi.org/10.1016/0031-0182(89)90084-9)
- Thomas, C.D., Franco, A.M.A., Hill, J.K., 2006. Range retractions and extinction in the face of climate warming. *Trends Ecol. Evol.* 21, 415–416. <https://doi.org/10.1016/j.tree.2006.05.012>
- Torrence, C., Compo, G.P., 1998. A Practical Guide to Wavelet Analysis. *Bull. Am. Meteorol. Soc.* 79, 61–78. [https://doi.org/10.1175/1520-0477\(1998\)079<0061:APGTWA>2.0.CO;2](https://doi.org/10.1175/1520-0477(1998)079<0061:APGTWA>2.0.CO;2)
- Trouet, V., Esper, J., Graham, N.E., Baker, A., Scourse, J.D., Frank, D.C., 2009. Persistent Positive North Atlantic Oscillation Mode Dominated the Medieval Climate Anomaly. *Science* 324, 78. <https://doi.org/10.1126/science.1166349>
- Turney, C.S.M., Kershaw, A.P., Clemens, S.C., Branch, N., Moss, P.T., Keith Fifield, L., 2004. Millennial and orbital variations of El Niño/Southern Oscillation and high-latitude climate in the last glacial period. *Nature* 428, 306.
- Tzedakis, P., 2007. Seven ambiguities in the Mediterranean palaeoenvironmental narrative. *Quat. Sci. Rev.* 26, 2042–2066.

- USGS, 2006. Shuttle Radar Topography Mission, 3 Arc Second scene SRTM3n37w003V2. (Global Land Cover Facility, University of Maryland, 2006).
- Valbuena-Carabaña, M., de Heredia, U.L., Fuentes-Utrilla, P., González-Doncel, I., Gil, L., 2010. Historical and recent changes in the Spanish forests: A socio-economic process. *Iber. Floras Time Land Divers. Surviv.* 162, 492–506. <https://doi.org/10.1016/j.revpalbo.2009.11.003>
- Valle, F., 2003. Mapa de series de vegetación de Andalucía 1: 400 000. Editorial Rueda.
- Valle Tendero, F., 2004. Modelos de Restauración Forestal: Datos botánicos aplicados a la gestión del Medio Natural Andaluz II: Series de vegetación. Cons. Medio Ambiente Junta Andal. Sevilla.
- Van der Hammen, T., Wijmstra, T.A., Zagwijn, H., 1971. The floral record of the Late Cenozoic of Europe. In: Turekian, K.K. (Ed.), *The Late Cenozoic Glacial Ages*. Yale University Press, New Haven, pp. 391–424.
- Van Geel, B., Coope, G.R., Hammen, T.V.D., 1989. Palaeoecology and stratigraphy of the lateglacial type section at Usselo (the Netherlands). *Rev. Palaeobot. Palynol.* 60, 25–129. [http://dx.doi.org/10.1016/0034-6667\(89\)90072-9](http://dx.doi.org/10.1016/0034-6667(89)90072-9)
- Van Geel, B., Hallewas, D.P., Pals, J.P., 1983. A late holocene deposit under the Westfriese Zeedijk near Enkhuizen (Prov. of Noord-Holland, The Netherlands): Palaeoecological and archaeological aspects. *Rev. Palaeobot. Palynol.* 38, 269–335. [http://dx.doi.org/10.1016/0034-6667\(83\)90026-X](http://dx.doi.org/10.1016/0034-6667(83)90026-X)
- Vaquero, J.M., Gallego, M.C., García, J.A., 2002. A 250-year cycle in naked-eye observations of sunspots. *Geophys. Res. Lett.* 29, 58–1. <https://doi.org/10.1029/2002GL014782>
- Villegas Molina, F., 1967. Laguna de Padul: Evolución geológico-histórica. *Estud. Geográficos* 28, 561.
- Visbeck, M.H., Hurrell, J.W., Polvani, L., Cullen, H.M., 2001. The North Atlantic Oscillation: Past, present, and future. *Proc. Natl. Acad. Sci.* 98, 12876–12877. <https://doi.org/10.1073/pnas.231391598>
- Waelbroeck, C., Labeyrie, L., Michel, E., Duplessy, J.C., McManus, J.F., Lambeck, K., Balbon, E., Labracherie, M., 2002. Sea-level and deep water temperature changes derived from benthic foraminifera isotopic records. *EPILOG* 21, 295–305. [https://doi.org/10.1016/S0277-3791\(01\)00101-9](https://doi.org/10.1016/S0277-3791(01)00101-9)
- Wassenburg, J.A., Immenhauser, A., Richter, D.K., Niedermayr, A., Riechelmann, S., Fietzke, J., Scholz, D., Jochum, K.P., Fohlmeister, J., Schröder-Ritzrau, A., Sabaoui, A., Riechelmann, D.F.C., Schneider, L., Esper, J., 2013. Moroccan speleothem and tree ring records suggest a variable positive state of the North Atlantic Oscillation during the Medieval Warm Period. *Earth Planet. Sci. Lett.* 375, 291–302. <https://doi.org/10.1016/j.epsl.2013.05.048>
- Whitlock, C., Anderson, R.S., 2003. Fire History Reconstructions Based on Sediment Records from Lakes and Wetlands, in: Veblen, T.T., Baker, W.L., Montenegro, G., Swetnam, T.W. (Eds.), *Fire and Climatic Change in Temperate Ecosystems of the Western Americas*. Springer New York, New York, NY, pp. 3–31. https://doi.org/10.1007/0-387-21710-X_1

- Wick, L., Lemcke, G., Sturm, M., 2003. Evidence of Lateglacial and Holocene climatic change and human impact in eastern Anatolia: high-resolution pollen, charcoal, isotopic and geochemical records from the laminated sediments of Lake Van, Turkey. *The Holocene* 13, 665–675. <https://doi.org/10.1191/0959683603hl653rp>
- Wieder, R.K., Lang, G.E., 1988. Cycling of inorganic and organic sulfur in peat from Big Run Bog, West Virginia. *Biogeochemistry* 5, 221–242. <https://doi.org/10.1007/BF02180229>
- Wiles, G.C., D'Arrigo, R.D., Villalba, R., Calkin, P.E., Barclay, D.J., 2004. Century-scale solar variability and Alaskan temperature change over the past millennium. *Geophys. Res. Lett.* 31, n/a-n/a. <https://doi.org/10.1029/2004GL020050>
- Wu, J., Yu, Z., Zeng, H., Wang, N., 2009. Possible solar forcing of 400-year wet–dry climate cycles in northwestern China. *Clim. Change* 96, 473–482. <https://doi.org/10.1007/s10584-009-9604-4>
- Xu, D., Lu, H., Chu, G., Wu, N., Shen, C., Wang, C., Mao, L., 2014. 500-year climate cycles stacking of recent centennial warming documented in an East Asian pollen record 4, 3611.
- Yu, Z., Ito, E., 1999. Possible solar forcing of century-scale drought frequency in the northern Great Plains. *Geology* 27, 263–266.
- Zanchettin, D., Rubino, A., Traverso, P., Tomasino, M., 2008. Impact of variations in solar activity on hydrological decadal patterns in northern Italy. *J. Geophys. Res. Atmospheres* 113, n/a–n/a. <https://doi.org/10.1029/2007JD009157>
- Ziegler, M., Jilbert, T., de Lange, G.J., Lourens, L.J., Reichert, G., 2008. Bromine counts from XRF scanning as an estimate of the marine organic carbon content of sediment cores. *Geochem. Geophys. Geosystems* 9.
- Zielhofer, C., Fletcher, W.J., Mischke, S., De Batist, M., Campbell, J.F.E., Joannin, S., Tjallingii, R., El Hamouti, N., Junginger, A., Stele, A., Bussmann, J., Schneider, B., Lauer, T., Spitzer, K., Strupler, M., Brachert, T., Mikdad, A., 2017. Atlantic forcing of Western Mediterranean winter rain minima during the last 12,000 years. *Quat. Sci. Rev.* 157, 29–51. <https://doi.org/10.1016/j.quascirev.2016.11.037>

